ESA-EOPG-EBA-TN-5, issue 1.1

ENVIromental SATellite (ENVISAT)
MICHELSON INTERFEROMETER for PASSIVE ATMOSPHERIC SOUNDING (MIPAS)

ESA Level 2 version 8.22 products - Product Quality Readme File

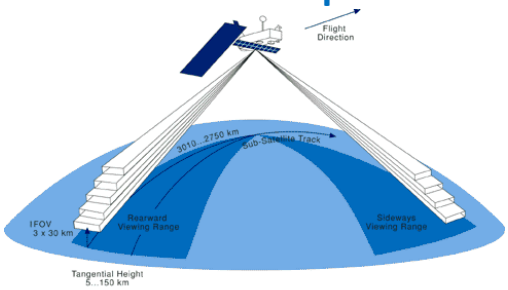

September 2021

P. Raspollini, A. Piro, D. Hubert, A. Keppens, J.-C. Lambert, G. Wetzel, D. Moore, S. Ceccherini, M. Gai, F. Barbara, N. Zoppetti,
with MIPAS Quality Working Group, MIPAS validation teams, MIPAS IDEAS+ (Instrument Data quality Evaluation and Analysis Service) team
Approved by: A. Dehn ESA-ESRIN

Contact people:
A. Dehn –ESA-ESRIN: angelika.dehn@esa.int
Alessandro Piro – SERCO: alessandro.piro@serco.com
Piera Raspollini – IFAC-CNR: p.raspollini@ifac.cnr.it
Marco Gai – IFAC-CNR: m.gai@ifac.cnr.it

TABLE OF CONTENTS

0 Scope and background of this document

This document describes the geophysical atmospheric data products following the reprocessing of the measurements of the complete MIPAS mission with ESA Level 2 processor version 8.22. It is targeted at users of MIPAS V8 data.

The version 8 data release (Dinelli et al., in preparation) is the fourth public release of MIPAS ESA full mission data. Earlier releases were performed for V5.0x, V6.0x (Raspollini et al., 2013) and V7.0x (README FILE V7).
In addition to guidance on how to use and screen the data, this document describes the quality for the L2 V8.22 data products, and contains a brief outline of the algorithms used to generate Level 2 data from the Level 1 data (calibrated middle infrared radiance observations).
More information on the MIPAS instrument can be found here.
The theoretical basis for the Level 2 software is described in (Ridolfi et al., 2000), (Raspollini et al, 2006), (Raspollini et al., 2013). (Raspollini et al., in preparation) describes the modifications implemented in both the L2 processor V8 and in the auxiliary data.

In particular, Chapter 1 of this document details relevant aspects of the MIPAS mission.

Chapter 2 describes the L2 V8.22 processor used to reprocess the full mission, from the theoretical basis of the algorithm to the latest modifications in the algorithm and in the auxiliary data. There is also a short revision of the changes in the L1 V8.03 products, used as input by the L2 V8.22 processor and having an impact on L2 products.

Chapter 3 describes the V8.22 dataset, how the products are organised, how they have to be filtered, how they can be characterised in terms of Averaging Kernels, random and systematic errors.

Chapter 4 provides product-specific information on the main differences with respect to previous versions and on the quality of the geophysical products of V8 dataset.

1 MIPAS mission overview

MIPAS is a Fourier transform spectrometer that measured atmospheric limb emission spectra from a polar sun-synchronous orbit on board the European ENVISAT satellite. The measured spectra cover the mid-infrared region, from 680 to 2410 cm^{-1}, and are recorded in both the daytime (descending node around 10:00 local solar time) and nighttime (ascending node around 22:00 local solar time) part of the orbit.
The ENVISAT mission with the MIPAS instrument on-board lasted ten years, from the 1st of March 2002 until the 8th of April 2012. MIPAS operated at 100% of its duty cycle from July 2002 to the 26th of March 2004, when, due to a major anomaly affecting the Interferometer Drive Unit (IDU), its regular operations were interrupted to avoid the mechanical blockage of the instrument. ESA succeeded in recovering the instrument in January 2005, after various tests with different spectral resolutions, at a reduced spectral resolution but an increased vertical sampling.

At the beginning of 2005, MIPAS operated at only 30% duty cycle which was progressively increased until December 2007, when it was successfully recovered back to 100% operations.

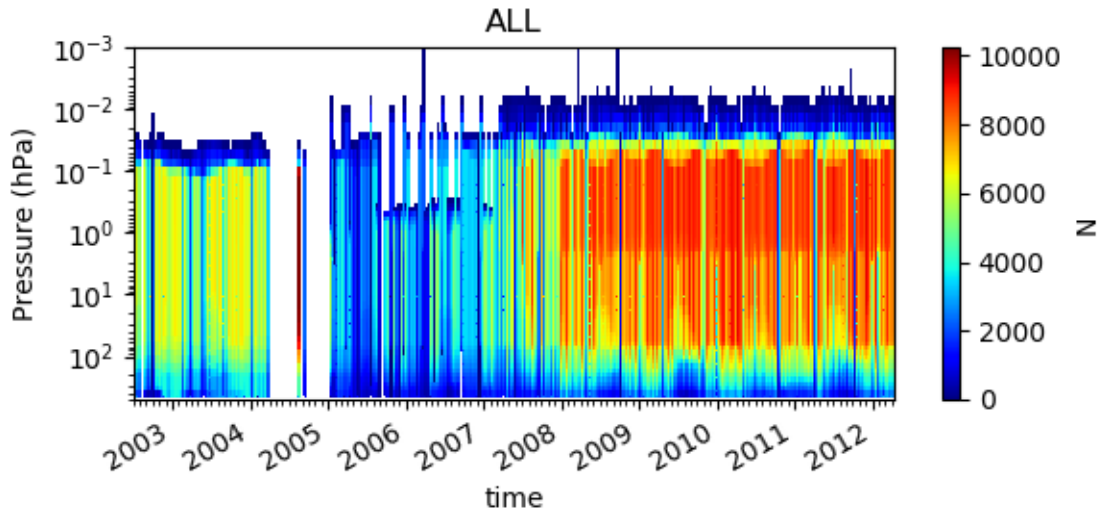

Figure 1-1 Timeseries of altitude dependent number of retrieved temperature values on a weekly basis. All considered measurement modes are included.

Figure 1-1 reports the timeseries of the number of retrieved temperature values at the different altitudes computed on a weekly basis. It is clearly visible the reduced duty cycle in the period 2005-2007 and the increase of the number of retrieved profiles in the Optimised Resolution Phase (when duty cycle returned to 100%) coming from the reduced measurement time of each scan sequence.

During all MIPAS lifetime the acquisition baseline was defined by the "MIPAS Science Team" and was regularly revised during the mission in order to adapt the measuring scenario to scientific requirements, such as special operations in support to calibration/validation campaigns or special events. Different measurements modes were thus implemented. In more detail, the following phases can be identified along the MIPAS mission.

- **Commissioning Phase: 1st March – July 2002**

ENVISAT launch, SODAP (Switch-On and Data Acquisition Phase, where the instrument operation are verified and the calibration /validation activities are carried out) and MIPAS cal/val phase. Data from this period are not released to the public.

- **Full Resolution (FR) phase: 1st July 2002 – 26th March 2004**

The original measurement mode for MIPAS, acquiring full spectral resolution measurements (0.025 cm^{-1}). During this phase, measurements were mainly acquired in Nominal Mode with 17 sweeps per scan sequence. Only a few orbits were commanded in the Special observation Mode or in the Upper Atmosphere observational scenario for scientific purposes. ORM V8 processed only the measurements acquired in nominal mode.

- **Mission suspended: 26th March 2004 – 9th August 2004**

- **Reduced Resolution (RR) phase: 9th August 2004 – 17th September 2004**

MIPAS was tested to acquire measurements at reduced spectral resolution (from 0.025 to 0.0625 cm^{-1}). For this phase, Nominal Mode operations have 17 sweeps per scan sequence.

- **Mission suspended: 17th September 2004 – 10th January 2005**

- **Optimised Resolution (OR) phase: 10th January 2005 – 21st October 2010**

MIPAS acquired reduced spectral resolution measurements (0.0625 cm^{-1}). The new Nominal Mode has 27 sweeps per scan sequence, with the reduced measurement time being exploited to make the vertical sampling of the scan finer. During this phase, beside the most frequent Nominal Mode, several measurements were acquired in, e.g., UTLS-1 (Upper Troposphere-Lower Stratosphere), mainly in the 2005-2007 period, and MA (Middle Atmosphere) and UA (Upper Atmosphere) modes, regularly measured in a sequence with 8 days of NOM measurements, 1 day of MA and 1 day of UA in the 2007-2009 period, and in a sequence of 1 day of MA , four days of NOM and one day of UA in the period 2010-2012. Other measurement modes (NLC and AE) were occasionally used. Operations were based on an "event driven scenario" with priority to validation campaigns and special observations. The instrument duty cycle increased from 30% up to 100%, with continuous operations resumed on 1st December 2007. .

- **ENVISAT extended mission: 21st October 2010 – 8th April 2012**

MIPAS continued operations as in the Optimised Resolution phase but the ENVISAT platform was moved to a lower altitude with a drifting orbit equator crossing time. On 8th April 2012 contact with the ENVISAT platform was lost unexpectedly and efforts to re-establish communication with the satellite were unsuccessful, thereby ending the MIPAS mission.

The description of the different MIPAS measurement modes can be found here, while the mission planning for each year of the MIPAS mission can be found at this link.

In Table 1.1 the list of all measurements modes which were analysed by ORM V8.22 is provided, together with the indication of the number of measured sweeps per scan of each mode, the measured altitude range, the percentage of the scans measured in each mode, information on whether a floating altitude is used. Some modes are characterised by a floating altitude-sampling grid, where the altitudes varies with latitude but maintaining fixed steps from sweep to sweep in order to follow roughly the tropopause height along the orbit with the requirement to collect at least one spectrum within the troposphere but to avoid too many cloud-affected spectra which are hard to analyse. It has to be noted that the retrieval range may be smaller than the measured altitude range and different for the different species (see Sect. 4).

L2-algorithm		L2-V8-overview		Altitude		TEMP	H_2O	O_3	HNO_3	CH_4	N_2O	NO_2	CFC-11
$ClONO_2$	N_2O_5	CFC-12	COF_2	CCl_4	HCN	CFC-14	HCFC22	C_2H_2	C_2H_6	CH_3Cl	$COCl_2$	OCS	HDO

Table 1-1 List of the measurement modes analysed by ORM_V8.22

Measurement mode	Number of tangent altitudes	Altitude range of the measurements (at latitude 45° if floating altitude) (km)	Floating altitude	% of scans per mode wrt total scans
FR NOM	17	6-68	No	20.01
OR NOM	27	7-72	Yes	74.07
OR UTLS-1	19	8.5-52	Yes	5.28
OR UTLS-1 old	18	8.5-49	No	0.41
OR UTLS-2	11	12-42	No	0.22
OR AE	12	7-38	No	0.16
OR NLC	25	39-102	No	1.71
OR MA	29	18-102	No	8.07
OR UA	35	42-172	No	6.55
RR 17 (Aug-Sep 2004)	17	6-68	No	0.89

2 Level 2 full mission reprocessing with ORM V8

The Version 8 reprocessing of the full mission consists of a complete reprocessing of both level1b and level2 data. The MIPAS L2 V8 dataset was obtained from the analysis of L1V8.03 dataset with Level 2 Optimised Retrieval Model (ORM) processor version 8.22. In this Section the theoretical basis of the L2 algorithm is reviewed, as well as the improvements implemented in the latest version of the L2 algorithm, in the used auxiliary data, and in the input L1b V8 data.

2.1 Review of theoretical basis of the L2 algorithm

The Level 2 processor (Ridolfi et al., 2000, Raspollini et al., 2006, Raspollini et al., 2013) has been specifically designed to operate in near real time, and hence to work automatically in different atmospheric conditions, aimed to use a minimum amount of a priori information that may introduce a bias in the profiles. To this end, the altitude grid of the retrieval coincides with the tangent points of the limb measurements (or a sample of them) where the sensitivity of the measurements peaks and the non-linear least-square fit is used. A global fit (Carlotti, 1988) is performed, consisting in the simultaneous fit of the whole limb scanning sequence of the spectra acquired at different tangent altitudes. The ill-conditioned problem of the measurements is handled with the regularizing Levenberg–Marquardt approach (Levenberg, 1944; Marquardt, 1963; Hanke, 1997) during the iterations and an a posteriori regularization with a self-adapting constraint dependent on the random error of each profile (Ceccherini, 2005; Ridolfi and Sgheri, 2011). An accurate method specifically designed for the regularizing Levenberg–Marquardt approach is used for the computation of the diagnostic quantities (covariance and averaging kernels) (Ceccherini and Ridolfi, 2010).

The forward model computes the radiative transfer integral properly taking into account vertical inhomogeneities in the atmosphere, and, since V8, also inhomogeneities in the horizontal direction (represented by gradients of temperature, water vapour and ozone along the line of sight, derived from ERA INTERIM reanalysis products).
The atmosphere is assumed to be in local thermodynamic equilibrium (LTE) and in hydrostatic equilibrium. The characteristics of the instrument (Instrument Line Shape (ILS) and Instantaneous Field of View (IFOV)) are modelled accurately. Scattering is not included in the radiative transfer integral, and the spectra affected by thick clouds, identified by the cloud filtering algorithm (Spang et al.,2002, 2004; Raspollini et al.,2006), are not included in the analysis.

The impact of unaccounted atmospheric effects (non-LTE, interfering species, etc.) is minimized through the selection of spectral intervals (microwindows, MW) containing relevant information on target parameters and minimizing the systematic errors (Dudhia et al., 2002).

For each scan, the pressure corresponding to the tangent altitudes and the related temperature values are retrieved simultaneously (pT retrieval), which is followed by a sequential retrieval of trace gas VMR profiles (first H_2O, then O_3, and all other species). The retrieval vector includes, in addition to the species profile, MW-dependent continuum transmission profiles and MW-dependent, but height-independent offset calibration values. These are jointly retrieved with either VMR or pT retrieval.

2.2 ORM V8 algorithm upgrades

The MIPAS Level 2 ORM processor version 8.22, used to perform the reprocessing of the full MIPAS mission, includes improvements in the retrieval algorithms, an update of the output data format and provides products of six new species.

2.2.1 Algorithm modifications

The upgrades implemented in ORM V8.22 that impact the quality of the data are:

Handling of horizontal inhomogeneities

The horizontal variability of the atmosphere is modelled with a user supplied horizontal gradient for both temperature and trace gases taken from ECMWF data, derived from ERA INTERIM reanalysis.
This reduces the systematic difference (of 1 to 2 K) in retrieved temperature profiles in the ascending and descending part of the orbit at mid- to higher latitudes, while preserving the naturally occurring ascending-descending temperature differences due to solar tides in Equatorial regions. For trace gas retrievals, the handling of gradients has a smaller effect on the ascending-descending differences.

Height-dependent cloud-index thresholds for cloud detection

The cloud detection algorithm uses a cloud index (CI), that is defined as the ratio between the mean radiance in two spectral intervals, the first (788-796 cm^{-1}) is dominated by CO_2 and weak ozone emissions, the second interval (832-834 cm^{-1}) is characterized by aerosols and cloud emissions, and some weak ozone and CFC-11 emission lines and is relatively insensitive to temperature.
Typical band A CI values for the upper troposphere are: CI = 1.8 corresponding to thick cloud, CI=6.0 meaning no cloud and 1.8 < CI _< 4.0 corresponding to thick and thin clouds. CI values between 4 and 6 are produced by weaker cirrus clouds such as sub-visible cirrus clouds, or by clouds partially covering the MIPAS line of sight. Spectra with CI smaller than a given threshold are not included in the analysis. In previous versions the CI threshold was taken fixed in altitude and latitude and equal to 1.8, as a consequence only spectra affected by thick clouds were filtered out. This caused a problem especially in the polar winter, where polar stratospheric clouds were not filtered out and they were responsible of some outliers in the retrieved H_2O and other species retrievals.
For level 2 processor version 8 the altitude-dependent and latitude-dependent cloud filtering threshold (Sembhi et al., 2012, Griessbach et al., 2016) was used, because this approach was considered significantly more sensitive in detecting critical clouds.
These thresholds were multiplied by the factor 0.8 in order to slightly reduce the sensitivity of this approach and to avoid the removal of points whose VMR is not significantly affected by the clouds.
The use of the altitude and latitude dependent cloud filtering has as effect that outliers in polar winters are significantly avoided. Furthermore, the number of points retrieved at higher altitudes are in general greater, due to the fact that now no a posteriori filtering (acting on the whole profile) is needed for removing the outliers. At intermediate altitudes, the new cloud filtering algorithm removes a greater number of points than the previous one, in particular in equatorial regions, and the number of points retrieved is lower. At low altitudes, the new cloud filter is weaker and the number of retrieved points is greater.

Optimal Estimation

The Optimal Estimation (OE) approach (Rodgers, 2000) is used for the following species: HCN, CF_4, C_2H_2, C_2H_6, CH_3Cl, OCS, $COCl_2$, HDO.
For all species, except HDO, a fixed (in time and latitude) a priori profile is used (obtained as the mean of climatological profiles of the considered species at different latitudes). The use of a fixed a priori profile guarantees that observed variability in the retrieved products comes from the measurements and not from the a priori profile. The diagonal elements of the covariance matrix of the a priori profile at a given altitude is given by the square of a constant plus a given percentage of the value of the a priori profile at the considered altitude, while the off-diagonal elements are obtained considering an exponential decrease with altitude with a given correlation length.

Choice in the selection of Initial Guess profiles/ assumed profiles of interfering species
Different databases are available for the definition of initial guess profiles, interfering species profiles and computation of the gradients. These are: Climatological profiles (Remedios et al., 2012) IG2, ECMWF profiles, MIPAS retrieved profiles from previous reanalysis, retrieved profiles of previous scans, retrieved profiles from the same scan. The selection of the profiles is made according to a priority list defined in the settings files. The L2 V8 products have been processed using the following settings: profiles retrieved by ORM in the previous retrievals of the chain or in the previous scan are used; if they are not available, climatological profiles are used. The gradients have been computed using ECMWF profiles.

Filtering
The filtering of the retrieved profiles was performed as described below:

- only retrieved profiles reaching convergence and having chi-square and maximum error smaller than the corresponding thresholds are used in subsequent retrievals as initial guess and interfering species profiles
- flagging of profiles in the output files are performed with the same criteria.

2.2.2 Additional retrieved species

The output products generated by the new processor ORM V8.22 contain also the files for the following six additional species, retrieved at the end of the chain: C_2H_2, C_2H_6, $COCl_2$, CH_3Cl, OCS and HDO.

2.3 Upgrades in the L2 Auxiliary Data Files

The main upgrade to the Level 2 Auxiliary Data Files v9.06 used by the processor ORM V8.22 comes from the use of the MIPAS dedicated spectroscopic database v4.45 (instead of v3.2), and of up-to-date cross-sections for the following heavy molecules (CFC-11, CFC-12, CFC-14, CCl_4, HCFC-22, CFC-113, $ClONO_2$, HNO_4, SF_6), (see TN 'Assessment of Molecular Cross-Section Data v. 2', here).

The spectroscopic database v4.45 is based on HITRAN08 (Rothman et al., 2009), but spectroscopic parameters for the molecules O_2, SO_2, OCS, CH_3Cl, C_2H_2, C_2H_6 are taken from HITRAN 2012 (Rothman et al., 2012). The spectroscopic parameters of HNO_3 were derived by Perrin et al., 2016, the spectroscopic data for the $COCl_2$ were derived by Tchana et al., 2015. Both HNO_3 and $COCl_2$ data are now contained in HITRAN 2016. Spectroscopic data for the new molecule C_3H_8 (Flaud et al., 2010 and Nixon et al., 2009)), which are not present in HITRAN dataset up to 2016, have been included in the dataset pf4.45. Among the species for which spectroscopic data have changed significantly with respect to previous MIPAS spectroscopic database HITRAN_mipas_pf3_2 we have to mention HCN, for which spectroscopy as described in (Maki et al., 1996, 2000) is used.

The use of the new spectroscopic database and new cross-sections leads in many cases to a reduction of the residuals. In some cases, it has a strong impact on the profiles. This is discussed in the product-specific description, Sect. 4.

Another change in the auxiliary data involves the ECMWF data files, which are now taken from the ERA Interim reanalysis.

New auxiliary data were needed for using the Optimal Estimation approach for some species, which implies the availability of a priori profiles and their covariance matrices.

New MWs for MA and UA measurement modes have been used, as well as for some trace gases (see product-specific description, Sect. 4).

2.4 Input L1b V8 dataset

The MIPAS full mission reprocessing with ORM V8.22 processor takes advantage of the use of the latest available Level 1b dataset V8 [Kleinert et al., 2018 and [AD-10]]. L1V8 data are characterized by:

- Better radiometric accuracy coming from an improved in-flight characterisation of detector non-linearity (important for trend estimation from MIPAS L2 products). This modification was an upgrade of the correction already implemented in L1V7 data. The impact of the correction in L1V8 data is mainly on the bias of the L2 products, but there is also a small change in the drift over the 10 year (see details in product specific Section 4).
- Lower discontinuities in the time series: Although gain measurements were acquired on a daily basis, the gain function used for radiometric calibration was updated only once per week. The gain variation is usually sufficiently slow that the error introduced by the temporal drift of the gain function is small. However, in some situations, generally after a decontamination period, some abrupt changes in the gain occasionally occur especially in band B, and hence the gain variation is significantly better captured when using the daily gain measurements (as far as they are available). Therefore the daily gain measurements were used for processing L1 version 8. This leads to a reduction of the discontinuities in the timeseries of retrieved profiles from band B (CH_4, N_2O and N_2O_5).
- Larger accuracy in the Line of Sight (LOS) engineering tangent altitude. From the comparison of MIPAS LOS with correlative measurements (ozone sonde), an annual cycle and negative trend were deduced in the LOS. The cycle and trend were characterized and a corresponding correction was applied to the tangent altitude information. Smaller pointing residual errors are found in L1 V8 data with respect to previous versions (smaller than 200 m at high altitudes, smaller than 400 m at low altitudes).

3 Level 2 version 8.22 dataset

3.1 Product overview

The MIPAS Level 2 V8 dataset is the result of the full-mission reprocessing campaign performed on L1V8 products using the ORM processor version 8.22. The reprocessed dataset covers the entire MIPAS operational mission lifetime period, from the 1st of July 2002 up to the 8th of April 2012. The following products are provided on a pressure grid and altitude grid: H_2O, O_3, HNO_3, CH_4, N_2O, NO_2, CFC-11, $ClONO_2$, N_2O_5, CFC-12, COF_2, CCl_4, HCN, CFC-14, HCFC-22, HDO, C2H2, C2H6, CH3Cl, OCS, COCl2, as well as Temperature.

In total products relative to 35147 orbits were generated with a total data volume of about 2.3 TB. Table 3-1 gives an overview of the number of orbits available. The status of the MIPAS consolidated Level 2 data set version 8.22 is also available here.

Table 3-1 Number of orbits available in the different years of MIPAS mission, distinguishing between total L0, L1b V8 and L2 V8 orbits. The last column reports the percentage of available L2 V8 orbits wrt L1 orbits (L2/L1)

Year	Total Envisat orbits	L1b v8 Products available	L2 v8 Products available	Percentage of availability
2002 (since 01/07)	2634	2003	1994	99.60%
2003	5224	4544	4453	98.33%
2004	5239	1157	1115	94.99%
2005	5225	1679	1648	98.15%
2006	5225	2051	2023	98.63%
2007	5224	3302	3214	97.33%
2008	5240	4827	4806	99.56%
2009	5224	4864	4840	99.51%
2010	5229	4841	4832	99.81%
2011	5243	4884	4868	99.67%
2012 (up to 08/04)	1415	1354	1354	100.00%
Total	**51122**	***35506***	**35147**	**98.99%**

3.2 Products identifiers

The Level 2 products generated by ORM V8.22 are identified by the retrieval identifier '01' reported in the product filename (last 2 digit before file extension '.nc') and by the fields reported in Table 3-2 inside the output files themselves:

Table 3-2 Fields reported in the output files providing information on the version of the used code and auxiliary data

Output file Field	Value
processor_version	ORM_V8.xx
auxdata_version	9.xx
processor_patchlevel	22
auxdata_subversion	6

Level 2 data files are disseminated per species and per orbit, and users can either download a standard product or an extended product (see Section 3.4). Table 3-3 shows the structure of the filenames of both standard and extended files.

L2-algorithm		L2-V8-overview		Altitude		TEMP	H_2O	O_3	HNO_3	CH_4	N_2O	NO_2	CFC-11
$ClONO_2$	N_2O_5	CFC-12	COF_2	CCl_4	HCN	CFC-14	HCFC22	C_2H_2	C_2H_6	CH_3Cl	$COCl_2$	OCS	HDO

Table 3-3 Structure of the filename of the output files

Standard product filename
MIPAS_2PS_[species]_[Start_time]_[Stop_time]_[orbit#]_01.nc
Extended product filename
MIPAS_2PE_[species]_[Start_time]_[Stop_time]_[orbit#]_01.nc

3.3 How to access the data

See further details for data registration and access here.

3.4 Product format and content

The MIPAS Level 2 products generated with ORM V8.22 have a completely new format, i.e. NetCDF-4. The content of the data and the format is described in the TN 'Input/Output Data Definition (IODD)' TN IFAC_GA_2018_1_FB.

For each retrieved species (H_2O, O_3, HNO_3, CH_4, N_2O, NO_2, CFC-11, $ClONO_2$, N_2O_5, CFC-12, COF_2, CCl_4, HCN, CFC-14, HCFC-22, HDO, C2H2, C2H6, CH3Cl, OCS, COCl2, as well as Temperature) and orbit two files are provided with a different level of detail:

- The *standard file* provides the information needed by most data users, namely geolocation information, information on the measurement mode, altitude, pressure, temperature, retrieved VMR profile and related Covariance Matrices (CM) and vertical Averaging Kernels Matrices (AKM), quality flags, profiles on an extended vertical grid. The standard file includes a single orbit and a single species.
- The *extended file* is mainly used for diagnostics and targeted at users who need complete information about the retrieval process. It includes the full state vector (retrieved profiles, atmospheric continuum and instrumental offset) with related CM and AK, and additional information about the retrieval. The full state vector is needed, e.g., when performing data fusion (Ceccherini et al., 2015). Due to the composition of the state vector, variables in the data file have different units. The extended file contains a single orbit and a single retrieval.

3.5 Product quality filtering

Profiles with post_quality_flag = 0 are considered of good quality. This flag is based on a number of quality indicators (see below) and provides an easy and robust way to remove unreliable data.

Furthermore, when treating data users have to take into account also the information of the 'useful vertical range', according to recommendation contained in Sect. 3.5.2.
The useful vertical ranges, intended as a limitation to the used retrieval range reported in the output files, is provided in the summary table of each species in Sect. 4.

3.5.1 Quality control indicators that define quality_flag and post_quality_flag

The quality indicators that determine the post-quality flag are listed in Table 3-4.

L2-algorithm		L2-V8-overview		Altitude		TEMP	H_2O	O_3	HNO_3	CH_4	N_2O	NO_2	CFC-11
$ClONO_2$	N_2O_5	CFC-12	COF_2	CCl_4	HCN	CFC-14	HCFC22	C_2H_2	C_2H_6	CH_3Cl	$COCl_2$	OCS	HDO

Table 3-4. Quality indicators

Field name	Description	Threshold
chi2	Final chi_square	chi2 smaller than chi2_Threshold
lambda_marq	Final Marquardt lambda	lambda Marquardt smaller than lambda_Threshold
Profile_error	Error of the retrieved profile	maximum error smaller than max_err_Threshold
conv_id	It provides information on convergence of the retrieval. Possible values: 0, convergence reached 1, maximum number of macro-iterations exceeded 2, maximum number of micro-iterations exceeded 3, maximum run-time exceeded 4, retrieval failed 5, convergence reached and final matrix singular 6, maximum number of macro-iterations exceeded and final matrix singular 7, maximum number of micro-iterations exceeded and final matrix was singular	0 or 5

The used thresholds for chi-square, Marquardt and maximum error are given as attributes of the variable "obs_mod_flag", that gives the information about the processed observation mode (see 'Input/Output Data Definition (IODD)' TN IFAC_GA_2018_1_FB, Sect. 7.1.2).

The field 'quality_flag', which is also contained in the standard output file, is 0 when all following conditions are satisfied

- chi2 < chi2_Threshold
- lambda_marq < lambda_Threshold
- maximum error < max_err_Threshold

The 'post_quality_flag' is set to 0 when 'quality_flag' is 0 and 'conv_id' is either 0 or 5.

3.5.2 Useful vertical range

Each retrieved profile is properly and fully characterised on the full retrieval range provided in the output files by the corresponding CM and AKM. Altitude regions of the retrieved profile with poor retrieval information (i.e. determined only by the a priori information) can be identified by low values of diagonal elements of the AKM and/or large values of diagonal elements of the CM.
Since the AKM and the CM are calculated considering the retrieval on the full vertical range, the use of only a part of the profile, with the association of sub-matrices of the provided AKM and CM, implies an approximation in the AKM and CM.
Therefore recommendation is to use the profile, with its CM and AKM, on the full range.
However, for each species an altitude range where the retrieval is 'useful' has been evaluated on the basis of considerations on the average Degrees of Freedom (DOF) distribution (Ceccherini et al., 2013) and other

considerations on the physical meaning of the measurements. The DOF per unity height is computed as the ratio between the diagonal element of the Averaging Kernel Matrix and the step in altitude ; it goes to zero at the altitudes where the information on the retrieved quantity contained in the observations goes to zero. As an example, the curve of the DOF distribution profile, as well as the curve of the vertical resolution profile, is reported in each plot containing the AK functions for representative scans and each species in Sect. 4.

For the species retrieved using the OE technique, the useful vertical range is identified as the range with DOF distribution larger than a threshold of 0.05 km^{-1}, which corresponds, in an ideal condition of the AK equal a triangle, to a vertical resolution of 20 km. This criterium is not sufficient to identify a useful range for retrievals performed using Levenberg-Marquardt technique, for which the profiles of some retrieved species, at either the high or low boundary of the retrieval range, may be characterised by very small values of the VMR and larger retrieval error in correspondence to DOF distribution values larger than the threshold. In some of these cases, also negative values in the average profiles are found, indicating the presence of a systematic error. The altitude ranges with negative averages are excluded from the useful range. Limitation to the useful range is reported in the summary table of each species in Sect. 4.
We stress that the information on the useful range must be used only if the AKM and CM are not taken into account for the characterization of the products. Comparison with independent measurements which use the AKMs should be performed on the full range, while the results of the comparison should be evaluated only in the useful range.

3.6 Handling of negative values

When the VMR is small and comparable to the retrieval error, negative retrieved VMRs can occur. While negative VMRs are not physical, these estimates make perfect sense from the statistical point of view given the non-zero uncertainty in the measurement and retrieval process. As a consequence, when considering a single profile, negative values have to be filtered out, but when computing averages as part of the scientific analysis it is important that negative values are not masked, in order not to introduce a positive bias in the averaged profile.

3.7 Averaging Kernel and covariance matrices

The elements of the AKM **A** are defined as the derivatives of the components of the retrieved profile $\hat{x}$ with respect to the components of the true profile x:

$$A_{ij} = \frac{\partial \hat{x}_i}{\partial x_j} .$$

The elements of the CM **S** are defined as the expectation value of the products of the components of the retrieval error **σ**:

$$S_{ij} = \left\langle \sigma_i \, \sigma_j \right\rangle$$

For the species retrieved using the Levenberg-Marquardt regularizing method the AKM and CM of the retrieved state vectors are calculated taking into account all the steps performed during the retrieval process as described in (Ceccherini and Ridolfi, 2010). When the a posteriori Tikhonov regularization is applied, the AKM and CM are updated in order to take into account the regularization.

For the species retrieved using the optimal estimation method the formulas of the AK and CM reported in (Rodgers, 2000) are used.
The usage of the AK and CM for performing validation activities is described in (Keppens et al., 2019)

The AK and CM are included in the output files as described in the 'Input/Output Data Definition (IODD)', TN IFAC_GA_2018_1_FB.

3.8 Precision and Accuracy of the retrieved profiles

The accuracy of the retrieved profiles is described in terms of the noise error and the forward model errors. The noise error is the mapping of the measurement noise in the retrieved profile and its covariance matrix S is computed as described in Sect. 3.7.

The forward model errors are given by the propagation in the retrieved profiles of the uncertainties present in the instrument and in the atmospheric model parameters, as well as of the approximations in the forward model itself (Dudhia et al., 2002).

Among the forward model errors, some are random, like the propagation of temperature and pressure noise errors on the VMR profiles (pT propagation error (Raspollini and Ridolfi, 2000)), and some are systematic, such as the spectroscopic errors. Others have a value and a variability that may depend on either the time or spatial scale of the profiles that are considered for the statistical analysis.

3.8.1 Random error component

The main contributions to the random error component are the noise error (provided in the output standard file in the field 'profile_error' together with the CM of the retrieved profiles 'covariance_matrix') and the pT propagation error in VMR retrievals, the latter being computed a posteriori and provided for each scan in the output standard files as CM in the field 'error_p_t_cm'. The single scan total random error for VMR retrievals has been estimated by summing quadratically the average single scan noise error and the average single scan error in VMR profiles due to the pT propagation error. In Sect. 4, the plots of the average single scan random error (both noise error and the combination of noise error and pT error) are reported for five reference atmospheres among the product specific information of each trace species for both FR and OR nominal modes.

3.8.2 Systematic error component

Full error analyses have been computed for five reference atmospheres and the main three MIPAS operating modes. Results and details of the calculations can be found on https://earth.esa.int/eogateway/instruments/mipas/cal-val which includes a list of errors considered and a Technical Note describing the method used.

It is emphasised that these analyses characterise the systematic error budget for a single profile and the web-page also contains some guidance on how these might be adapted for averaged products.

Please consider that for the noise error and the pT error propagation on VMR profiles (see Sect. 3.8.1), which are also provided at https://earth.esa.int/eogateway/instruments/mipas/cal-val, the dedicated profiles provided in the output files for each scan have to be used.

3.9 Critical issues

3.9.1 Issues in L1V8 data with impact on L2 data

After the L2 full mission reanalysis, a problem was found in the L1 V8 data, consisting in the fact that about 4% of the scans of MA, 4,7% of the scans in NLC e 1.4% of the scans in UA have one tangent altitude set to 0, generally the one with nominal tangent altitude equal to 85 km. The corresponding spectrum is also corrupted. From further investigations it was found that also other

measurement modes are affected, but for a smaller amount. It was verified that also V7 has this problem, but not always in the same scans as V8. On the contrary, V5 L1 files seem not affected by this problem.

Different causes have been identified in the different L1 products: the first one is the fact that the procedure in CFI* that performs the ray tracing for the determination of the tangent altitude is failing because there is a hard limit to the number of points to be considered along the Line of Sight, and this occurs both in V7, which uses CFC v5.8.1 and in V8, which uses CFC v.5.9. The problem is however more critical for V8, since a larger accuracy (obtained using the input parameter iray=10) is searched; V7 uses iray=30, which means smaller accuracy. V7 products have in addition the problem that in correspondence of the transmission error, all sweep information and spectra are set to 0. This check was removed in V8, since no major problems were found in spectra with transmission error.

A new version of CFI is now under test. Tests on a significant number of cases for the various affected measurement modes are needed. The consistency of the results of the new CFI version with respect to the old one for non critical orbits have also to be verified. The recommendation is to provide improved L1b products to the users based on the reprocessing of only the orbits with this problem and then perform the L2 analysis on these orbits.

Even if ORM V8 performs the analysis of the MA, NLC and UA modes only below 80 km, some products have been anyhow impacted by this problem. The cause has to be searched in the procedure used for the cloud filtering, which performs the checks on all tangent altitudes smaller than 40 Km, and hence also on the tangent altitude which has been set to zero. At 85 km this check may not provide realistic results, since the cloud detection method does not work properly above 40 km. With a tangent altitude equal to 0 at high altitudes the cloud filtering algorithm may wrongly flag as cloudy all the sweeps below it. For this reason, about half of the scans with a tangent altitude set to 0, even if outside the retrieval range, was not processed by ORM V8.

It has to be underlined that this problem in the L1b data reduces the number of the provided L2 products, but does not degrade the quality of the provided L2 data.

* The **Envisat CFI software** is a collection of multiplatform precompiled C libraries for timing, coordinate conversions, orbit propagation, satellite pointing calculations, and target visibility calculations, specifically parametrized and configured for the **Envisat satellite**.

3.9.2 New species

The comparison of the new V8 species (C_2H_2, C_2H_6, $COCl_2$, OCS, and CH_3Cl) in general exhibits somewhat larger deviations in the retrieved VMR of MIPAS and the validation instruments (compared to the other species). Some altitude regions of C_2H_2 and, to a lesser extent, C_2H_6 are characterized by negative MIPAS values (mainly in the Arctic winter). While VMR deviations for the gases $COCl_2$ and OCS stay (for the MIPAS-Balloon comparison) within about 20% in the upper troposphere and lower stratosphere (FR and OR phase), VMR differences for the molecule CH_3Cl exceed the 50% limit in this altitude region in the FR period. Hence, we state that MIPAS V8 data of the species C_2H_2, C_2H_6, and CH_3Cl (FR phase) should be used carefully in scientific studies.

4 PRODUCT-SPECIFIC INFORMATION

This section summarizes the main results of the verification and validation performed on the L2 products. Full details of the validation of MIPAS L2 V8.22 retrieved species are provided in the following validation reports ('Long-term validation of MIPAS ESA operational products using MIPAS-B measurements', 'Long-term validation of MIPAS ESA operational products using ACE v3/v4 measurements' (for ACE-FTS V4 data see Boone et al., 2020), 'Ground-based validation of MIPAS ESA operational products (ORM 8.22): T, altitude, O3, CH4, HNO3 and N2O', which can be downloaded here).

4.1 Altitude

Introduction

MIPAS measurements contain information on the pressures corresponding to the tangent altitudes of the scan. And indeed, for every measured scan, the pressure and temperature corresponding to each tangent altitude (estimated from pointing information of platform and instrument) are retrieved. Then, the altitude grid is rebuilt from the retrieved pressure and temperature profiles using the hydrostatic equilibrium equation and assuming the lowest altitude is known correctly. Any error in this anchor point will lead to an artificial shift of the entire altitude grid. For L2 data versions prior to V7 the error on the anchor point was considerable and it was therefore recommended to only use pressure as the vertical coordinate for retrieved profiles.

Since then, a large effort on the L1 processor led to more accurate engineering tangent altitudes, and the L2 processor now corrects the lowest engineering tangent altitude using information from co-located ECMWF z-p profiles, when available. This reduces the altitude registration of the anchor point considerably. In fact, the earlier recommendation is now obsolete and V8 profiles can be represented versus pressure or altitude without loss of data quality.

The altitude grid (variable 'height') reported in the L2 V8 data files is reconstructed as described above, but the anchor point can have two origins depending on the availability of ECMWF auxiliary files

- when ECMWF auxiliary files are available, the lowest altitude is computed from co-located ECMWF z-p profiles. The variable 'ECMWF_altitude_shift' gives the correction applied to the lowest engineering tangent altitude. These *ECMWF-corrected* altitude profiles are very accurate and constitute 97.9% of the measurements.
- when ECMWF auxiliary files are not available, the lowest altitude is estimated from pointing information of platform and instrument . In this case, the variable 'ECMWF_altitude_shift' is set to Fill value. These *MIPAS-corrected* altitude profiles are slightly less accurate and represent 2.1% of the measurements.

Validation

Reference instrument	Source	Coverage validation analysis		
		Time	Horizontal	Vertical
Radiosonde	NDACC, WOUDC, SHADOZ	2002-2012	86 sites, 82°N – 90°S	500-7 hPa

MIPAS profiles of altitude versus pressure were compared to coincident in-situ measurements by radiosondes. These reference data were collected across the globe during the entire mission.

The median bias between MIPAS and reference data is less than 20 m at the bottom of the profile and gradually increases away from the anchor point, to at most 100 m at 10 hPa. A similar vertical dependence is also noted in the spread of the comparisons, with values of 40-50 m at the anchor point, gradually increasing to 100-150 m at 10 hPa. The latitudinal dependence of these quality indicators is generally negligible (Figure 4-1).

There are no noticeable patterns in the comparison time series. The amplitude of the annual cycle is less than 50 m. Stability over the 2005-2012 period is better than 50-100 m/decade. No clear difference in data quality was found between the Full Resolution (FR, 2002-2004) and the Optimised Resolution (OR, 2005-2012) phase of the mission, except at mid latitudes.

It is important to realise that the excellent agreement MIPAS-radiosonde at the lowest profile level can be due to the fact that the ECMWF auxiliary data (used to anchor the MIPAS profile) include assimilated radiosonde measurements. The comparison is therefore not completely independent and any global shift of the MIPAS altitude profile should be evaluated using other, more independent means. Any patterns (vertical, latitudinal and temporal) in comparisons at other grid levels are a result of patterns in errors in the MIPAS pressure-temperature retrieval. These errors accumulate through the hydrostatic equation which leads to increased uncertainty away from the anchor point. Bias and spread at the top of the MIPAS altitude profile are larger than the 100 m quoted earlier.

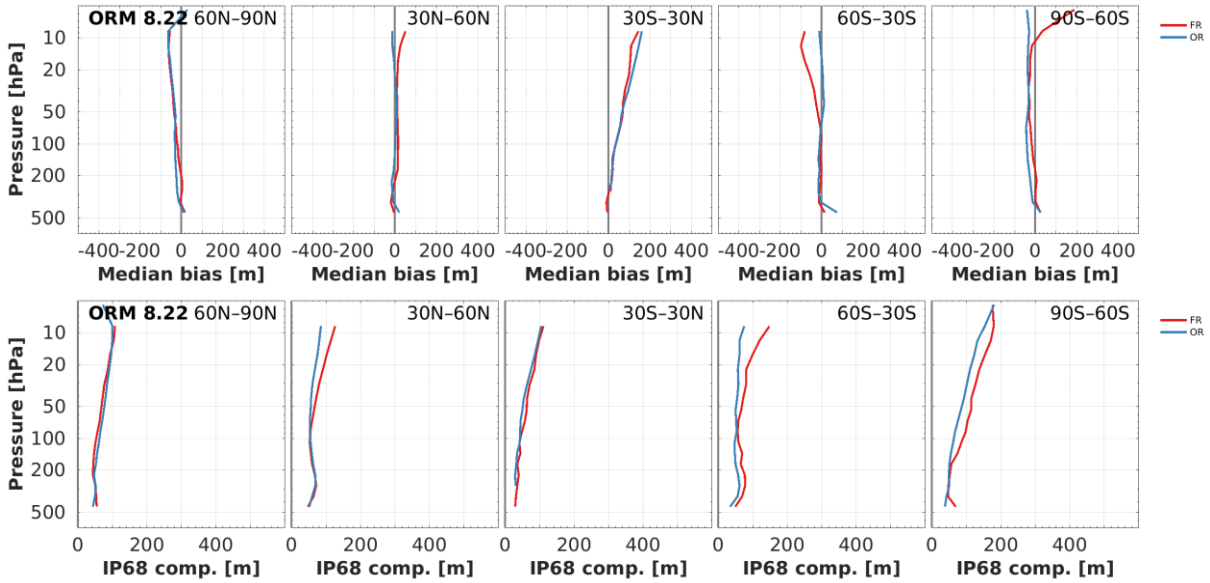

Figure 4-1. Median bias (top) and 68% interpercentile (bottom) of the absolute difference between co-located MIPAS V8.22 altitude and radiosonde profiles. Results are differentiated by latitude band and by mission phase. Positive bias values indicate that MIPAS data are larger than the reference.

4.2 Temperature (T)

LEVEL 2 V8 TEMPERATURE RETRIEVED PRODUCTS										
Operational modes:	FR	RR	OR							
	NOM		NOM	UTLS1	MA	UA	AE	NLC	UTLS2	UTLS1_o
Nominal Vertical range [Km]	*6-68*	*6-68*	*6-71*	*8.5-52*	*18-78*	*42-78*	*7-38*	*39-78*	*12-42*	*8.5-49*
Useful range	*Full range*									
Microwindows:	*Link for downloading*									
Systematic errors:	*Link for downloading* *Link errors*									

Introduction

Temperature profile is retrieved jointly with the pressure at the tangent altitudes of the scan.

As an example, Figure 4-2 reports the timeseries of weekly mean of Temperature on the full mission averaged on the latitude band 90S-60S. A strong seasonal variation in the time series is clearly visible, with the coldest temperatures in the troposphere in the polar winters.

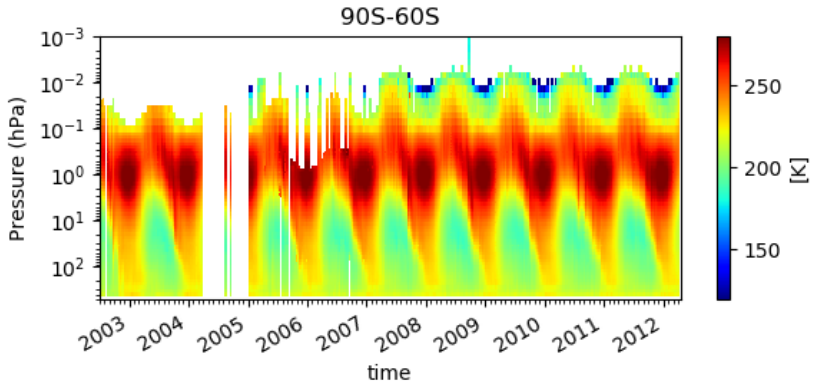

Figure 4-2 Timeseries of weekly mean of Temperature profiles on the full mission averaged on the latitude band 90S-60S

Verification and changes wrt V7 products

Handling horizontal inhomogeneities along the line of sight (as in V8) or not (as in V7) has a minor impact on individual retrieved temperature and pressure profiles. Differences with and without consideration of horizontal gradients are smaller than the retrieval error. Larger changes are expected where horizontal gradients are the largest, i.e. in the polar regions in wintertime and in the lower stratosphere. However, the impact of horizontal gradients is significant when the differences in temperature for the ascending and descending parts of the orbit are averaged over many scans. Figure 4-3 shows such ascending-descending differences for latitude band 60N-75N for various retrieval set-ups (horizontal gradient taken into account or not; two retrieval codes, namely ESA L2 processor (ORM) and KOPRAFIT retrieval algorithm,

developed at IMK-IAA (Stiller et al., 2002; Hoepfner et al., 2001)). A significant reduction in the ascending-descending difference is found when horizontal gradients of temperature are taken into account, while the contribution from the handling of horizontal gradients of the trace species is much smaller.

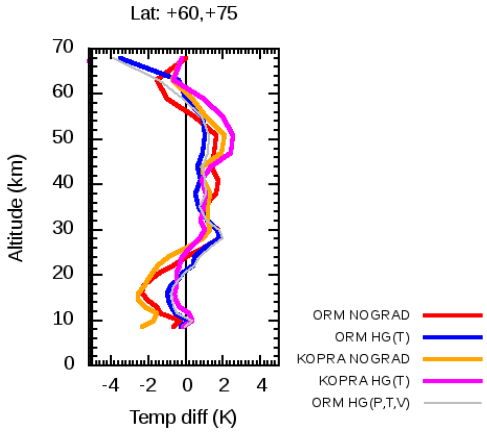

Figure 4-3 Ascending-descending 3-day average differences for temperature retrieved by MIPAS ORM V8 and KOPRAFIT. ORM V8 : without horizontal gradients (HGs) (red), with modelled temperature HGs (blue), and with modelled temperature, pressure and (H2O, O3) VMR HGs (grey). KOPRAFIT : without HGs (brown), and with temperature HGs (magenta).

Figure 4-4 reports the differences between V8 and V7 temperature profiles all over the mission. Among the changes implemented in the L1V8 and L2V8 processors and in the L2 auxiliary database, the one with the largest impact on V8 temperature profile comes from the use of the L1V8 products, which in particular take advantage of the new radiometric calibration: this indeed is responsible of an average increase in temperature of about +0.5 K all over the mission (see Figure 4-5), which leads to a reduction of the negative bias introduced in the V7 temperature profiles in the FR measurements (see README FILE V7). Other changes in the L2V8 products come from changes in the spectroscopic database, impacting mainly the high altitudes of OR measurements, and from changes in the handling of profiles below the lowest retrieved altitude causing lower temperatures at low altitudes for both FR and OR measurements.

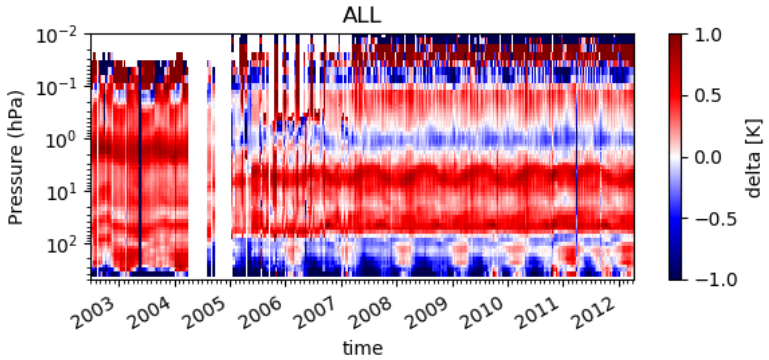

Figure 4-4 Timeseries of weekly mean differences between V8 and V7 Temperature profiles all over the mission. Positive values mean that V8 temperature is larger than V7.

The time-dependent radiometric calibration correction also has an impact on the stability of temperature along the mission: resulting differences between L2V8 and L2V7 temperature trends are mainly seen at

low altitudes in the tropical regions (see Figure 4-6).

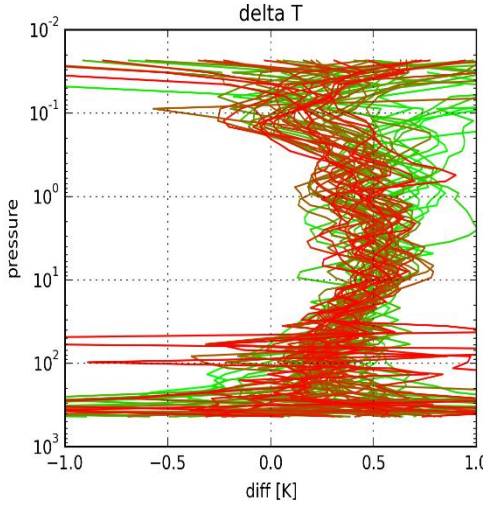

Figure 4-5 Change in retrieved temperature profiles due to the radiometric calibration implemented in L1V8 files (with respect to the one implemented in L1V7) for several orbits all over the mission (from the beginning of the mission (light green) to the end of the mission (brown).

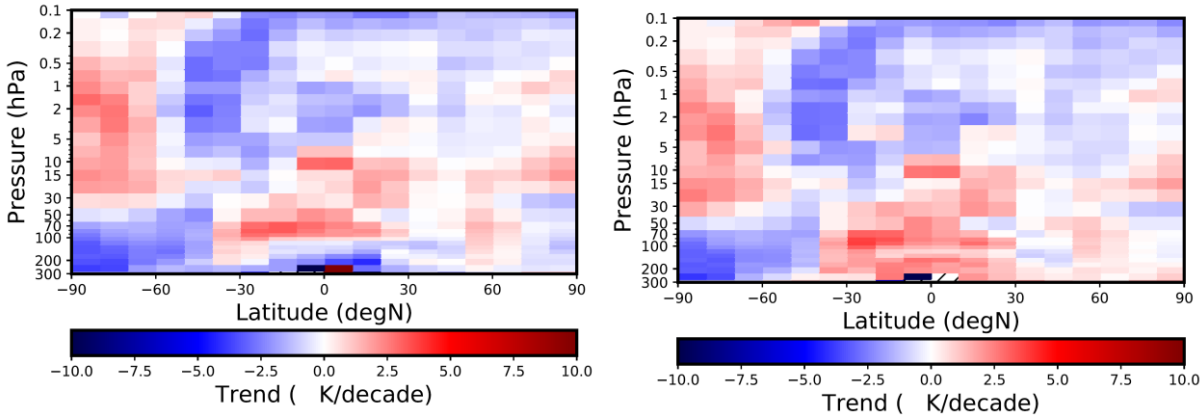

Figure 4-6. Temperature trend over the 2002-2012 period in L2V7 products (left) and in the L2V8 products (right). Trends were estimated using a regression model that also fits an offset between MIPAS temperature data for the 2002-2004 and 2005-2012 periods. This procedure avoids a bias in the trend due to a bias between the MIPAS mission phases (Figure 4-9).

Quality quantifiers (AK and retrieval errors)

The vertical averaging kernels of the temperature retrieval are shown in Figure 4-7 for two representative profiles in Full Resolution nominal mode (left panel) and Optimised Resolution nominal mode (right panel). The selected scans are not affected by clouds. Also the vertical resolution profile is reported in red and the DOF distribution profile in blue. The vertical resolution profile of the considered scan is also reported in red in the same plot and the DOF distribution profile (see Sect. 3.5.2) in blue. A mean vertical resolution profile has been also computed considering all scans in the nominal mode of 2003 (for FR plots) and 2010 (for OR plots). It is 2.5-3 km for FR measurements and 4 km for OR measurements between 6 and 40 km. Above 40 km the vertical resolution starts degrading in both cases as a consequence of the increased measurement step.

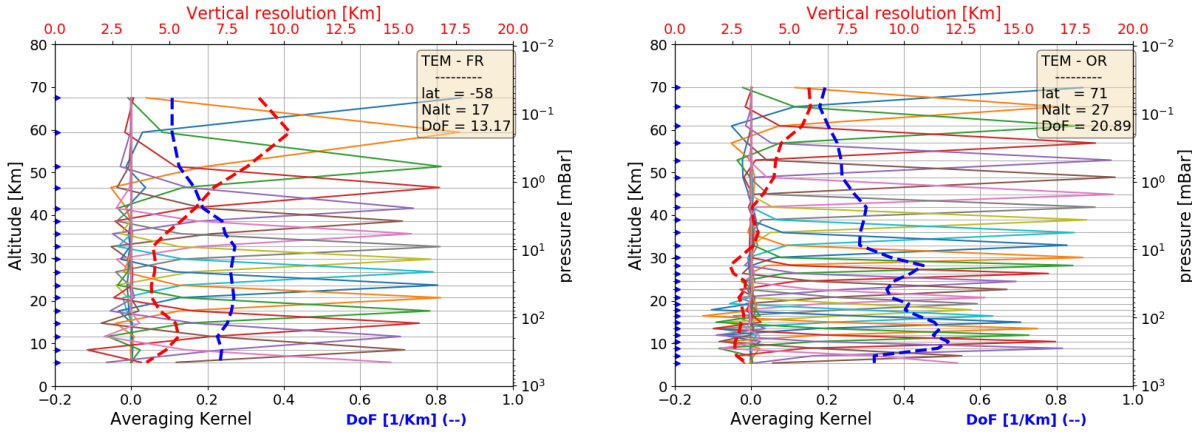

Figure 4-7 Example of Temperature vertical averaging kernel (AK) computed for a representative Full Resolution (left panel) and Optimised Resolution (right panel) scan. Together with the AKs, the plots show the vertical resolution (red dashed line) and the Degree of Freedom for unity height (blue dashed line). The yellow box on the top right of each panel contains the latitude of the observation, the number of the measurement sweeps and the total Degree of Freedom (DoF).

Figure 4-8 shows the average temperature values (left plots) and their associated average noise error, in absolute (middle plots) and relative (right plots) scale. The average quantities are representative of 5 reference atmospheres, namely polar summer daytime, polar winter nightime, mid-latitudes (both daytime and nightime) and equatorial daytime atmospheres. The averages have been computed using information on retrieved profiles and noise error which are contained in the output files for each scan. For mid latitude atmospheres all scans in the nominal mode of 2003 (for FR plots) and 2010 (for OR plots) in the latitude band 30-60 (both hemispheres) have been taken into account (considering either daytime or nightime scans), for equatorial atmosphere the scans in the latitude band 30S-30N, for polar winter nighttime atmosphere all nightime scans in the nominal mode of June-July-August of 2003 (for FR) and of 2005-2011 years (for OR) in the band 60S-90S, for polar summer daytime atmosphere all daytime scans in the nominal mode of December-January-February of 2003 (for FR) and 2005-2011 (for OR) in the latitude band 60S-90S. Solid lines of middle and right plots represent the noise error, given by the mapping of the measurement error on the retrieved profile. Very similar performances are obtained for FR and OR measurements. Random errors are between 0.3-0.5 K for pressures larger than 0.4 hPa (below 55 km). Only errors relative to the polar winter atmosphere are a bit larger for OR measurements.

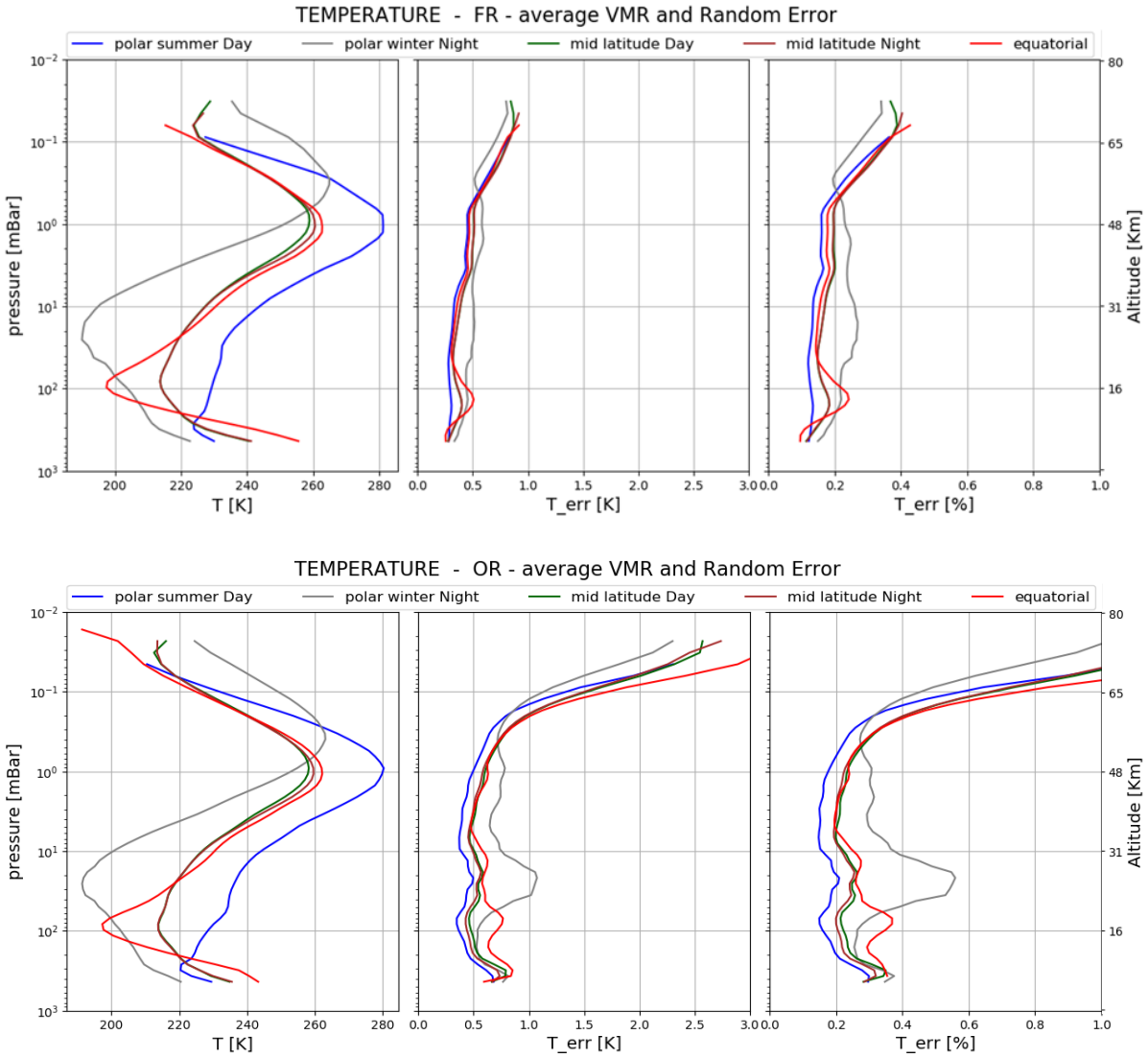

Figure 4-8 Average Temperature (left plots), absolute (mid plots) and relative (right plots) noise error for the 5 reference atmospheres described in the text. Top panel: Full Resolution nominal mode; bottom panel: Optimized Resolution nominal mode.

Validation

Reference instrument	Source	Coverage validation analysis		
		Time	Horizontal	Vertical
Radiosonde	NDACC, WOUDC, SHADOZ	2002-2012	86 sites, 82°N–90°S	500–7 hPa
Temperature lidar	NDACC	2002-2012	9 sites, 80°N–21°S	10–0.1 hPa
MIPAS-B	KIT-IMK	8 flights + 2-day trajectories	3 sites, 68°N–5°S	200–2 hPa

The validation analyses find that MIPAS L2V8 temperature data are of better quality than the L2V7 data release. When compared to the latter, the V8 temperature data

- *are 0.2-0.5 K warmer in the stratosphere and cooler in the UT/LS region,*
- *show a smaller spread in the comparisons,*
- *drift less over the OR period,*
- *have a clearly reduced seasonal pattern in the bias.*

More details are provided below.

MIPAS temperatures are systematically colder than radiosonde and lidar data. The cold bias remains less than ~1 K in the stratosphere but increases to 2 K in the lower mesosphere (Figure 4-9). The bias with respect to MIPAS-B has opposite sign and shows a peak in the tropical lowermost stratosphere (not shown) and tropopause region during the OR phase (Figure 4-10). Overall, the mean bias seen in MIPAS V8 comparisons exhibits some vertical structure but is mostly independent of latitude. Biases remain less than ±2 K over the entire profile, which is within the combined systematic error of the compared data records. However, the combined precision is too small to explain the 1-4 K standard deviation in the comparisons (Figure 4-10). An underestimation of the precision reported in the MIPAS products is just one of several possible factors to this discrepancy. Surely, at least part of this underestimation can be explained by the not perfect coincidence of the measurements and hence by the atmospheric variability (Sheese et al., 2020).

Comparison time series show evidence of a positive drift of MIPAS L2V8 with respect to radiosonde and lidar data, between 0.2-0.5 K per decade over the 2005-2012 time period over most of the stratosphere (Figure 4-11). Around the stratopause, the drift changes sign and reaches its peak value of -1.2 K per decade at 0.5 hPa. Highest confidence in the detection of drift lies in the middle stratosphere. In any case, users who analyse the complete MIPAS time series for temperature trends should be aware of a bias between the FR and OR periods of the MIPAS mission. They should anticipate a step change of at most 1 K around the stratopause and less than about 0.5 K elsewhere.

Ground-based comparisons also reveal signs of a seasonal pattern in MIPAS bias. Phase and amplitude depend on latitude and pressure, but peak-to-peak values are usually less than 0.5-1 K and never exceed 1.5 K.

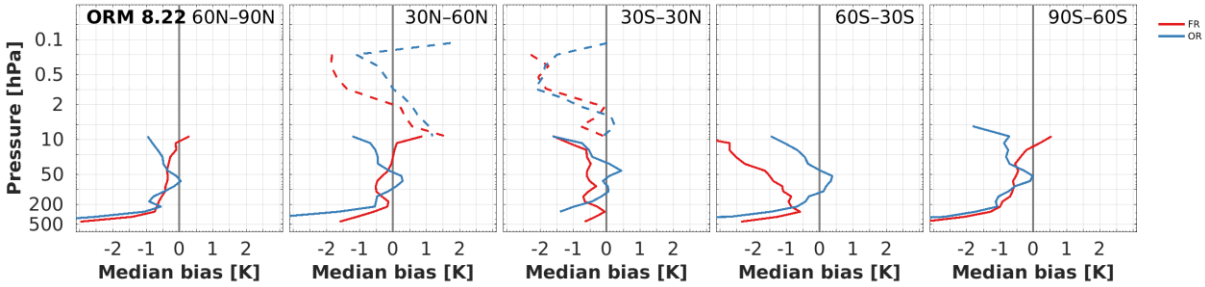

Figure 4-9. Median bias of the absolute difference between co-located MIPAS V8.22 temperature and reference profiles by radiosonde (solid) and lidar (dashed). Results are differentiated by latitude band and by mission phase (FR: 2002-2004; OR: 2005-2012). Positive values indicate that MIPAS data are warmer than the reference.

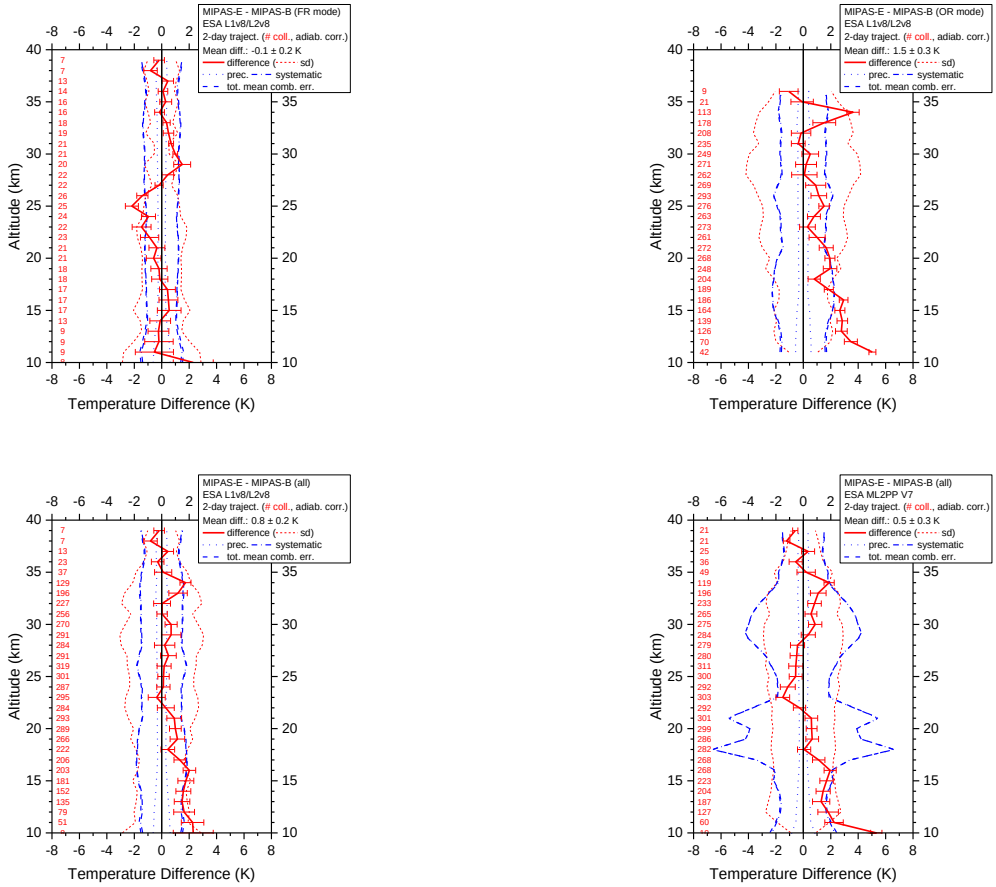

Figure 4-10. Mean temperature difference (red solid line) of all trajectory match collocations (red numbers) between MIPAS-Envisat and MIPAS-Balloon including standard deviation (red dotted lines) and standard error of the mean (plotted as error bars). Precision (blue dotted lines), systematic (blue dash-dotted lines), and total (blue dashed lines) mean combined errors are shown, too. Top: v8 FR mode (left) and v8 OR mode (right) collocations; bottom: all FR plus OR v8 (left) and all FR plus OR v7 (right) collocations.

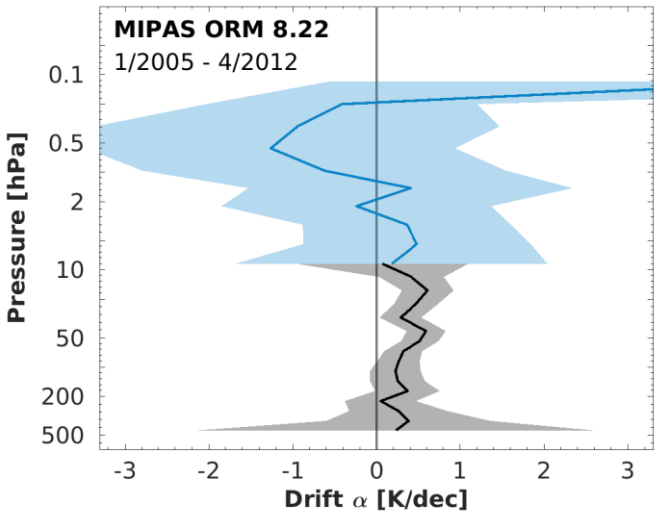

Figure 4-11. Drift of MIPAS V8.22 temperature versus sonde (black) and lidar (blue) networks over the OR phase of the mission (2005-2012). The shaded area represents the estimated 95% confidence interval. Positive drift values indicate that MIPAS temperature biases become progressively more positive over time wrt reference.

4.3 Water Vapor (H2O)

LEVEL 2 V8 WATER VAPOUR PRODUCTS										
Operational modes:	FR	RR	OR							
	NOM		NOM	UTLS1	MA	UA	AE	NLC	UTLS2	UTLS1_o
Nominal Vertical range [Km]	*6-68*	*6-68*	*6-71*	*6-49*	*18-72*	*42-72*	*7-38*	*39-72*	*12-16*	*8.5-16*
Useful range	*Full range*									
Microwindows:	*Link for downloading*									
Systematic errors:	*Link for downloading* *Link errors*									

Introduction

Time series of V8 H_2O profiles are reported in Figure 4-12 for the latitude band 0-30N. The tape recorder effect is clearly visible in the time series.

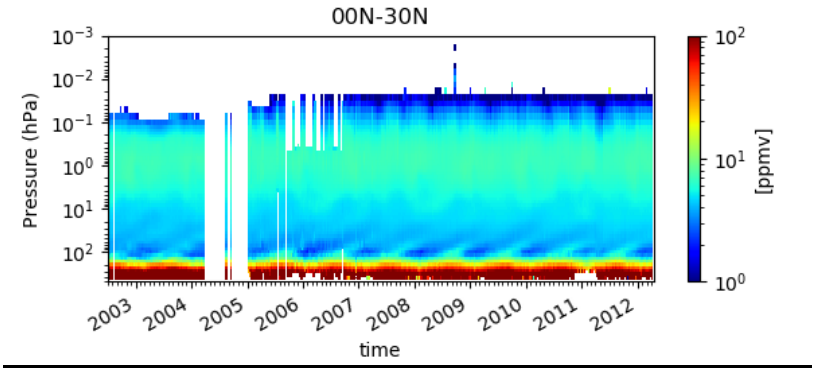

Figure 4-12 Timeseries of weekly mean of H_2O on the full mission averaged on the latitude band 0-30N

For the analysis of H_2O V8 OR products, a completely new selection of microwindows was performed. This was needed because a 5% positive bias was observed when using the old MWs (in particular MW H2O_0332) with the new spectroscopic database. Since the systematic difference increased the discrepancy between MIPAS and correlative measurements, and since the new (v4.45) spectroscopic data are more accurate than the old ones, the reason of this bias has to be searched in a under-compensation of other systematic error components (e.g. continuum).

Verification and changes wrt V7 products

With the new MW selection, very similar results are obtained with the old and the new spectroscopic database in the stratosphere. Some differences are found below the tropopause (see Figure 4-13).

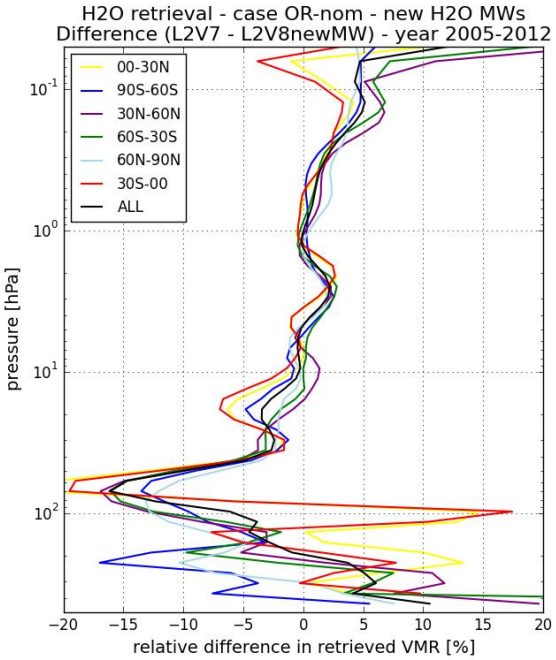

Figure 4-13 Relative difference in the retrieved H2O profiles when either the old MWs and the old spectroscopic database (v3.2) or the new MWs and the new spectroscopic database (v4.45) are used. Different colours refer to different latitude bands as described in the legend.

Main modifications in H_2O V8 profiles come from the modification in the radiometric calibration in L1b V8 files that is responsible of a 3-4% smaller H_2O wrt V7 data in the range 0.5-40 hPa all over the mission (see Figure 4-14). We have also to mention that with the new cloud filtering approach we have a smaller number of outliers in H_2O profiles in the polar winter.

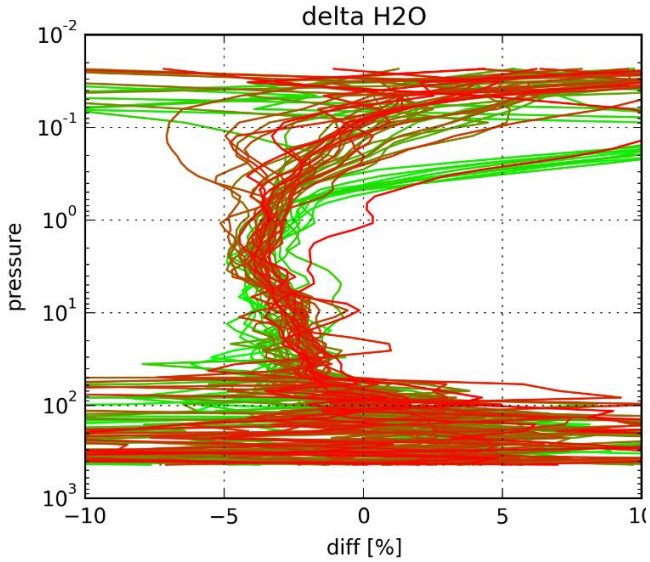

Figure 4-14 Change in retrieved water vapour profiles due to the radiometric calibration implemented in L1V8 files (with respect to the one implemented in L1V7) for several orbits all over the mission (from the beginning of the mission (light green) to the end of the mission (brown)).

As a result of all the implemented modifications in the L1 products and in the auxiliary data V8 water vapour profiles are about 5% smaller than V7 products at all altitudes and both phases of the mission, with the exception of the low border of the retrieval range, where V8 water vapour values are significantly larger (see Figure 4-15).

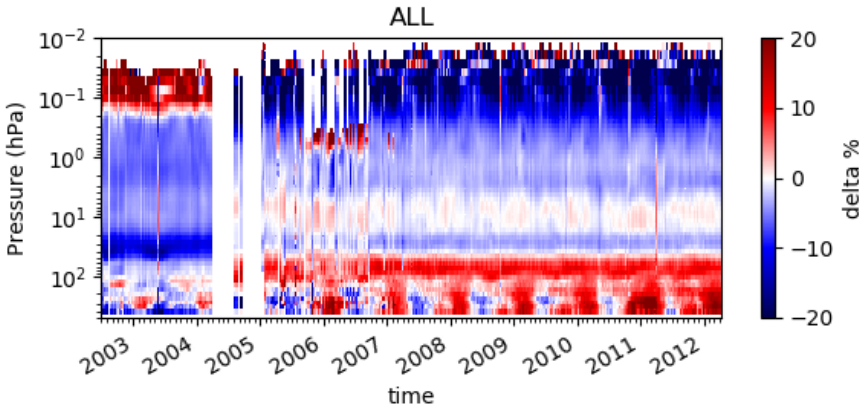

Figure 4-15 Timeseries of weekly mean differences between V8 and V7 H2O profiles all over the mission. Positive values indicate that V8 is larger than V7.

Quality quantifiers (AK and errors)

The vertical averaging kernels of the water vapour retrieval are shown in Figure 4-16 for two representative profiles in Full Resolution nominal mode (left panel) and Optimised Resolution nominal mode (right panel). The selected scans are not affected by clouds. The vertical resolution profile of the considered scan is also reported in red in the same plot and the DOF distribution profile (see Sect. 3.5.2) in blue. A mean vertical resolution profile has been also computed considering all scans in the nominal mode of 2003 (for FR plots) and 2010 (for OR plots). Similar performances are obtained for FR and OR measurements, vertical resolution is about 3 at 10 km, then it slowly degrades, 5-6 km at 20 km, 7.5 at 30-40 km, 10 at 50 km, 12.5-15 at 60 km.

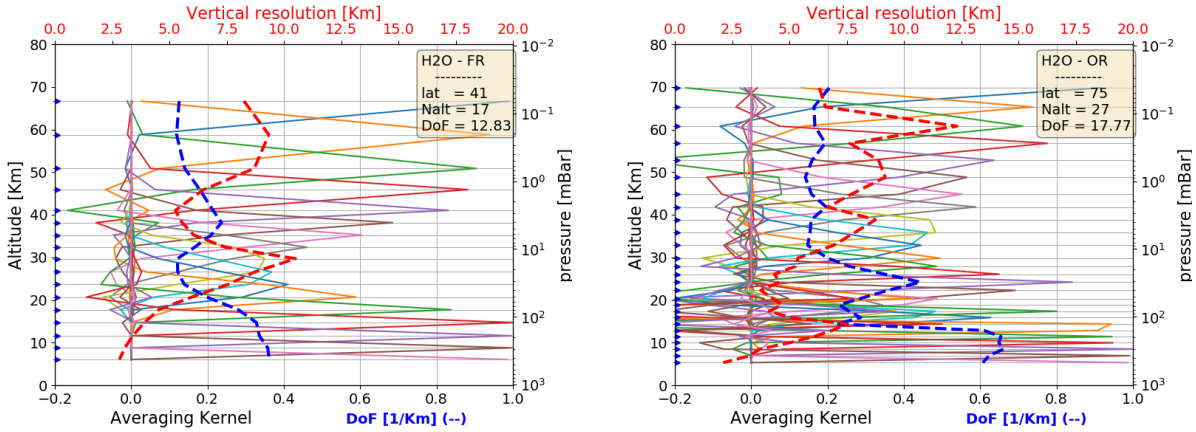

Figure 4-16 Example of water vapour vertical averaging kernel (AK) computed for two representative Full Resolution (left panel) and Optimized Resolution (right panel) scans. Together with the AKs, the plots show the vertical resolution (red dashed line) and the Degree of Freedom for unity height (blue dashed line). The yellow box on the top right of each panel contains the latitude of the observation, the number of the measurement sweeps and the total Degree of Freedom (DoF).

Figure 4-17 shows the average water vapour VMR values (left plots) and its associated average random error, in absolute (middle plots) and relative (right plots) scale. The average quantities are representative of 5 reference atmospheres, namely polar summer daytime, polar winter nightime, mid-latitudes (both daytime and nightime) and equatorial daytime atmospheres. The averages have been computed using information on retrieved profiles, noise error and pT error which are contained in the output files for each scan. For mid latitude atmospheres all scans in the nominal mode of 2003 (for FR plots) and 2010 (for OR plots) in the latitude band 30-60 (both hemispheres) have been taken into account (considering either daytime or nightime scans), for equatorial atmosphere the scans in the latitude band 30S-30N, for polar winter nighttime atmosphere all nightime scans in the nominal mode of June-July-August of 2003 (for FR) and of 2005-2011 years (for OR) in the band 60S-90S, for polar summer daytime atmosphere all daytime scans in the nominal mode of December-January-February of 2003 (for FR) and 2005-2011 (for OR) in the latitude band 60S-90S. Solid lines of middle and right plots represent the total random error, coming from the quadratic summation of the noise error (dotted curves, given by the mapping of the measurement error on the retrieved profile) and the pT error (given by the propagation of the random error of retrieved pressure and temperature profiles on VMR profile). The contribution coming from the pT error propagation is generally smaller than the noise contribution. The total random error is about 1-2% in the range 50 hPa-1 hPa for all atmospheres except polar winter, where it may reach values even larger than 5%. The tropopause is characterized by large percent random noise (also due to the minimum of the VMR), in the mesosphere random error rapidly increases with the altitude. In general larger values are found for the OR measurements.

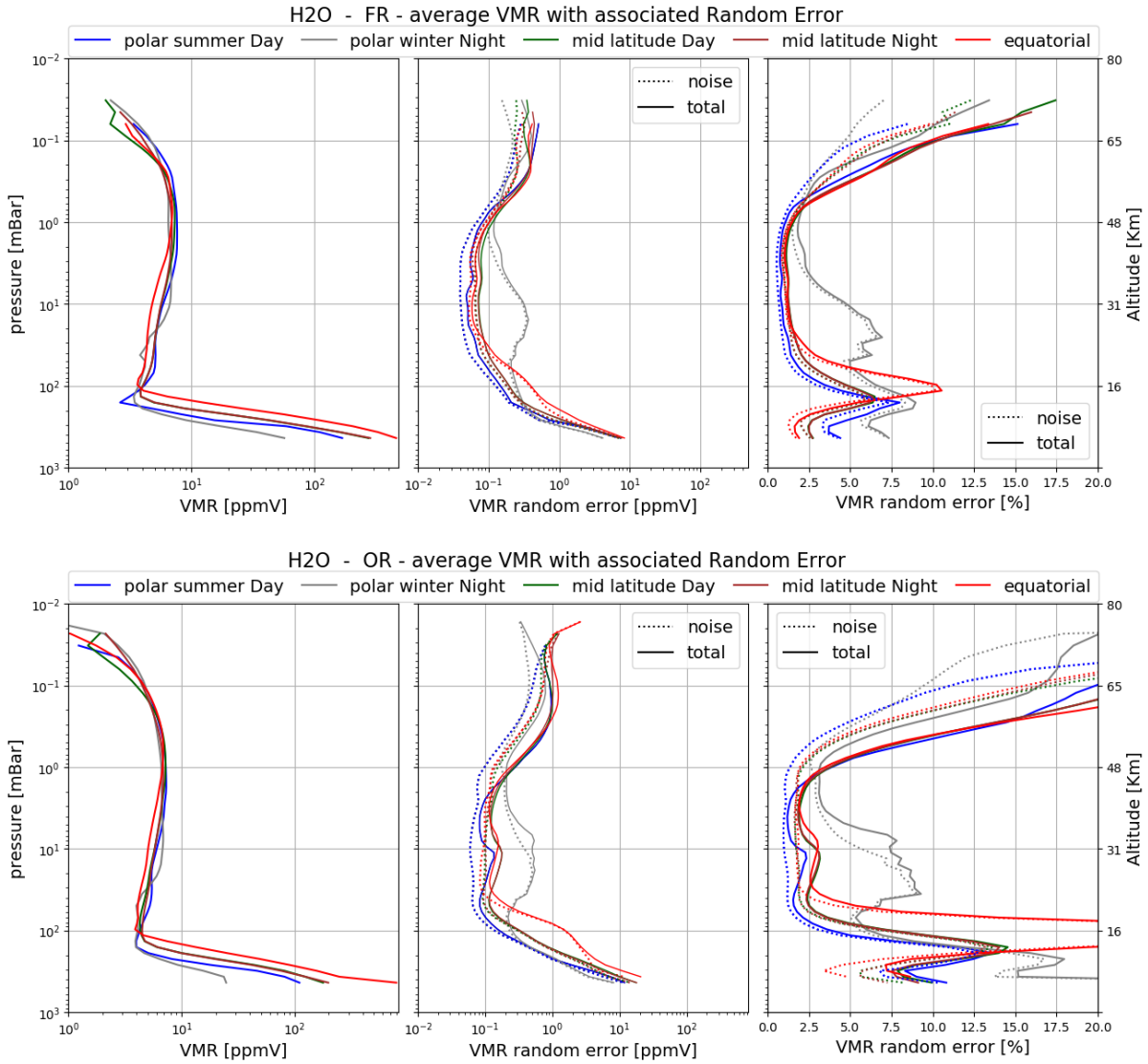

Figure 4-17 Average H_2O VMR (left plots), absolute (mid plots) and relative (right plots) H2O random error for the 5 reference atmospheres described in the text. The noise error (dotted curves) is calculated by the retrieval; the total random error (solid curves) includes the contribution to the random error coming from propagation of the pT random error on VMR profiles. Top panel: Full Resolution nominal mode; bottom panel: Optimized Resolution nominal mode.

Validation

Reference instrument	Source	Coverage validation analysis		
		Time	Horizontal	Vertical
MIPAS-B	KIT-IMK	8 flights + 2-day trajectories	3 sites, 68°N–5°S	200–2 hPa

FR and OR mode comparisons show different vertical shapes of the differences between MIPAS-E and MIPAS-B (see Figure 4-18). In the lowermost stratosphere and upper troposphere MIPAS-E significantly overestimates H_2O and exceeds the combined systematic error bars around 15 km in the OR mode. This general behaviour remains also in the statistical analysis of all collocations. In the middle and upper stratosphere, a positive bias of MIPAS-E vs. MIPAS-B (increasing with altitude in the FR period) of 5-20% is visible although the errors stay (except at 37 km) within the predicted error budget. The growing bias towards higher altitudes in the FR period was already recognized in a comprehensive validation study comparing v4.61 MIPAS data with observations of different instruments (Wetzel et al., 2013a). This bias is slightly reduced compared to v7 data due to somewhat (~0.1 ppmv) lower H_2O values in the MIPAS-E retrievals.

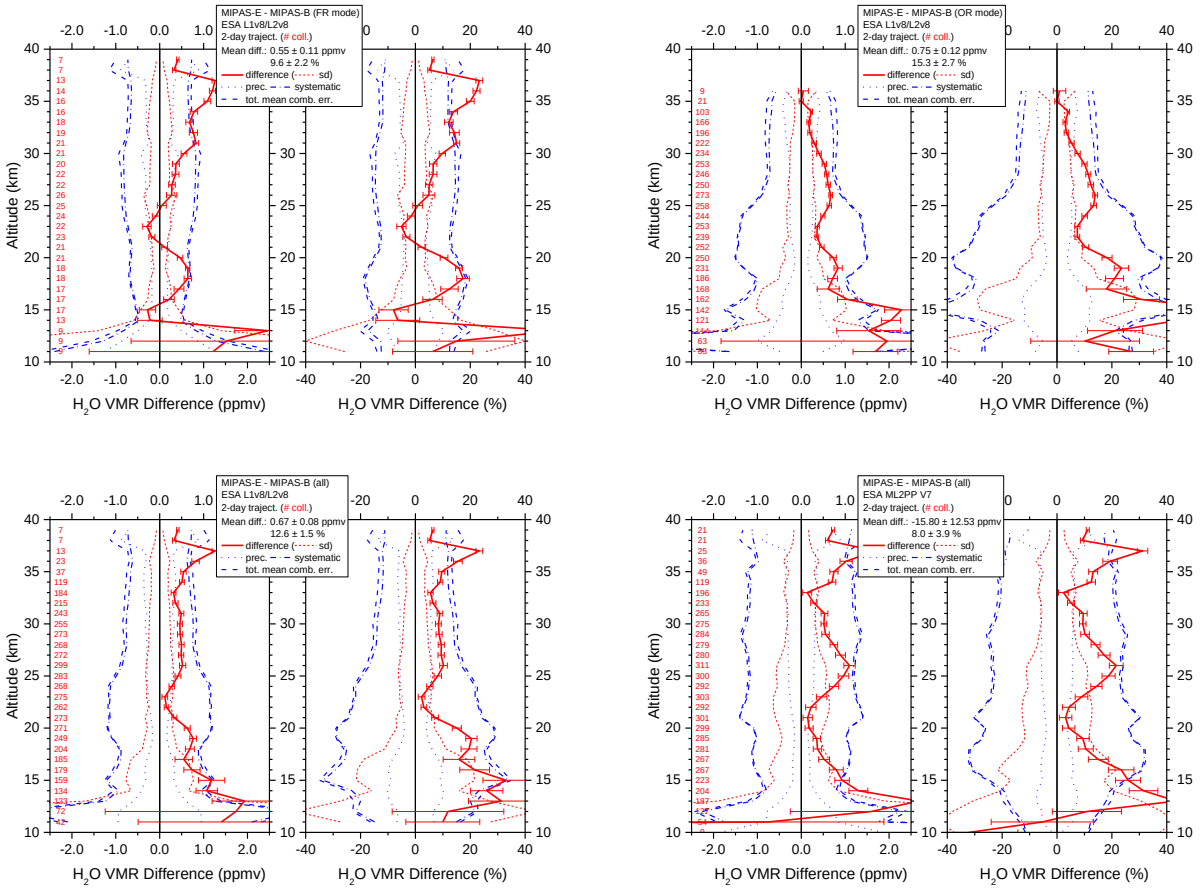

Figure 4-18 Mean absolute and relative H_2O VMR difference of all trajectory match collocations (red numbers) between MIPAS-E and MIPAS-B (red solid line) including standard deviation (red dotted lines) and standard error of the mean (plotted as error bars). Precision (blue dotted lines), systematic (blue dash-dotted lines), and total (blue dashed lines) mean combined errors are shown, too. Top: v8 FR mode (left) and v8 OR mode (right) collocations; bottom: all FR plus OR v8 (left) and all FR plus OR v7 (right) collocations.

4.4 Ozone (O3)

LEVEL 2 V8 OZONE PRODUCTS										
Operational modes:	FR	RR	OR							
	NOM		NOM	UTLS1	MA	UA	AE	NLC	UTLS2	UTLS1_o
Nominal Vertical range [Km]	*6-68*	*6-68*	*6-71*	*6-49*	*18-78*	*42-78*	*7-38*	*39-78*	*12-42*	*8.5-49*
Useful range	*Full range*									
Microwindows:	*Link for downloading*									
Systematic errors:	*Link for downloading* *Link errors*									

Introduction

Figure 4-19 illustrates, as an example, time series of MIPAS V8.22 ozone in the latitude band 90S-60S. It is clearly visible the seasonal dependence of the Ozone profile in the stratosphere, with maximum ozone values in the summer and the ozone hole in the spring.

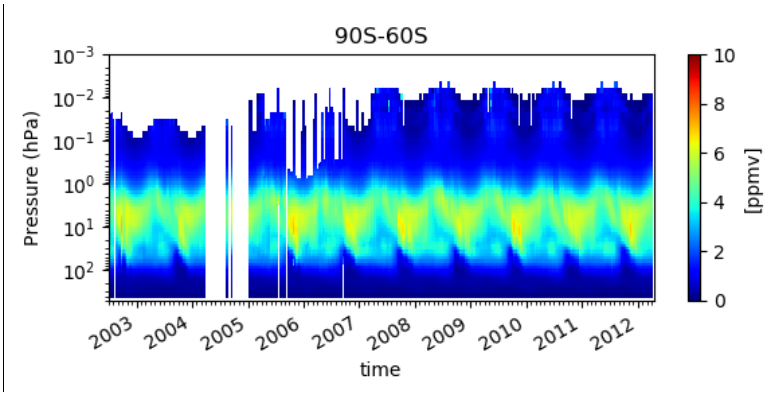

Figure 4-19 Time series of weekly mean of MIPAS V8.22 ozone for the full mission averaged over 90S-60S.

Verification and changes wrt V7 products

The changes implemented in both L1V8 and L2V8 processors, as well as in the auxiliary data, have a very small impact on the O_3 retrieval, as visible in Figure 4-20, where the time series of the relative difference between V8 and V7, averaged over all latitudes, are reported. Differences are well below 2% in the whole retrieval range, except at very high altitudes for MA, UA, and NLC modes, for which different microwindows are used for the retrieval by V8 processor, and at the lowest border of the retrieval, where differences may be due to changes in the handling of the profile below the lowest retrieved altitude.

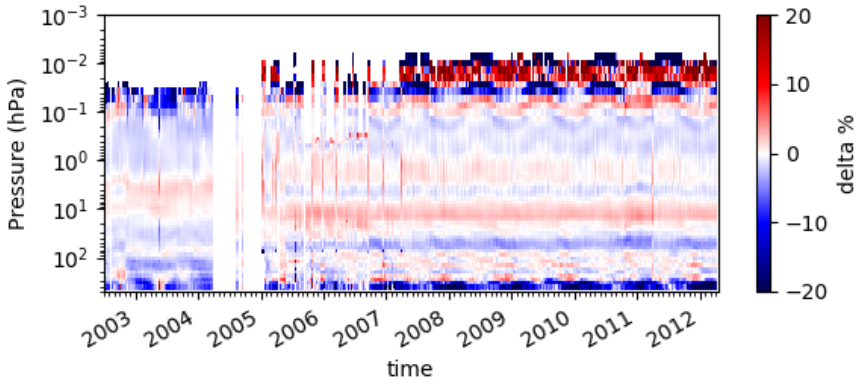

Figure 4-20 Time series of global, weekly mean relative difference of V8-V7 ozone over the entire mission. Blue values indicate that V8 O3 is smaller than V7 O3

Quality quantifiers (AK and errors)

The vertical averaging kernels of the ozone retrieval are shown in Figure 4-21 for two representative profiles in Full Resolution nominal mode (left panel) and Optimised Resolution nominal mode (right panel). The selected scans are not affected by clouds. The vertical resolution profile of the considered scan is also reported in red in the same plot and the DOF distribution profile (see Sect. 3.5.2) in blue. A mean vertical resolution profile has been also computed considering all scans in the nominal mode of 2003 (for FR plots) and 2010 (for OR plots). Below 40 km it is around 3 km in FR measurements and around 2 km in the OR measurements due to the finer vertical sampling of the OR measurements.

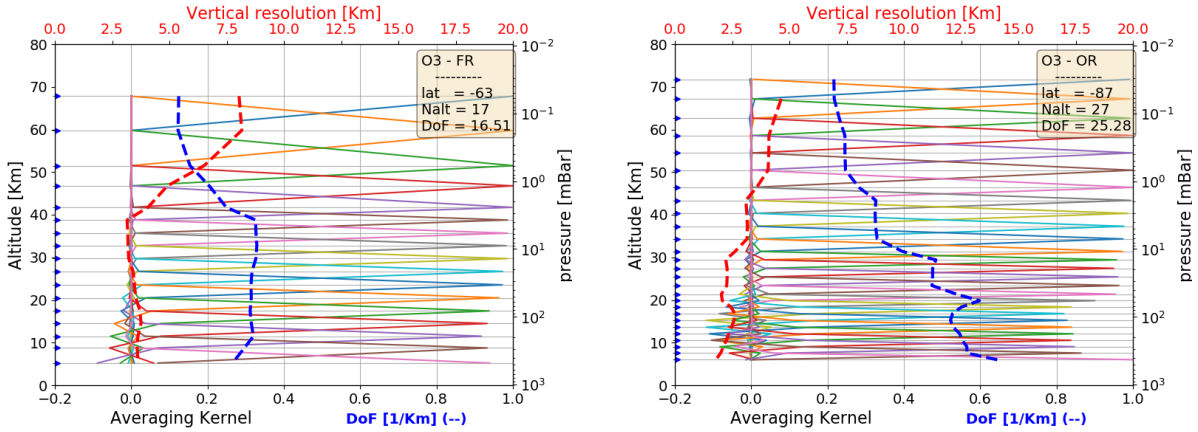

Figure 4-21 Example of ozone vertical averaging kernel (AK) computed for a representative Full Resolution (left panel) and Optimized Resolution (right panel) scan. Together with the AKs, the plots show the vertical resolution (red dashed line, red scale at the top) and the Degree of Freedom for unity height (blue dashed line). The yellow box on the top right of each panel contains the latitude of the observation, the number of the measurement sweeps and the total number of Degrees of Freedom (DoF).

Figure 4-22 shows the average ozone VMR values (left plots) and its associated average random error, in absolute (middle plots) and relative (right plots) scale. The average quantities are representative of 5 reference atmospheres, namely polar summer daytime, polar winter nightime, mid-latitudes (both daytime and nightime) and equatorial daytime atmospheres. The averages have been computed using information on retrieved profiles, noise error and pT error which are contained in the output files for each scan. For mid latitude atmospheres all scans in the nominal mode of 2003 (for FR plots) and 2010 (for OR plots) in the

latitude band 30-60 (both hemispheres) have been taken into account (considering either daytime or nightime scans), for equatorial atmosphere the scans in the latitude band 30S-30N, for polar winter nighttime atmosphere all nightime scans in the nominal mode of June-July-August of 2003 (for FR) and of 2005-2011 years (for OR) in the band 60S-90S, for polar summer daytime atmosphere all daytime scans in the nominal mode of December-January-February of 2003 (for FR) and 2005-2011 (for OR) in the latitude band 60S-90S. Solid lines of middle and right plots represent the total random error, coming from the quadratic summation of the noise error (dotted curves, given by the mapping of the measurement error on the retrieved profile) and the pT error (given by the propagation of the random error of retrieved pressure and temperature profiles on VMR profile). The contribution coming from the pT error propagation is generally smaller than the noise contribution, but it is not negligible. The total random error varies between 3 and 5% in the stratosphere, with the largest values in the polar winter; above and below the stratosphere the errors rapidly increases, also due to the much lower VMR. In general larger values are found for the OR measurements.

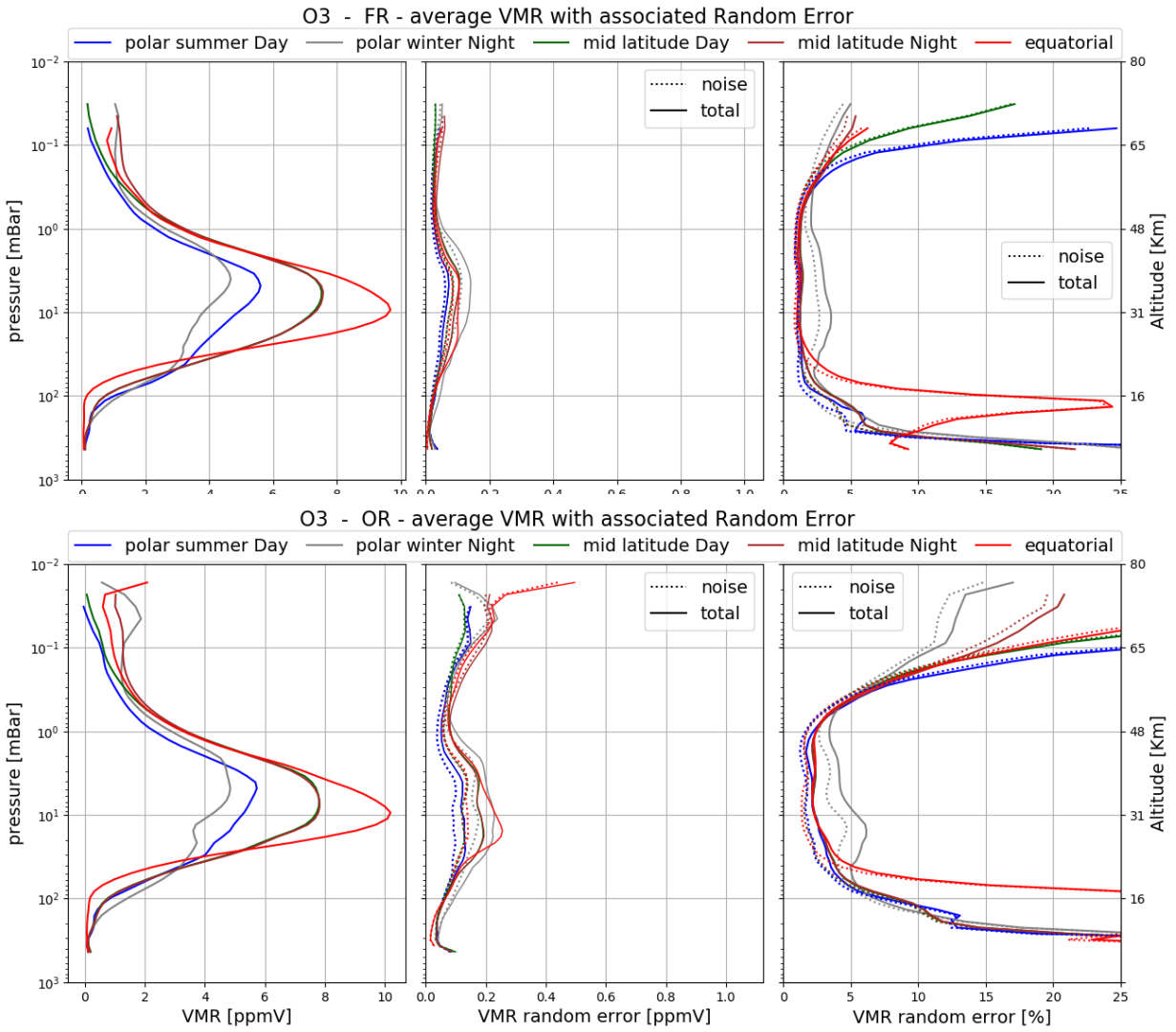

Figure 4-22 Average ozone VMR (left plots), absolute (mid plots) and relative (right plots) ozone random error for the 5 reference atmospheres described in the text. The noise error (dotted curves) is calculated by the retrieval; the total random error (solid curves) includes the contribution to the random error coming from propagation of the pT random error on VMR profiles. Top panel: Full Resolution nominal mode; bottom panel: Optimized Resolution nominal mode.

Validation

Reference instrument	Source	Coverage validation analysis		
		Time	Horizontal	Vertical
Ozonesonde	NDACC, WOUDC, SHADOZ	2002-2012	86 sites, 82°N–90°S	500–7 hPa
Ozone lidar	NDACC	2002-2012	12 sites, 80°N–21°S	100–1 hPa
Ozone MWR	NDACC	2002-2012	4 sites, 47°N–45°S	10–0.04 hPa
MIPAS-B	KIT-IMK	8 flights + 2-day trajectories	3 sites, 68°N–5°S	200–2 hPa
ACE-FTS v4	U Waterloo	2005-2012	global	500-0.04 hPa

The validation analyses find that MIPAS L2V8 ozone data are of similar quality than the L2V7 data release. On average, V7 and V8 ozone VMR values differ less than ±2%. Long-term stability, seasonal structure and the overall spread in the comparisons are similar. More details are reported below.

MIPAS ozone VMR profiles in the stratosphere are systematically higher than all co-located data records, in both FR and OR phases of the mission. Between 100 hPa/15 km and the stratopause the positive MIPAS bias is 5-10% and mostly less than 5% w.r.t. MIPAS-B and ACE-FTS (Figure 4-23, Figure 4-24 and Figure 4-25) respectively. At the lower end of the profile, systematic disagreement increases to 20-30% or (much) higher, in part due to the (much) lower VMRs. The bias changes sign around the stratopause. Mesospheric MIPAS ozone underestimates microwave radiometer and ACE-FTS data by up to 20%. Overall, the observed mean differences to MIPAS-B and ACE-FTS remain within the combined systematic errors. The spread in the comparisons amounts to 5-10% in the stratosphere and grows in the UTLS and mesosphere. The combined random error of the data records under comparison explains most of the differences in the stratosphere, but that is not the case at the profile ends. In order to conclude that MIPAS random errors are underestimated the missing terms in the error budget (such as sampling and/or smoothing mismatch) should be quantified as well.

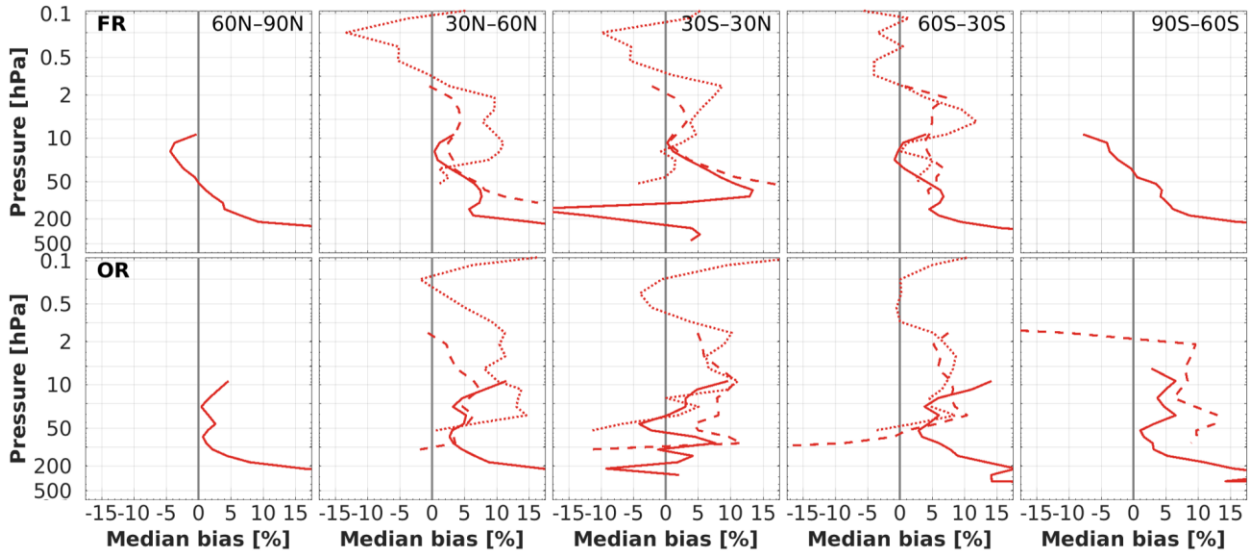

Figure 4-23. Median bias of the relative difference between co-located MIPAS V8.22 ozone and reference profiles by ozonesonde (solid), lidar (dashed) and microwave radiometer (dotted). Results are differentiated by latitude band and by mission phase (FR: 2002-2004; OR: 2005-2012). Positive values indicate that MIPAS O3 VMRs are larger than the reference.

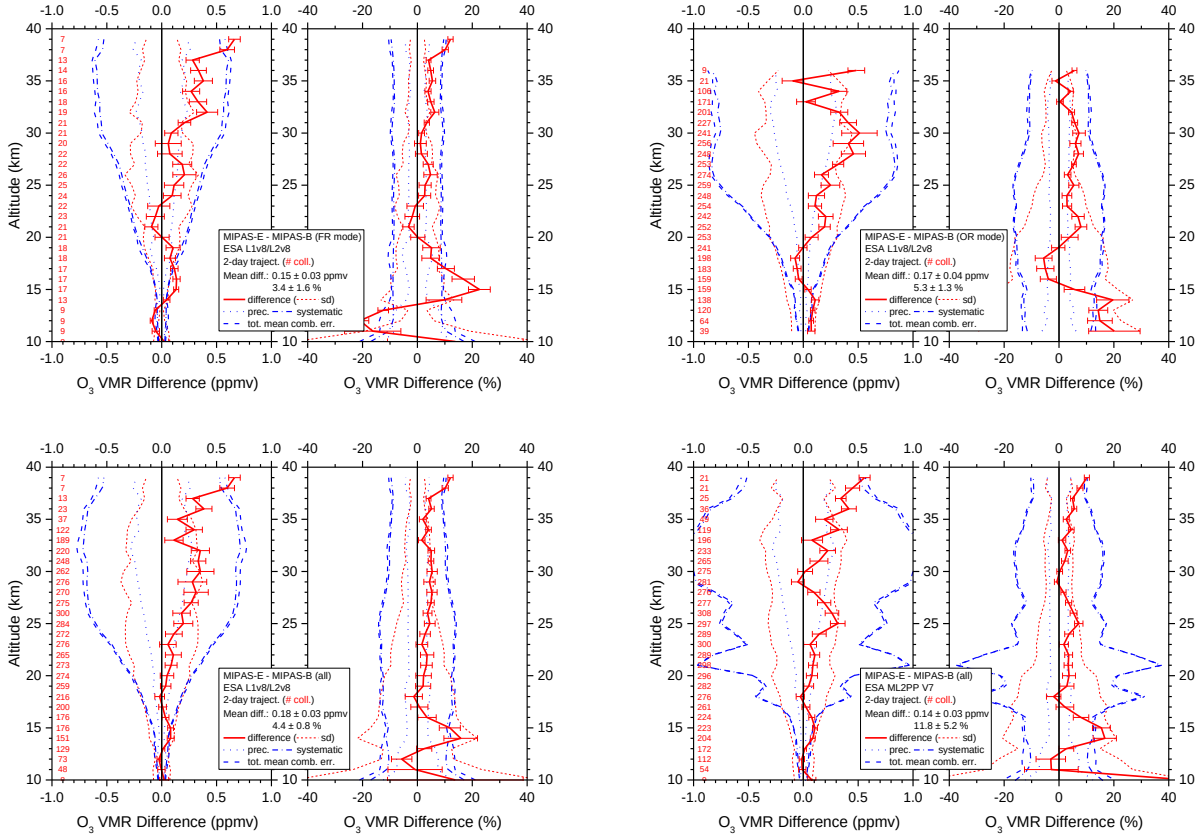

Figure 4-24. Mean absolute and relative O3 VMR difference of all trajectory match collocations (red numbers) between MIPAS-E and MIPAS-B (red solid line) including standard deviation (red dotted lines) and standard error of the mean (plotted as error bars). Precision (blue dotted lines), systematic (blue dash-dotted lines), and total (blue dashed lines) mean combined errors are shown, too. Top: v8 FR mode (left) and v8 OR mode (right) collocations; bottom: all FR plus OR v8 (left) and all FR plus OR v7 (right) collocations.

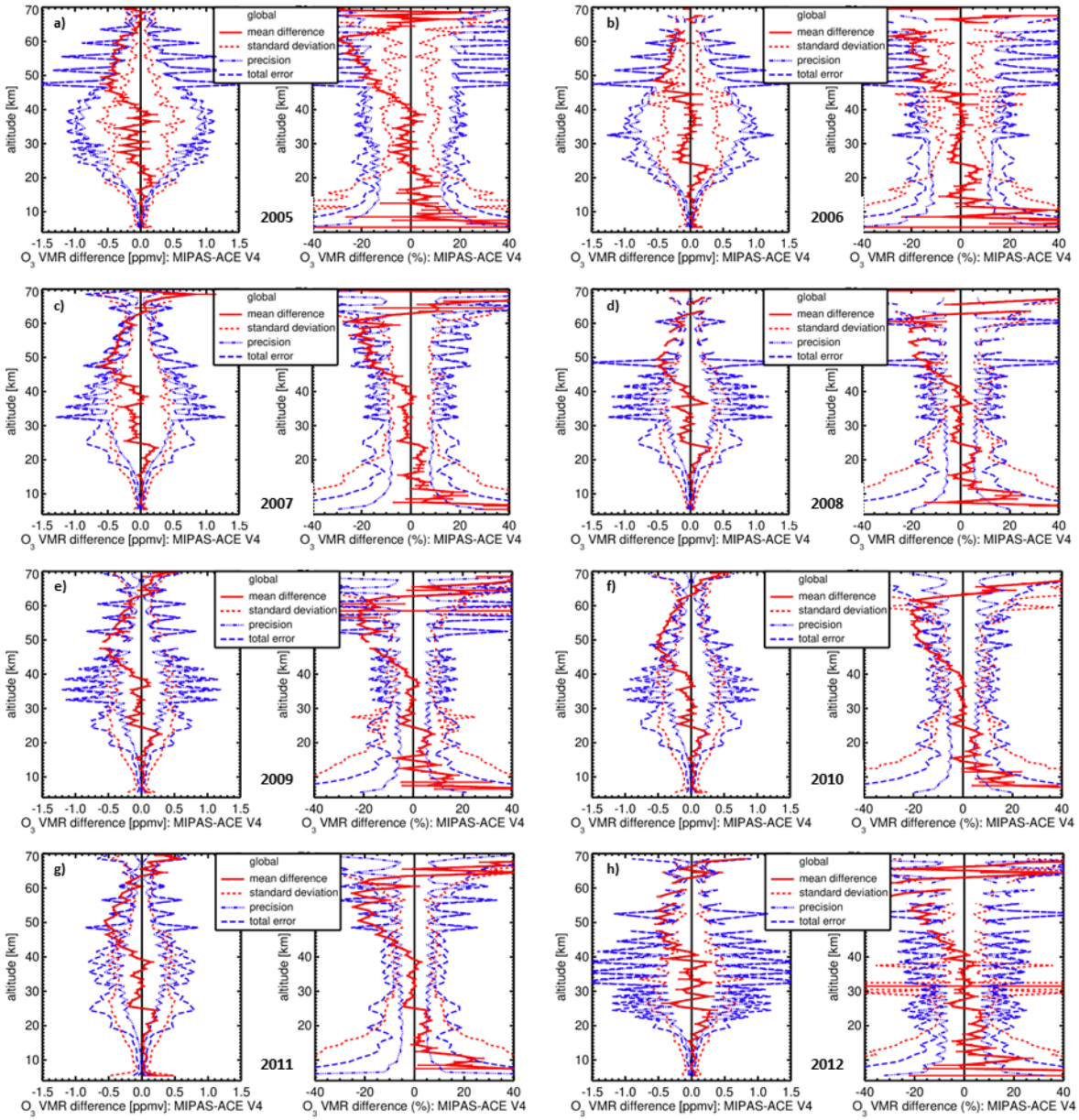

Figure 4-25. Annual mean absolute and relative O3 VMR difference of all match collocations between MIPAS V8.22 and ACE V4 data (red solid line) including standard deviation (red dotted lines) and standard error of the mean (plotted as error bars). Precision (blue dotted lines) and total (blue dashed lines) mean combined errors are shown, too. Global matchups. a) 2005, b) 2006, c) 2007, d) 2008, e) 2009, f) 2010 g) 2011, h) 2012.

Comparison time series show evidence of a positive drift of MIPAS L2V8 with respect to ozonesonde, lidar and –to lesser extent– MWR data of up to 5% per decade over the 2005-2012 time period in the middle stratosphere (20-5 hPa, 25-35 km). In this region annual mean biases w.r.t. ACE-FTS do not change significantly (since 2005), on the other hand. Ground-based drift estimates are not significantly different from zero outside the middle stratosphere (Figure 4-26, left). Users who analyse the complete MIPAS time series for ozone trends should be aware of an offset of about 5% between the FR (2002-2004) and OR (2005-2012) periods of the MIPAS mission (Figure 4-23). They should anticipate an artificial drop in the time series below the 50-20 hPa / 20-25 km level and a jump at higher altitudes.

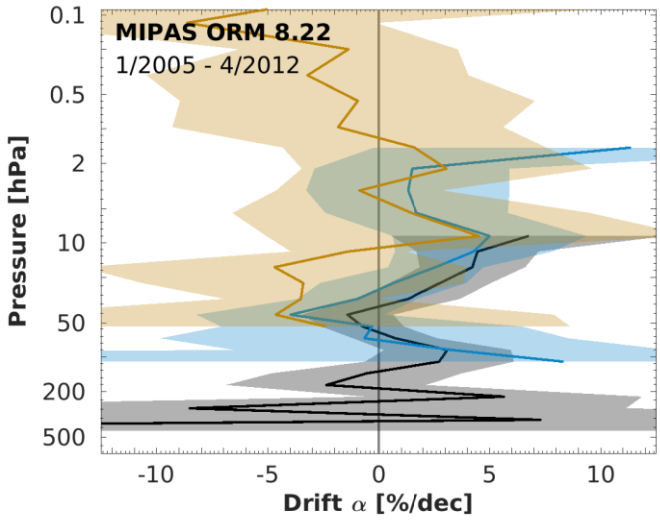

Figure 4-26. Drift of MIPAS V8.22 ozone versus sonde (black), lidar (blue) and MWR (orange) networks over the OR phase of the mission (2005-2012). The shaded area represents the estimated 95% confidence interval. Positive drift values indicate that MIPAS ozone biases become progressively more positive over time wrt reference.

Ground-based comparisons show no coherent seasonal structures in MIPAS bias. The only clear seasonal feature is the Antarctic ozone hole season between 150-50 hPa/13-20 km. MIPAS overestimates lower stratospheric ozone by 10-15% during June-August and underestimates by 15% during September-November. Previous values are indicative since co-location mismatch errors are not taken into account and these can be especially large around the polar vortex and its strong spatial gradients in the ozone field.

4.5 Nitric Acid (HNO_3)

LEVEL 2 V8 HNO_3 PRODUCTS										
Operational modes:	FR	RR	OR							
	NOM		NOM	UTLS1	MA	UA	AE	NLC	UTLS2	UTLS1_o
Nominal Vertical range [Km]	*6-42*	*6-42*	*9-43*	*11.5-43*	*1839*	*-*	*8.5-38*	*-*	*1.27-42*	*8.5-44*
Useful range	*Full range*									
Microwindows:	*Link for downloading*									
Systematic errors:	*Link for downloading* *Link errors*									

Introduction

In Figure 4-27 the time series of V8 HNO_3 weekly mean profiles all over the mission are reported for the latitude band 90S-60S. A strong seasonality is clearly visible in the timeseries, with HNO_3 peaking in the winter.

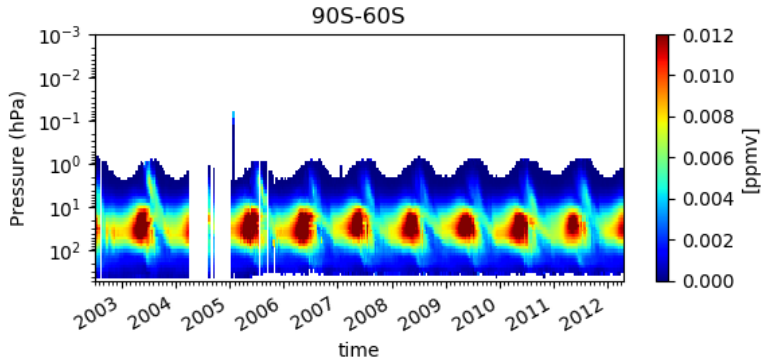

Figure 4-27 Timeseries of weekly mean of HNO3 on the full mission averaged on the latitude band 90S-60S

Verification and changes wrt V7 products

L2V8 HNO_3 profile is about 2-5% greater than L1V7 HNO_3 profile (see Figure 4-28), the main contribution to the differences coming from the changes in the spectroscopic database. Significant improvements were introduced in the spectroscopic parameters of HNO_3 by A.Perrin et al., 2016, now contained in HITRAN 2016 dataset. The new spectroscopy of HNO_3 helps in reducing significantly the residuals of the retrieval.

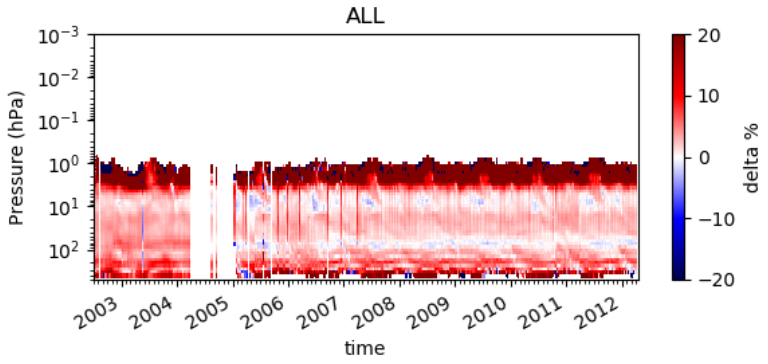

Figure 4-28 Timeseries of weekly mean differences between V8 and V7 HNO_3 profiles all over the mission. Red values indicate that V8 HNO_3 VMRs are greater than V7 VMRs.

As already said for retrieved temperature profiles, handling horizontal inhomogeneities along the line of sight (as in V8) or not (as in V7) has a minor impact on individual retrieved VMR profiles. Differences with and without consideration of horizontal gradients are smaller than the retrieval error. Larger changes are expected where horizontal gradients are the largest, i.e. in the polar regions in wintertime and in the lower stratosphere. However, the impact of horizontal gradients is significant when the differences in HNO_3 VMR for the ascending and descending parts of the orbit are averaged over many scans. Figure 4-29 shows such ascending-descending differences for different latitude bands for various retrieval set-ups (horizontal gradient taken into account or not, two retrieval codes, namely ESA L2 processor (ORM) and KOPRAFIT retrieval algorithm, developed at IMK-IAA (Stiller et al., 2001; Hoepfner et al., 2001). A significant reduction in the ascending-descending difference is found for latitude bands 75°-60° and 60°-45°, both hemispheres, when horizontal gradients of temperature are taken into account, while a smaller but not negligible contribution comes also from handling the horizontal gradients of the trace species. For latitudes near the equator horizontal gradients are negligible and hence the impact of handling horizontal gradients is almost zero.

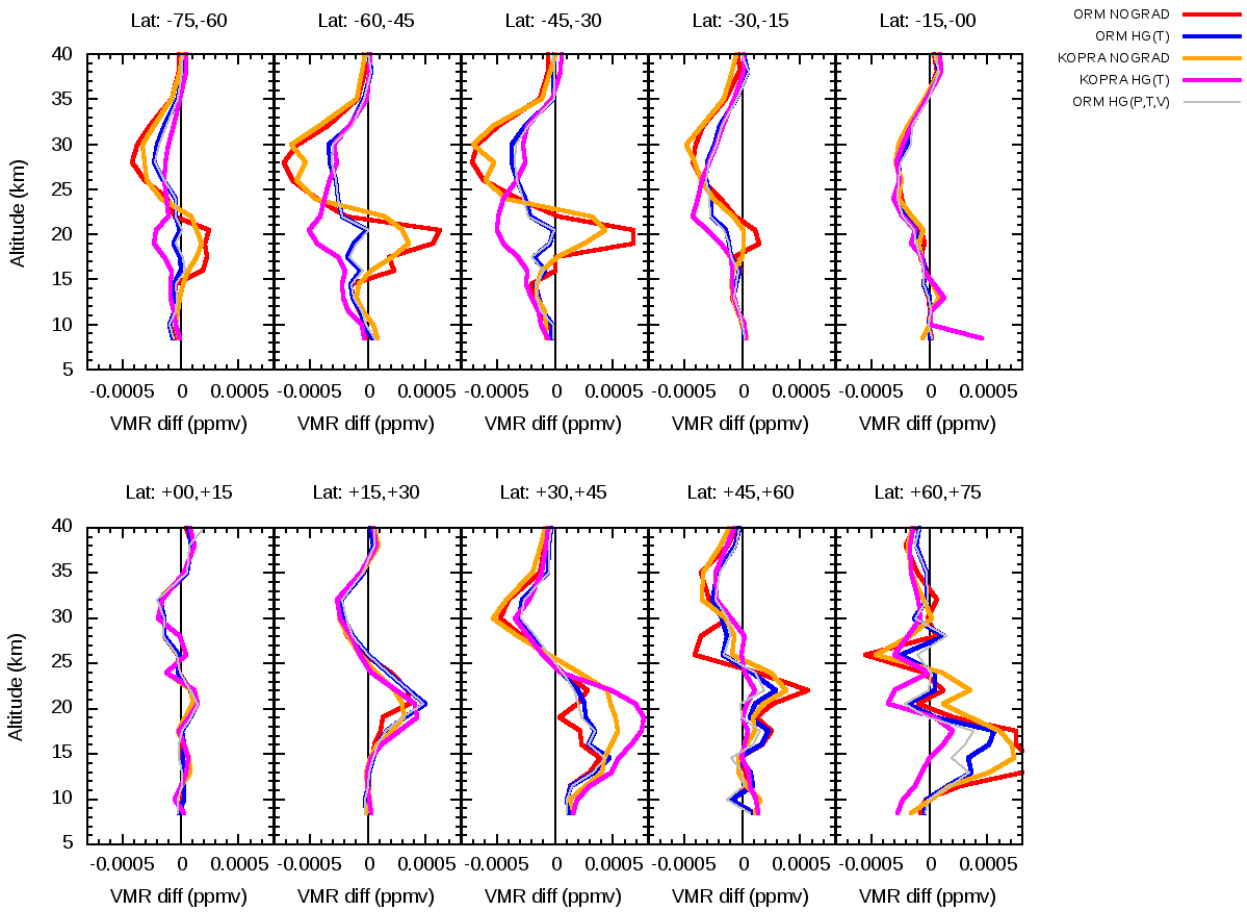

Figure 4-29 Ascending-descending 3-day average differences for HNO_3 retrieved VMR by MIPAS ORM V8 and KOPRAFIT. ORM V8 : without horizontal gradients (HGs) (red), with modelled temperature HGs (blue), and with modelled temperature, pressure and (H2O, O3) VMR HGs (grey). KOPRAFIT : without HGs (brown), and with temperature HGs (magenta).

Quality quantifiers (AK and errors)

The vertical averaging kernels of the HNO_3 retrieval are shown in Figure 4-30 for two representative profiles in Full Resolution nominal mode (left panel) and Optimised Resolution nominal mode (right panel). The selected scans are not affected by clouds. The vertical resolution profile of the considered scan is also reported in red in the same plot and the DOF distribution profile (see Sect. 3.5.2) in blue. A mean vertical resolution profile has been also computed considering all scans in the nominal mode of 2003 (for FR plots) and 2010 (for OR plots). It is about 3 km for FR measurements, about 2 km up to 30 km for the OR measurements.

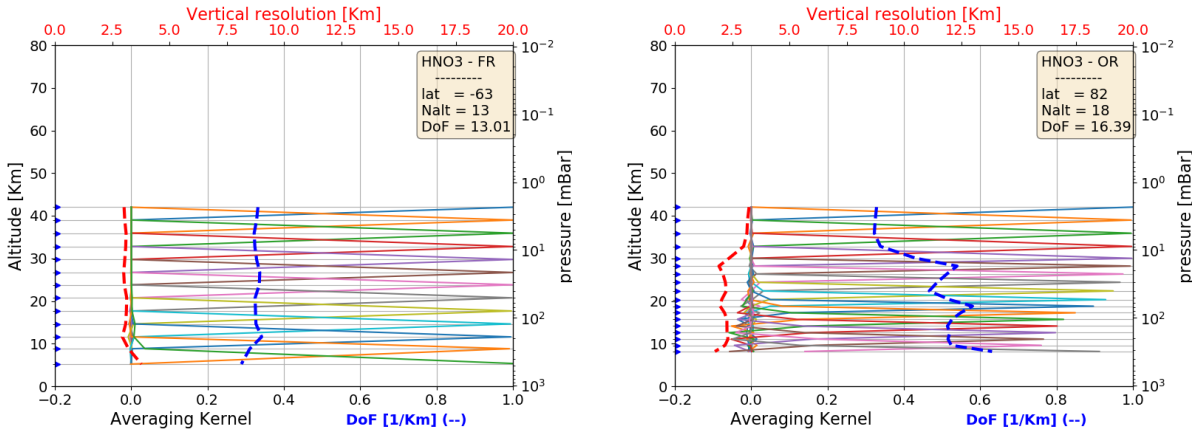

Figure 4-30 Example of HNO_3 vertical averaging kernel (AK) computed for a representative Full Resolution (left panel) and Optimized Resolution (right panel) scan. Together with the AKs, the plots show the vertical resolution (red dashed line) and the Degree of Freedom for unity height (blue dashed line). The yellow box on the top right of each panel contains the latitude of the observation, the number of the measurement sweeps and the total Degree of Freedom (DoF).

Figure 4-31 shows the average nitric acid VMR profiles (left plots) and their associated average random error profiles, in absolute (middle plots) and relative (right plots) scale. The average quantities are representative of 5 reference atmospheres, namely polar summer daytime, polar winter nightime, mid-latitudes (both daytime and nightime) and equatorial daytime atmospheres. The averages have been computed using information on retrieved profiles, noise error and pT error which are contained in the output files for each scan. For mid latitude atmospheres all scans in the nominal mode of 2003 (for FR plots) and 2010 (for OR plots) in the latitude band 30-60 (both hemispheres) have been taken into account (considering either daytime or nightime scans), for equatorial atmosphere the scans in the latitude band 30S-30N, for polar winter nighttime atmosphere all nightime scans in the nominal mode of June-July-August of 2003 (for FR) and of 2005-2011 years (for OR) in the band 60S-90S, for polar summer daytime atmosphere all daytime scans in the nominal mode of December-January-February of 2003 (for FR) and 2005-2011 (for OR) in the latitude band 60S-90S. Solid lines of middle and right plots represent the total random error, coming from the quadratic summation of the noise error (dotted curves, given by the mapping of the measurement error on the retrieved profile) and the pT error (given by the propagation of the random error of retrieved pressure and temperature profiles on VMR profile). The total random error is smaller than 5% in the range 100 hPa-6 hPa, where the VMR peaks, outside this range it rapidly increases. In the equatorial band the percent errors are larger due to the smaller VMR. Errors of the OR measurements are a bit larger than the ones of the FR measurements. The contribution of the pT error to the total random error is not negligible.

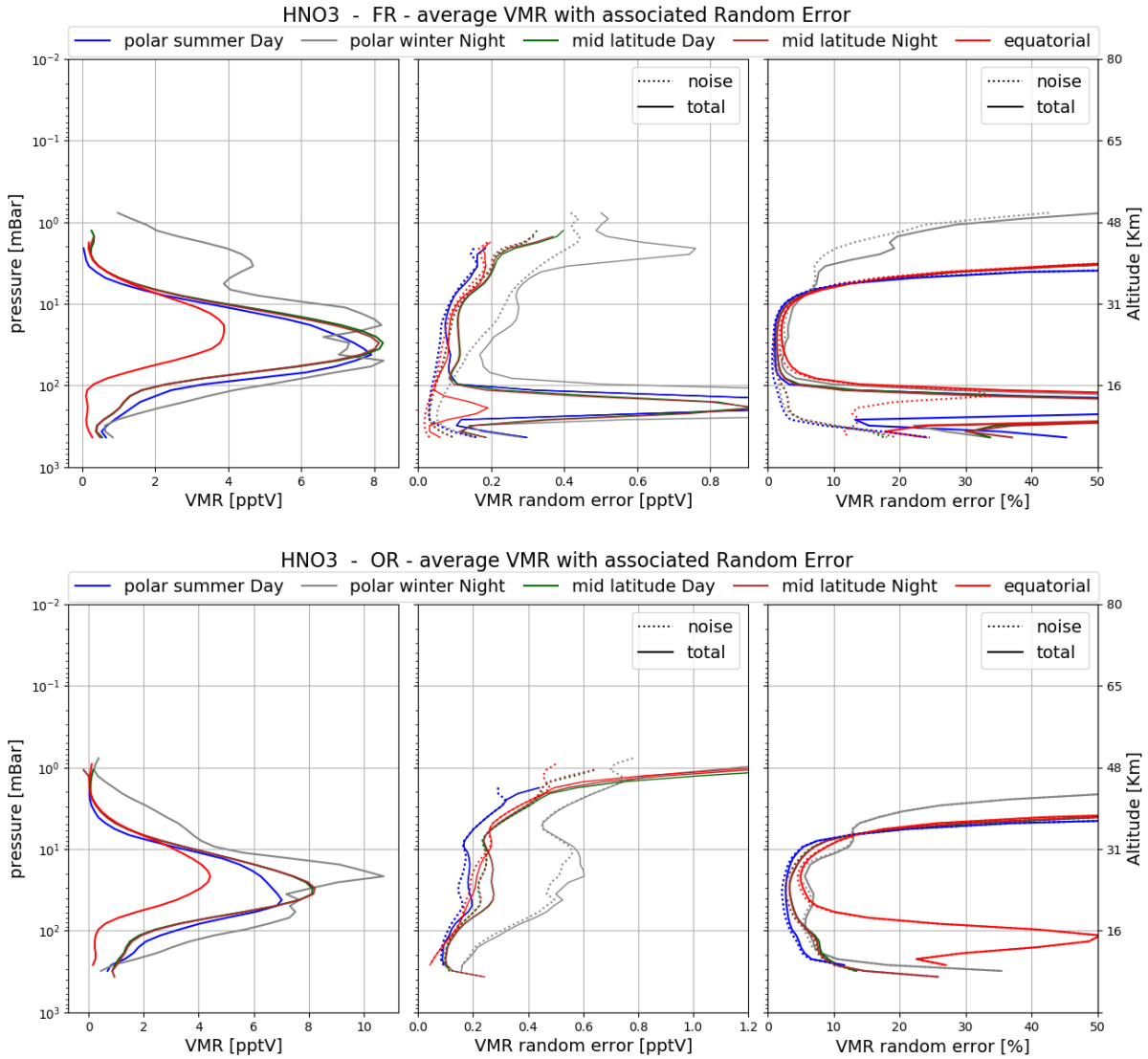

Figure 4-31 Average HNO_3 VMR (left plots), absolute (mid plots) and relative (right plots) HNO_3 random error for the 5 reference atmospheres described in the text. The noise error (dotted curves) is calculated by the retrieval; the total random error (solid curves) includes the contribution to the random error coming from propagation of the pT random error on VMR profiles. Top panel: Full Resolution nominal mode; bottom panel: Optimized Resolution nominal mode.

Validation

Reference instrument	Source	Coverage validation analysis		
		Time	Horizontal	Vertical
FTIR	NDACC			
MIPAS-B	KIT-IMK	8 flights + 2-day trajectories	3 sites, 68°N–5°S	200–2 hPa
ACE-FTS v4	U Waterloo	2005-2012	global	500-0.04 hPa

Comparison with both MIPAS-balloon and ACE-FTS indicates a positive bias of HNO3 MIPAS V8 (within 5-20%) in the altitude range 12-25 km, while comparison with FTIR measurements indicate a negative bias in the same altitude range, with a peak at 21 km. Above 25 km MIPAS is smaller than ACE-FTS (10-30%). Details of results of validation are reported below.

VMR difference profiles of both MIPAS instruments for the stratospheric nitrogen reservoir species HNO_3 are presented in Figure 4-32. MIPAS-E tends to overestimate the HNO_3 abundance when compared to MIPAS-B below about 27 km. This bias is most prominent in the OR mode data between 19 and 26 km around the altitude of the VMR maximum of the HNO_3 profile and somewhat enhanced compared to the v7 data. Biases are typically in the order of 5-20% in relative units. Standard deviations clearly exceed the expected precision. We have to consider that the precision does not include the contribution of the pT error propagation (see Figure 4-31), while the expected precision includes also the atmospheric variability coming from the non-exact co-location of the measurements.

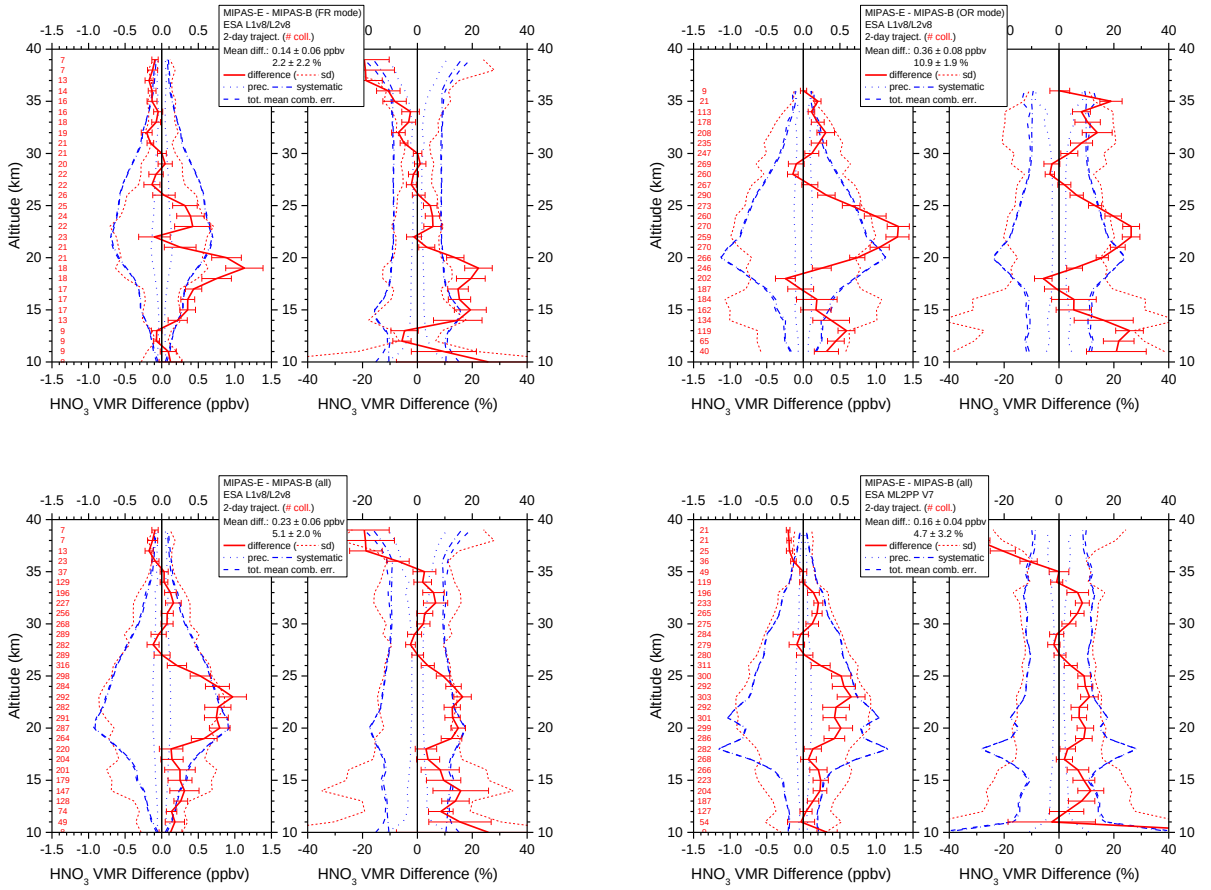

Figure 4-32 Mean absolute and relative HNO_3 VMR difference of all trajectory match collocations (red numbers) between MIPAS-E and MIPAS-B (red solid line) including standard deviation (red dotted lines) and standard error of the mean (plotted as error bars). Precision (blue dotted lines), systematic (blue dash-dotted lines), and total (blue dashed lines) mean combined errors are shown, too. Top: v8 FR mode (left) and v8 OR mode (right) collocations; bottom: all FR plus OR v8 (left) and all FR plus OR v7 (right) collocations.

In the upper troposphere and lowermost stratosphere (12 km to 17 km) differences between the MIPAS and ACE-FTS satellites are within ±10% (see Figure 4-33). In the lower stratosphere (17 km to 25 km) MIPAS is generally higher than ACE by up to 10%. By the upper stratosphere (25 km to 40 km) MIPAS is generally between 10%-30% lower than the ACE values. Overall, biases are typically in the order of 5-20% in relative units.

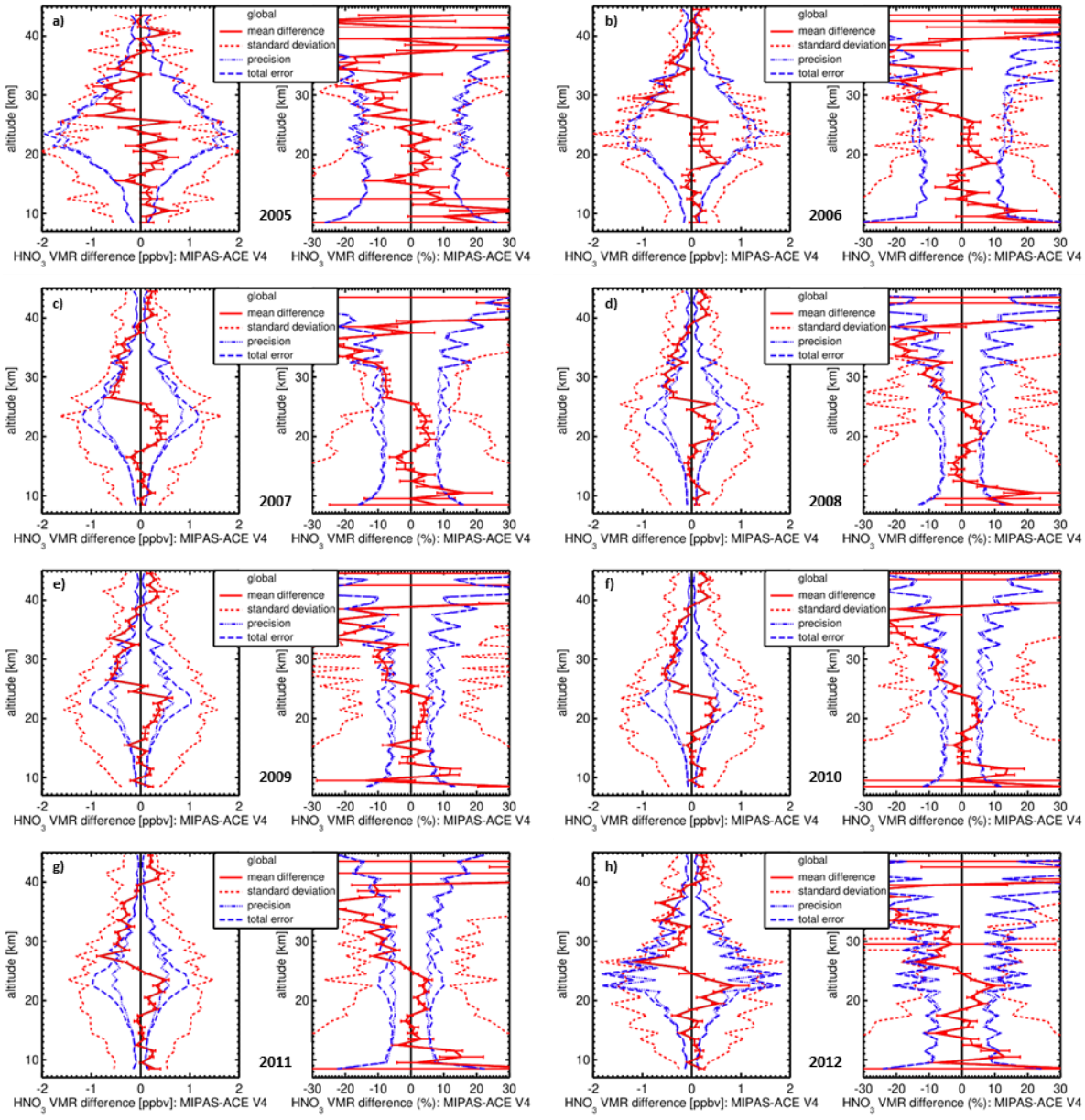

Figure 4-33. Mean absolute and relative HNO_3 VMR difference of all match collocation (red numbers) between MIPAS and ACE version 4 data (red solid line) including standard deviation (red dotted lines) and standard error of the mean (plotted as error bars). Precision (blue dotted lines) and total (blue dashed lines) mean combined errors are shown, too. Global matchups. a) 2005, b) 2006, c) 2007, d) 2008, e) 2009, f) 2010 g) 2011, h) 2012.

The MIPAS HNO3 V8 product has also been validated with respect to ground-based FTIR (Fourier-transform infrared) spectrometer observations that were obtained from the Network for the Detection of Atmospheric Composition Change (NDACC, www.ndacc.org). Using collocation criteria of 300 km and 3 hours, 2508 unique HNO_3 profile measurements from nine FTIR stations have been found to coincide with the MIPAS L2 V8 observations. Differences between collocated measurements were calculated for

vertically integrated HNO_3 subcolumns with about one unit of information [Vigouroux et at., 2007; Payan et al., 2009] and for vertically regridded HNO_3 profiles between 12 and 30 km [Calisesi et al., 2005]. Yearly medians (as relative bias) and 68 % interpercentiles (as vertical errors bars) of HNO_3 subcolumn differences are shown for four MIPAS L2 versions at the Arctic Kiruna station in Figure 4-34. The median (bias) and 68 % interpercentile (spread) of the corresponding profile differences are added as well, whereby the MIPAS profiles have been vertically smoothed using the coincident FTIR averaging kernel matrices [Rodgers, 2000]. The subcolumn difference statistics for all nine FTIR stations, subdivided over five latitude bands, are collected in Table 4-1. The comparison results overall show a less than 5 % negative V8 bias (no Southern hemisphere data), which is smaller than for previous retrieval versions, and an order of 10 % comparison spread, which is well within the typical FTIR spectrometer uncertainty. However, the comparisons show a significant vertical dependence, with a strong negative MIPAS HNO3 bias above 16-26 km, reaching a minimum at roughly 22 km in the Arctic or higher towards the equator, and spreads between 5 and 50 %, with a minimum around the altitude of the most negative bias. This vertical dependence is also seen in the MIPAS balloon comparisons, although with an offset (different overall bias). A significant seasonal bias dependence is also observed, with values that are more negative in local winter times around the bias minimum.

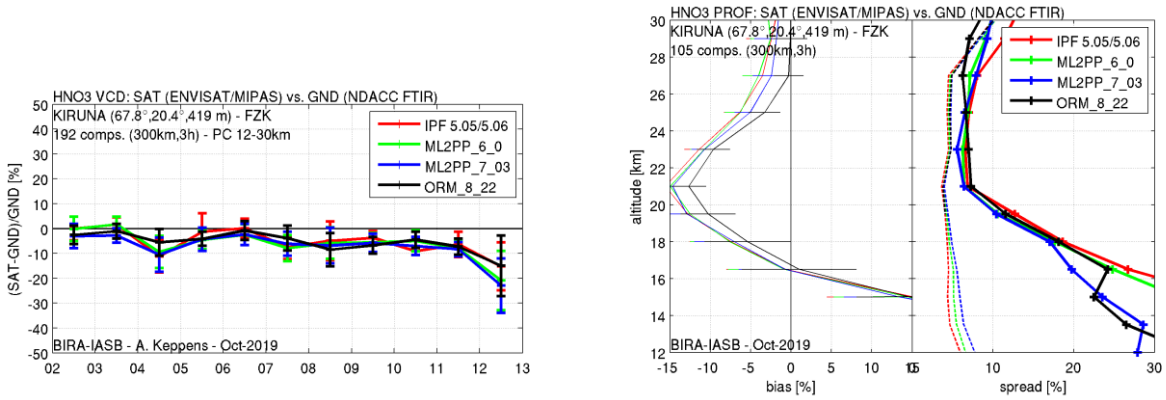

Figure 4-34 The left plot shows yearly medians (as relative bias) and 68 % interpercentiles (as vertical errors bars) of MIPAS-FTIR HNO3 subcolumn differences (12-30 km) for four MIPAS L2 versions at the Arctic Kiruna station. The right plot shows the median (bias) and 68 % interpercentile (spread) of the corresponding 12-30 km profile differences. The MIPAS profiles are thereby vertically smoothed using the coincident FTIR averaging kernel matrices.

Table 4-1 HNO3 12-30 km subcolumn difference statistics for MIPAS L2 V8 retrievals versus coincident FTIR measurements, subdivided over five latitude bands.

	# stats.	# comps.	V8 bias [%]	V8 spread [%]
60N-90N	4	2042	-4.1	8.1
30N-60N	3	220	-4.8	9.2
30N-30S	2	246	-2.5	10.9
30S-60S	0	0	/	/
60S-90S	0	0	/	/

4.6 Methane (CH_4)

LEVEL 2 V8 OZONE PRODUCTS										
Operational modes:	FR	RR	OR							
	NOM		NOM	UTLS1	MA	UA	AE	NLC	UTLS2	UTLS1_o
Nominal Vertical range [Km]	*6-68*	*6-68*	*6-71*	*6-49*	*18-69*	*42-69*	*7-38*	*39-69*	*12-42*	*10-49*
Useful range	*All altitudes up to 68 km (pressures greater than 0.05 hPa)*									
Microwindows:	*Link for downloading*									
Systematic errors:	*Link for downloading* *Link errors*									

Introduction

CH_4 is a long-lived tracer of similar lifetime of N_2O and a strong green-house gas. In Figure 4-35 the timeseries of V8 CH_4 weekly mean profiles all over the mission averaged in the latitude band 90S-60S are reported as an example. It is visible the air subsidence in the polar winter bringing CH_4 poor air from the highest altitudes to the lowest ones.

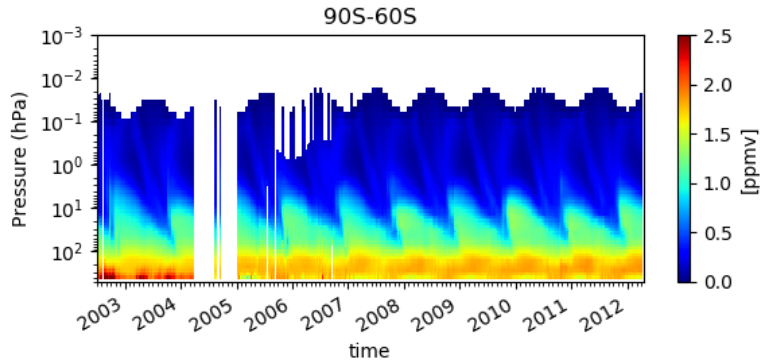

Figure 4-35 Timeseries of weekly mean of CH4 on the full mission averaged on the latitude band 90S-60S

Verification and changes wrt V7 products

In Figure 4-36 the time series of the weekly mean of the differences between V8 and V7 CH_4 profiles, averaged on all latitude bands are reported. The FR and the OR phases are affected differently by the changes in the code, in the auxiliary data and in the L1V8 files, but in general differences are small (within 2-3%), mainly due to the correction in the radiometric calibration of L1V8 files. At low altitudes, the new spectroscopic database and the changes implemented in the L2 retrieval are responsible of some changes in the retrieved profiles. Larger relative differences are found at the highest end of the retrieval range, also due to smaller CH_4 values.

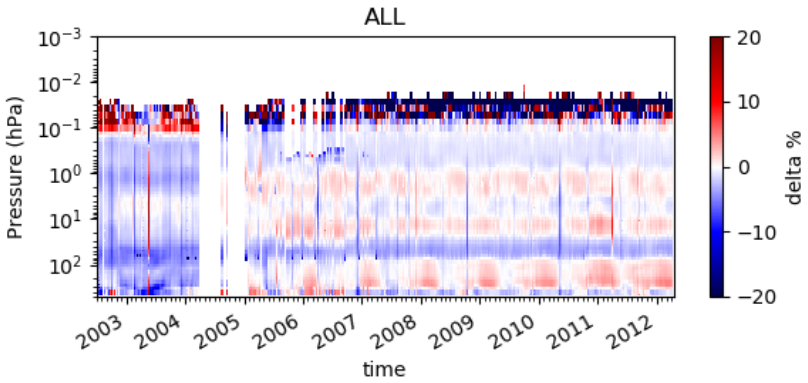

Figure 4-36 Timeseries of weekly mean differences on all latitude bands between V8 and V7 CH4 profiles all over the mission. Positive values indicate that V8 CH4 is larger than V7 CH4.

As stated in Errera et al., 2016, two problems were identified in V6 and V7 CH_4 data: discontinuities in the time series and poor correlation between MIPAS and MLS and ACE-FTS in the tropical lower stratosphere.

Indeed, time series of MIPAS V6 and V7 CH4 profiles show unexpected discontinuities which are due to the abrupt change in the radiometric gain of the instrument, not correctly handled with a weekly update of the gain.
In Figure 4-37 we show that the use of the daily calibration reduces these discontinuities in timeseries of V8 CH_4, with respect to the timeseries of V7 CH_4.

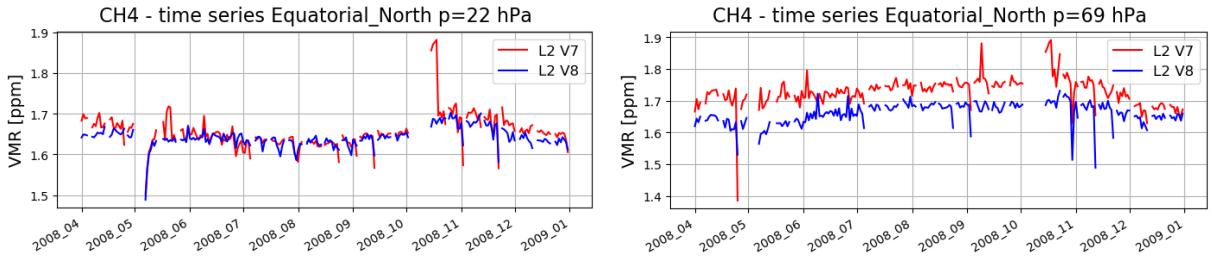

Figure 4-37 Timeseries of CH_4 at pressure 22 and 69 hPa in the period April-December 2008 where Herrera et al. found large discontinuities in April and October after the decontamination operations.

Second, the correlations between BASCOE analyses and independent observations from MLS and ACE–FTS are poor in the tropical lower stratosphere. This is due to outlier profiles which are not flagged out in the presence of clouds. Since L2V8 uses new altitude and latitude dependent thresholds for the cloud filtering, an improvement may be possible.
The comparison of the timeseries of CH4 from L2V7 and L2V8 in Figure 4-38 and Figure 4-39 indicates that at least in the FR the timeseries do contain less outliers.

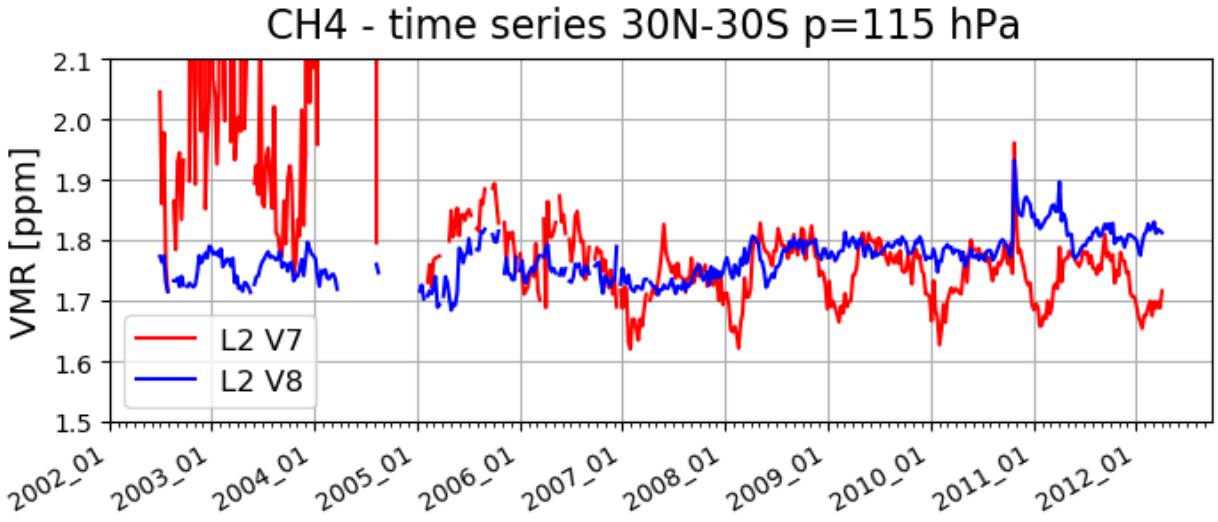

Figure 4-38 Time series of CH4 in the tropics at pressure 115 hPa

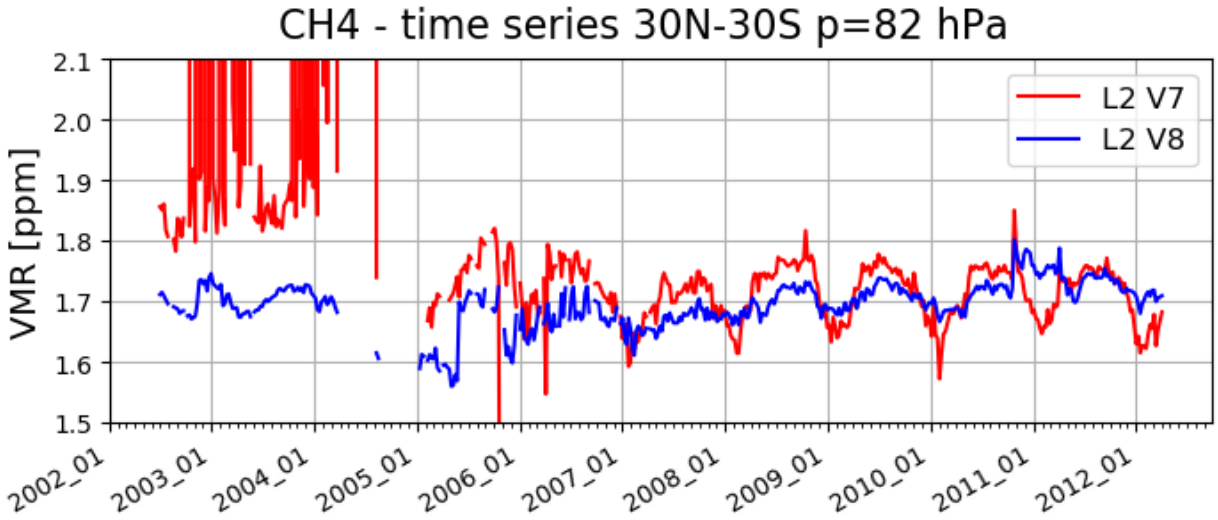

Figure 4-39 Time series of CH_4 in the tropics at pressure 82 hPa

Quality quantifiers (AK and errors)

The vertical averaging kernels of the methane retrieval are shown in Figure 4-40 for two representative profiles in Full Resolution nominal mode (left panel) and Optimised Resolution nominal mode (right panel). The selected scans are not affected by clouds. The vertical resolution profile of the considered scan is also reported in red in the same plot and the DOF distribution profile (see Sect. 3.5.2) in blue. A mean vertical resolution profile has been also computed considering all scans in the nominal mode of 2003 (for FR plots) and 2010 (for OR plots). It is between 4 and 5 km in both phases up to 50 km. Indeed, even if the measurement grid is finer in the OR phase, retrieval is performed on a subsample of the measurement grid up to 29 km, i.e. only one point every two is retrieved in order to reduce the retrieval instabilities.

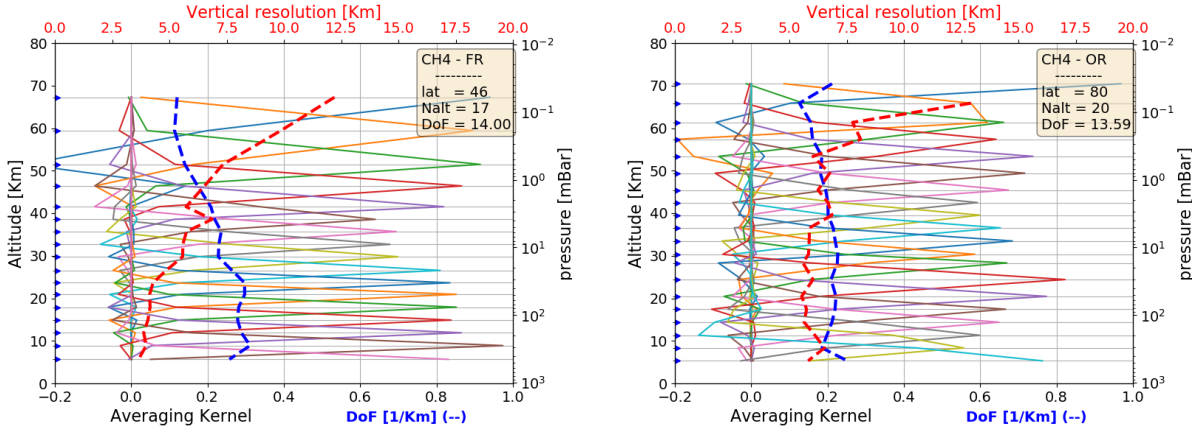

Figure 4-40 Example of methane vertical averaging kernel (AK) computed for a representative Full Resolution (left panel) and Optimized Resolution (right panel) scan. Together with the AKs, the plots show the vertical resolution (red dashed line) and the Degree of Freedom for unity height (blue dashed line). The yellow box on the top right of each panel contains the latitude of the observation, the number of the measurement sweeps and the total Degree of Freedom (DoF)

Figure 4-41 shows the average methane VMR profiles (left plots) and their associated average random error profiles, in absolute (middle plots) and relative (right plots) scale. The average quantities are representative of 5 reference atmospheres, namely polar summer daytime, polar winter nightime, mid-latitudes (both daytime and nightime) and equatorial daytime atmospheres. The averages have been computed using information on retrieved profiles, noise error and pT error which are contained in the output files for each scan. For mid latitude atmospheres all scans in the nominal mode of 2003 (for FR plots) and 2010 (for OR plots) in the latitude band 30-60 (both hemispheres) have been taken into account (considering either daytime or nightime scans), for equatorial atmosphere the scans in the latitude band 30S-30N, for polar winter nighttime atmosphere all nightime scans in the nominal mode of June-July-August of 2003 (for FR) and of 2005-2011 years (for OR) in the band 60S-90S, for polar summer daytime atmosphere all daytime scans in the nominal mode of December-January-February of 2003 (for FR) and 2005-2011 (for OR) in the latitude band 60S-90S. Solid lines of middle and right plots represent the total random error, coming from the quadratic summation of the noise error (dotted curves, given by the mapping of the measurement error on the retrieved profile) and the pT error (given by the propagation of the random error of retrieved pressure and temperature profiles on VMR profile). The total random error is approximately constant around 2% until 1 hPa for all atmospheres except the polar winter, where it reaches 10 % at 10 hPa. In general larger errors are found for the OR measurements. Especially for the OR measurements, the pT error gives a large contribution to the total random error.

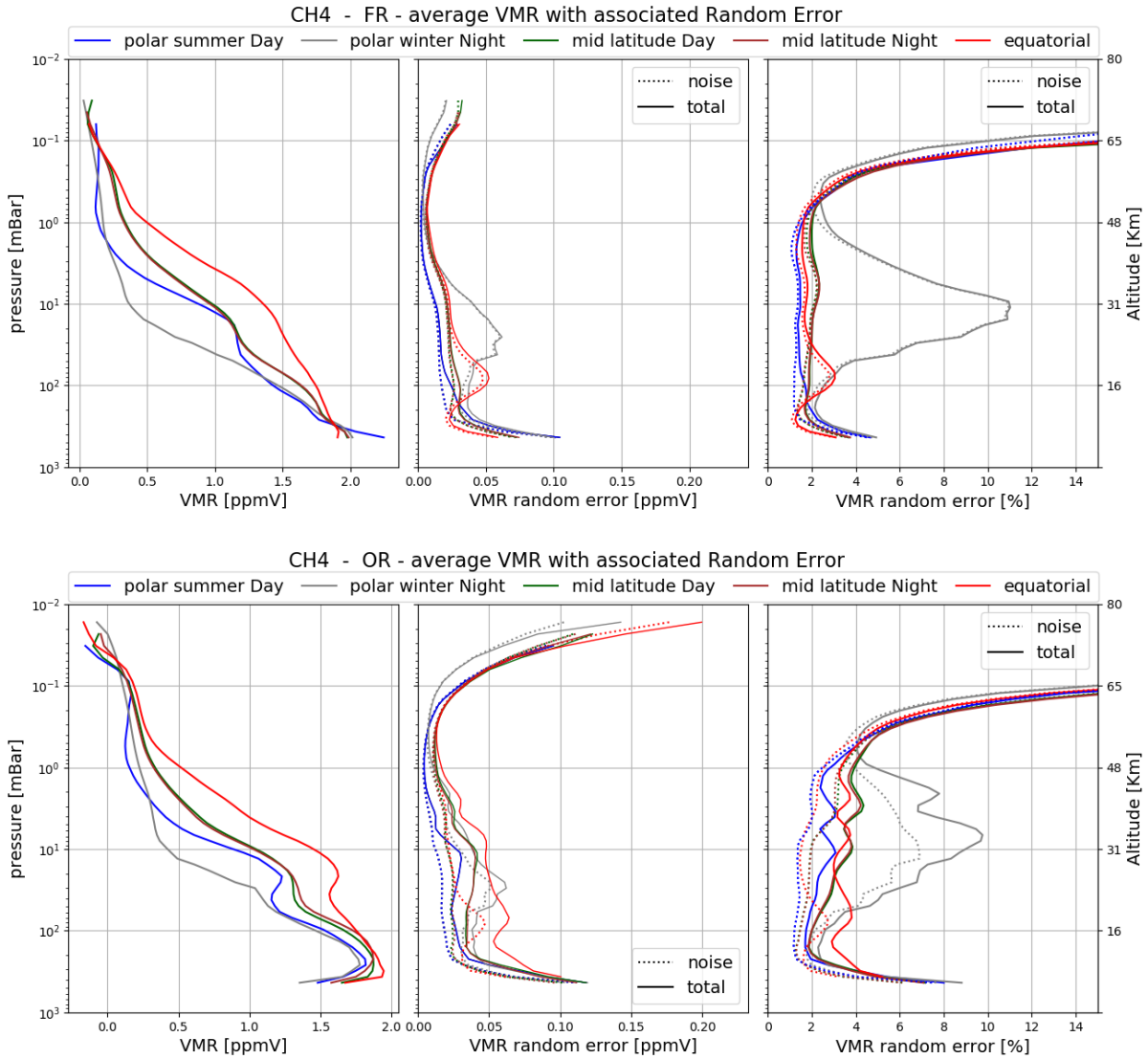

Figure 4-41 Average CH_4 VMR (left plots), absolute (mid plots) and relative (right plots) CH_4 random error for the 5 reference atmospheres described in the text. The noise error (dotted curves) is calculated by the retrieval; the total random error (solid curves) includes the contribution to the random error coming from propagation of the pT random error on VMR profiles. Top panel: Full Resolution nominal mode (average 2003); bottom panel: Optimized Resolution nominal mode (average on 2010).

L2-algorithm		L2-V8-overview		Altitude		TEMP	H_2O	O_3	HNO_3	CH_4	N_2O	NO_2	CFC-11
$ClONO_2$	N_2O_5	CFC-12	COF_2	CCl_4	HCN	CFC-14	HCFC22	C_2H_2	C_2H_6	CH_3Cl	$COCl_2$	OCS	HDO

Validation

Reference instrument	Source	Coverage validation analysis		
		Time	Horizontal	Vertical
FTIR	NDACC	2002-2012	4 sites, 47°N–45°S	10–0.04 hPa
MIPAS-B	KIT-IMK	8 flights + 2-day trajectories	3 sites, 68°N–5°S	200–2 hPa

MIPAS exhibits a significant positive bias of 3. to 15% in the stratosphere and upper troposphere with respect to both, the ground-based FTIR and the balloon-borne MIPAS measurements. This holds for both MIPAS observation periods (FR and OR mode) and different geographical regions. More details are reported below.

Figure 4-42 presents the results for the molecule CH_4 based on the statistical trajectory analysis of all MIPAS satellite and balloon collocations available. MIPAS-E tends to overestimate the abundance of CH_4 in the stratosphere below about 35 km by 5-15% and standard deviations exceed the expected precision. Somewhat larger positive deviations occur in the Tropics around 30 km. Changes in the VMR differences using the current L1v8/L2v8 data set compared to the VMR differences taking the v7 data are small.

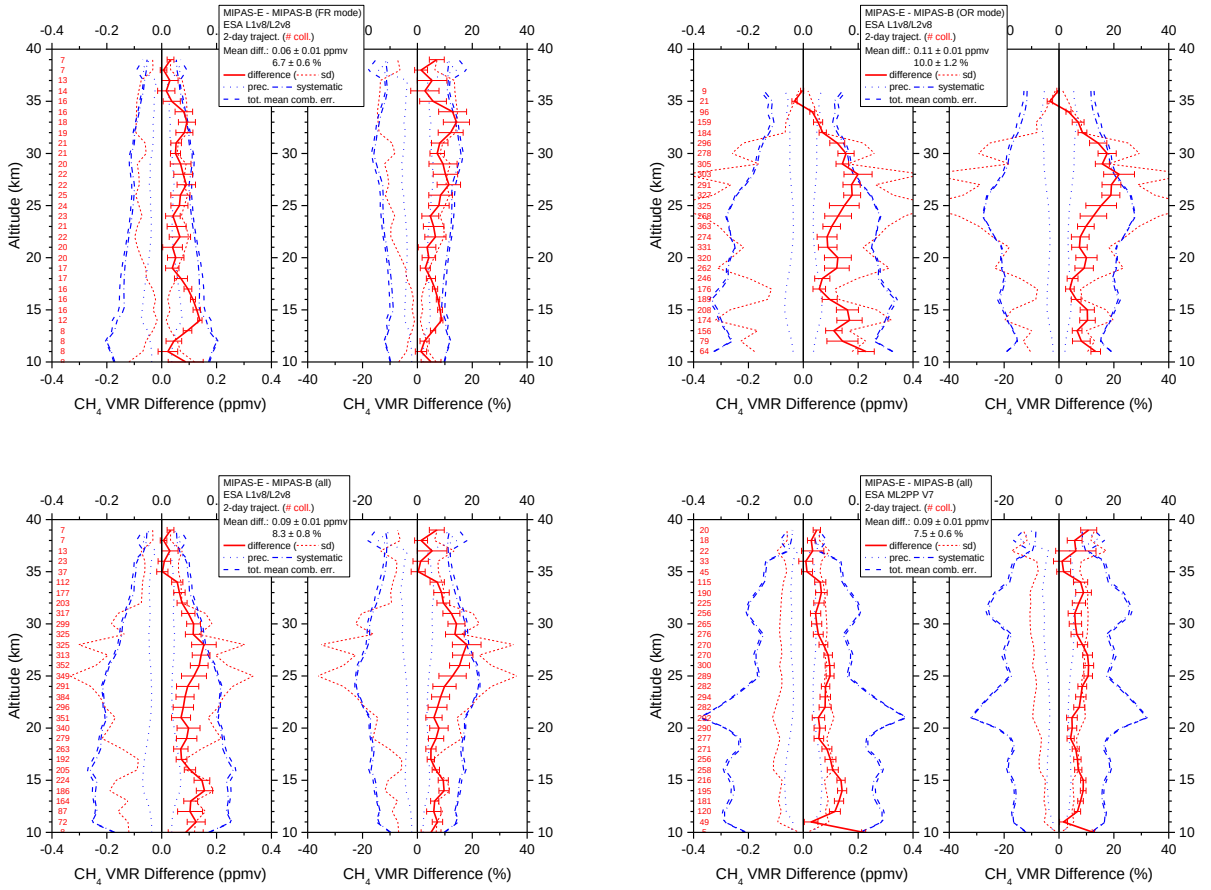

Figure 4-42 Mean absolute and relative CH_4 VMR difference of all trajectory match collocations (red numbers) between MIPAS-E and MIPAS-B (red solid line) including standard deviation (red dotted lines) and standard error of the mean (plotted as error bars). Precision (blue dotted lines), systematic (blue dash-dotted lines), and total (blue dashed lines) mean combined errors are shown, too. Top: v8 FR mode (left) and v8 OR mode (right) collocations; bottom: all FR plus OR v8 (left) and all FR plus OR v7 (right) collocations.

The MIPAS CH4 V8 product has also been validated with respect to ground-based FTIR (Fourier-transform infrared) spectrometer observations that were obtained from the Network for the Detection of Atmospheric Composition Change (NDACC, www.ndacc.org). Using collocation criteria of 300 km and 3 hours, 2767 unique CH4 profile measurements from nine FTIR stations have been found to coincide with the MIPAS L2 V8 observations. Differences between collocated measurements were calculated for three vertically integrated CH4 subcolumns (9-12, 12-30, and 30-60 km) with about one unit of information each [Vigouroux et al., 2007; Payan et al., 2009], and for vertically regridded CH4 profiles between 12 and 30 km [Calisesi et al., 2005]. Yearly medians (as relative bias) and 68 % interpercentiles (as vertical errors bars) of CH4 subcolumn differences are shown for four MIPAS L2 versions at the Arctic Kiruna station in Figure 4-43. The median (bias) and 68 % interpercentile (spread) of the corresponding profile differences are added as well, whereby the MIPAS profiles have been vertically smoothed using the coincident FTIR averaging kernel matrices [Rodgers, 2000]. The subcolumn difference statistics for all nine FTIR stations, subdivided over five latitude bands, are collected in Table 4-2. The comparison results show a globally (without the Antarctic) and vertically consistent MIPAS CH4 V8 positive bias of about 3 to 10 % and a similar spread below 30 km, increasing above due to decreasing concentrations (and appearance of

fluctuations). This means that median differences are at the edge of being significant. The V8 (and V7) CH4 bias is slightly reduced with respect to the V5 and V6 bias results in the full resolution period, yet at the cost of a small bias increase (few %) in the optimised resolution period. The unsmoothed difference profile shape seems to be in agreement with the MIPAS balloon comparisons (also at Kiruna), with a small vertical dependence, being mostly constant above 18 to 20 km, while going down to lower values below. The large comparison uncertainties make it difficult to detect seasonal dependences or trends.

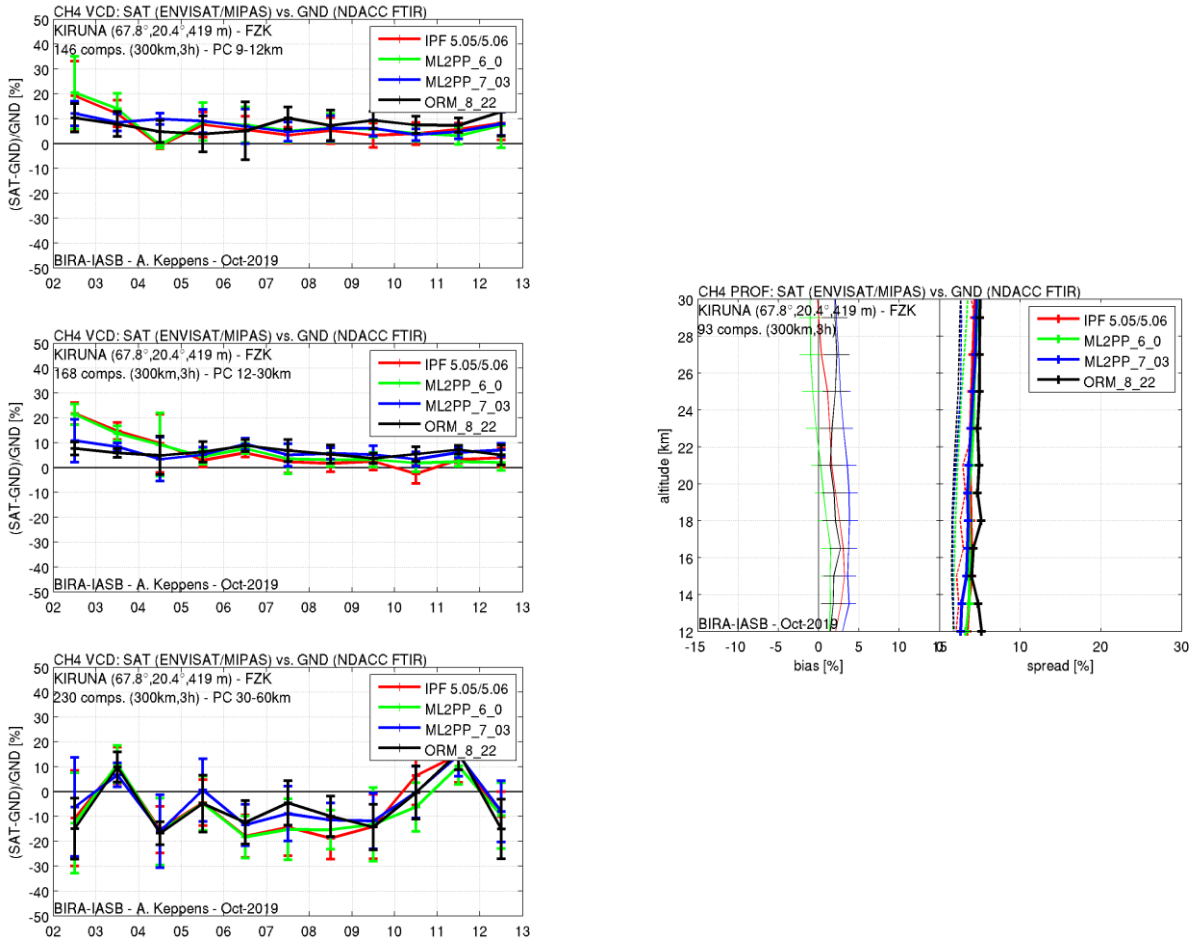

Figure 4-43 Yearly medians (as relative bias) and 68 % interpercentiles (as vertical errors bars) of MIPAS-FTIR CH4 subcolumn differences (left, 9-12 km, 12-30 km, 30-60 km from top to bottom) for four MIPAS L2 versions at the Arctic Kiruna station. The right plot shows the median (bias) and 68 % interpercentile (spread) of the 12-30 km profile differences. The MIPAS profiles are thereby vertically smoothed using the coincident FTIR averaging kernel matrices.

Table 4-2 CH4 subcolumn difference statistics for MIPAS L2 V8 retrievals versus coincident FTIR measurements, subdivided over five latitude bands.

	# stats.	# comps.	V8 bias [%]	V8 spread [%]	V8 bias [%]	V8 spread [%]	V8 bias [%]	V8 spread [%]
			9-12 km		12-30 km		30-60 km	
60N-90N	4	1385	6.5	5.9	7.4	6.1	3.1	19.1
30N-60N	3	664	5.0	7.7	4.0	6.8	6.3	15.5
30N-30S	1	358	6.5	6.5	4.5	6.3	13.0	6.5
30S-60S	1	360	10.5	3.3	7.0	5.8	18.5	10.5
60S-90S	0	0	/	/	/	/	/	/

4.7 Nitrous Oxide (N_2O)

LEVEL 2 V8 NITROUS OXIDE PRODUCTS										
Operational modes:	FR	RR	OR							
	NOM		NOM	UTLS1	MA	UA	AE	NLC	UTLS2	UTLS1_o
Nominal Vertical range [Km]	*6-68*	*6-52*	*6-58*	*6-49*	*18-63*	*42-63*	*7-38*	*39-63*	*12-42*	*10-49*
Useful range	*All altitudes up to 60 km (pressure greater than 0.2 hPa)*									
Microwindows:	*Link for downloading*									
Systematic errors:	*Link for downloading* *Link errors*									

Introduction

N_2O is a long-lived tracer of similar lifetime of methane and a strong green-house gas. In Figure 4-44 the time series of V8 N_2O weekly mean profiles all over the mission averaged in the latitude band 90S-60S are reported. As for CH_4, it is visible the air subsidence in the polar winter bringing N_2O poor air from the highest altitudes to the lower ones.

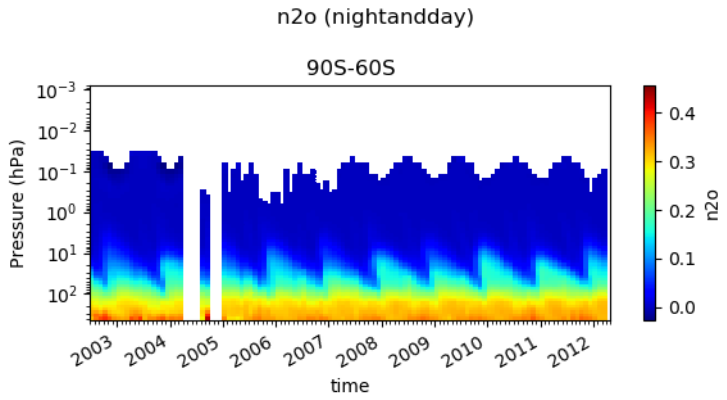

Figure 4-44 Timeseries of weekly mean of N2O on the full mission averaged on the latitude band 90S-60S

Verification and changes wrt V7 products

Differences between V8 and V7 N_2O profiles are small (see Figure 4-45), with N_2O V8 values about 5% smaller than N_2O V7 ones. Differences are mainly due to the new calibration in the L1V8 files and the use of new spectroscopic database.

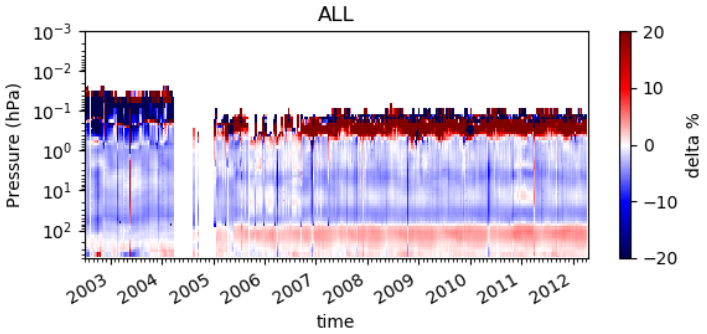

Figure 4-45 Timeseries of weekly mean differences between V8 and V7 N2O profiles all over the mission. Blue values means that V8 N2O is smaller than V7 N2O.

As already discussed for CH_4 and as stated in Errera et al., 2016, time series of MIPAS V6 and V7 profiles show unexpected discontinuities which have been attributed to the abrupt change in the radiometric gain of the instrument, not correctly handled with a weekly update of the gain.
In Figure 4-37 we show that the use of the daily calibration reduces these discontinuities in the V8 N_2O timeseries, compared with the V7 N_2O ones.

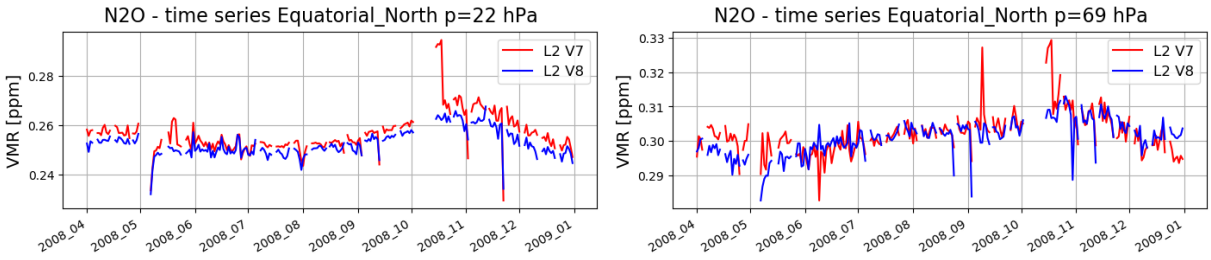

Figure 4-46 Timeseries of N2O at pressure 22 hPa (left plot) and 69 hPa (right plot) in the period April-December 2008 where Herrera et al. found large discontinuities in April and October after the decontamination operations.

Quality quantifiers (AK and errors)

The vertical averaging kernels of the N_2O retrieval are shown in Figure 4-47 for two representative profiles in Full Resolution nominal mode (left panel) and Optimised Resolution nominal mode (right panel). The selected scans are not affected by clouds. The vertical resolution profile of the considered scan is also reported in red in the same plot and the DOF distribution profile (see Sect. 3.5.2**Error! Reference source n ot found.**) in blue. A mean vertical resolution profile has been also computed considering all scans in the nominal mode of 2003 (for FR plots) and 2010 (for OR plots). For both phases it is about 4 km up to 30 km, above it slowly degrades with altitude. The measurement grid of the OR phase is finer than the one of FR phase, but for N2O retrieval is performed on a subsample of the measurement grid up to 21 km, i.e. only one point every two is taken in order to reduce the retrieval instabilities. This explains that similar performances are obtained in the two phases.

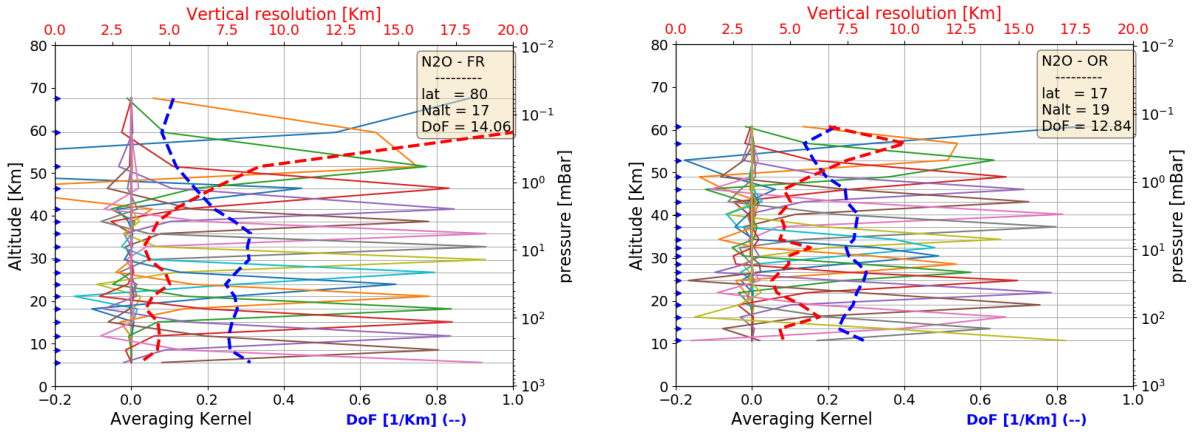

Figure 4-47 Example of N_2O vertical averaging kernel (AK) computed for a representative Full Resolution (left panel) and Optimized Resolution (right panel) scan. Together with the AKs, the plots show the vertical resolution (red dashed line) and the Degree of Freedom for unity height (blue dashed line). The yellow box on the top right of each panel contains the latitude of the observation, the number of the measurement sweeps and the total Degree of Freedom (DoF)

Figure 4-48 shows the average N_2O VMR profiles (left plots) and their associated average random error profiles, in absolute (middle plots) and relative (right plots) scale. The average quantities are representative of 5 reference atmospheres, namely polar summer daytime, polar winter nightime, mid-latitudes (both daytime and nightime) and equatorial daytime atmospheres. The averages have been computed using information on retrieved profiles, noise error and pT error which are contained in the output files for each scan. For mid latitude atmospheres all scans in the nominal mode of 2003 (for FR plots) and 2010 (for OR plots) in the latitude band 30-60 (both hemispheres) have been taken into account (considering either daytime or nightime scans), for equatorial atmosphere the scans in the latitude band 30S-30N, for polar winter nighttime atmosphere all nightime scans in the nominal mode of June-July-August of 2003 (for FR) and of 2005-2011 years (for OR) in the band 60S-90S, for polar summer daytime atmosphere all daytime scans in the nominal mode of December-January-February of 2003 (for FR) and 2005-2011 (for OR) in the latitude band 60S-90S. Solid lines of middle and right plots represent the total random error, coming from the quadratic summation of the noise error (dotted curves, given by the mapping of the measurement error on the retrieved profile) and the pT error (given by the propagation of the random error of retrieved pressure

and temperature profiles on VMR profile). The contribution coming from the pT error propagation is smaller than the noise contribution but it is not negligible. The total random error is about 2% in the range 300 hPa-10 hPa for all atmospheres, then it rapidly increases with the altitude. Polar winter is an exception, with relative errors increasing with altitude, reaching 10% at 10 hPa.

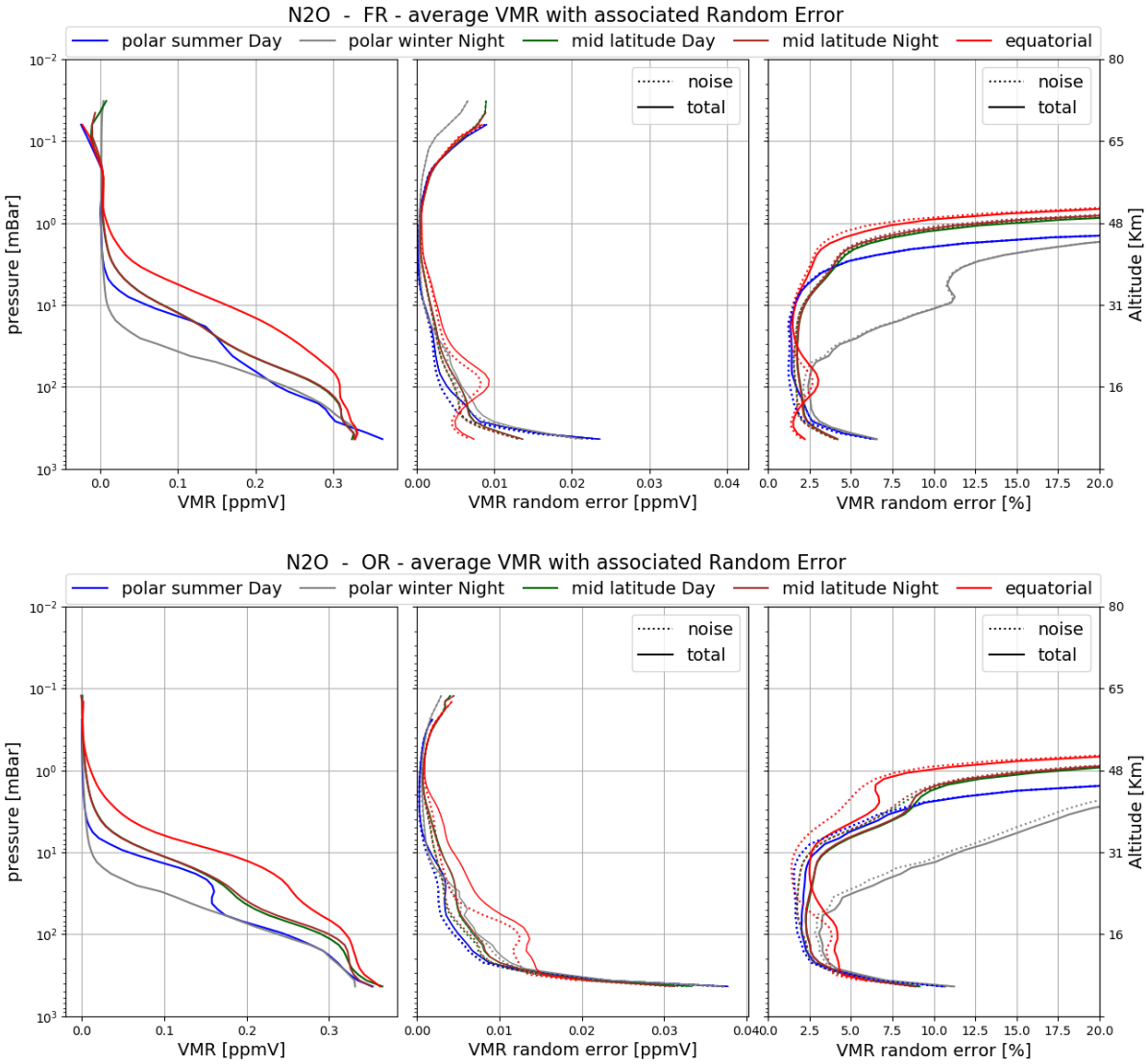

Figure 4-48 Average N_2O VMR (left plots), absolute (mid plots) and relative (right plots) N_2O random error for the 5 reference atmospheres described in the text. The noise error (dotted curves) is calculated by the retrieval; the total random error (solid curves) includes the contribution to the random error coming from propagation of the pT random error on VMR profiles. Top panel: Full Resolution nominal mode; bottom panel: Optimized Resolution nominal mode.

Validation

Reference instrument	Source	Coverage validation analysis		
		Time	Horizontal	Vertical
FTIR	NDACC	2002-2012	4 sites, 47°N–45°S	10–0.04 hPa
MIPAS-B	KIT-IMK	8 flights + 2-day trajectories	3 sites, 68°N–5°S	200–2 hPa

MIPAS exhibits a significant positive bias of about 5% with respect to the ground-based FTIR measurements. In the comparison to the balloon observation, this positive bias is even more pronounced reaching values typically between 10 and 20%. This holds for both MIPAS observation periods (FR and OR mode) and different geographical regions. More details are reported below.

Results for the molecule N_2O based on the trajectory analysis of MIPAS satellite and balloon collocations are depicted in Figure 4-49. The species N_2O shows an altitude-dependent behaviour of the mean difference quite similar to CH_4 while standard deviations exceed the expected precision. Comparable to the case of CH_4, MIPAS-E tends to overestimate the abundance of N_2O in the stratosphere below about 35 km by 10-20%. Somewhat larger positive deviations occur in the Tropics around 30 km. Changes in the VMR differences using the current L1v8/L2v8 data set compared to the VMR differences taking the v7 data are small.

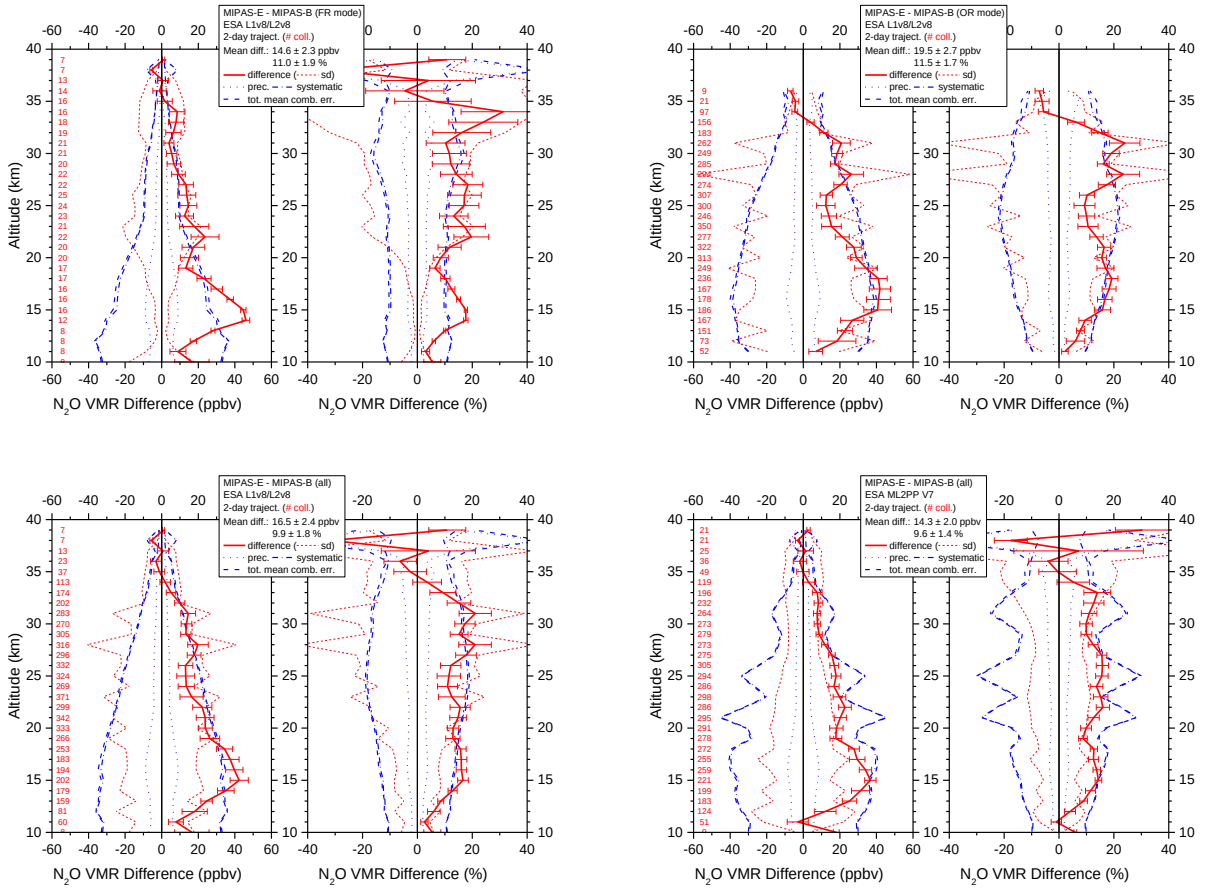

Figure 4-49 Mean absolute and relative N_2O VMR difference of all trajectory match collocations (red numbers) between MIPAS-E and MIPAS-B (red solid line) including standard deviation (red dotted lines) and standard error of the mean (plotted as error bars). Precision (blue dotted lines), systematic (blue dash-dotted lines), and total (blue dashed lines) mean combined errors are shown, too. Top: v8 FR mode (left) and v8 OR mode (right) collocations; bottom: all FR plus OR v8 (left) and all FR plus OR v7 (right) collocations.

The MIPAS N_2O V8 product has also been validated with respect to ground-based FTIR (Fourier-transform infrared) spectrometer observations that were obtained from the Network for the Detection of Atmospheric Composition Change (NDACC, www.ndacc.org). Using collocation criteria of 300 km and 3 hours, 3055 unique N_2O profile measurements from eight FTIR stations have been found to coincide with the MIPAS L2 V8 observations. Differences between collocated measurements were calculated for two vertically integrated N_2O subcolumns (9-12 and 12-30 km) with about one unit of information each [Vigouroux et at., 2007; Payan et al., 2009], and for vertically regridded N_2O profiles between 12 and 30 km [Calisesi et al., 2005]. Yearly medians (as relative bias) and 68 % interpercentiles (as vertical errors bars) of N2O subcolumn differences are shown for four MIPAS L2 versions at the Arctic Kiruna station in Figure 4-50. The median (bias) and 68 % interpercentile (spread) of the corresponding profile differences are added as well, whereby the MIPAS profiles have been vertically smoothed using the coincident FTIR averaging kernel matrices [Rodgers, 2000]. The subcolumn difference statistics for all eight FTIR stations, subdivided over five latitude bands, are collected in Table 4-3. The comparison results show a globally (without the Antarctic) and vertically consistent MIPAS N2O V8 bias of about 5 % positive and a similar spread, meaning that median differences are at the edge of being significant. The V8 (and V7) N2O bias is slightly

reduced with respect to the V5 and V6 bias results in the full resolution period, yet at the cost of a small bias increase in the optimised resolution period. Note however that the smoothed difference profile shape does not seem to be in agreement with the MIPAS balloon comparisons (also at Kiruna). The large comparison uncertainties moreover make it difficult to detect seasonal dependences or trends.

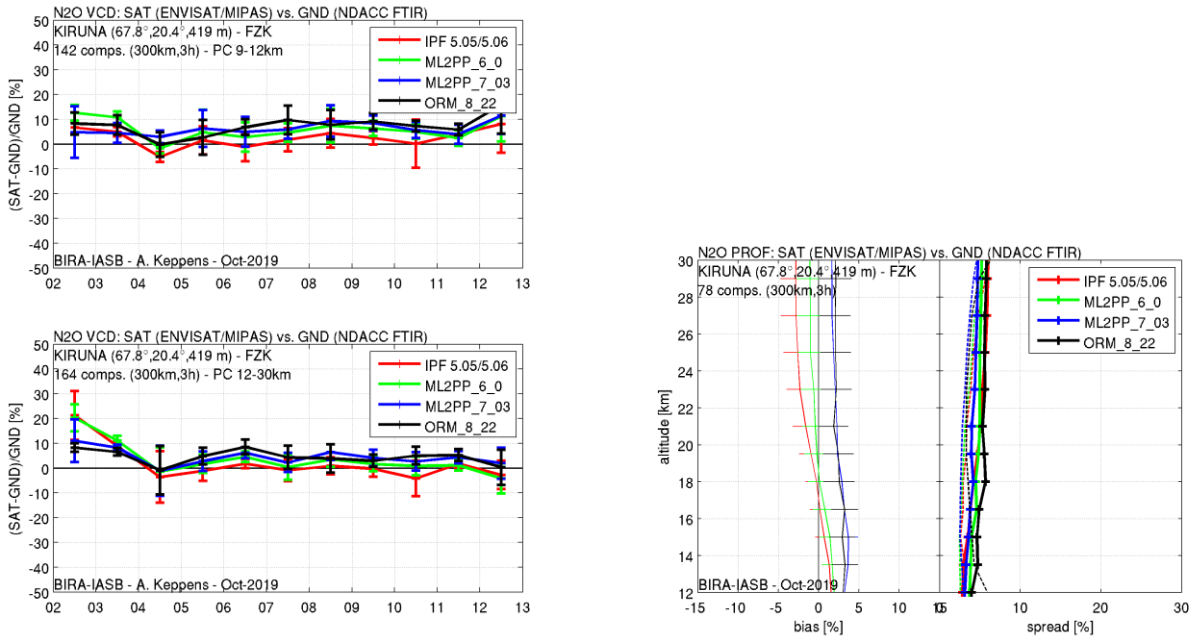

Figure 4-50 Yearly medians (as relative bias) and 68 % interpercentiles (as vertical errors bars) of MIPAS-FTIR N2O subcolumn differences (left, 9-12 km on top, 12-30 km bottom) for four MIPAS L2 versions at the Arctic Kiruna station. The right plot shows the median (bias) and 68 % interpercentile (spread) of the corresponding 12-30 km profile differences. The MIPAS profiles are thereby vertically smoothed using the coincident FTIR averaging kernel matrices.

Table 4-3 N2O subcolumn difference statistics for MIPAS L2 V8 retrievals versus coincident FTIR measurements, subdivided over five latitude bands.

	# stats.	# comps.	V8 bias [%]	V8 spread [%]	V8 bias [%]	V8 spread [%]
			9-12 km		12-30 km	
60N-90N	3	1394	6.7	6.2	6.3	5.6
30N-60N	3	1109	6.5	5.8	4.5	4.7
30N-30S	1	179	4.5	6.3	3.5	3.3
30S-60S	1	373	8.5	4.5	4.0	4.0
60S-90S	0	0	/	/	/	/

4.8 Nitrogen Dioxide (NO_2)

LEVEL 2 V8 NITROGEN DIOXIDE PRODUCTS										
Operational modes:	FR	RR	OR							
	NOM		NOM	UTLS1	MA	UA	AE	NLC	UTLS2	UTLS1_o
Nominal Vertical range [Km]	*12-68*	*18-68*	*18-70*	*18-49*	*18-69*	*42-69*	*17-38*	*39-69*	*12-42*	*22-49*
Useful range	*Full range*									
Microwindows:	*Link for downloading*									
Systematic errors:	*Link for downloading* *Link errors*									

Introduction

NO_2 exhibits a strong diurnal variation in the stratosphere and is in photochemical equilibrium with NO and N_2O_5. In Figure 4-51the time series of V8 NO_2 weekly mean profiles all over the mission averaged in the latitude band 90S-60S are reported for nighttime and daytime measurements. Large NO_2 values are visible in the mesosphere in the polar winter in correspondence of the solar proton events.

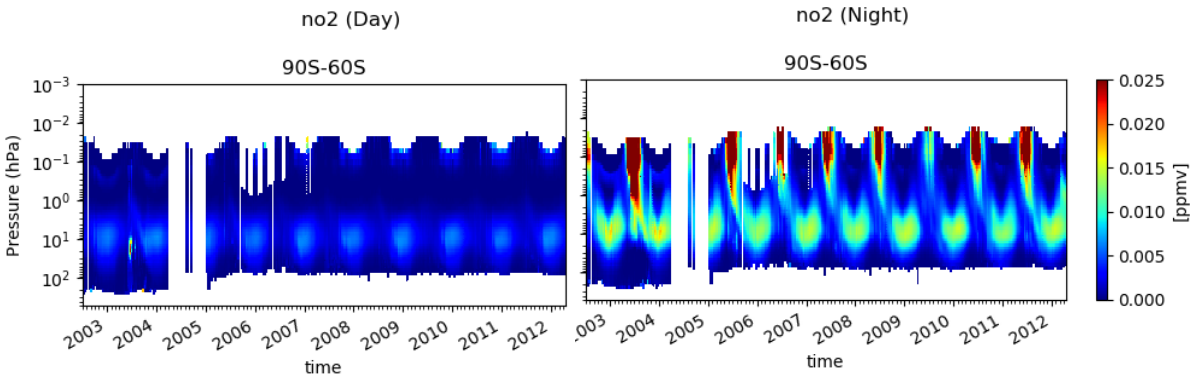

Figure 4-51 Timeseries of weekly mean of NO_2 on the full mission averaged on the latitude band 90S-60S for day-time and night-time conditions

For the analysis of OR measurements, a new MW selection was performed using the new error spectra for Non-LTE (link.). In particular, the old MW NO2_334 (1602.5-1605.5 cm-1), considered to be responsible of a positive bias of NO_2 during daytime at high altitudes due to the interference with a line of H_2O affected by Non-LTE, was removed and replaced by other MWs.

Verification and changes wrt V7 products

The effect of the change of the MWs used for the analysis of the OR measurements is a significant reduction of NO_2 daytime retrieved profile above 1 hPa, while the NO_2 nighttime profile is significantly less affected (see Figure 4-52).

The use of the new L1V8 files leads to a 3-5% reduction in NO_2 retrieved profiles.

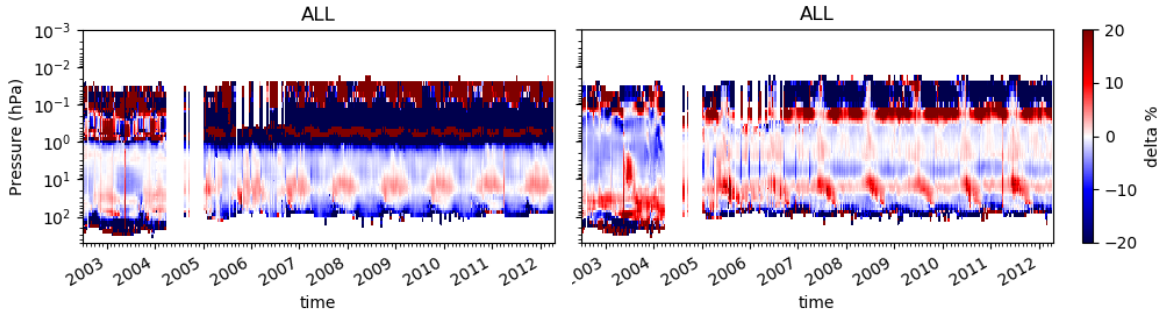

Figure 4-52 Timeseries of weekly mean differences between V8 and V7 NO_2 profiles all over the mission for daytime (left plot) and nighttime (right plot) conditions. Blue values mean that V8 NO_2 is smaller than V7 NO_2.

Quality quantifiers (AK and errors)

The vertical averaging kernels of the NO_2 retrieval are shown in Figure 4-53 for two representative profiles in Full Resolution nominal mode (left panel) and Optimised Resolution nominal mode (right panel). The selected scans are not affected by clouds. The vertical resolution profile of the considered scan is also reported in red in the same plot and the DOF distribution profile (see Sect.3.5.2) in blue. A mean vertical resolution profile has been also computed considering all scans in the nominal mode of 2003 (for FR plots) and 2010 (for OR plots). It is between 5 and 7 km in the altitude range 15-50 km for both FR and OR measurements, above it degrades up to 20-30 km.

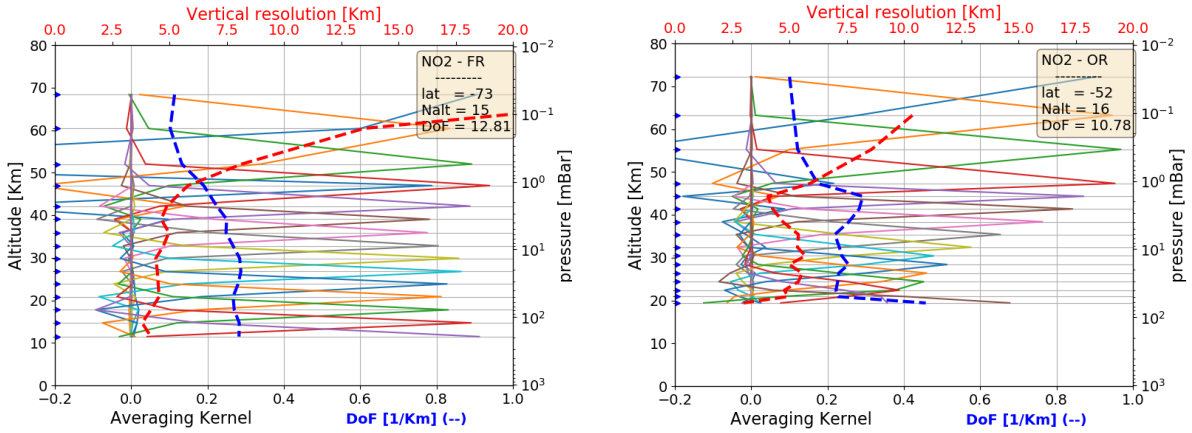

Figure 4-53 Example of NO_2 vertical averaging kernel (AK) computed for a representative Full Resolution (left panel) and Optimized Resolution (right panel) scan. Together with the AKs, the plots show the vertical resolution (red dashed line) and the Degree of Freedom for unity height (blue dashed line). The yellow box on the top right of each panel contains the latitude of the observation, the number of the measurement sweeps and the total Degree of Freedom (DoF)

Figure 4-54 shows the average NO_2 VMR profiles (left plots) and their associated average random error profiles, in absolute (middle plots) and relative (right plots) scale. The average quantities are representative of 5 reference atmospheres, namely polar summer daytime, polar winter nightime, mid-latitudes (both daytime and nightime) and equatorial daytime atmospheres. The averages have been computed using information on retrieved profiles, noise error and pT error which are contained in the output files for each scan. For mid latitude atmospheres all scans in the nominal mode of 2003 (for FR plots) and 2010 (for OR plots) in the latitude band 30-60 (both hemispheres) have been taken into account (considering either daytime or nightime scans), for equatorial atmosphere the scans in the latitude band 30S-30N, for polar winter nighttime atmosphere all nightime scans in the nominal mode of June-July-August of 2003 (for FR) and of 2005-2011 years (for OR) in the band 60S-90S, for polar summer daytime atmosphere all daytime scans in the nominal mode of December-January-February of 2003 (for FR) and 2005-2011 (for OR) in the latitude band 60S-90S. Solid lines of middle and right plots represent the total random error, coming from the quadratic summation of the noise error (dotted curves, given by the mapping of the measurement error on the retrieved profile) and the pT error (given by the propagation of the random error of retrieved pressure and temperature profiles on VMR profile). The contribution coming from the pT error propagation is generally smaller than the noise contribution. The percent error varies with altitude and for the different atmospheres but it is within 5% in all cases between 20 and 2 hPa.

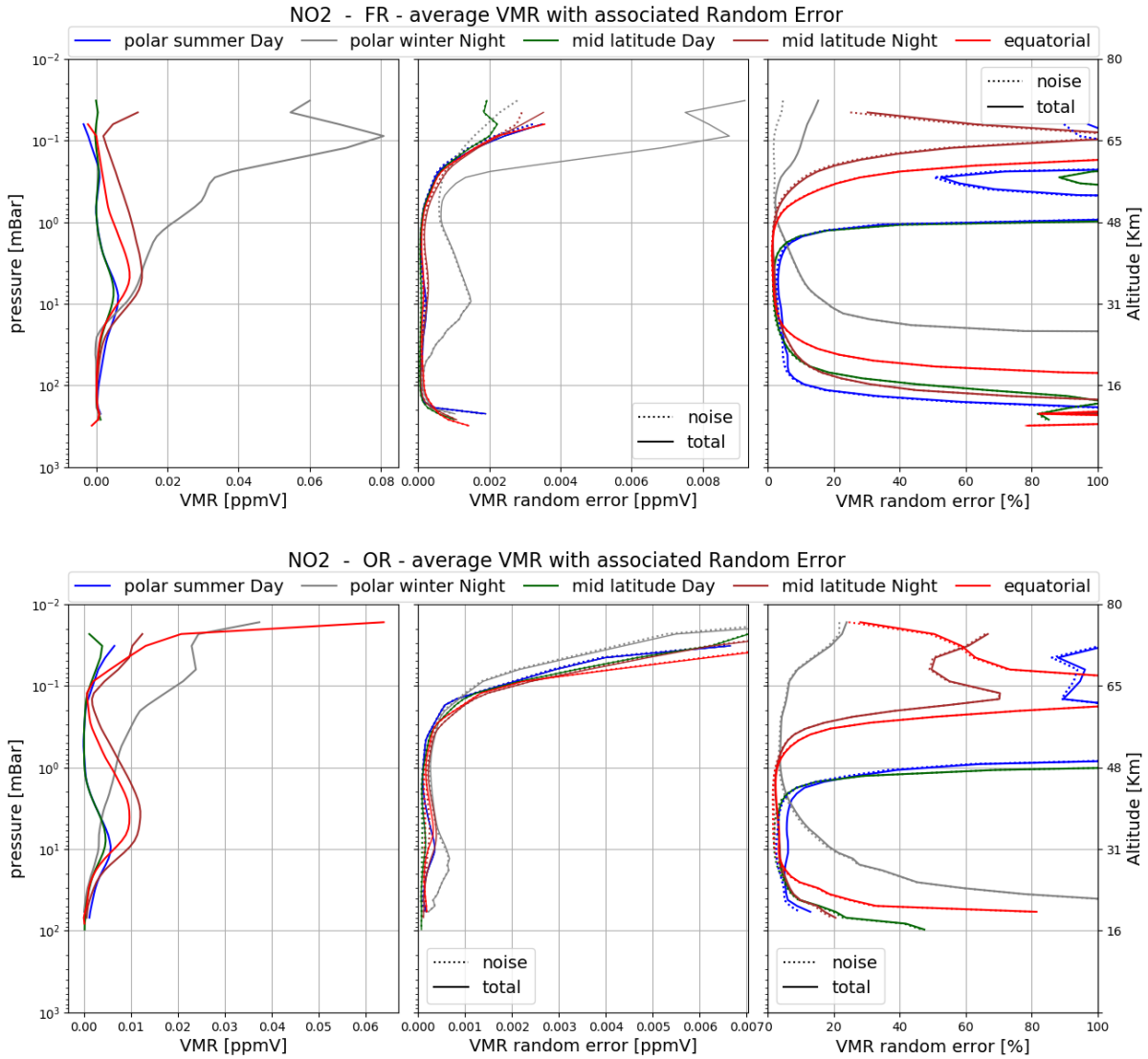

Figure 4-54 Average NO_2 VMR (left plots), absolute (mid plots) and relative (right plots) NO_2 random error for the 5 reference atmospheres described in the text. The noise error (dotted curves) is calculated by the retrieval; the total random error (solid curves) includes the contribution to the random error coming from propagation of the pT random error on VMR profiles. Top panel: Full Resolution nominal mode; bottom panel: Optimized Resolution nominal mode.

Validation

Reference instrument	Source	Coverage validation analysis		
		Time	Horizontal	Vertical
MIPAS-B	KIT-IMK	8 flights + 2-day trajectories	3 sites, 68°N–5°S	100–2 hPa

Figure 4-55 presents the statistical trajectory match analysis between both MIPAS instruments Potential VMR differences due to different solar zenith angles during the data recording were corrected with the help

of photochemical modelling (see Wetzel et al., 2007, and Technical Note by Wetzel et al., 2020). It indicates a positive bias (up to 20%, exceeding the combined systematic errors above 31 km) of MIPAS-E NO_2 in the FR period that is becoming increasingly significant from lower to higher altitudes. In the OR period, the positive bias (above 27 km) between both sensors is smaller (~10%). No striking changes compared to the previous v7 data can be recognized.

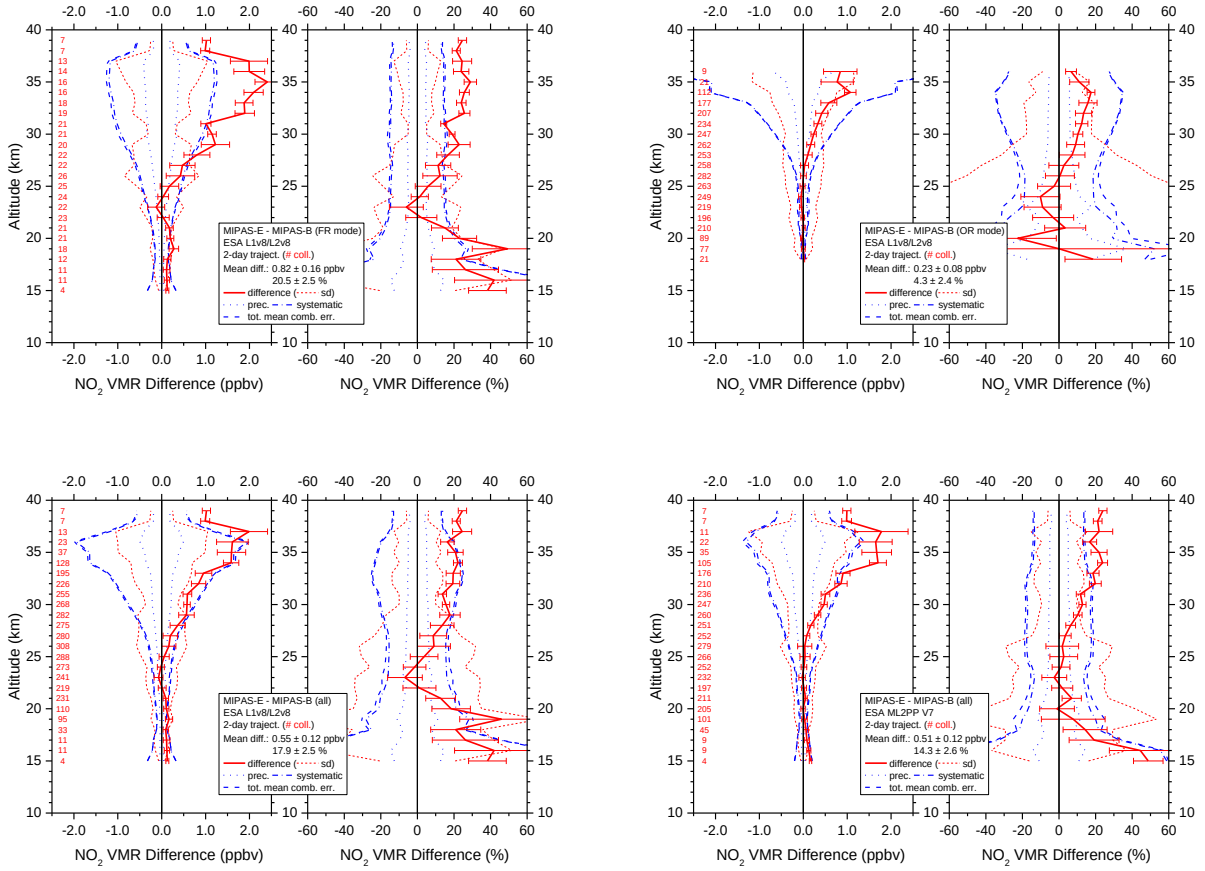

Figure 4-55 Mean absolute and relative NO_2 VMR difference of all trajectory match collocations (red numbers) between MIPAS-E and MIPAS-B (red solid line) including standard deviation (red dotted lines) and standard error of the mean (plotted as error bars). Precision (blue dotted lines), systematic (blue dash-dotted lines), and total (blue dashed lines) mean combined errors are shown, too. Top: v8 FR mode (left) and v8 OR mode (right) collocations; bottom: all FR plus OR v8 (left) and all FR plus OR v7 (right) collocations.

4.9 Trichloro(fluoro)methane (CFC-11)

LEVEL 2 V8 CFC-11 ***PRODUCTS***

Operational modes:	FR	RR	OR							
	NOM		NOM	UTLS1	MA	UA	AE	NLC	UTLS2	UTLS1_o
Nominal Vertical range [Km]	*6-33*	*6-33*	*6-34*	*6-34*	*18-33*	---	*7-33.5*	---	*12-33*	*10-39*
Useful range	*Full range*									
Microwindows:	*Link for downloading*									
Systematic errors:	*Link for downloading* *Link errors*									

Introduction

CFC-11 is an ozone depleting substance regulated by Montreal protocol and a powerful green-house gas. In Figure 4-56 the timeseries of CFC-11 profiles on the full mission averaged on latitude band 60N-90N are reported.

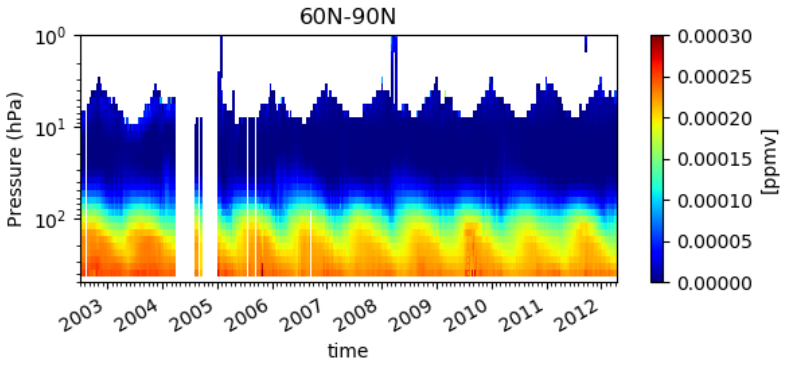

Figure 4-56 Timeseries of weekly mean of CFC-11 on the full mission averaged on all latitudes

A negative trend is clearly observed in the timeseries.

Verification and changes wrt V7 products

In Figure 4-57 we report the difference between V8 and V7 products. Below 20 hPa V8 is 2-3% smaller than V7, above 20 hPa V8 is larger.

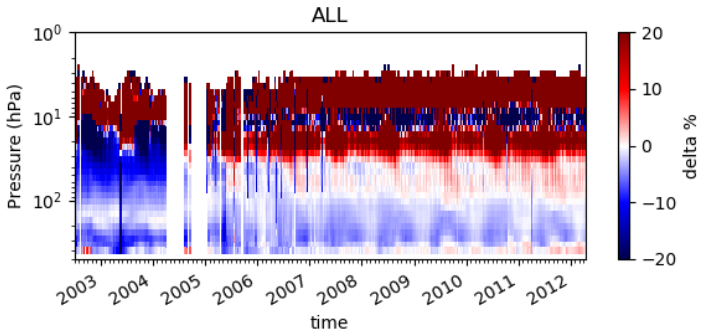

Figure 4-57 Timeseries of weekly mean differences between V8 and V7 CFC-11 profiles all over the mission. Blue values indicate that V8 CFC-11 is smaller than V7 CFC-11.

The main change in V8 reprocessing comes from the use of the new cross-sections for CFC-11 (Harrison, 2018). The use of the new cross-sections brings to a 2-3% reduction of the retrieved profile.

Quality quantifiers (AK and errors)

The vertical averaging kernels of the CFC-11 retrieval are shown in Figure 4-58 for two representative profiles in Full Resolution nominal mode (left panel) and Optimised Resolution nominal mode (right panel). The selected scans are not affected by clouds. The vertical resolution profile of the considered scan is also reported in red in the same plot and the DOF distribution profile (see Sect.3.5.2) in blue. A mean vertical resolution profile has been also computed considering all scans in the nominal mode of 2003 (for FR plots) and 2010 (for OR plots). It varies from 5 to 7 km in the range 6 - 35 km for both FR and OR measurements.

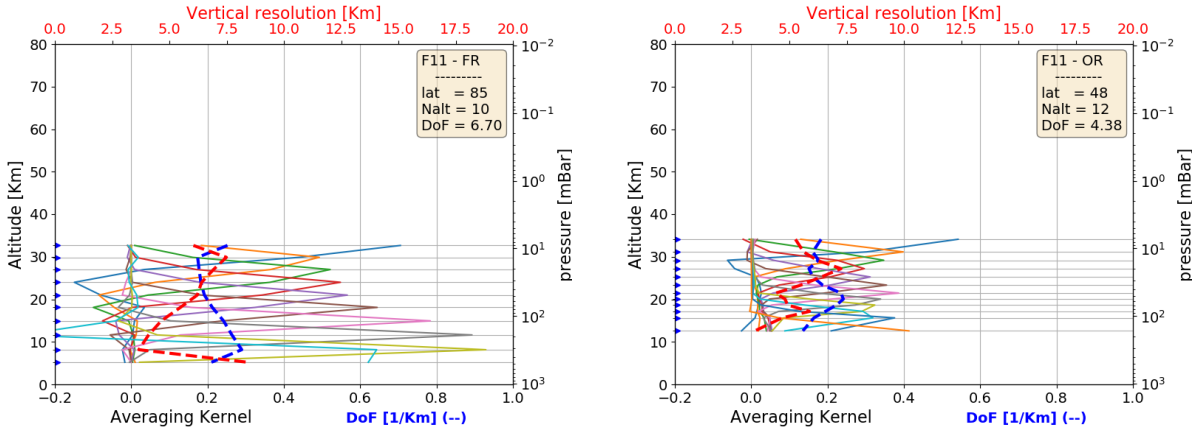

Figure 4-58 Example of CFC-11 vertical averaging kernel (AK) computed for a representative Full Resolution (left panel) and Optimized Resolution (right panel) scan. Together with the AKs, the plots show the vertical resolution (red dashed line) and the Degree of Freedom for unity height (blue dashed line). The yellow box on the top right of each panel contains the latitude of the observation, the number of the measurement sweeps and the total Degree of Freedom (DoF)

Figure 4-59 shows the average CFC-11 VMR profiles (left plots) and their associated average random error profiles, in absolute (middle plots) and relative (right plots) scale. The average quantities are representative of 5 reference atmospheres, namely polar summer daytime, polar winter nightime, mid-latitudes (both daytime and nightime) and equatorial daytime atmospheres. The averages have been computed using information on retrieved profiles, noise error and pT error which are contained in the output files for each scan. For mid latitude atmospheres all scans in the nominal mode of 2003 (for FR plots) and 2010 (for OR plots) in the latitude band 30-60 (both hemispheres) have been taken into account (considering either daytime or nightime scans), for equatorial atmosphere the scans in the latitude band 30S-30N, for polar winter nighttime atmosphere all nightime scans in the nominal mode of June-July-August of 2003 (for FR) and of 2005-2011 years (for OR) in the band 60S-90S, for polar summer daytime atmosphere all daytime scans in the nominal mode of December-January-February of 2003 (for FR) and 2005-2011 (for OR) in the latitude band 60S-90S. Solid lines of middle and right plots represent the total random error, coming from the quadratic summation of the noise error (dotted curves, given by the mapping of the measurement error on the retrieved profile) and the pT error (given by the propagation of the random error of retrieved pressure and temperature profiles on VMR profile). The contribution coming from the pT error propagation is generally smaller than the noise contribution. The relative random error is 2-3% up to 100 hPa, then it rapidly increases also as a consequence of the reduction of the VMR.

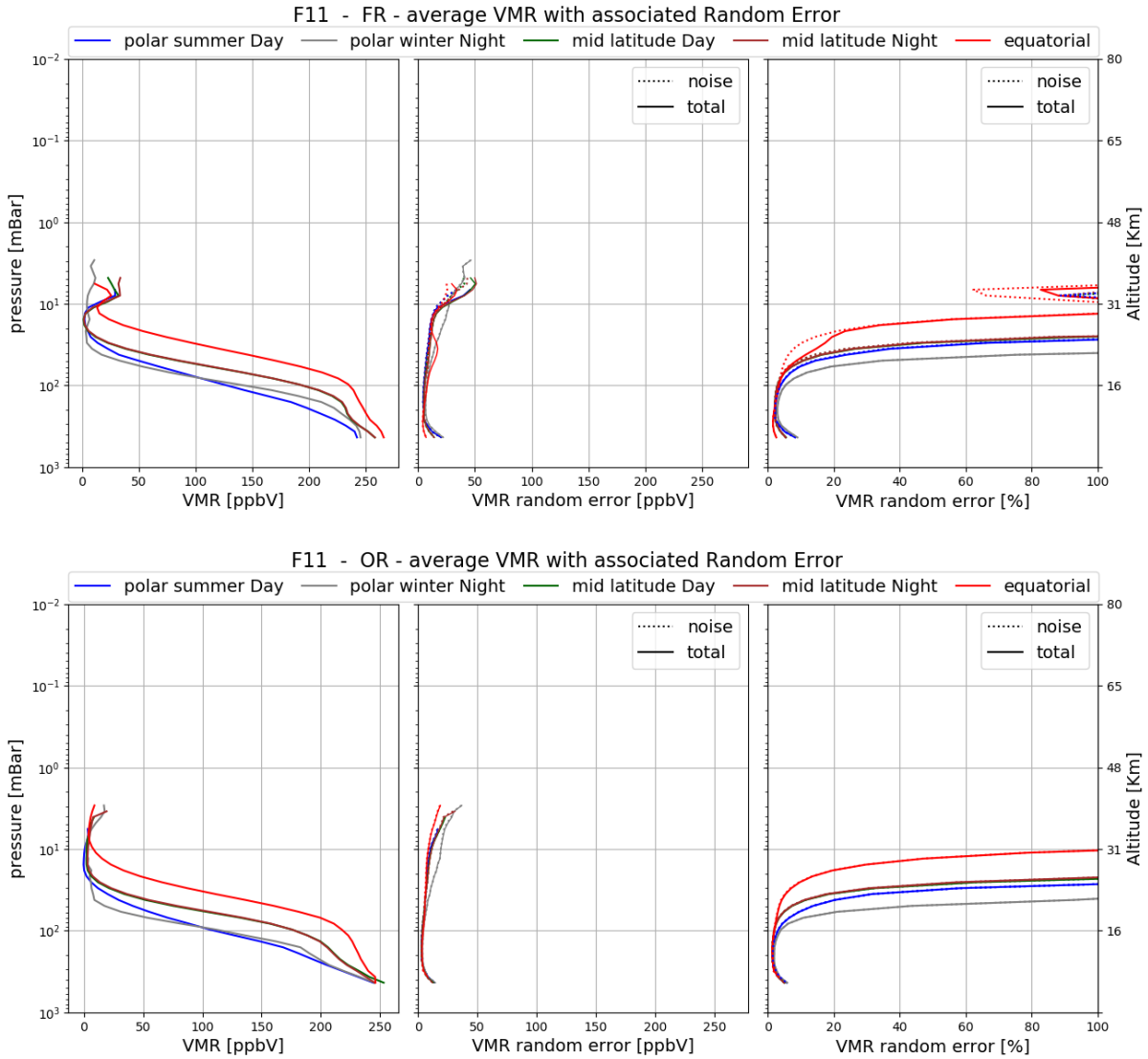

Figure 4-59 Average CFC-11 VMR (left plots), absolute (mid plots) and relative (right plots) CFC-11 random error for the 5 reference atmospheres described in the text. The noise error (dotted curves) is calculated by the retrieval; the total random error (solid curves) includes the contribution to the random error coming from propagation of the pT random error on VMR profiles. Top panel: Full Resolution nominal mode (average 2003); bottom panel: Optimized Resolution nominal mode (average on 2010).

Validation

Reference instrument	Source	Coverage validation analysis		
		Time	Horizontal	Vertical
MIPAS-B	KIT-IMK	8 flights + 2-day trajectories	3 sites, 68°N–5°S	200–10 hPa

Results for the long-lived chlorofluorocarbon CFC-11 (CCl_3F) are shown in Figure 4-60. Deviations between both MIPAS instruments amount up to ±10% below 20 km. An increasing positive bias is visible above this altitude level. Some enhanced negative deviations below 15 km compared to previous V7 data are obvious.

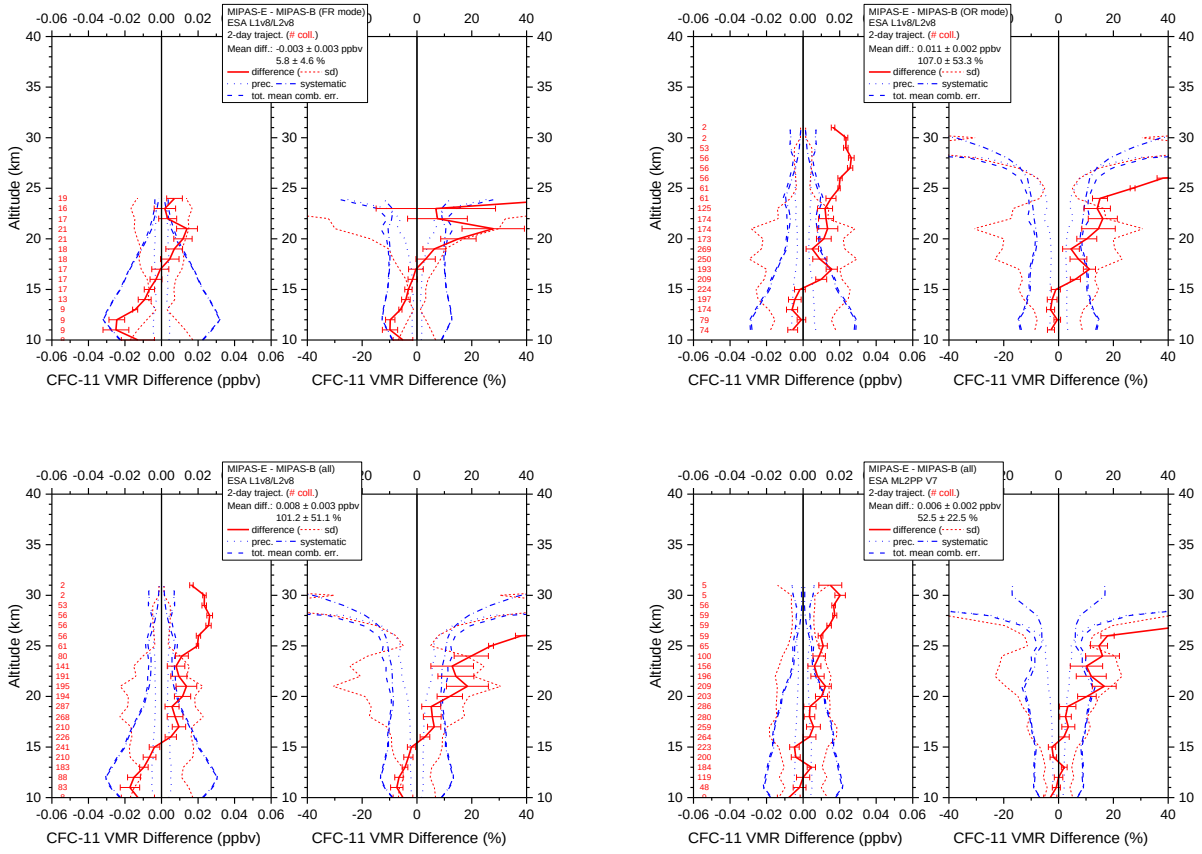

Figure 4-60 Mean absolute and relative CFC-11 VMR difference of all trajectory match collocations (red numbers) between MIPAS-E and MIPAS-B (red solid line) including standard deviation (red dotted lines) and standard error of the mean (plotted as error bars). Precision (blue dotted lines), systematic (blue dash-dotted lines), and total (blue dashed lines) mean combined errors are shown, too. Top: v8 FR mode (left) and v8 OR mode (right) collocations; bottom: all FR plus OR v8 (left) and all FR plus OR v7 (right) collocations.

4.10 Chlorine Nitrate ($ClONO_2$)

LEVEL 2 V8 CHLORINE NITRATE PRODUCTS

Operational modes:	FR	RR	OR							
	NOM		NOM	UTLS1	MA	UA	AE	NLC	UTLS2	UTLS1_o
Nominal Vertical range [Km]	*15-42*	*15-42*	*13.5-43**	*13.5-43**	*18-42*	---	*13-38*	---	*12-42*	*17.5-39-*
Useful range	*All altitudes up to 40 km (pressures greater than 3 hPa)*									
Microwindows:	*Link for downloading*									
Systematic errors:	*Link for downloading* *Link errors*									

*Floating altitude

Introduction

$ClONO_2$ is a major reservoir of reactive chlorine in the stratosphere and is involved in heterogeneous chemistry in the context of ozone depletion at high latitudes. It undergoes diurnal variations at higher altitudes during periods of stronger illumination. In Figure 4-61 we present the timeseries of V8 $ClONO_2$ in the latitude band 90S-60S and 30S-0 on the full mission for both daytime and nighttime observations.

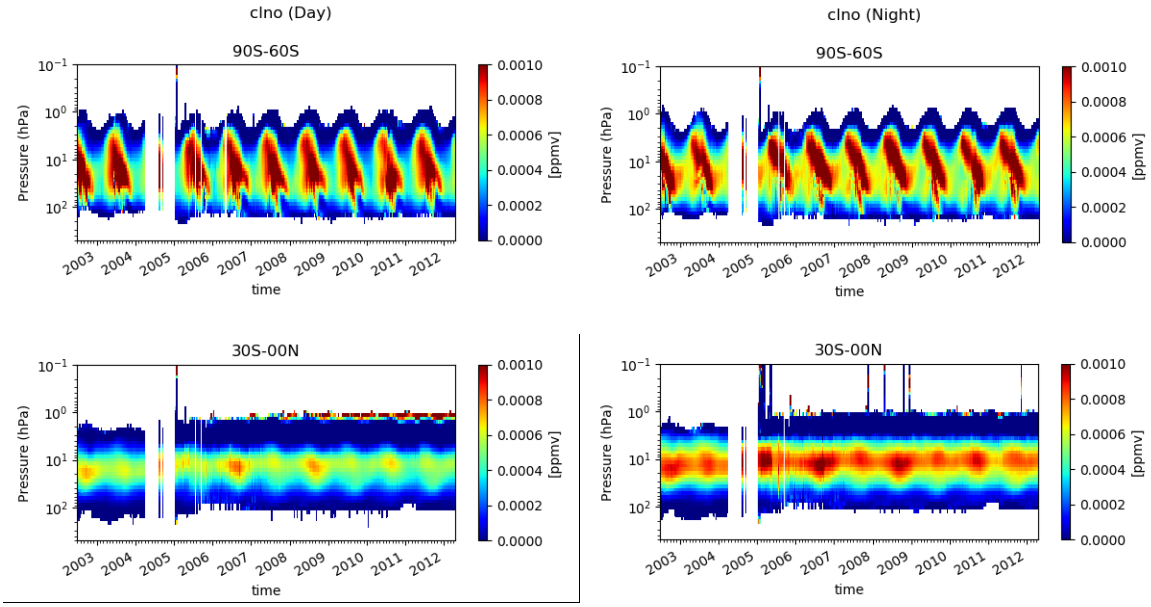

Figure 4-61 Timeseries of weekly mean of $ClONO_2$ on the full mission averaged on the latitude band 90S-60S and 30S-0 for both day-time (maps on the left) and night-time (maps on the right) conditions.

Verification and changes wrt V7 products

Relative differences between V8 $ClONO_2$ and V7 $ClONO_2$ are significant close to the borders of the retrieval range, where the VMR decreases, see Figure 4-62.

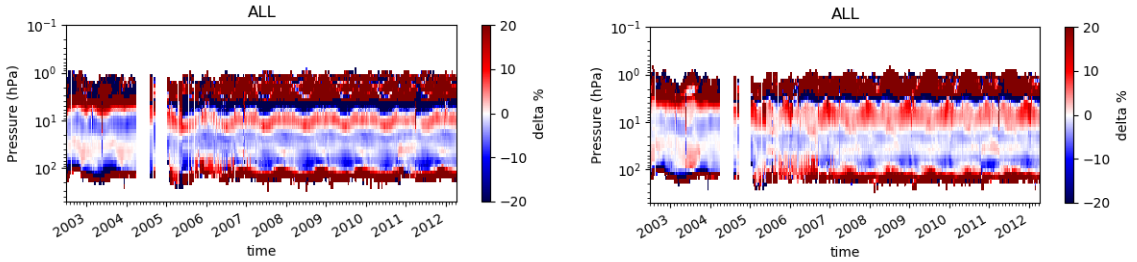

Figure 4-62 Timeseries of weekly mean differences between V8 and V7 $ClONO_2$ profiles all over the mission for both day-time (map on the left) and night-time (map on the right) conditions

Quality quantifiers (AK and errors)

The vertical averaging kernels of the $ClONO_2$ retrieval are shown in Figure 4-63 for two representative profiles in Full Resolution nominal mode (left panel) and Optimised Resolution nominal mode (right panel). The selected scans are not affected by clouds. The vertical resolution profile of the considered scan is also reported in red in the same plot and the DOF distribution profile (see Sect. 3.5.2) in blue. A mean vertical resolution profile has been also computed considering all scans in the nominal mode of 2003 (for FR plots) and 2010 (for OR plots). It goes from 3 (5) km at 12 km to 7.5 (10) at 45 km for FR (OR) measurements.

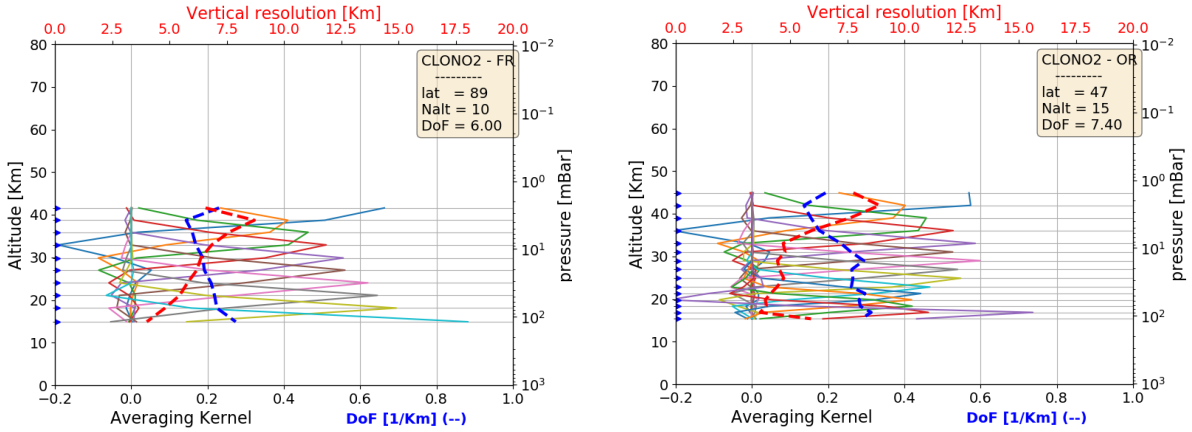

Figure 4-63 Example of $ClONO_2$ vertical averaging kernel (AK) computed for a representative Full Resolution (left panel) and Optimized Resolution (right panel) scan. Together with the AKs, the plots show the vertical resolution (red dashed line) and the Degree of Freedom for unity height (blue dashed line). The yellow box on the top right of each panel contains the latitude of the observation, the number of the measurement sweeps and the total Degree of Freedom (DoF)

Figure 4-64 shows the average $ClONO_2$ VMR profiles (left plots) and their associated average random error profiles, in absolute (middle plots) and relative (right plots) scale. The average quantities are representative of 5 reference atmospheres, namely polar summer daytime, polar winter nightime, mid-latitudes (both daytime and nightime) and equatorial daytime atmospheres. The averages have been computed using information on retrieved profiles, noise error and pT error which are contained in the output files for each scan. For mid latitude atmospheres all scans in the nominal mode of 2003 (for FR plots) and 2010 (for OR plots) in the latitude band 30-60 (both hemispheres) have been taken into account (considering either daytime or nightime scans), for equatorial atmosphere the scans in the latitude band 30S-30N, for polar winter nighttime atmosphere all nightime scans in the nominal mode of June-July-August of 2003 (for FR) and of 2005-2011 years (for OR) in the band 60S-90S, for polar summer daytime atmosphere all daytime scans in the nominal mode of December-January-February of 2003 (for FR) and 2005-2011 (for OR) in the latitude band 60S-90S. Solid lines of middle and right plots represent the total random error, coming from the quadratic summation of the noise error (dotted curves, given by the mapping of the measurement error on the retrieved profile) and the pT error (given by the propagation of the random error of retrieved pressure and temperature profiles on VMR profile). The contribution coming from the pT error propagation is generally smaller than the noise contribution. Relative random errors of about 5% are obtained for most atmospheres around the peak of the profile, errors rapidly increase at high and low altitudes.

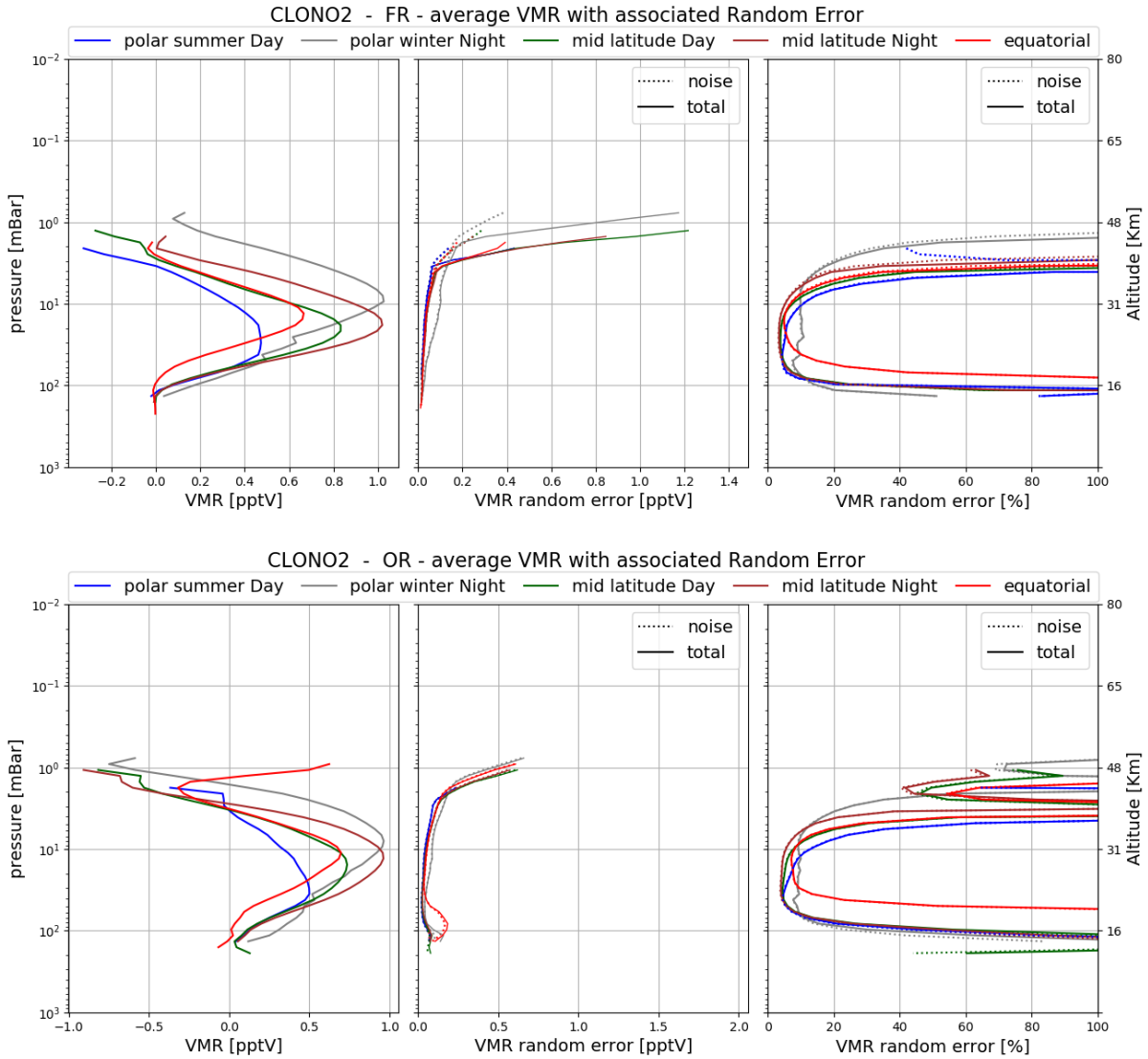

Figure 4-64 Average $ClONO_2$ VMR (left plots), absolute (mid plots) and relative (right plots) $ClONO_2$ random error for the 5 reference atmospheres described in the text. The noise error (dotted curves) is calculated by the retrieval; the total random error (solid curves) includes the contribution to the random error coming from propagation of the pT random error on VMR profiles. Top panel: Full Resolution nominal mode; bottom panel: Optimized Resolution nominal mode.

Validation

Reference instrument	Source	Coverage validation analysis		
		Time	Horizontal	Vertical
MIPAS-B	KIT-IMK	8 flights + 2-day trajectories	3 sites, 68°N–5°S	200–2 hPa

Figure 4-65 presents the intercomparison results for all MIPAS satellite and balloon collocations. In the altitude region where $ClONO_2$ concentrations are most relevant both data sets are consistent. Differences are within ±10% between 17 and 34 km without a clear bias. Only at the upper and lower altitude edge of the comparisons the mean differences exceed the combined systematic errors. However, standard deviations clearly exceed the expected precision. No striking changes compared to v7 data are visible.

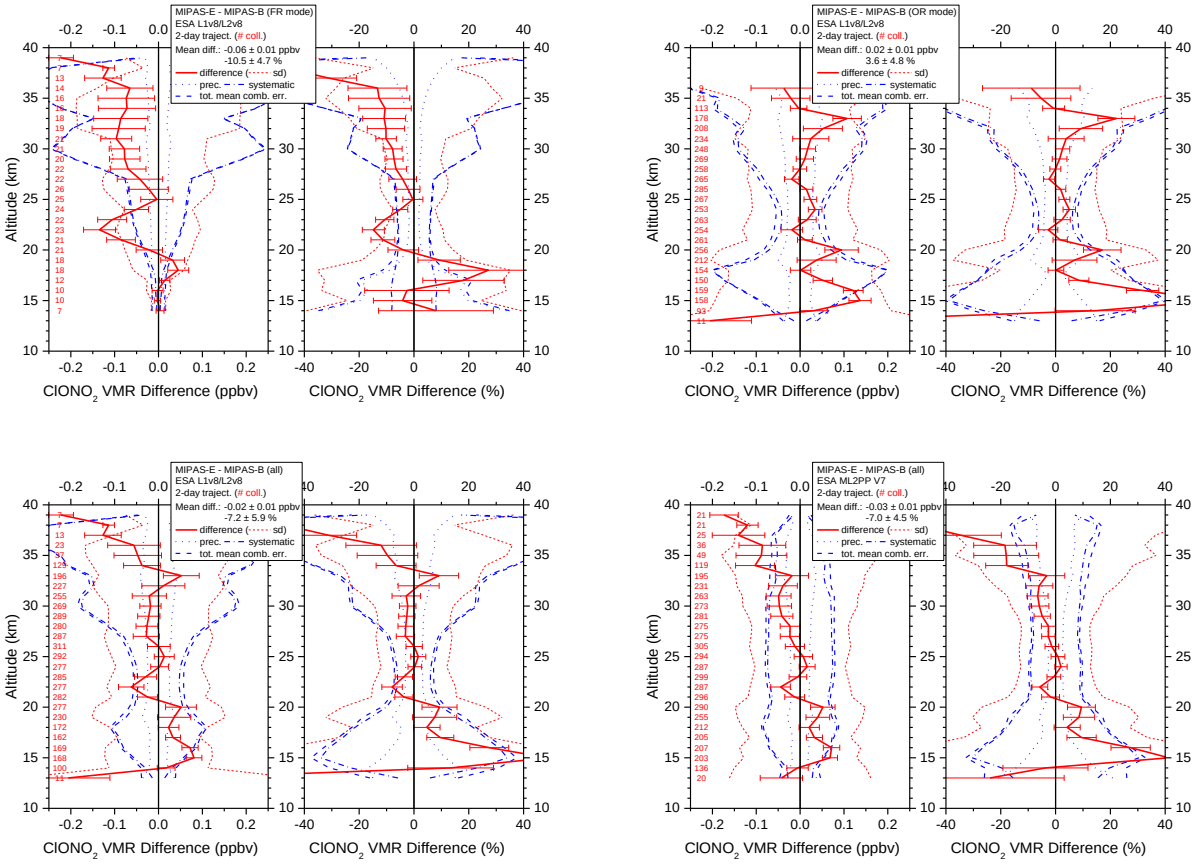

Figure 4-65 Mean absolute and relative $ClONO_2$ VMR difference of all trajectory match collocations (red numbers) between MIPAS-E and MIPAS-B (red solid line) including standard deviation (red dotted lines) and standard error of the mean (plotted as error bars). Precision (blue dotted lines), systematic (blue dash-dotted lines), and total (blue dashed lines) mean combined errors are shown, too. Top: v8 FR mode (left) and v8 OR mode (right) collocations; bottom: all FR plus OR v8 (left) and all FR plus OR v7 (right) collocations.

4.11 Dinitrogen Pentoxide (N_2O_5)

LEVEL 2 V8 DINITROGEN PENTOXIDE PRODUCTS										
Operational modes:	FR	RR	OR							
	NOM		NOM	UTLS1	MA	UA	AE	NLC	UTLS2	UTLS1_o
Nominal Vertical range [Km]	*15-42*	*15-42*	*15-46**	*16-46**	*18-45*	---	*15-38*	---	*12-42*	*19-49*
Useful range	*All altitudes greater than 18 km (pressures smaller than 100 hPa)*									
Microwindows:	*Link for downloading*									
Systematic errors:	*Link for downloading* *Link errors*									

*Floating altitude

Introduction

N_2O_5 is a temporary reservoir of reactive nitrogen in the stratosphere and exhibits a prominent diurnal variation with maxima just before sunrise and minima just before sunset. In Figure 4-66 we present the timeseries of V8 N_2O_5 in the latitude band 90S-60S on the full mission for day-time and night-time observations.

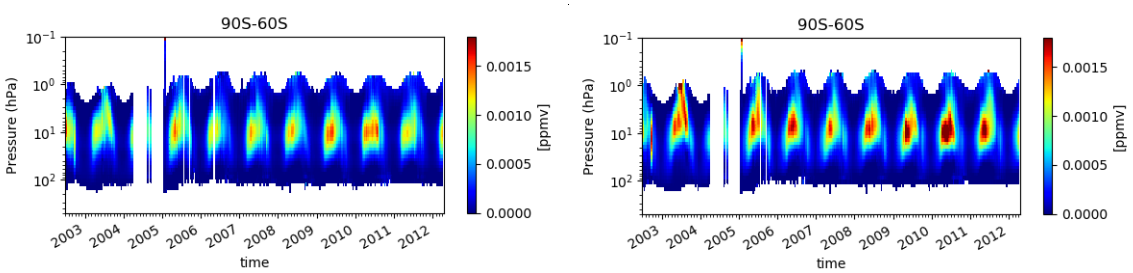

Figure 4-66 Timeseries of weekly mean of N_2O_5 on the full mission averaged on the latitude band 90S-60S for both day-time and night-time conditions

Verification and changes wrt V7 products

In Figure 4-67 the time series of weekly mean relative differences between V8 and V7 N_2O_5 for both day-time (map on the left) and night-time (map on the right) conditions are shown. Large percent differences are found at the borders of the retrieval range where the VMR is very small, differences smaller than 3% are found around the peak. As for V7, a single profile for the atmospheric continuum across the N_2O_5 emission features instead of one for each used microwindow is retrieved. This improves the stability of the retrieval but leads to a reduction of up to 10% of the values of the retrieved profile.

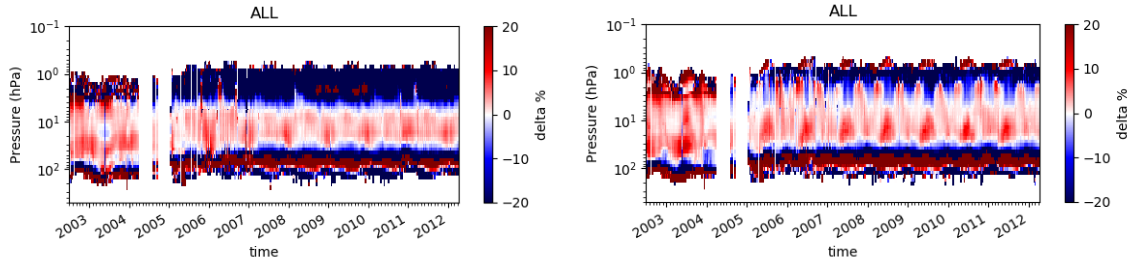

Figure 4-67 Timeseries of weekly mean percent differences between V8 and V7 N_2O_5 profiles for both day-time (map on the left) and night-time (map on the right) conditions all over the mission.

Quality quantifiers (AK and errors)

The vertical averaging kernels of the N_2O_5 retrieval are shown in Figure 4-68 for two representative profiles in Full Resolution nominal mode (left panel) and Optimised Resolution nominal mode (right panel). The selected scans are not affected by clouds. The vertical resolution profile of the considered scan is also reported in red in the same plot and the DOF distribution profile (see Sect. 3.5.2) in blue. A mean vertical resolution profile has been also computed considering all scans in the nominal mode of 2003 (for FR plots) and 2010 (for OR plots). It varies from 5 km at 15 km to 7km at 30 km, to 7.5 at 50 km for both FR and OR measurements.

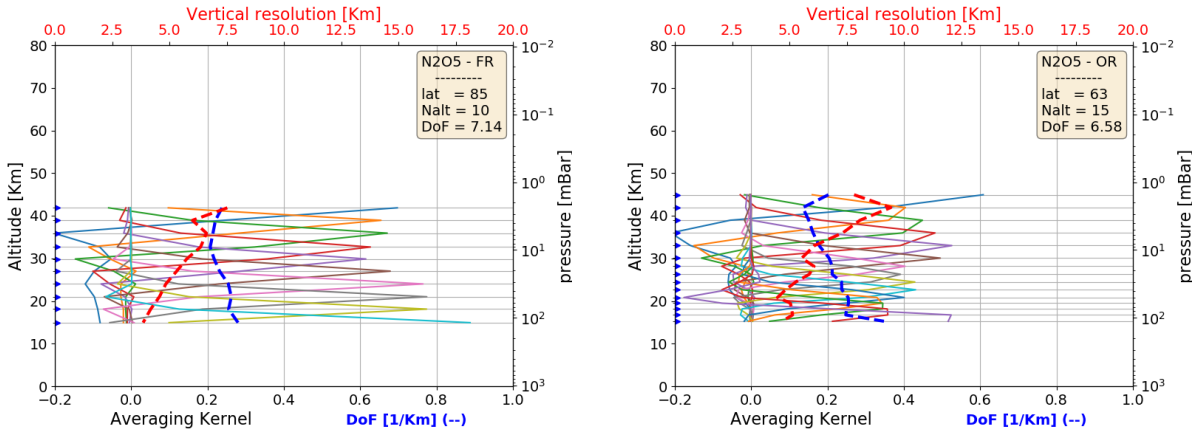

Figure 4-68 Example of N_2O_5 vertical averaging kernel (AK) computed for a representative Full Resolution (left panel) and Optimized Resolution (right panel) scan. Together with the AKs, the plots show the vertical resolution (red dashed line) and the Degree of Freedom for unity height (blue dashed line). The yellow box on the top right of each panel contains the latitude of the observation, the number of the measurement sweeps and the total Degree of Freedom (DoF)

Figure 4-69 shows the average N_2O_5 VMR profiles (left plots) and their associated average random error profiles, in absolute (middle plots) and relative (right plots) scale. The average quantities are representative of 5 reference atmospheres, namely polar summer daytime, polar winter nightime, mid-latitudes (both daytime and nightime) and equatorial daytime atmospheres. The averages have been computed using information on retrieved profiles, noise error and pT error which are contained in the output files for each scan. For mid latitude atmospheres all scans in the nominal mode of 2003 (for FR plots) and 2010 (for OR plots) in the latitude band 30-60 (both hemispheres) have been taken into account (considering either daytime or nightime scans), for equatorial atmosphere the scans in the latitude band 30S-30N, for polar winter nighttime atmosphere all nightime scans in the nominal mode of June-July-August of 2003 (for FR) and of 2005-2011 years (for OR) in the band 60S-90S, for polar summer daytime atmosphere all daytime scans in the nominal mode of December-January-February of 2003 (for FR) and 2005-2011 (for OR) in the latitude band 60S-90S. Solid lines of middle and right plots represent the total random error, coming from the quadratic summation of the noise error (dotted curves, given by the mapping of the measurement error on the retrieved profile) and the pT error (given by the propagation of the random error of retrieved pressure and temperature profiles on VMR profile). The contribution coming from the pT error propagation is generally smaller than the noise contribution. With the only exception of the polar summer case where the profile is very small and hence the relative random error is very large, for all other atmospheres relative random errors of about 5% are obtained around the peak of the profile, errors rapidly increase at high and low altitudes.

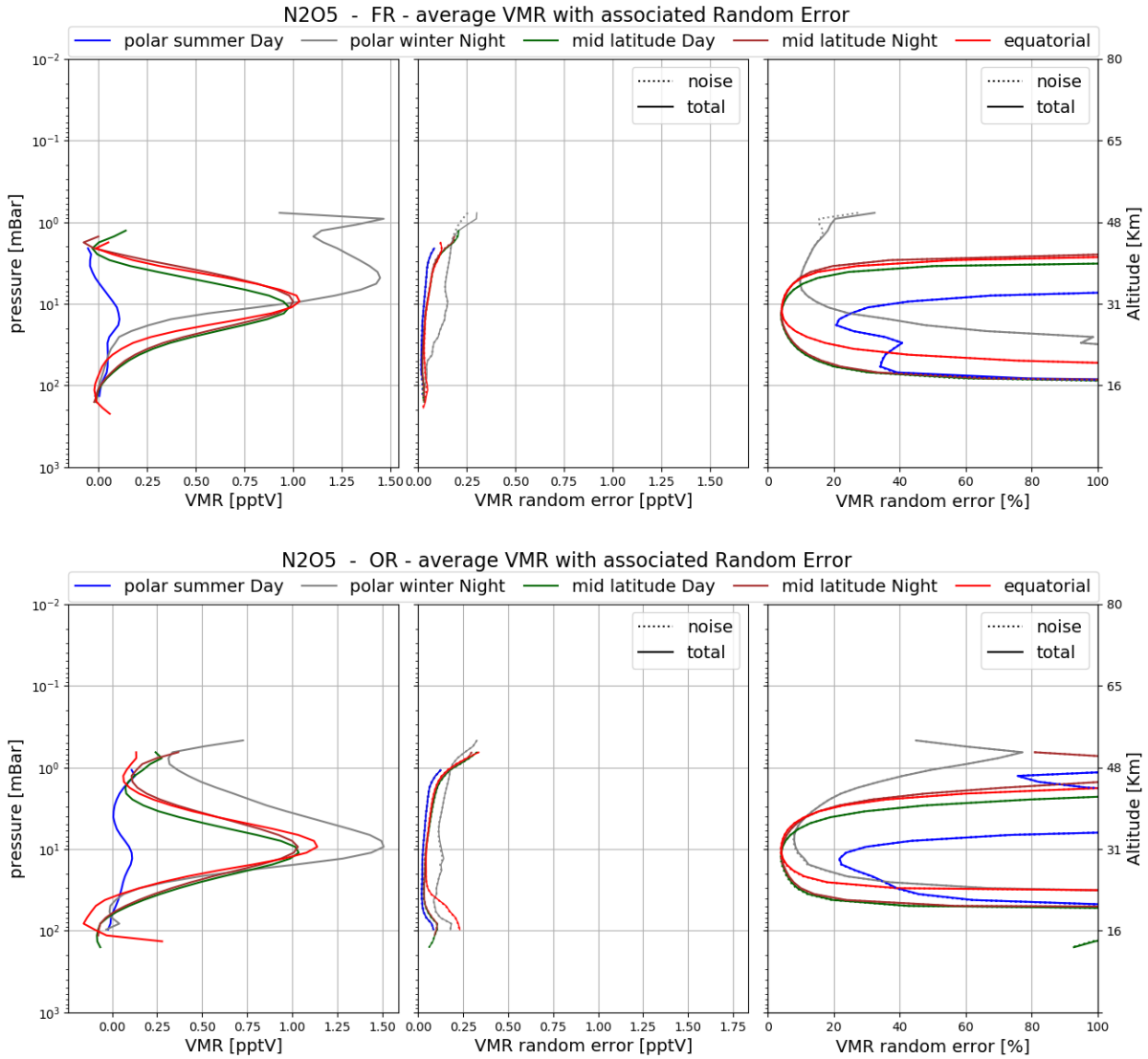

Figure 4-69 Average N_2O_5 VMR (left plots), absolute (mid plots) and relative (right plots) N_2O_5 random error for the 5 reference atmospheres described in the text. The noise error (dotted curves) is calculated by the retrieval; the total random error (solid curves) includes the contribution to the random error coming from propagation of the pT random error on VMR profiles. Top panel: Full Resolution nominal mode; bottom panel: Optimized Resolution nominal mode.

Validation

Reference instrument	Source	Coverage validation analysis		
		Time	Horizontal	Vertical
MIPAS-B	KIT-IMK	8 flights + 2-day trajectories	3 sites, 68°N–5°S	100–2 hPa

The general agreement between MIPAS-E and MIPAS-B (Figure 4-70) is within ±10% between 24 and 34 km for the mean of all collocations. Potential VMR differences due to different solar zenith angles during the data recording were corrected with the help of photochemical modelling (see Wetzel et al., 2013b, and Technical Note by Wetzel et al., 2020). The behaviour of the complete vertical profile of the mean difference suggests slightly different VMR profiles measured by both instruments (especially in the tropics). Below 24 km and above 34 km mean differences exceed at least partly the systematic errors suggesting a careful use of the MIPAS-E N_2O_5 data for scientific studies in these altitude regimes. No significant bias is visible in the OR mode but a small negative bias is obvious in the FR period. No striking changes compared to v7 data are noticeable.

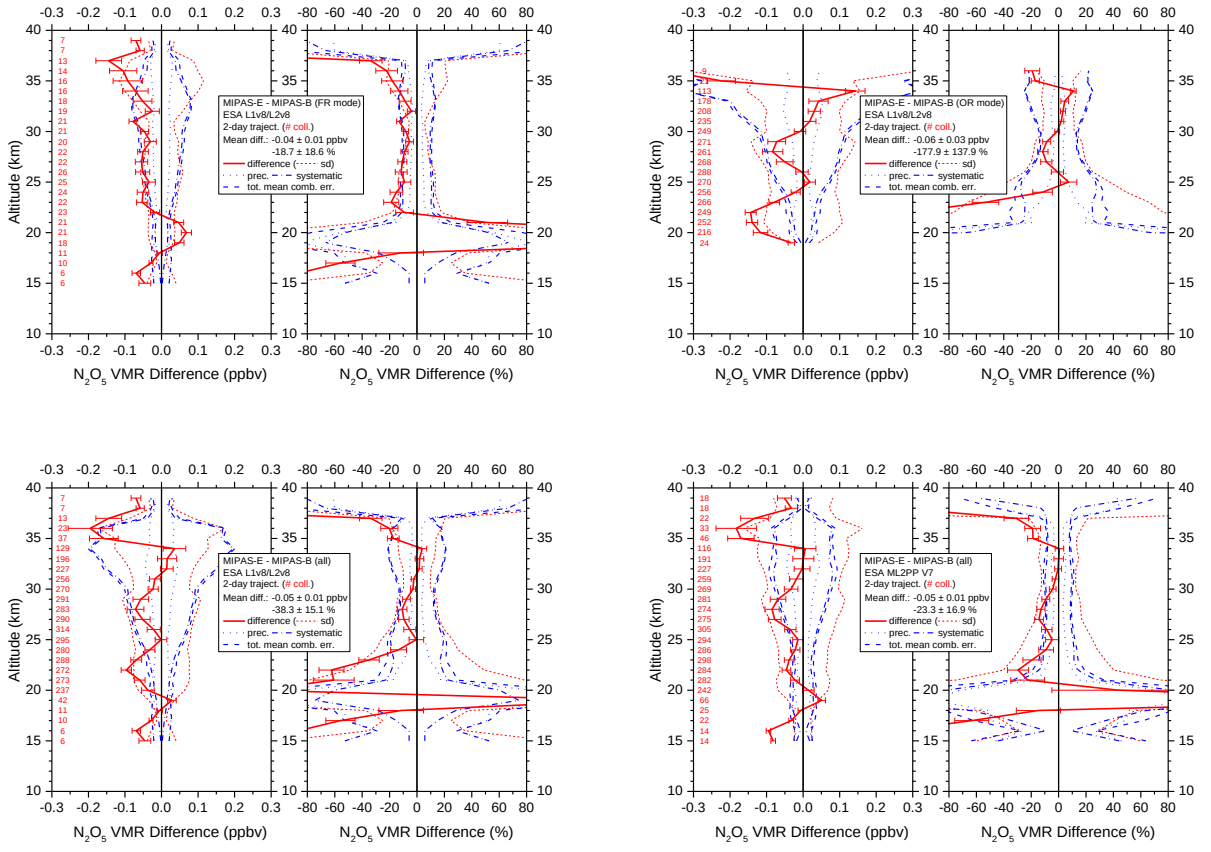

Figure 4-70 Mean absolute and relative N_2O_5 VMR difference of all trajectory match collocations (red numbers) between MIPAS-E and MIPAS-B (red solid line) including standard deviation (red dotted lines) and standard error of the mean (plotted as error bars). Precision (blue dotted lines), systematic (blue dash-dotted lines), and total (blue dashed lines) mean combined errors are shown, too. Top: v8 FR mode (left) and v8 OR mode (right) collocations; bottom: all FR plus OR v8 (left) and all FR plus OR v7 (right) collocations.

4.12 Dichloro(difluoro)methane (CFC-12)

LEVEL 2 V8 CFC-12 PRODUCTS										
Operational modes:	FR	RR	OR							
	NOM		NOM	UTLS1	MA	UA	AE	NLC	UTLS2	UTLS1_o
Nominal Vertical range [Km]	*6-39*	*6-39*	*6-40*	*8.5-43*	*18-39*	---	*7-38*	---	*12-42*	*10-49*
Useful range	*Full range*									
Microwindows:	*Link for downloading*									
Systematic errors:	*Link for downloading* *Link errors*									

Introduction

CFC-12 is an ozone depleting substance regulated by the Montreal protocol and a green-house gas. As an example, in Figure 4-71 the timeseries of V8 CFC-12 weekly mean profiles averaged in the latitude band 90S-60S are reported.

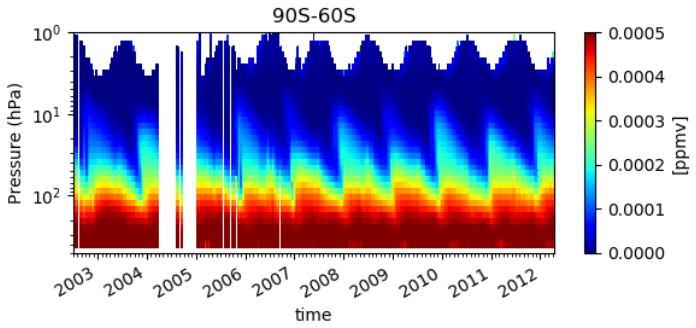

Figure 4-71 Timeseries of weekly mean of CFC-12 on the full mission averaged on the latitude band 90S-60S

The effect of the Montreal protocol regulation is a negative trend in the concentration of CFC-12. Due to the long lifetime of this trace species, the concentration of CFC-12 reduces very slowly.

Verification and changes wrt V7 products

Figure 4-72 show the timeseries of the differences between V8 and V7 CFC-12 profiles all over the mission. Differences in the algorithm, in the auxiliary data, in the L1V8 products produce an opposite behaviour in FR and OR products in the range 100 hPa-10 hPa (see Figure 4-72), the differences in the OR measurements being dominated by the change in the cross-sections (Harrison, 2015).

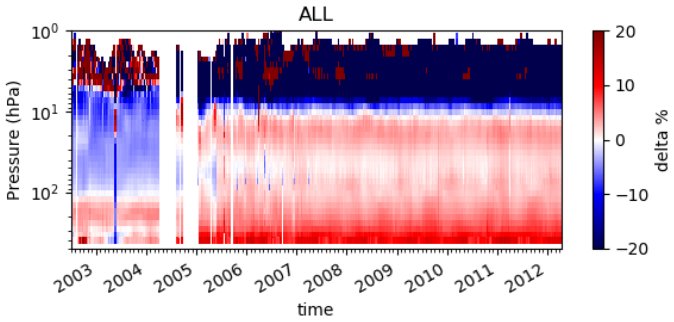

Figure 4-72 Timeseries of weekly mean percent differences between V8 and V7 CFC-12 profiles all over the mission. Red values indicates that V8 CFC-12 is larger than V7 CFC-12.

Quality quantifiers (AK and errors)

The vertical averaging kernels of the CFC-12 retrieval are shown in Figure 4-73 for two representative profiles in Full Resolution nominal mode (left panel) and Optimised Resolution nominal mode (right panel). The selected scans are not affected by clouds. The vertical resolution profile of the considered scan is also reported in red in the same plot and the DOF distribution profile (see Sect. 3.5.2 in blue. A mean vertical resolution profile has been also computed considering all scans in the nominal mode of 2003 (for FR plots) and 2010 (for OR plots). It varies from 5 km at 6 km to 7.5 at 40 km for both FR and OR measurements.

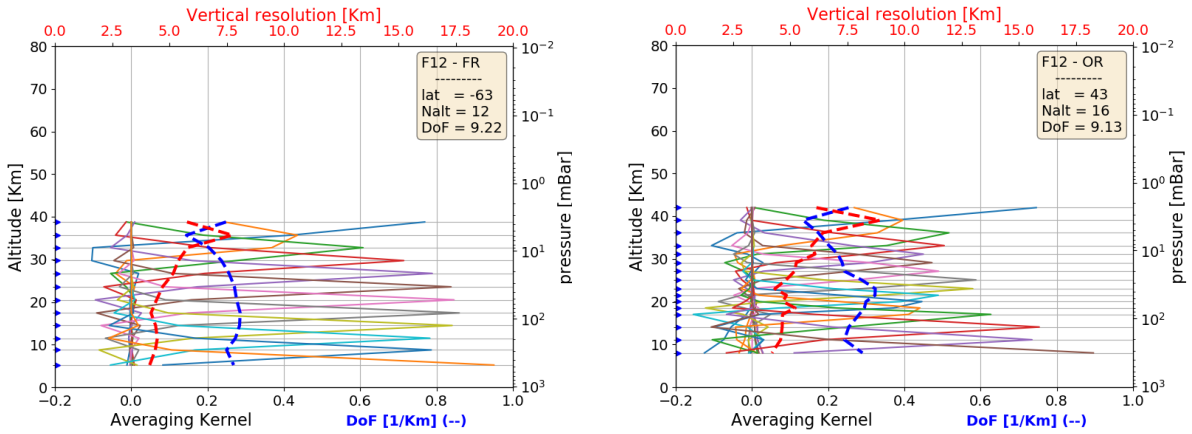

Figure 4-73 . Example of CFC-12 vertical averaging kernel (AK) computed for a representative Full Resolution (left panel) and Optimized Resolution (right panel) scan. Together with the AKs, the plots show the vertical resolution (red dashed line) and the Degree of Freedom for unity height (blue dashed line). The yellow box on the top right of each panel contains the latitude of the observation, the number of the measurement sweeps and the total Degree of Freedom (DoF)

Figure 4-74 shows the average CFC-12 VMR profiles (left plots) and their associated average random error profiles, in absolute (middle plots) and relative (right plots) scale. The average quantities are representative of 5 reference atmospheres, namely polar summer daytime, polar winter nightime, mid-latitudes (both daytime and nightime) and equatorial daytime atmospheres. The averages have been computed using information on retrieved profiles, noise error and pT error which are contained in the output files for each scan. For mid latitude atmospheres all scans in the nominal mode of 2003 (for FR plots) and 2010 (for OR plots) in the latitude band 30-60 (both hemispheres) have been taken into account (considering either daytime or nightime scans), for equatorial atmosphere the scans in the latitude band 30S-30N, for polar winter nighttime atmosphere all nightime scans in the nominal mode of June-July-August of 2003 (for FR) and of 2005-2011 years (for OR) in the band 60S-90S, for polar summer daytime atmosphere all daytime scans in the nominal mode of December-January-February of 2003 (for FR) and 2005-2011 (for OR) in the latitude band 60S-90S. Solid lines of middle and right plots represent the total random error, coming from the quadratic summation of the noise error (dotted curves, given by the mapping of the measurement error on the retrieved profile) and the pT error (given by the propagation of the random error of retrieved pressure and temperature profiles on VMR profile). The contribution coming from the pT error propagation is generally smaller than the noise contribution. The random error is approximately constant and equal to 5% up to 40 hPa (22 km), up to 20 hPa (28 km) for equatorial atmosphere, then it rapidly increases.

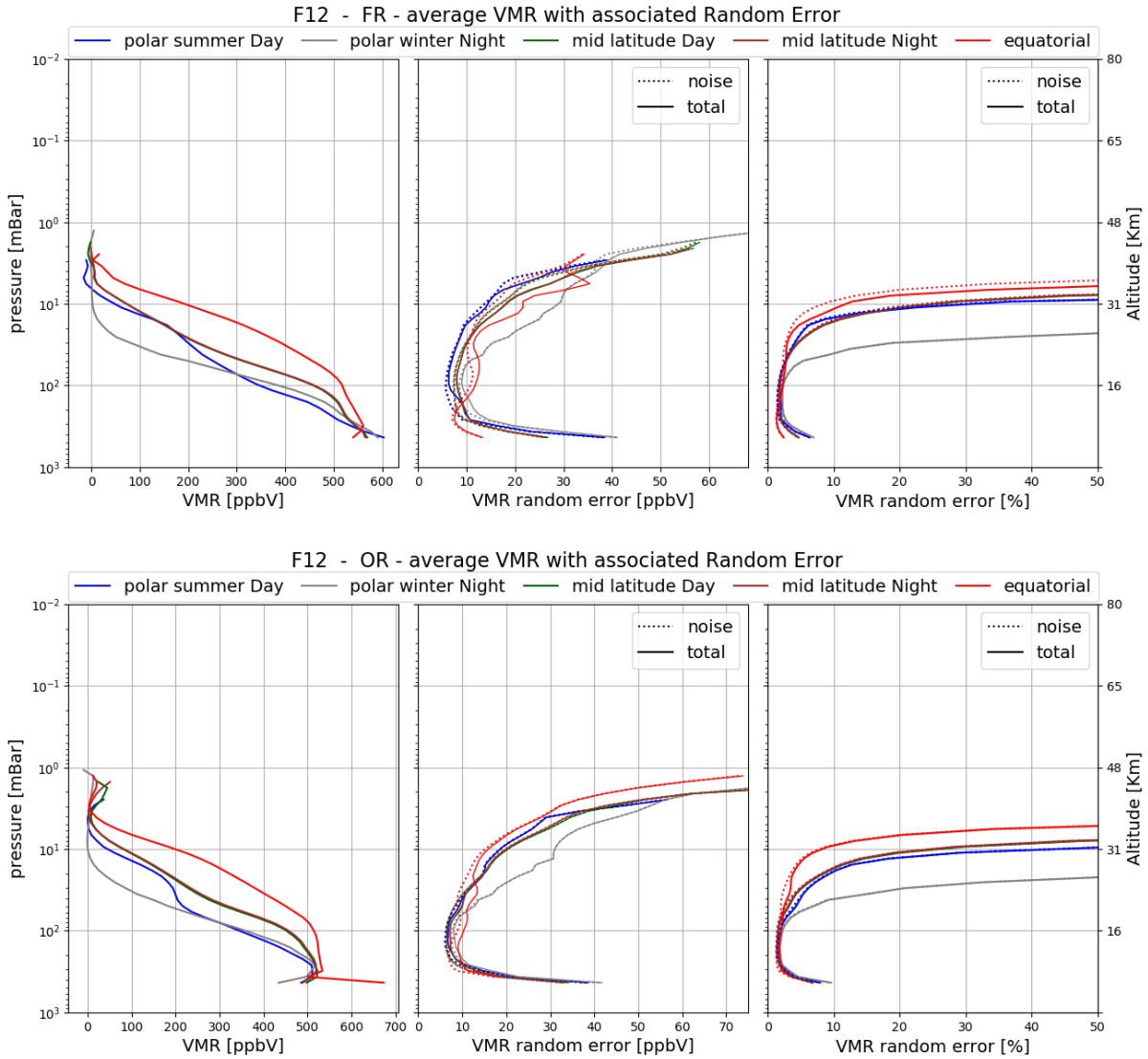

Figure 4-74 Average CFC-12 VMR (left plots), absolute (mid plots) and relative (right plots) CFC-12 random error for the 5 reference atmospheres described in the text. The noise error (dotted curves) is calculated by the retrieval; the total random error (solid curves) includes the contribution to the random error coming from propagation of the pT random error on VMR profiles. Top panel: Full Resolution nominal mode ; bottom panel: Optimized Resolution nominal mode.

Validation

Reference instrument	Source	Coverage validation analysis		
		Time	Horizontal	Vertical
MIPAS-B	KIT-IMK	8 flights + 2-day trajectories	3 sites, 68°N–5°S	200–2 hPa

Results for the long-lived chlorofluorocarbon CFC-12 (CCl_2F_2) are shown in Figure 4-75. Mean differences between both MIPAS instruments remain within the combined errors and are within ±5% below 20 km. Above this altitude, a significant positive bias is visible (up to 32 km) and standard deviations exceed the expected precision. Slightly reduced deviations below 16 km compared to v7 data are noticeable.

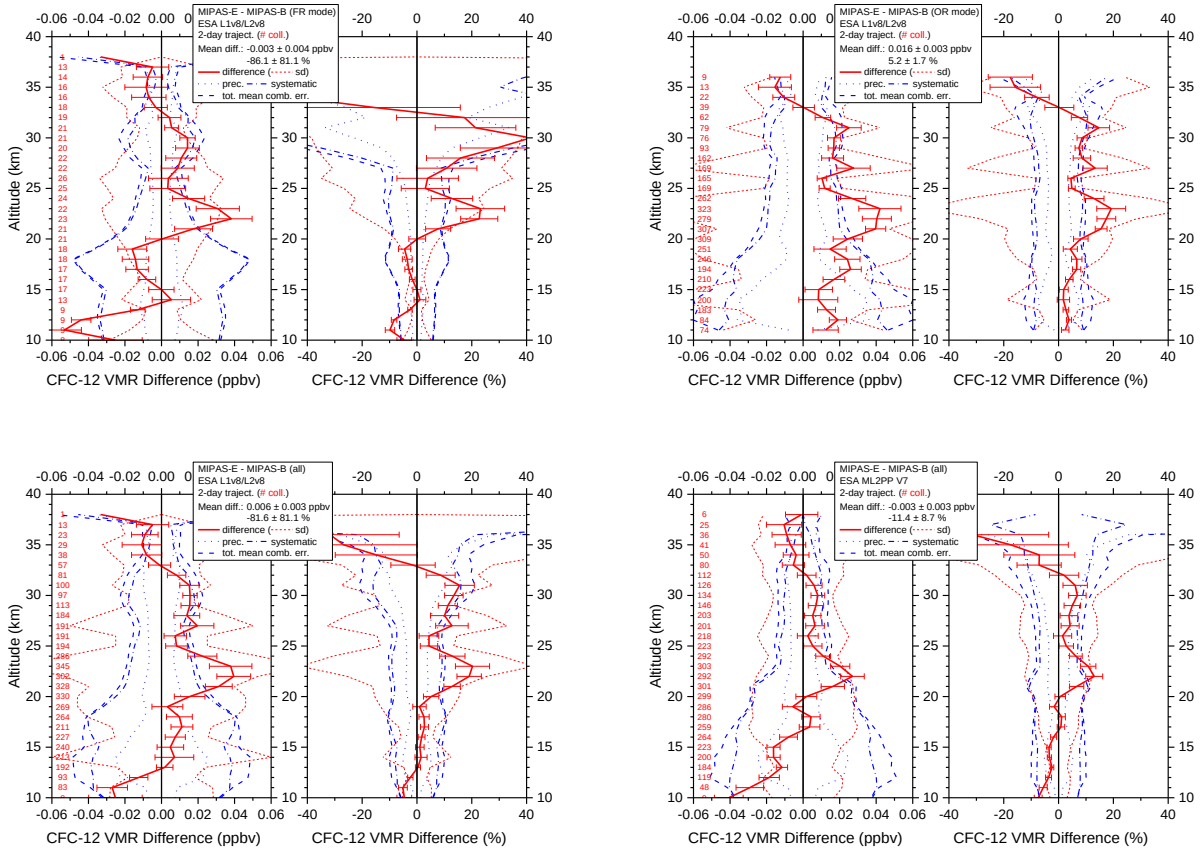

Figure 4-75 Mean absolute and relative CFC-12 VMR difference of all trajectory match collocations (red numbers) between MIPAS-E and MIPAS-B (red solid line) including standard deviation (red dotted lines) and standard error of the mean (plotted as error bars). Precision (blue dotted lines), systematic (blue dash-dotted lines), and total (blue dashed lines) mean combined errors are shown, too. Top: v8 FR mode (left) and v8 OR mode (right) collocations; bottom: all FR plus OR v8 (left) and all FR plus OR v7 (right) collocations.

4.13 Carbonyl Fluoride (COF_2)

LEVEL 2 V8 CARBONYL FLUORIDE PRODUCTS

Operational modes:	FR	RR	OR							
	NOM		NOM	UTLS1	MA	UA	AE	NLC	UTLS2	UTLS1_o
Nominal Vertical range [Km]	*6-42*	*9-42*	*7.5-46*	*10-47.5*	---	---	*8.5-38*	---	*12-42*	*11.5-49*
Useful range	*Full range*									
Microwindows:	*Link for downloading*									
Systematic errors:	*Link for downloading* *Link errors*									

Introduction

The molecule COF_2 is a stratospheric reservoir species for fluorine. As an example, in

Figure 4-76 we present the timeseries of V8 COF_2 in the latitude band 90S-60S on the full mission. Minima in the stratospheric concentration of COF_2 are found in correspondence of the polar vortex when mesospheric COF_2-poor air subsides in the stratosphere. A positive trend is visible in the time series.

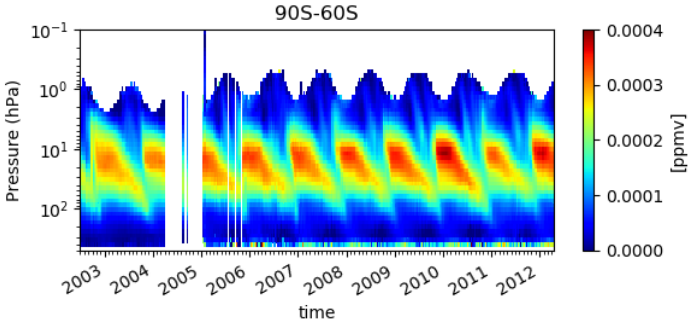

Figure 4-76 Timeseries of weekly mean of COF_2 on the full mission averaged on the latitude band 90S-60S

Verification and changes wrt V7 products

In Figure 4-77 we report the timeseries of the differences between V8 and V7 products. Differences are small around the peak of the profile, but they are large where the profile goes rapidly to small values. They seem to be dominated by the changes implemented in the algorithm.

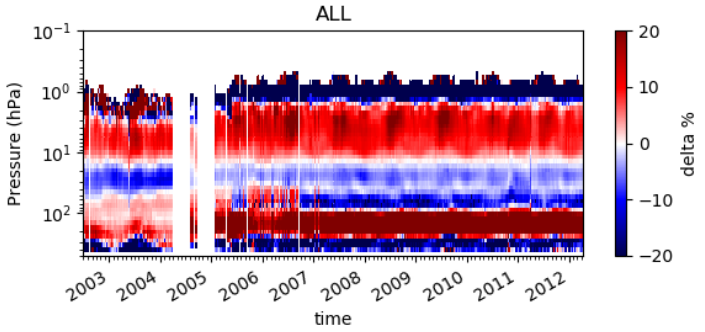

Figure 4-77 Timeseries of weekly mean percent differences between V8 and V7 COF_2 profiles all over the mission.

Quality quantifiers (AK and errors)

The vertical averaging kernels of the COF_2 retrieval are shown in Figure 4-78 for two representative profiles in Full Resolution nominal mode (left panel) and Optimised Resolution nominal mode (right panel). The selected scans are not affected by clouds. The vertical resolution profile of the considered scan is also reported in red in the same plot and the DOF distribution profile (see Sect. 3.5.2) in blue. A mean vertical resolution profile has been also computed considering all scans in the nominal mode of 2003 (for FR plots) and 2010 (for OR plots). It is 5 km at 10 km, 7.5 km at 40 km for both FR and OR measurements.

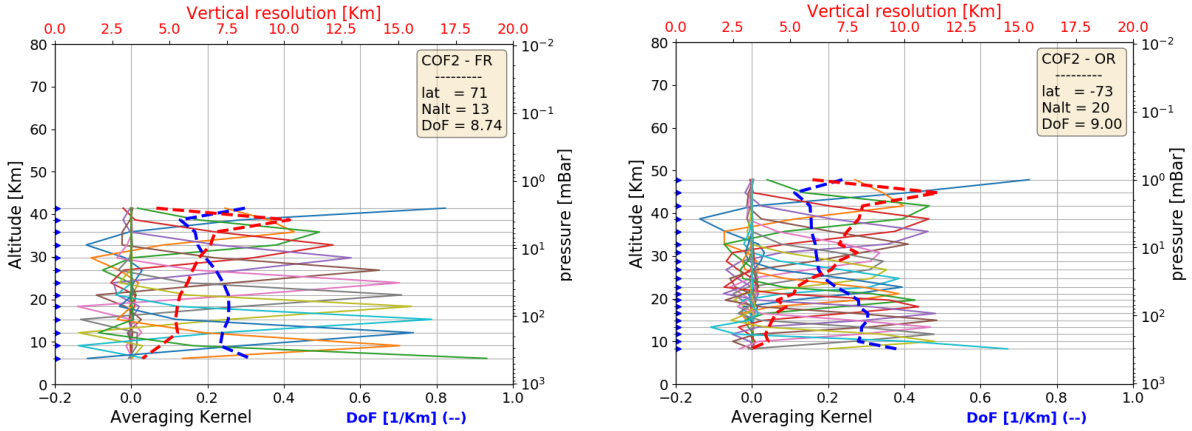

Figure 4-78 Example of COF_2 vertical averaging kernel (AK) computed for a representative Full Resolution (left panel) and Optimized Resolution (right panel) scan. Together with the AKs, the plots show the vertical resolution (red dashed line) and the Degree of Freedom for unity height (blue dashed line). The yellow box on the top right of each panel contains the latitude of the observation, the number of the measurement sweeps and the total Degree of Freedom (DoF)

Figure 4-79 shows the average COF2 VMR profiles (left plots) and their associated average random error profiles, in absolute (middle plots) and relative (right plots) scale. The average quantities are representative of 5 reference atmospheres, namely polar summer daytime, polar winter nightime, mid-latitudes (both daytime and nightime) and equatorial daytime atmospheres. The averages have been computed using information on retrieved profiles, noise error and pT error which are contained in the output files for each scan. For mid latitude atmospheres all scans in the nominal mode of 2003 (for FR plots) and 2010 (for OR plots) in the latitude band 30-60 (both hemispheres) have been taken into account (considering either daytime or nightime scans), for equatorial atmosphere the scans in the latitude band 30S-30N, for polar winter nighttime atmosphere all nightime scans in the nominal mode of June-July-August of 2003 (for FR) and of 2005-2011 years (for OR) in the band 60S-90S, for polar summer daytime atmosphere all daytime scans in the nominal mode of December-January-February of 2003 (for FR) and 2005-2011 (for OR) in the latitude band 60S-90S. Solid lines of middle and right plots represent the total random error, coming from the quadratic summation of the noise error (dotted curves, given by the mapping of the measurement error on the retrieved profile) and the pT error (given by the propagation of the random error of retrieved pressure and temperature profiles on VMR profile). The contribution coming from the pT error propagation is generally smaller than the noise contribution. The random error is about 5% in correspondence of the peak of the profile for all atmospheres, and between 100 and 10 hPa for all atmospheres except equatorial one.

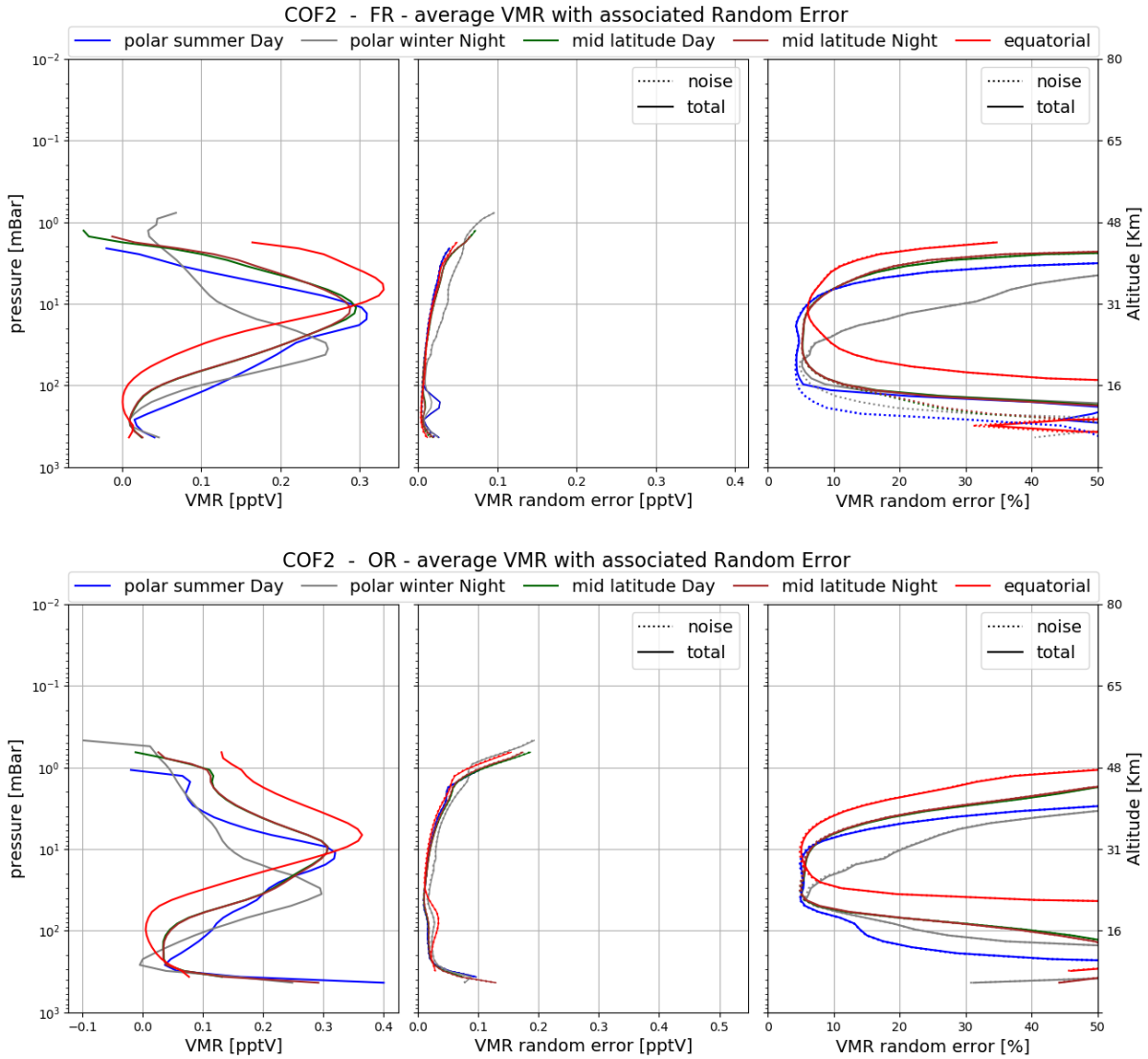

Figure 4-79 Average COF_2 VMR (left plots), absolute (mid plots) and relative (right plots) COF_2 random error for the 5 reference atmospheres described in the text. The noise error (dotted curves) is calculated by the retrieval; the total random error (solid curves) includes the contribution to the random error coming from propagation of the pT random error on VMR profiles. Top panel: Full Resolution nominal mode; bottom panel: Optimized Resolution nominal mode.

Validation

Reference instrument	Source	Coverage validation analysis		
		Time	Horizontal	Vertical
MIPAS-B	KIT-IMK	8 flights + 2-day trajectories	3 sites, 68°N–5°S	200–2 hPa
ACE-FTS v4	U Waterloo	2005-2012	global	500-0.04 hPa

MIPAS exhibits a profile consistency within ±20% in the stratosphere and upper troposphere with respect to both the balloon-borne MIPAS and ACE-FTS measurements. This holds for both MIPAS observation periods (FR and OR mode) for the balloon-borne MIPAS and different geographical regions. More details are reported below.

The general profile shape of COF_2 (as measured by MIPAS-B) is reproduced by MIPAS-E (see Figure 4-80). VMR differences stay within ±20% in the stratosphere (deviations in OR mode are larger than in FR mode). No unexplained biases (in terms of exceeding combined systematic error bars) are evident. A slightly different shape of deviations compared to v7 data is visible.

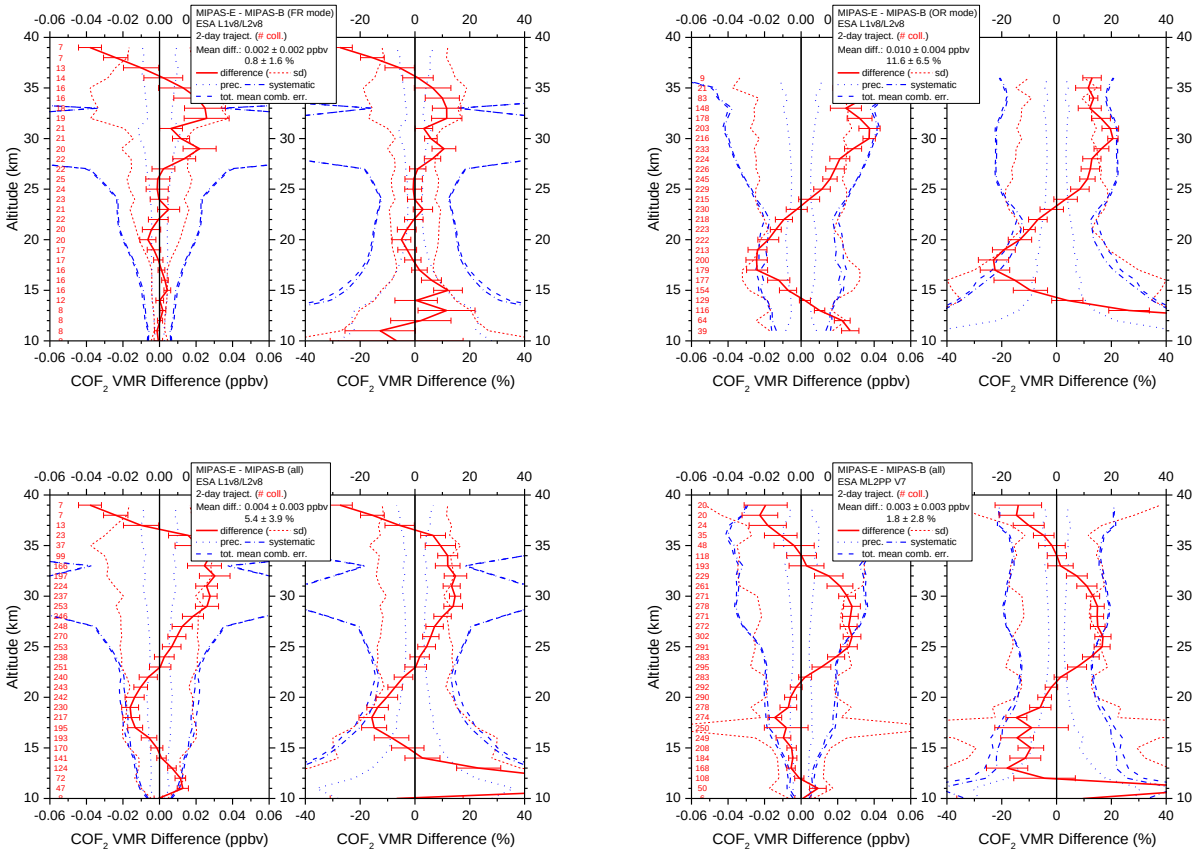

Figure 4-80 Mean absolute and relative COF_2 VMR difference of all trajectory match collocations (red numbers) between MIPAS-E and MIPAS-B (red solid line) including standard deviation (red dotted lines) and standard error of the mean (plotted as error bars). Precision (blue dotted lines), systematic (blue dash-dotted lines), and total (blue dashed lines) mean combined errors are shown, too. Top: v8 FR mode (left) and v8 OR mode (right) collocations; bottom: all FR plus OR v8 (left) and all FR plus OR v7 (right) collocations.

Data are generally consistent between MIPAS and ACE. VMR differences are smallest in the 15-18 km range across all years (±10%), see Figure 4-81. Above 18 km to the upper stratosphere (35 km) MIPAS is generally higher than ACE by between 20-40% across all years between 2005 and 2012. Above 20 km the differences exceed the expected total error on the differences.

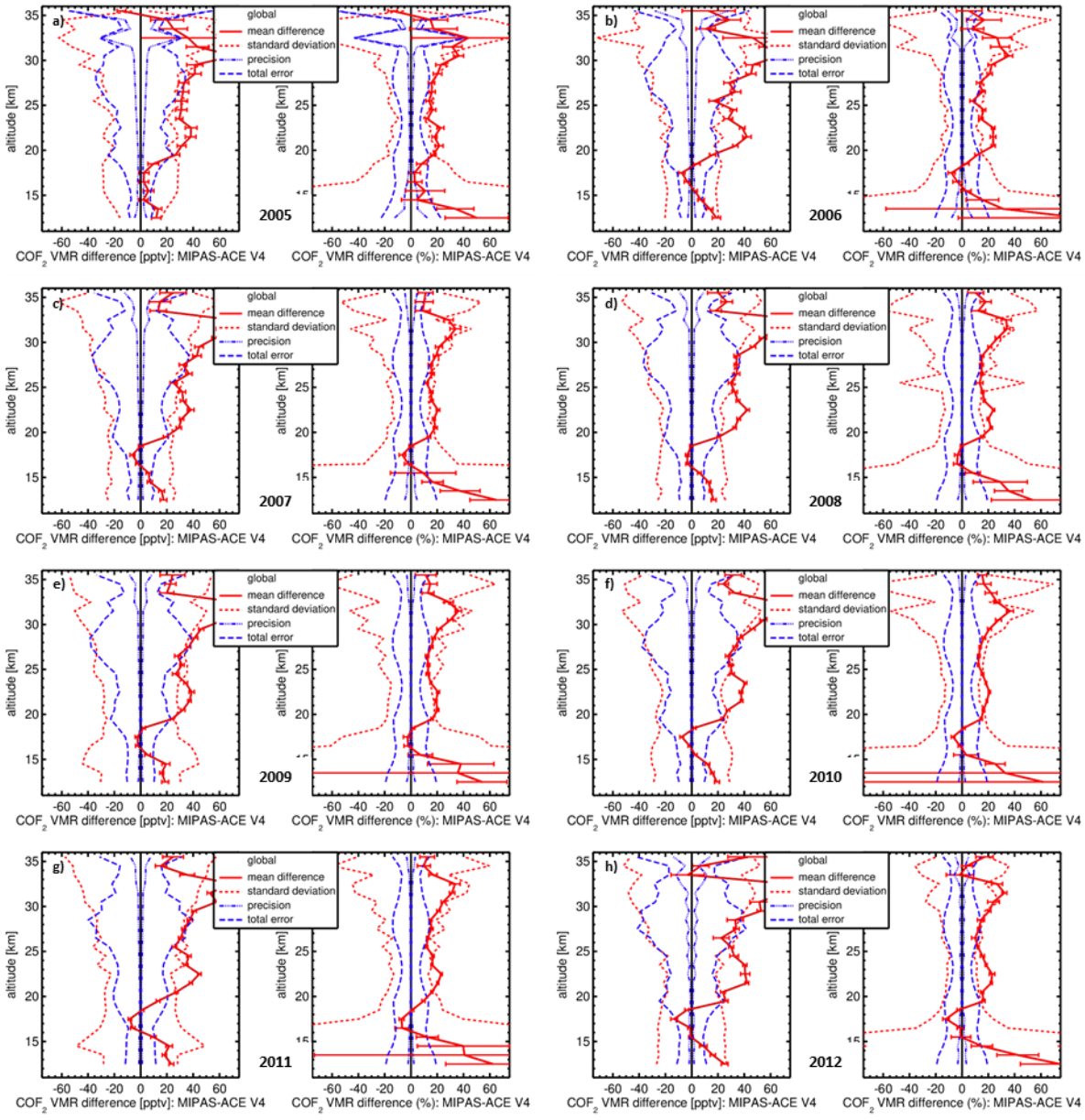

Figure 4-81. Mean absolute and relative COF_2 VMR difference of all match collocation (red numbers) between MIPAS and ACE version 4 data (red solid line) including standard deviation (red dotted lines) and standard error of the mean (plotted as error bars). Precision (blue dotted lines) and total (blue dashed lines) mean combined errors are shown, too. Global matchups. a) 2005, b) 2006, c) 2007, d) 2008, e) 2009, f) 2010 g) 2011, h) 2012.

4.14 Carbon Tetrachloride (CCl4)

LEVEL 2 V8 CARBON TETRACHLORIDE PRODUCTS										
Operational modes:	FR	RR	OR							
	NOM		NOM	UTLS1	MA	UA	AE	NLC	UTLS2	UTLS1_o
Nominal Vertical range [Km]	*6-27*	*9-27*	*9-27*	*11.5-28*	---	---	*10-29*	---	*12-33*	*13-31*
Useful range	*Full range*									
Microwindows:	*Link for downloading*									
Systematic errors:	*Link for downloading* *Link errors*									

Introduction

Carbon tetrachloride (CCl_4) is a strong ozone-depleting substance and a strong greenhouse gas (Valeri et al., 2017), which is regulated by the Montreal protocol. In Figure 4-82 the timeseries of V8 CCl_4 in the latitude band 90S-60S on the full mission are shown.

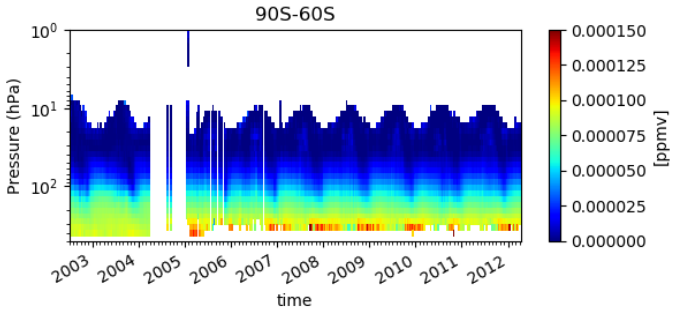

Figure 4-82 Timeseries of weekly mean of CCl4 on the full mission averaged on the latitude band 90S-60S

Verification and changes wrt V7 products

In Figure 4-83 we report the difference between V8 and V7 products. Most of the differences come from the use of the new cross-sections (Harrison et al., 2017; Assessment of Molecular Cross-Section Data v. 2 , here), responsible of about 10% lower VMR.

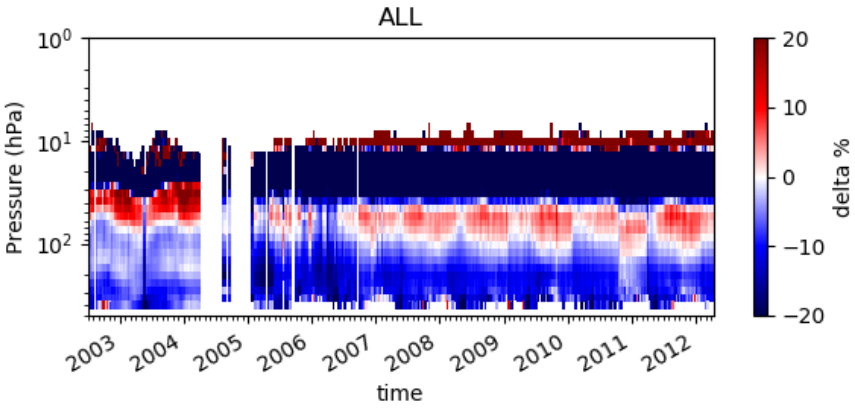

Figure 4-83 Timeseries of weekly mean percent differences between V8 and V7 CCl_4 profiles, averaged on all latitudes, all over the mission.

Quality quantifiers (AK and errors)

The vertical averaging kernels of the CCl_4 retrieval are shown in Figure 4-84 for two representative profiles in Full Resolution nominal mode (left panel) and Optimised Resolution nominal mode (right panel). The selected scans are not affected by clouds. The vertical resolution profile of the considered scan is also reported in red in the same plot and the DOF distribution profile (see Sect. 3.5.2) in blue. A mean vertical resolution profile has been also computed considering all scans in the nominal mode of 2003 (for FR plots) and 2010 (for OR plots). It is about 10 km at 6 km and 5-7.5 km between 10 and 30 km for both FR and OR measurements.

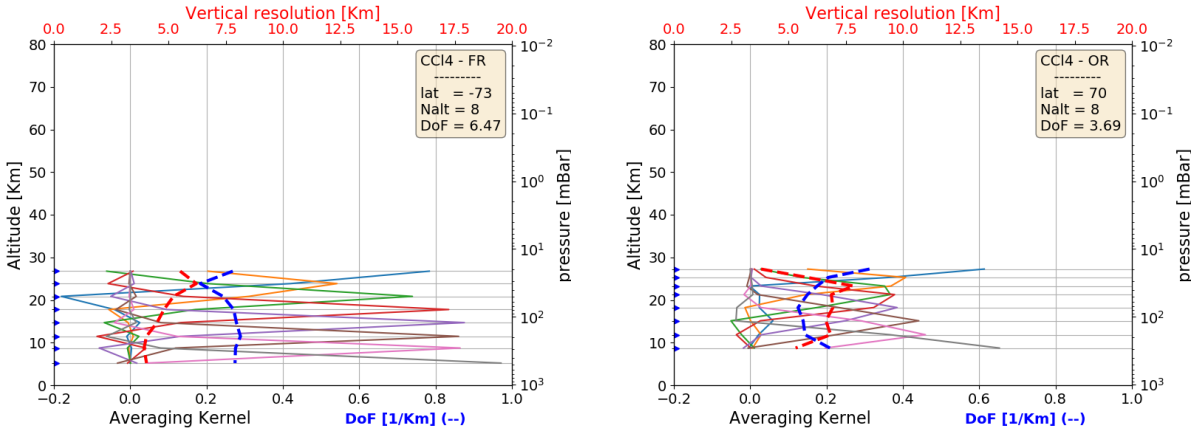

Figure 4-84 Example of CCl_4 vertical averaging kernel (AK) computed for a representative Full Resolution (left panel) and Optimized Resolution (right panel) scan. Together with the AKs, the plots show the vertical resolution (red dashed line) and the Degree of Freedom for unity height (blue dashed line). The yellow box on the top right of each panel contains the latitude of the observation, the number of the measurement sweeps and the total Degree of Freedom (DoF)

Figure 4-85 shows the average CCl_4 VMR profiles (left plots) and their associated average random error profiles, in absolute (middle plots) and relative (right plots) scale. The average quantities are representative of 5 reference atmospheres, namely polar summer daytime, polar winter nightime, mid-latitudes (both daytime and nightime) and equatorial daytime atmospheres. The averages have been computed using information on retrieved profiles, noise error and pT error which are contained in the output files for each scan. For mid latitude atmospheres all scans in the nominal mode of 2003 (for FR plots) and 2010 (for OR plots) in the latitude band 30-60 (both hemispheres) have been taken into account (considering either daytime or nightime scans), for equatorial atmosphere the scans in the latitude band 30S-30N, for polar winter nighttime atmosphere all nightime scans in the nominal mode of June-July-August of 2003 (for FR) and of 2005-2011 years (for OR) in the band 60S-90S, for polar summer daytime atmosphere all daytime scans in the nominal mode of December-January-February of 2003 (for FR) and 2005-2011 (for OR) in the latitude band 60S-90S. Solid lines of middle and right plots represent the total random error, coming from the quadratic summation of the noise error (dotted curves, given by the mapping of the measurement error on the retrieved profile) and the pT error (given by the propagation of the random error of retrieved pressure and temperature profiles on VMR profile). The contribution coming from the pT error propagation is generally smaller than the noise contribution. The random error is 5-6% between 6 and 100 hPa for both FR and OR measurements, then it rapidly increases as a consequence of the rapid decrease of the CCl_4 profile with altitude.

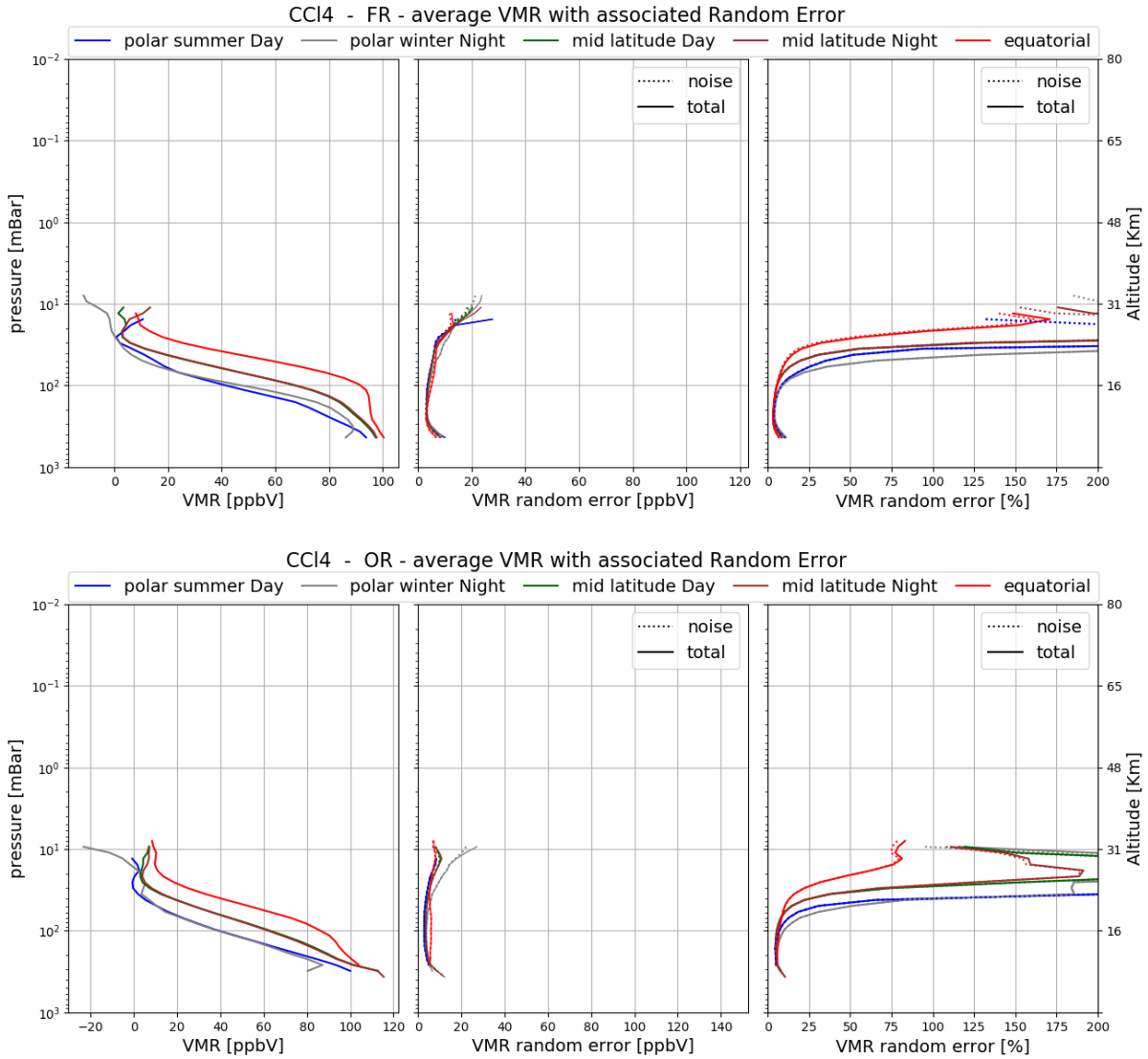

Figure 4-85 Average CCl_4 VMR (left plots), absolute (mid plots) and relative (right plots) CCl_4 random error for the 5 reference atmospheres described in the text. The noise error (dotted curves) is calculated by the retrieval; the total random error (solid curves) includes the contribution to the random error coming from propagation of the pT random error on VMR profiles. Top panel: Full Resolution nominal mode (average 2003); bottom panel: Optimized Resolution nominal mode (average on 2010).

Validation

Reference instrument	Source	Coverage validation analysis		
		Time	Horizontal	Vertical
MIPAS-B	KIT-IMK	8 flights + 2-day trajectories	3 sites, 68°N–5°S	200–10 hPa
ACE-FTS v4	U Waterloo	2005-2012	global	500-0.04 hPa

MIPAS exhibits a significant negative bias of up to 100% in the stratosphere above 21 km with respect to both the balloon-borne MIPAS measurements and the ACE-FTS measurements. MIPAS is consistent, within ±20% with respect to both the balloon-borne MIPAS measurements and the ACE-FTS measurements between 15 km and 21 km. Details of results of validation are reported below.

The comparison of both MIPAS instruments reveals a significant negative bias in the MIPAS-E CCl_4 data (full period) above 22 km (see Figure 4-86), which is at the brink of the combined systematic error limits. A significant positive bias is visible below 21 km during the OR phase. However, differences stay within ±20% up to about 22 km in both observation periods. A different shape of deviations compared to v7 data is recognized.

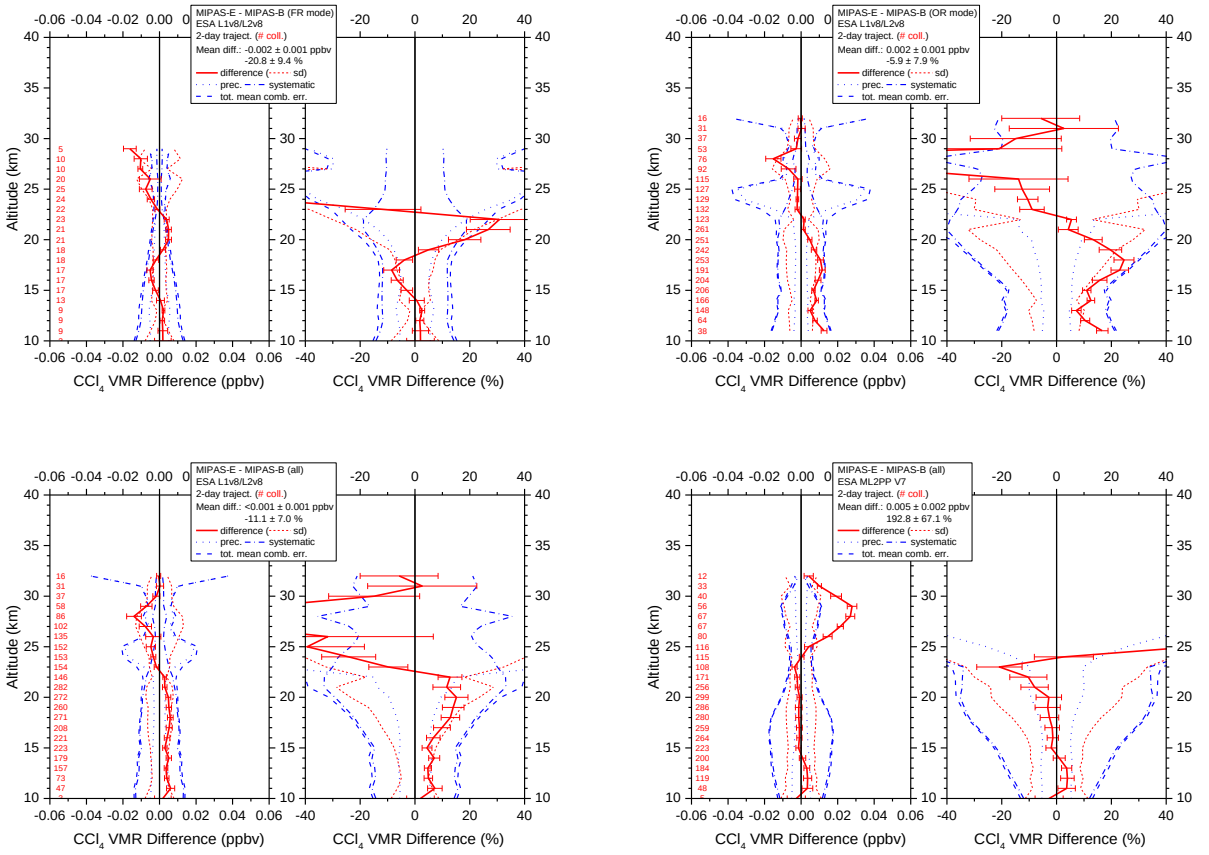

Figure 4-86 Mean absolute and relative CCl_4 VMR difference of all trajectory match collocations (red numbers) between MIPAS-E and MIPAS-B (red solid line) including standard deviation (red dotted lines) and standard error of the mean (plotted as error bars). Precision (blue dotted lines), systematic (blue dash-dotted lines), and total (blue dashed lines) mean combined errors are shown, too. Top: v8 FR mode (left) and v8 OR mode (right) collocations; bottom: all FR plus OR v8 (left) and all FR plus OR v7 (right) collocations.

The best consistency between MIPAS and ACE observations is between 15 and 21 km for each year where the differences are between ±10% (see Figure 4-87). There is a significant negative bias above 22 km of up to 100%, which is in some cases outside the total error. Below 15 km MIPAS VMRs are generally higher than ACE by between 5% and 40%.

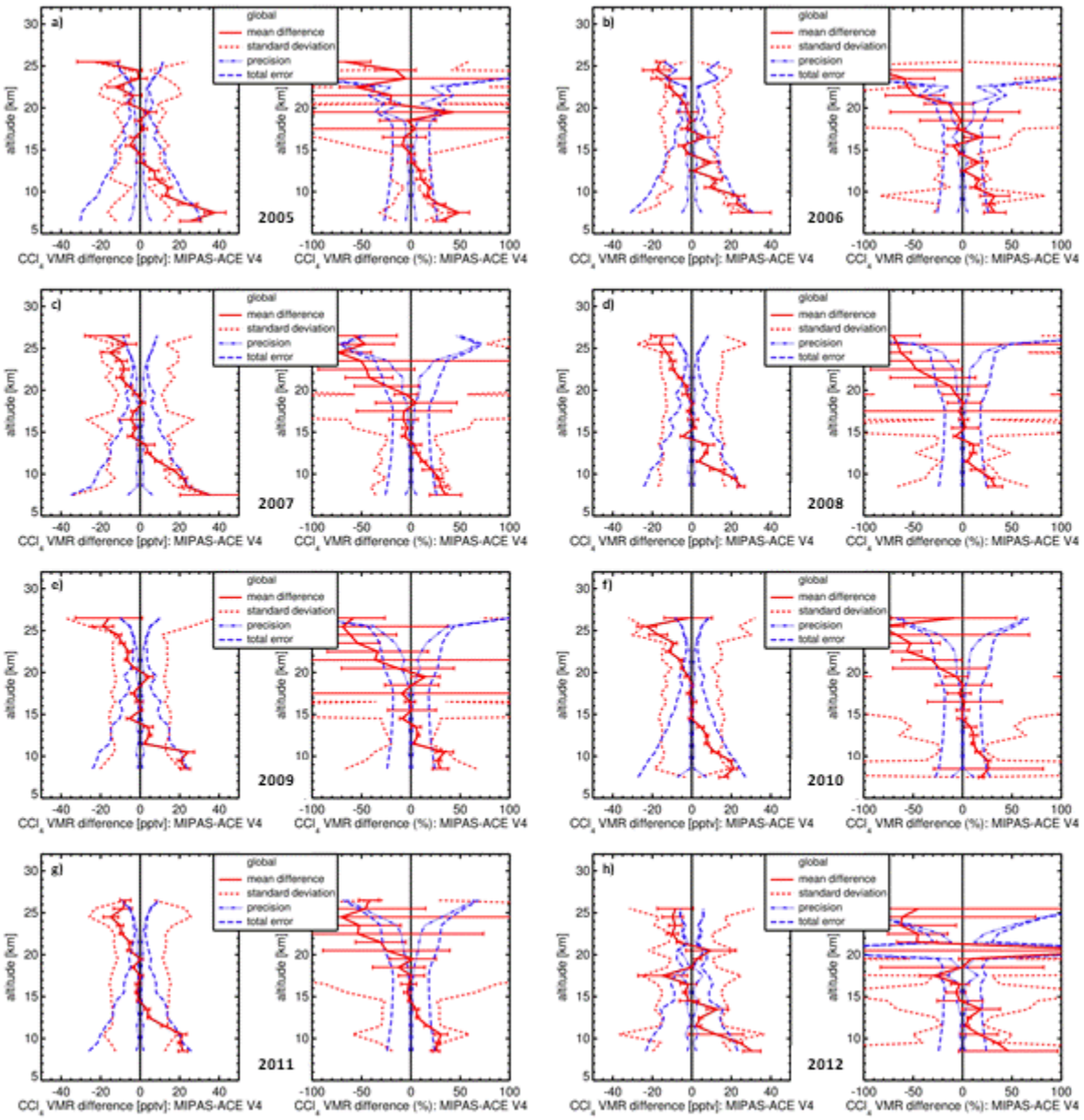

Figure 4-87. Mean absolute and relative CCl4 VMR difference of all match collocation (red numbers) between MIPAS and ACE version 4 data (red solid line) including standard deviation (red dotted lines) and standard error of the mean (plotted as error bars). Precision (blue dotted lines) and total (blue dashed lines) mean combined errors are shown, too. Global matchups. a) 2005, b) 2006, c) 2007, d) 2008, e) 2009, f) 2010 g) 2011, h) 2012.

4.15 Hydrogen Cyanide (HCN)

LEVEL 2 V8 HYDROGEN CYANIDE PRODUCTS										
Operational modes:	FR	RR	OR							
	NOM		NOM	UTLS1	MA	UA	AE	NLC	UTLS2	UTLS1_o
Nominal Vertical range [Km]	*6-60*	*6-60*	*6-62*	*8.5-525*	---	---	*7-38*	---	*12-42*	*10-49*
Useful range	*All altitudes up to 47 km (pressures greater than 1 hPa)*									
Microwindows:	*Link for downloading*									
Systematic errors:	*Link for downloading* *Link errors*									

Introduction

HCN is a tracer of biomass burning. In Figure 4-88 we report the timeseries of V8 HCN in the latitude band 30S-0 on the full mission. Some spots of enhanced HCN are regularly found in particular periods of each year in regions where large fires of biomass occur.

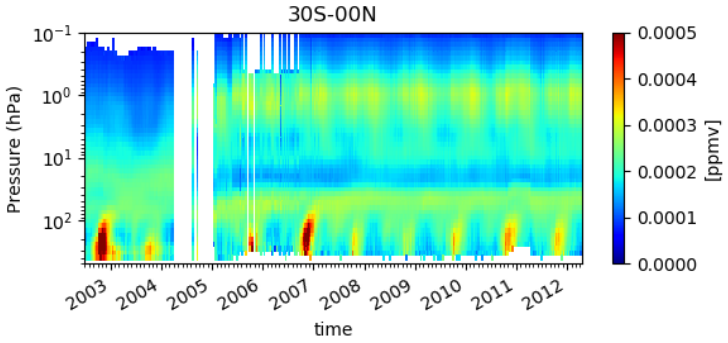

Figure 4-88 Timeseries of weekly mean of HCN on the full mission averaged on the latitude band 30S-00

Differently from L2 V7 reprocessing, V8 HCN was derived using the Optimal Estimation approach, with a fixed a priori profile given by the mean of the HCN climatological profiles.
The diagonal element of the CM of the a priori are computed as the square of the sum of a constant (10^{-6} ppmv) plus the 90% of the a priori profile, while the non diagonal elements are computed assuming a correlation length of 6 km.
This approach was needed to reduce strong oscillations present in the retrieved profiles when the standard retrieval approach is used.

Verification and changes wrt V7 products

In Figure 4-89 we report the difference between V8 and V7 products. The differences largely overcome 20%, V8 HCN being in general lower than V7 HCN.

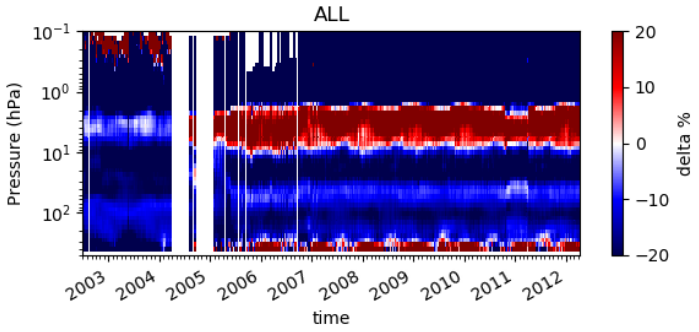

Figure 4-89 Timeseries of weekly mean percent differences between V8 and V7 HCN profiles all over the mission. Blue values mean that V8 HCN is smaller than V7 HCN.

The reason of this large difference is a major update in the HCN spectroscopic database. Line positions and intensities throughout the infrared have been revisited by Maki et al, 1996; 2000. The improvements apply to the three isotopologues present in HITRAN in the pure-rotation region and in the infrared from 500 to 3425 cm^{-1}. The new intensities are about 1.16 times larger than the previous ones which explains the found differences.

The cause of the stripe around 4 hPa in the differences between V8 HCN and V7 HCN is not clear, but it is located in a region where there is a large sensitivity of HCN profile to the temperature and pressure profiles, as can be deduced from the peak in the HCN total random error due to the large pT propagation error (see Figure 4-91). Even small changes in the temperature can induce a large change in the retrieved HCN in this altitude region.

Quality quantifiers (AK and errors)

The vertical averaging kernels of the HCN retrieval are shown in Figure 4-90 for two representative profiles in Full Resolution nominal mode (left panel) and Optimised Resolution nominal mode (right panel). The selected scans are not affected by clouds. The vertical resolution profile of the considered scan is also reported in red in the same plot and the DOF distribution profile (see Sect. 3.5.2) in blue. A mean vertical resolution profile has been also computed considering all scans in the nominal mode of 2003 (for FR plots) and 2010 (for OR plots). It is of 4-6 (5-10) km between 10 and 30 km for FR (OR), 10(12.5) at 40 km, above and below this range it rapidly increases.

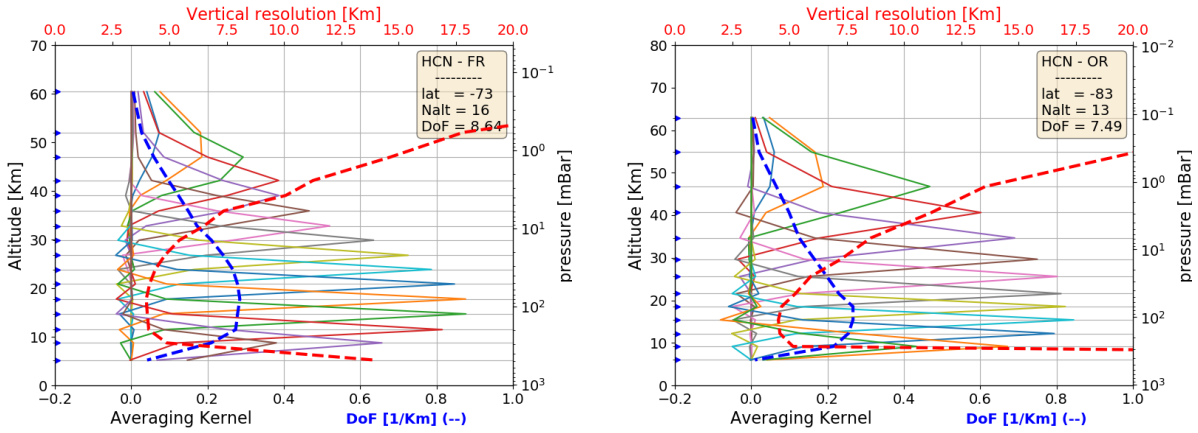

Figure 4-90 Example of HCN vertical averaging kernel (AK) computed for a representative Full Resolution (left panel) and Optimized Resolution (right panel) scan. Together with the AKs, the plots show the vertical resolution (red dashed line) and the Degree of Freedom for unity height (blue dashed line). The yellow box on the top right of each panel contains the latitude of the observation, the number of the measurement sweeps and the total Degree of Freedom (DoF)

Figure 4-91 shows the average HCN VMR profiles (left plots) and their associated average single scan random error profiles, in absolute (middle plots) and relative (right plots) scale. The average quantities are representative of 5 reference atmospheres, namely polar summer daytime, polar winter nightime, mid-latitudes (both daytime and nightime) and equatorial daytime atmospheres. The averages have been computed using information on retrieved profiles, noise error and pT error which are contained in the output files for each scan. For mid latitude atmospheres all scans in the nominal mode of 2003 (for FR plots) and 2010 (for OR plots) in the latitude band 30-60 (both hemispheres) have been taken into account (considering either daytime or nightime scans), for equatorial atmosphere the scans in the latitude band 30S-30N, for polar winter nighttime atmosphere all nightime scans in the nominal mode of June-July-August of 2003 (for FR) and of 2005-2011 years (for OR) in the band 60S-90S, for polar summer daytime atmosphere all daytime scans in the nominal mode of December-January-February of 2003 (for FR) and 2005-2011 (for OR) in the latitude band 60S-90S. Solid lines of middle and right plots represent the total random error, coming from the quadratic summation of the noise error (dotted curves, given by the mapping of the measurement error on the retrieved profile) and the pT error (given by the propagation of the random error of retrieved pressure and temperature profiles on VMR profile). It is clearly visible that especially at some altitudes (2hPa and 10 hPa) the noise error is significantly smaller than the total random error, indicating that the contribution of the pT error is very large. The mean single scan random error is about 20% between 200 and 20 (60) hPa for FR (OR) measurements, outside this range the error rapidly increases going to the highest and the lowest altitudes.

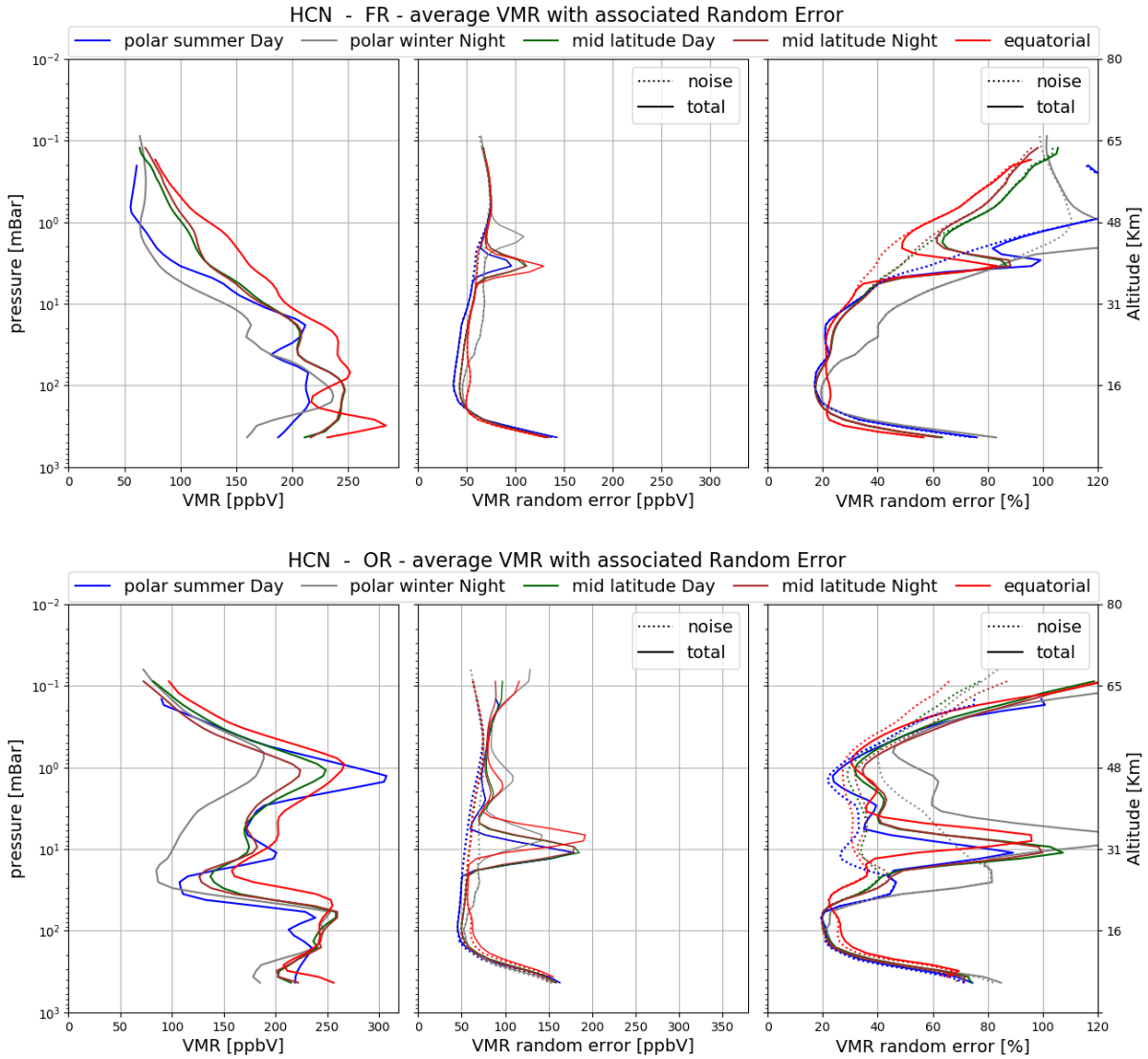

Figure 4-91 Average HCN VMR (left plots), absolute (mid plots) and relative (right plots) HCN random error for the 5 reference atmospheres described in the text. The noise error (dotted curves) is calculated by the retrieval; the total random error (solid curves) includes the contribution to the random error coming from propagation of the pT random error on VMR profiles. Top panel: Full Resolution nominal mode (average 2003); bottom panel: Optimized Resolution nominal mode (average on 2010).

Validation

Reference instrument	Source	Coverage validation analysis		
		Time	Horizontal	Vertical
MIPAS-B	KIT-IMK	8 flights + 2-day trajectories	3 sites, 68°N–5°S	200–2 hPa
ACE-FTS v4	U Waterloo	2005-2012	global	500-0.04 hPa

The intercomparison between MIPAS/ENVISAT vs MIPAS/balloon hints at a different quality of the HCN profiles retrieved from FR and OR measurements. Below 40 km, the differences between MIPAS/ENVISAT and MIPAS/balloon are smaller for OR measurements as compared to FR. The intercomparison to ACE is possible only in the altitude range 6-20 km and only for OR measurements. In the common altitude range, results of comparisons to MIPAS balloon and ACE are consistent, and indicate a positive bias in MIPAS/ENVISAT at 18-20 km. This bias is smaller than 15% in MIPAS balloon intercomparisons and consistent with the combined systematic error bounds. In the ACE-FTS intercomparisons the bias amounts to about 50%, which is larger than the combined systematic error bounds. Figure 4-90 shows that, at higher altitudes, immediately below 40 km and, especially, around 27-30 km, the HCN total random error is dominated by the pT error propagation. This is due to the extremely large sensitivity of the retrieved HCN to small variations in the retrieved temperature and pressure. We conclude that, at these altitudes, even a small bias in the retrieved Temperature and / or pressure may be the cause a significant bias in the retrieved HCN profiles.

Differences in the HCN amount measured by both MIPAS instruments are within ±20% below 34 km (see Figure 4-92). A significant positive bias (more than 20% above 20 km) is evident in the MIPAS-E profiles observed in the FR mode period exceeding the combined systematic error limits above 20 km. This pronounced bias is visible in each comparison of the three MIPAS-B flights in the FR phase. No clear bias can be seen in the OR period. The standard deviation between about 20 and 30 km exceeds the estimated precision in the OR phase. Deviations between both instruments are clearly reduced compared to previous v7 data.

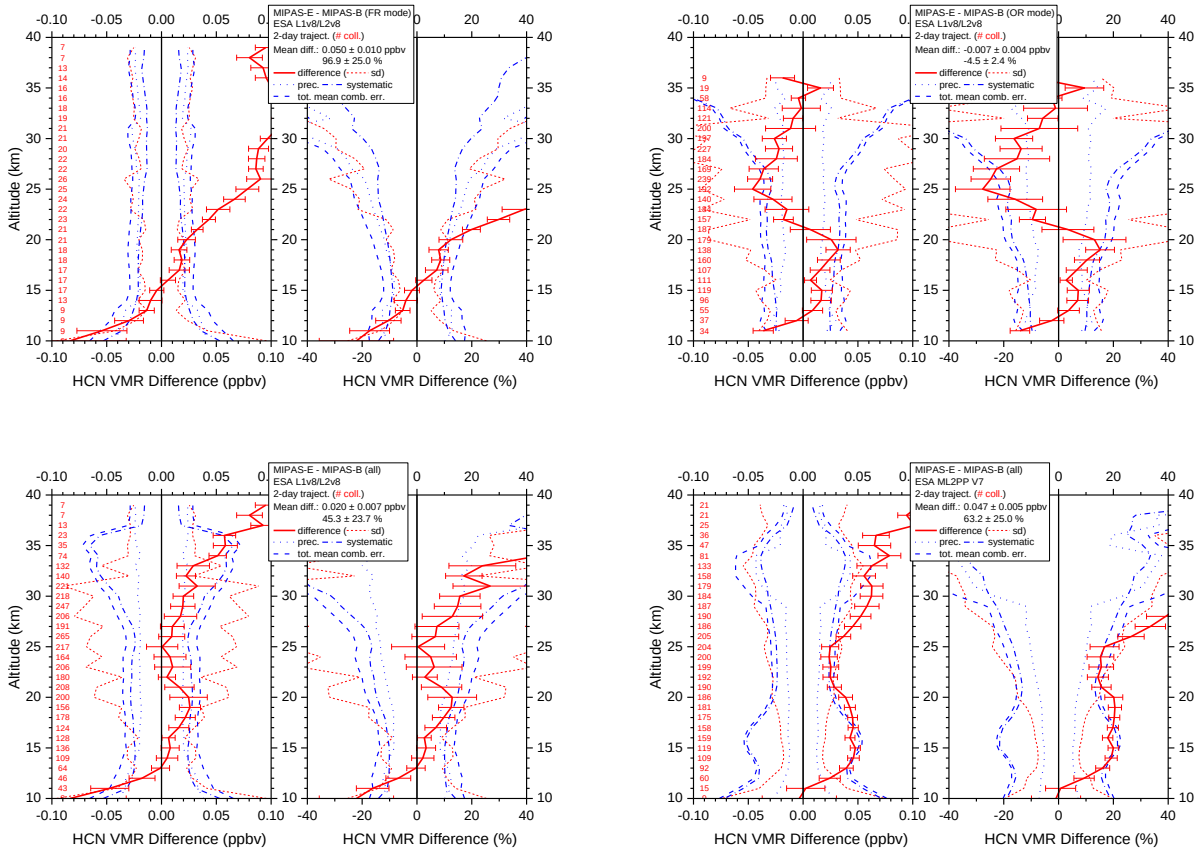

Figure 4-92 Mean absolute and relative HCN VMR difference of all trajectory match collocations (red numbers) between MIPAS-E and MIPAS-B (red solid line) including standard deviation (red dotted lines) and standard error of the mean (plotted as error bars). Precision (blue dotted lines), systematic (blue dash-dotted lines), and total (blue dashed lines) mean combined errors are shown, too. Top: v8 FR mode (left) and v8 OR mode (right) collocations; bottom: all FR plus OR v8 (left) and all FR plus OR v7 (right) collocations.

A significant positive bias of up to 100% is seen in the MIPAS data compared to the ACE v4 between 16 km and 19 km, exceeding the total error, and observed across all years in the 2005 to 2012 range (see Figure 4-93). Better consistency, between 10% to 30%, is observed between 9 and 15 km, where most of the elevated plumes of HCN occur after biomass burning events. Between 20 km and 23 km MIPAS VMRs are between 30% and 60% lower.

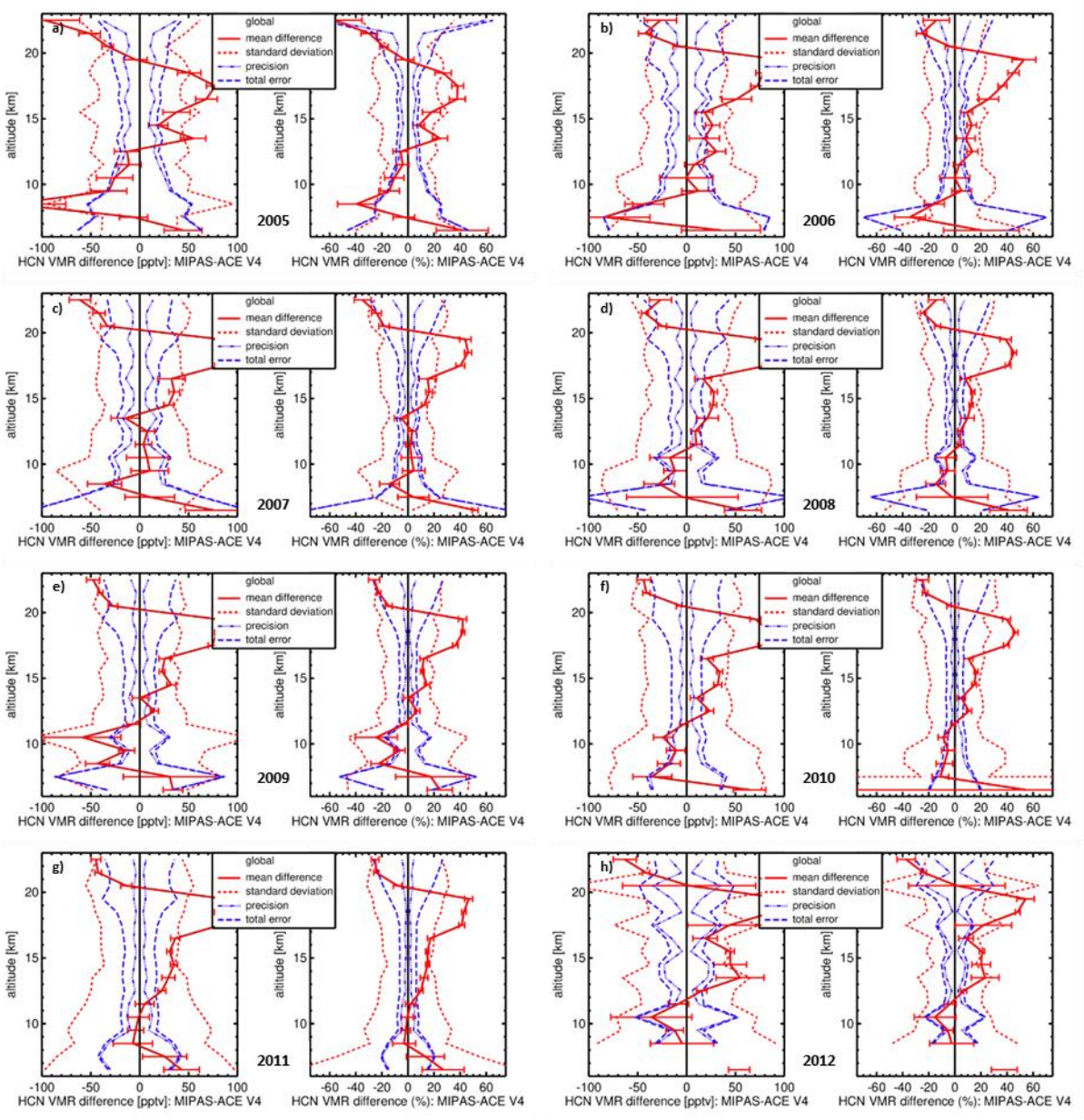

Figure 4-93. Mean absolute and relative HCN VMR difference of all match collocation (red numbers) between MIPAS and ACE version 4 data (red solid line) including standard deviation (red dotted lines) and standard error of the mean (plotted as error bars). Precision (blue dotted lines) and total (blue dashed lines) mean combined errors are shown, too. Global matchups. a) 2005, b) 2006, c) 2007, d) 2008, e) 2009, f) 2010 g) 2011, h) 2012.

4.16 Tetrafluoromethane (CFC-14 or CF_4)

LEVEL 2 V8 CFC-14PRODUCTS										
Operational modes:	FR	RR	OR							
	NOM		NOM	UTLS1	MA	UA	AE	NLC	UTLS2	UTLS1_o
Nominal Vertical range [Km]	*9-52*	*6-52*	*9-54*	*8.5-52*	---	---	*7-38*	---	*12-42*	*10-49*
Useful range	*Full range*									
Microwindows:	*Link for downloading*									
Systematic errors:	*Link for downloading* *Link errors*									

Introduction

The fluorocarbon CF_4 has an extremely long atmospheric lifetime of more than 50000 years and its atmospheric concentration is linearly increasing. In Figure 4-94 we report the timeseries of weekly means of V8 CF_4 profiles, averaged on all latitudes, for the full mission.

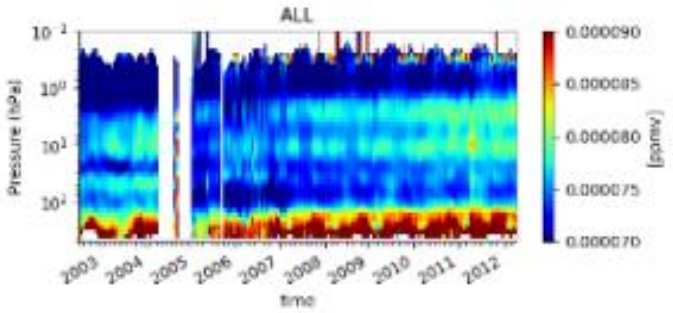

Figure 4-94 Timeseries of weekly mean of V8 CF_4 profiles on the full mission averaged on all latitudes

Differently from L2 V7 reprocessing, CF4 was processed by the L2V8 processor using the Optimal Estimation approach, with the a priori profile equal to the mean of the CF_4 climatological profiles. The diagonal element of the Covariance Matrix of the a priori are computed as the square of the 95% of the a priori profile, while the non diagonal elements are computed assuming a correlation length of 10 km. This approach allows to reduce strong oscillations present in the retrieved profiles from V7 L2 processor.

Verification and changes wrt V7 products

In Figure 4-95 we report the difference between V8 and V7 CF_4 products. Large oscillations are found in the differences, due to the reduced oscillations in V8 CF_4 retrieved profiles wrt V7 CF_4.

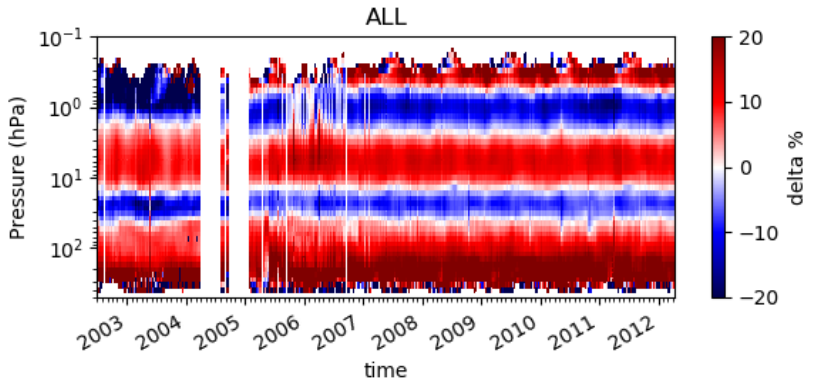

Figure 4-95 Timeseries of weekly mean percent differences between V8 and V7 CF_4 profiles averaged on all latitudes for the whole mission

Quality quantifiers (AK and errors)

The vertical averaging kernels of the CF_4 retrieval are shown in Figure 4-96 for two representative profiles in Full Resolution nominal mode (left panel) and Optimised Resolution nominal mode (right panel). The selected scans are not affected by clouds. The vertical resolution profile of the considered scan is also reported in red in the same plot and the DOF distribution profile (see Sect. 3.5.2) in blue. A mean vertical resolution profile has been also computed considering all scans in the nominal mode of 2003 (for FR plots) and 2010 (for OR plots). It is 3-5 (3-7.5) km in the range 10-40 km for FR (OR) measurements and 7 (10) km at 50 km.

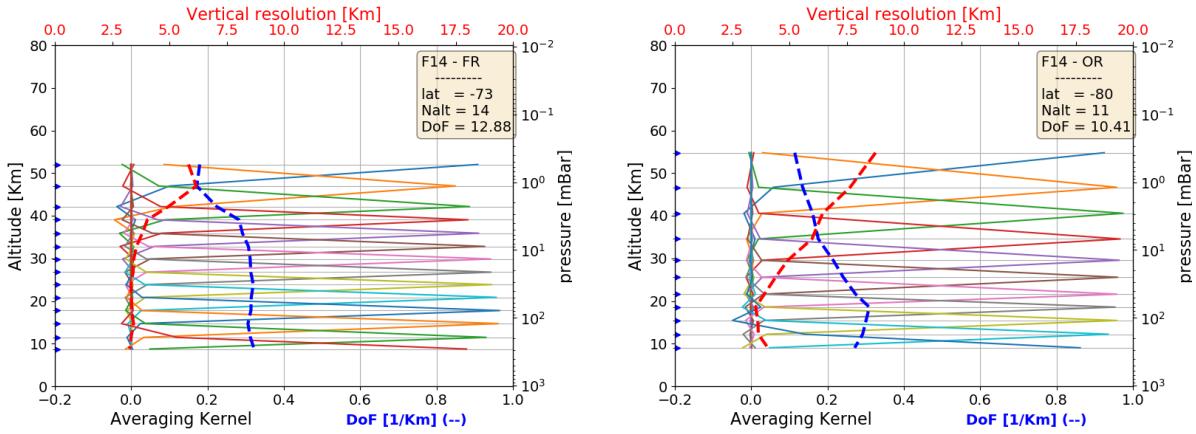

Figure 4-96 Example of CFC-14 vertical averaging kernel (AK) computed for a representative Full Resolution (left panel) and Optimized Resolution (right panel) scan. Together with the AKs, the plots show the vertical resolution (red dashed line) and the Degree of Freedom for unity height (blue dashed line). The yellow box on the top right of each panel contains the latitude of the observation, the number of the measurement sweeps and the total Degree of Freedom (DoF)

Figure 4-97 shows the average CF_4 VMR profiles (left plots) and their associated average single scan random error profiles, in absolute (middle plots) and relative (right plots) scale. The average quantities are representative of 5 reference atmospheres, namely polar summer daytime, polar winter nightime, mid-latitudes (both daytime and nightime) and equatorial daytime atmospheres. The averages have been computed using information on retrieved profiles, noise error and pT error which are contained in the output files for each scan. For mid latitude atmospheres all scans in the nominal mode of 2003 (for FR plots) and 2010 (for OR plots) in the latitude band 30-60 (both hemispheres) have been taken into account (considering either daytime or nightime scans), for equatorial atmosphere the scans in the latitude band 30S-30N, for polar winter nighttime atmosphere all nightime scans in the nominal mode of June-July-August of 2003 (for FR) and of 2005-2011 years (for OR) in the band 60S-90S, for polar summer daytime atmosphere all daytime scans in the nominal mode of December-January-February of 2003 (for FR) and 2005-2011 (for OR) in the latitude band 60S-90S. Solid lines of middle and right plots represent the total random error, coming from the quadratic summation of the noise error (dotted curves, given by the mapping of the measurement error on the retrieved profile) and the pT error (given by the propagation of the random error of retrieved pressure and temperature profiles on VMR profile).The contribution coming from the pT error propagation is significatly smaller than the noise contribution. The relative random error varies between 8 and 15% from 150 hPa to 2 hPa, outside this range it increases going to the highest and the lowest altitudes.

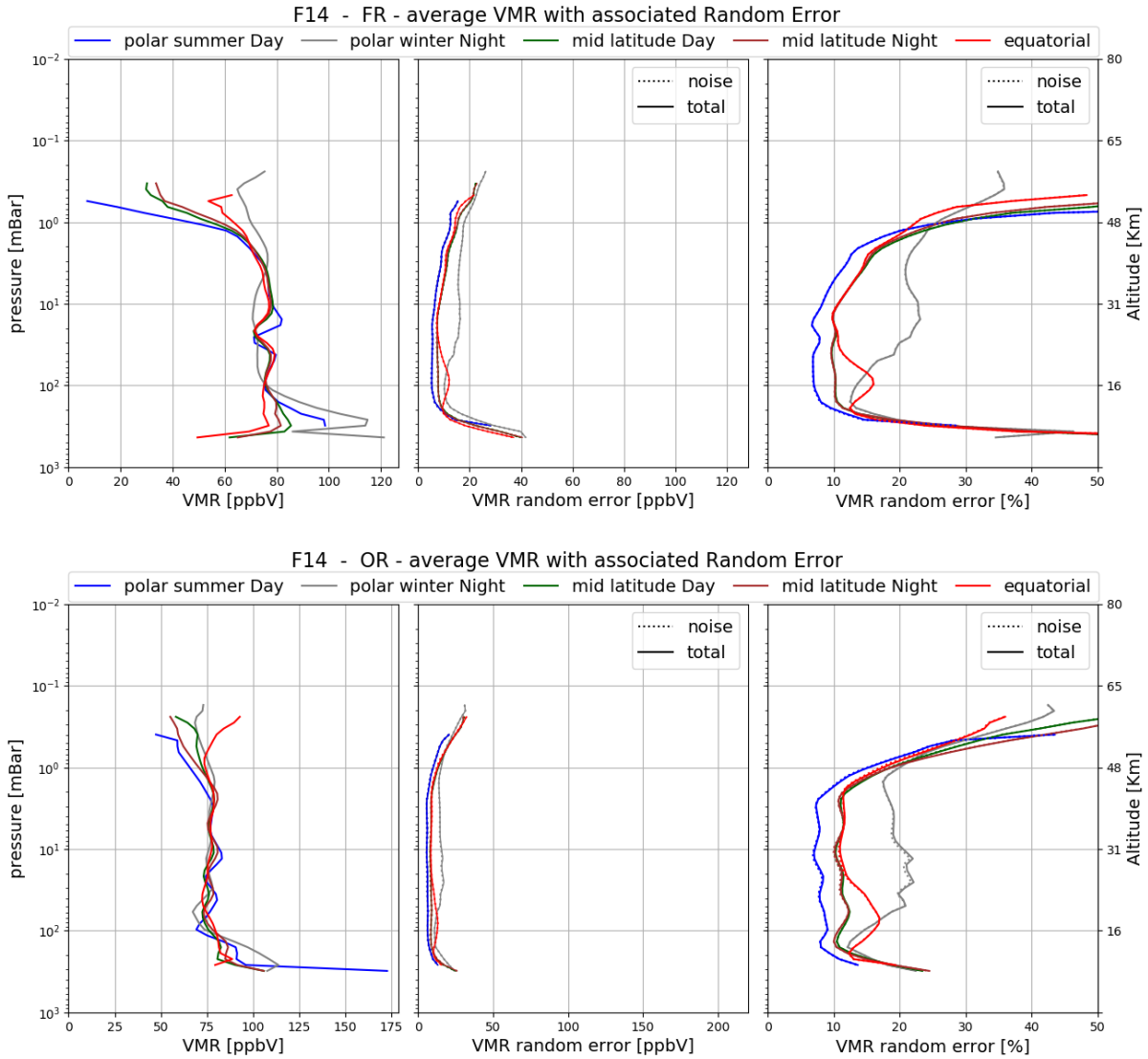

Figure 4-97 Average CF_4 VMR (left plots), absolute (mid plots) and relative (right plots) CFC-14 random error for the 5 reference atmospheres described in the text. The noise error (dotted curves) is calculated by the retrieval; the total random error (solid curves) includes the contribution to the random error coming from propagation of the pT random error on VMR profiles. Top panel: Full Resolution nominal mode; bottom panel: Optimized Resolution nominal mode.

Validation

Reference instrument	Source	Coverage validation analysis		
		Time	Horizontal	Vertical
MIPAS-B	KIT-IMK	8 flights + 2-day trajectories	3 sites, 68°N–5°S	200–2 hPa

Comparison results of both MIPAS instruments concerning the species CF_4 are shown in Figure 4-98. A general agreement between both instruments can be stated between 11 and 37 km (within ±10% in full observation period). In the FR phase, a significant positive bias above 10 km is visible. In contrast, no clear bias is obvious in the OR period where differences stay within ±10% at all altitudes. However, standard deviations exceed the expected precision in the OR phase. Clearly reduced deviations around 26 km compared to v7 are obvious.

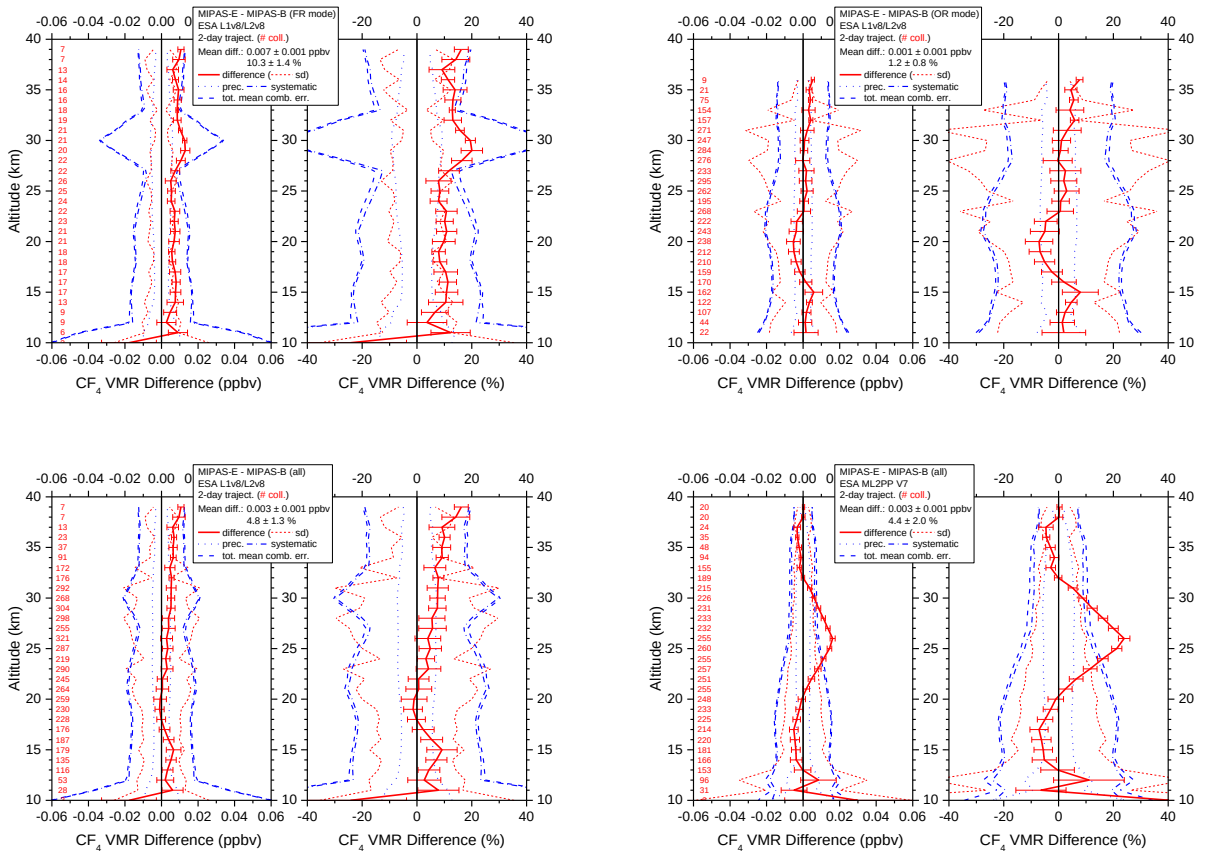

Figure 4-98 Mean absolute and relative CF_4 VMR difference of all trajectory match collocations (red numbers) between MIPAS-E and MIPAS-B (red solid line) including standard deviation (red dotted lines) and standard error of the mean (plotted as error bars). Precision (blue dotted lines), systematic (blue dash-dotted lines), and total (blue dashed lines) mean combined errors are shown, too. Top: v8 FR mode (left) and v8 OR mode (right) collocations; bottom: all FR plus OR v8 (left) and all FR plus OR v7 (right) collocations.

4.17 Chloro(difluoro)methane (HCFC-22)

LEVEL 2 V8 HCFC-22 PRODUCTS										
Operational modes:	FR	RR	OR							
	NOM		NOM	UTLS1	MA	UA	AE	NLC	UTLS2	UTLS1_o
Nominal Vertical range [Km]	*6-36*	*6-36*	*6-37*	*8.5-34*	---	---	*7-33.5*	---	*12-37*	*10-34*
Useful range	*Full range*									
Microwindows:	*Link for downloading*									
Systematic errors:	*Link for downloading* *Link errors*									

Introduction

HCFC-22 was used as temporary substitute of CFCs which were banned by Montreal protocol. In Figure 4-99 the timeseries of V8 HCFC-22 in the latitude band 0-30N on the full mission are shown. A positive trend of HCFC-22 VMR is clearly visible in the timeseries.

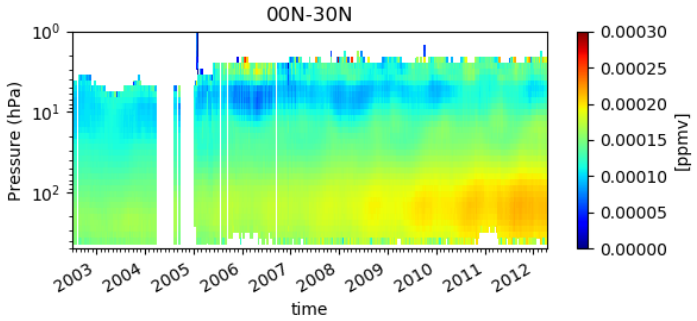

Figure 4-99 Timeseries of weekly mean of HCFC-22 on the full mission averaged on the latitude band 0-30N

Verification and changes wrt V7 products

In Figure 4-100 we report the difference between V8 and V7 products. V8 HCFC-22 is about 5-15% lower than V7 HCFC-22.

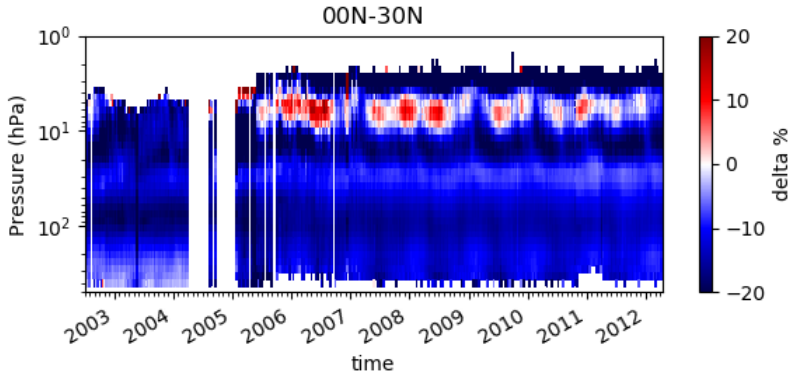

Figure 4-100 Timeseries of weekly mean percent differences between V8 and V7 HCFC-22 profiles all over the mission for latitude band 0-30N. Blue values indicate that V8 HCFC-22 is smaller than V7 HCFC-22.

The differences are due to the changed cross-sections for HCFC-22 (see Harrison, 2016 and 'Assessment of Molecular Cross-Section Data v. 2', here)

Quality quantifiers (AK and errors)

The vertical averaging kernels of the HCFC-22 retrieval are shown in Figure 4-101 for two representative profiles in Full Resolution nominal mode (left panel) and Optimised Resolution nominal mode (right panel). The selected scans are not affected by clouds. The vertical resolution profile of the considered scan is also reported in red in the same plot and the DOF distribution profile (see Sect. 3.5.2) in blue. A mean vertical resolution profile has been also computed considering all scans in the nominal mode of 2003 (for FR plots) and 2010 (for OR plots). It is 5 km at 10 km, 7.5-10 in the range 20-30 km, about 5 at 40 km for both FR and OR measurements.

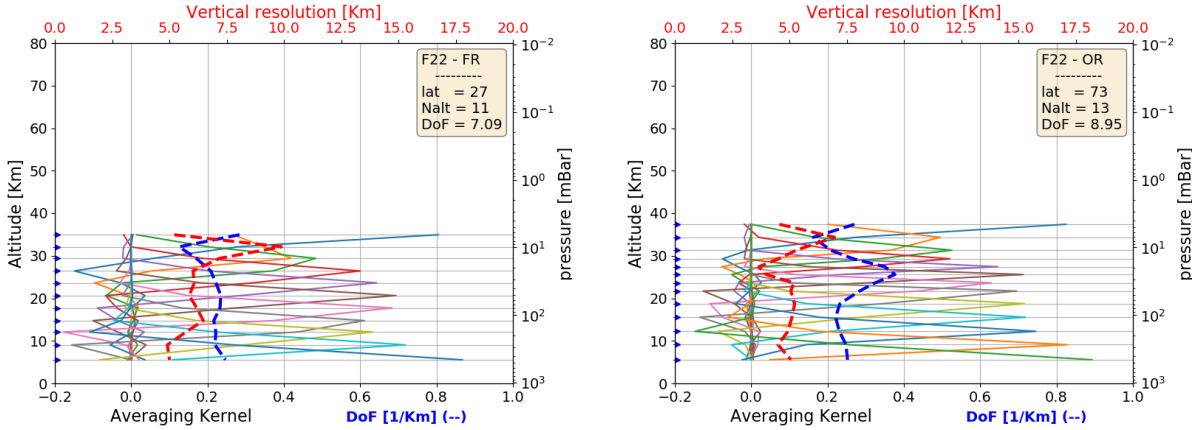

Figure 4-101 Example of HCFC-22 vertical averaging kernel (AK) computed for a representative Full Resolution (left panel) and Optimized Resolution (right panel) scan. Together with the AKs, the plots show the vertical resolution (red dashed line) and the Degree of Freedom for unity height (blue dashed line). The yellow box on the top right of each panel contains the latitude of the observation, the number of the measurement sweeps and the total Degree of Freedom (DoF)

Figure 4-102 shows the average HCFC-22 VMR profiles (left plots) and their associated average random error profiles, in absolute (middle plots) and relative (right plots) scale. The average quantities are representative of 5 reference atmospheres, namely polar summer daytime, polar winter nightime, mid-latitudes (both daytime and nightime) and equatorial daytime atmospheres. The averages have been computed using information on retrieved profiles, noise error and pT error which are contained in the output files for each scan. For mid latitude atmospheres all scans in the nominal mode of 2003 (for FR plots) and 2010 (for OR plots) in the latitude band 30-60 (both hemispheres) have been taken into account (considering either daytime or nightime scans), for equatorial atmosphere the scans in the latitude band 30S-30N, for polar winter nighttime atmosphere all nightime scans in the nominal mode of June-July-August of 2003 (for FR) and of 2005-2011 years (for OR) in the band 60S-90S, for polar summer daytime atmosphere all daytime scans in the nominal mode of December-January-February of 2003 (for FR) and 2005-2011 (for OR) in the latitude band 60S-90S. Solid lines of middle and right plots represent the total random error, coming from the quadratic summation of the noise error (dotted curves, given by the mapping of the measurement error on the retrieved profile) and the pT error (given by the propagation of the random error of retrieved pressure and temperature profiles on VMR profile).The contribution coming from the pT error propagation is generally smaller than the noise contribution. The relative random error is about 2% between 300 hPa and 50 hPa for both FR and OR measurements and 20% (40%) at 10 hPa for FR (OR) measurements.

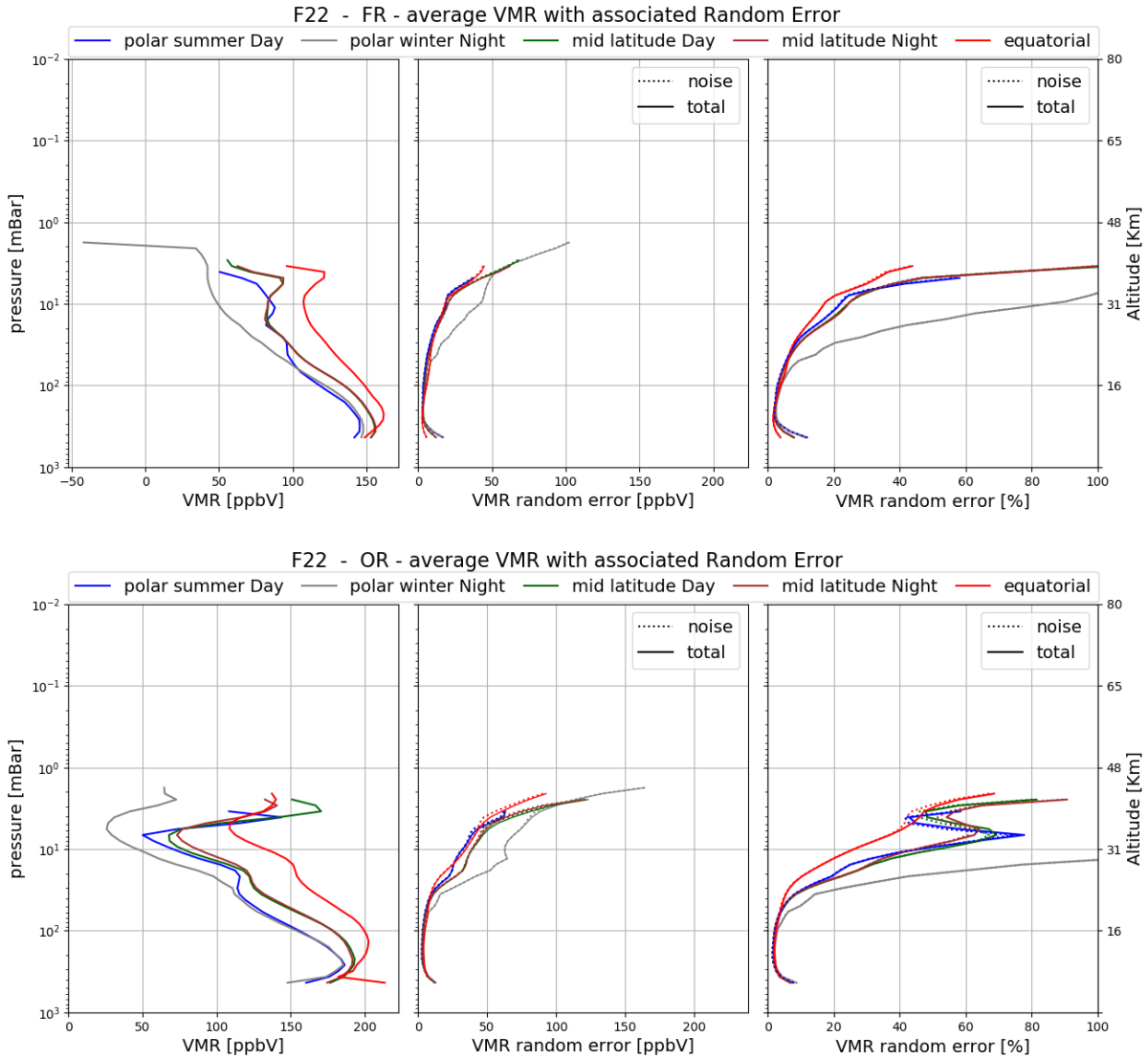

Figure 4-102 Average HCFC-22 VMR (left plots), absolute (mid plots) and relative (right plots) HCFC-22 random error for the 5 reference atmospheres described in the text. The noise error (dotted curves) is calculated by the retrieval; the total random error (solid curves) includes the contribution to the random error coming from propagation of the pT random error on VMR profiles. Top panel: Full Resolution nominal mode; bottom panel: Optimized Resolution nominal mode.

Validation

Reference instrument	Source	Coverage validation analysis		
		Time	Horizontal	Vertical
MIPAS-B	KIT-IMK	8 flights + 2-day trajectories	3 sites, 68°N–5°S	200–5 hPa

Comparison results of HCFC-22 ($CHClF_2$) are depicted in Figure 4-103. In the FR mode period differences between both MIPAS instruments remain within ±10% up to 26 km turning into a significant positive bias above this altitude. In the OR observation period, deviations stay within 10% for altitudes up to 28 km while a significant negative bias is visible in the MIPAS-E data above this altitude level. Standard deviations exceed the expected precision at higher altitudes (mainly OR phase). A slightly reduced negative bias above 28 km compared to previous v7 data is visible.

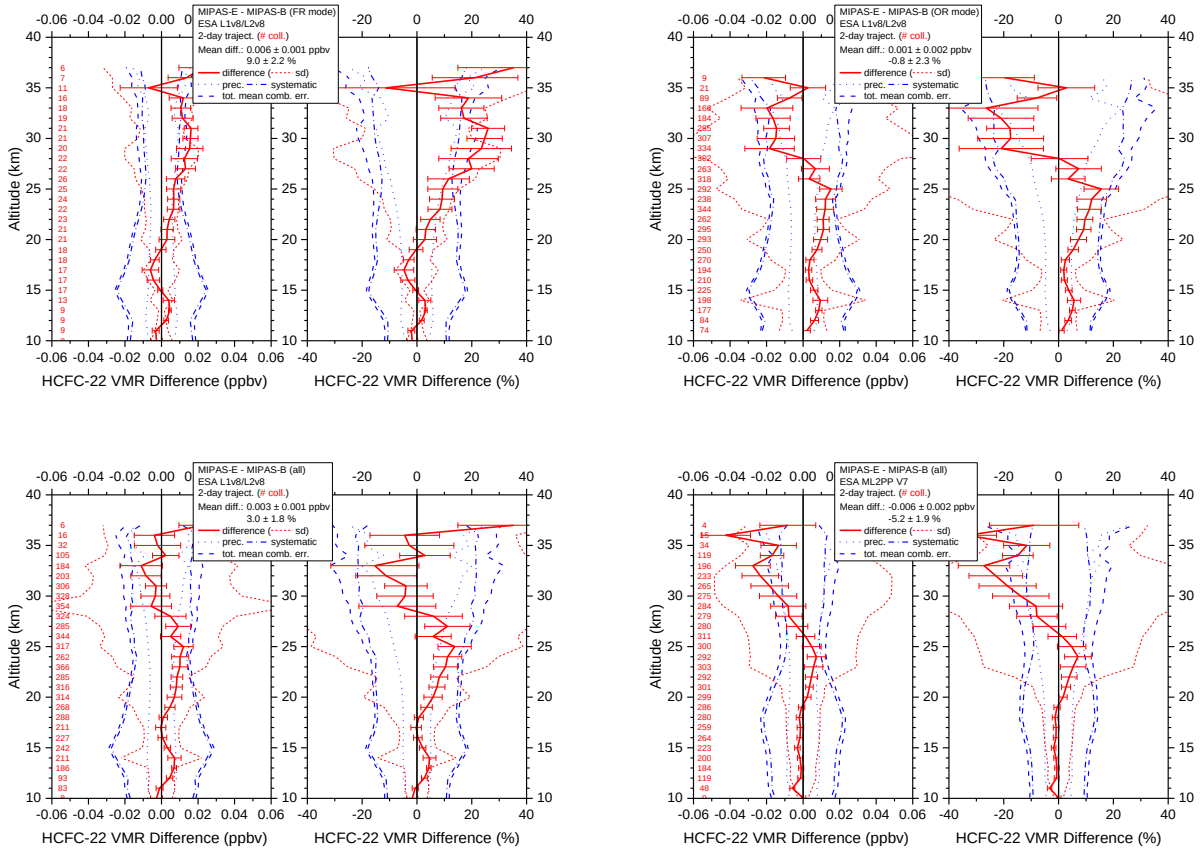

Figure 4-103 Mean absolute and relative HCFC-22 VMR difference of all trajectory match collocations (red numbers) between MIPAS-E and MIPAS-B (red solid line) including standard deviation (red dotted lines) and standard error of the mean (plotted as error bars). Precision (blue dotted lines), systematic (blue dash-dotted lines), and total (blue dashed lines) mean combined errors are shown, too. Top: v8 FR mode (left) and v8 OR mode (right) collocations; bottom: all FR plus OR v8 (left) and all FR plus OR v7 (right) collocations.

4.18 Acetylene (C_2H_2)

LEVEL 2 V8 ACETYLENE PRODUCTS										
Operational modes:	FR	RR	OR							
	NOM		NOM	UTLS1	MA	UA	AE	NLC	UTLS2	UTLS1_o
Nominal Vertical range [Km]	*6-36*	*6-21*	*6-23*	*8.5-24*	---	---	*7-20*	---	*12-23*	*8.5-22*
Useful range	*All altitudes up to 22 km (pressures greater than 60 hPa)*									
Microwindows:	*Link for downloading*									
Systematic errors:	*Link for downloading* *Link errors*									

Introduction

This molecule is a new molecule of MIPAS ESA L2V8 dataset.

Retrieval is performed with Optimal Estimation, with the a priori profile equal to the mean of the C_2H_2 climatological profiles. The diagonal element of the CM of the a priori are computed as the square of the sum of a constant ($5\ 10^{-8}$ ppmv) plus the 90% of the a priori profile, while the non diagonal elements are computed assuming a correlation length of 4 km.

C_2H_2 is mainly produced by biomass burning and, to a lesser extent, by biofuel burning. In Figure 4-104 the timeseries of V8 C_2H_2 in the latitude band 30N-60N are shown. Localized enhancements of C_2H_2 concentration in particular periods of each year are visible during the whole mission.

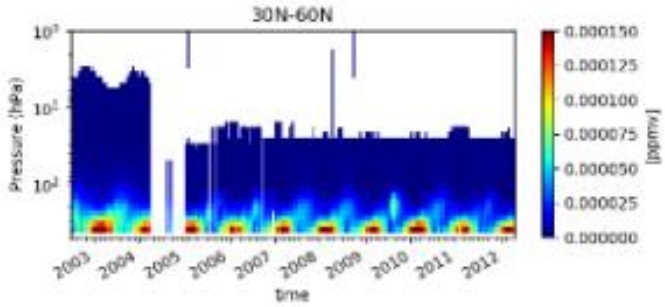

Figure 4-104 Timeseries of weekly mean of C2H2 on the full mission averaged on the latitude band 30N-60N

Quality quantifiers (AK and errors)

The vertical averaging kernels of the C_2H_2 retrieval are shown in Figure 4-105 for two representative profiles in Full Resolution nominal mode (left panel) and Optimised Resolution nominal mode (right panel). The selected scans are not affected by clouds. The vertical resolution profile of the considered scan is also reported in red in the same plot and the DOF distribution profile (see Sect. 3.5.2) in blue. A mean vertical resolution profile has been also computed considering all scans in the nominal mode of 2003 (for FR plots) and 2010 (for OR plots). It is 3-4 km between 6 and 13 km, and it is 10 km at 20 km for both FR and OR measurements.

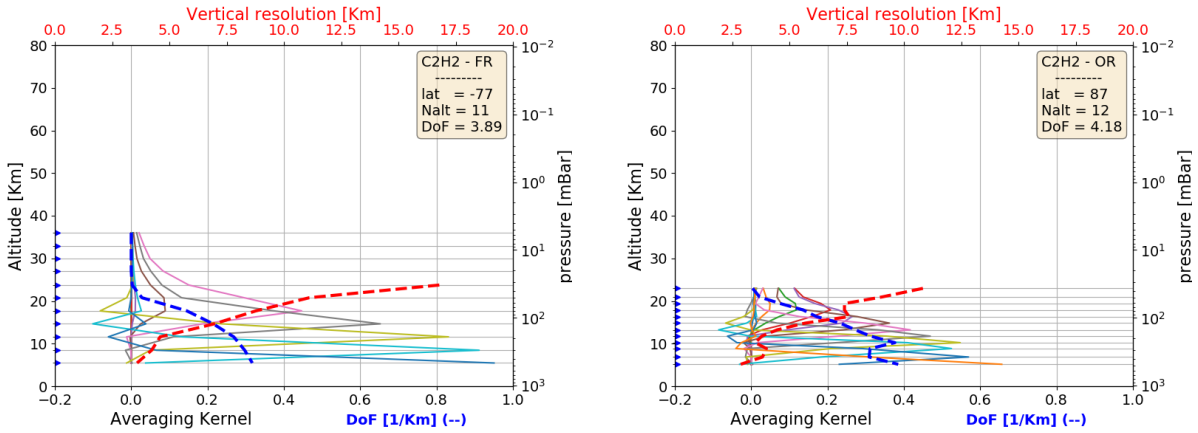

Figure 4-105 Example of C_2H_2 vertical averaging kernel (AK) computed for a representative Full Resolution (left panel) and Optimized Resolution (right panel) scan. Together with the AKs, the plots show the vertical resolution (red dashed line) and the Degree of Freedom for unity height (blue dashed line). The yellow box on the top right of each panel contains the latitude of the observation, the number of the measurement sweeps and the total Degree of Freedom (DoF)

Figure 4-106 shows the average C_2H_2 VMR profiles (left plots) and their associated average single scan random error profiles, in absolute (middle plots) and relative (right plots) scale. The average quantities are representative of 5 reference atmospheres, namely polar summer daytime, polar winter nightime, mid-latitudes (both daytime and nightime) and equatorial daytime atmospheres. The averages have been computed using information on retrieved profiles, noise error and pT error which are contained in the output files for each scan. For mid latitude atmospheres all scans in the nominal mode of 2003 (for FR plots) and 2010 (for OR plots) in the latitude band 30-60 (both hemispheres) have been taken into account (considering either daytime or nightime scans), for equatorial atmosphere the scans in the latitude band 30S-30N, for polar winter nighttime atmosphere all nightime scans in the nominal mode of June-July-August of 2003 (for FR) and of 2005-2011 years (for OR) in the band 60S-90S, for polar summer daytime atmosphere all daytime scans in the nominal mode of December-January-February of 2003 (for FR) and 2005-2011 (for OR) in the latitude band 60S-90S. Solid lines of middle and right plots represent the total random error, coming from the quadratic summation of the noise error (dotted curves, given by the mapping of the measurement error on the retrieved profile) and the pT error (given by the propagation of the random error of retrieved pressure and temperature profiles on VMR profile). The contribution to the random error coming from the pT error propagation is smaller than the noise contribution for FR measurements, while it is very large for OR measurements. The relative random error varies for the different atmospheres, but it is never smaller than 15%.

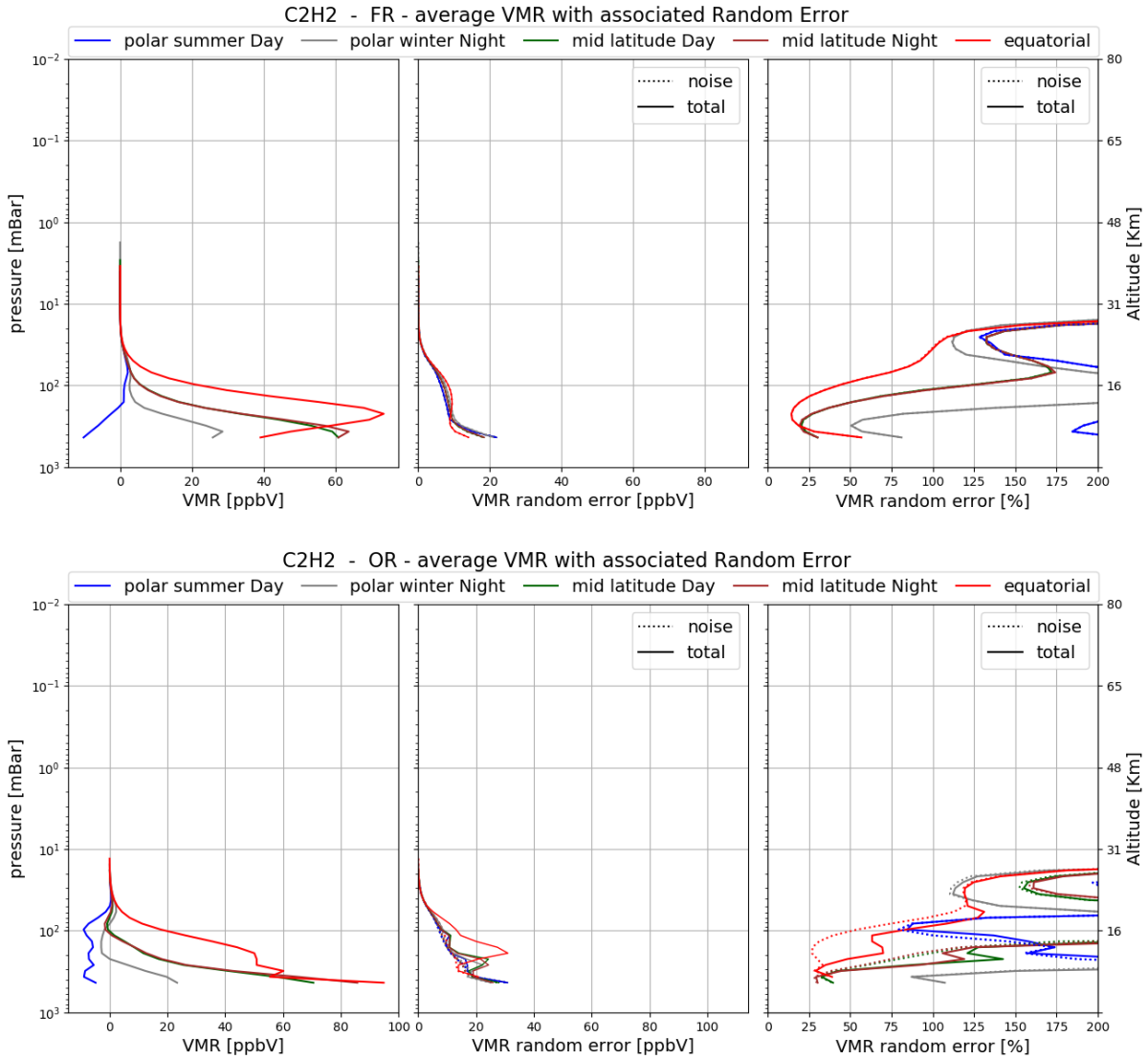

Figure 4-106 Average C_2H_2 VMR (left plots), absolute (mid plots) and relative (right plots) C_2H_2 random error for the 5 reference atmospheres described in the text. The noise error (dotted curves) is calculated by the retrieval; the total random error (solid curves) includes the contribution to the random error coming from propagation of the pT random error on VMR profiles. Top panel: Full Resolution nominal mode (average 2003); bottom panel: Optimized Resolution nominal mode (average on 2010).

Validation

Reference instrument	Source	Coverage validation analysis		
		Time	Horizontal	Vertical
MIPAS-B	KIT-IMK	8 flights + 2-day trajectories	3 sites, 68°N–5°S	200–20 hPa
ACE-FTS v4	U Waterloo	2005-2012	global	500-0.04 hPa

MIPAS contains a large number of negative C_2H_2 values, particularly in Arctic winter. MIPAS is consistent with the balloon-borne MIPAS measurements up to 24 km (within ±50 %). MIPAS is negatively biased with the ACE-FTS by between 5 and 50% below 25 km. Details of results of validation are reported below.

Differences in the C_2H_2 VMR of both MIPAS instruments are within ±50% up to 24 km (see Figure 4-107). A significant negative bias (within -50% difference limit) is evident in the FR mode (except 15-16 km). A significant negative bias below 20 km and above 23 km can be seen in the OR mode (exceeding combined systematic errors and the -50% difference limit). Lower stratospheric altitude regions in MIPAS-E retrievals sometimes show negative VMRs (in Arctic winter). Hence, this species should be carefully used in scientific studies.

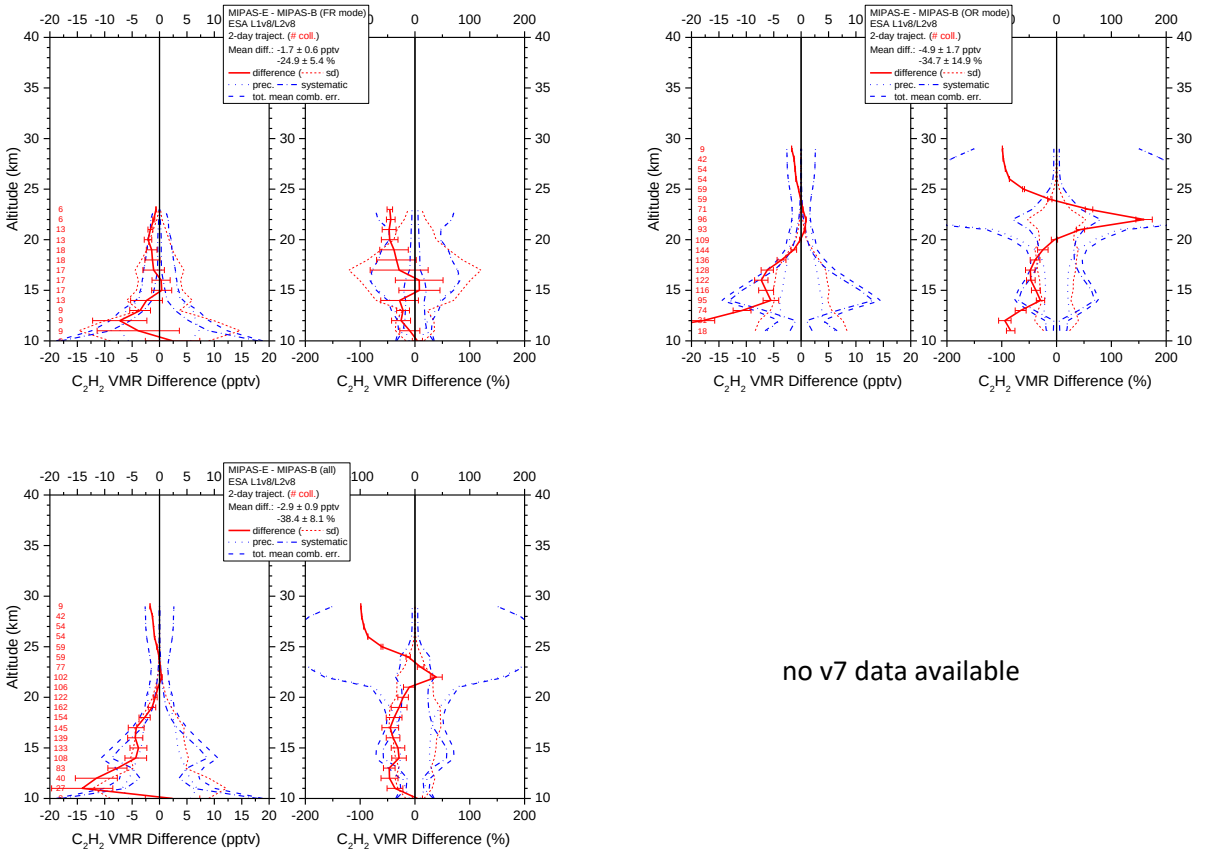

Figure 4-107 Mean absolute and relative C_2H_2 VMR difference of all trajectory match collocations (red numbers) between MIPAS-E and MIPAS-B (red solid line) including standard deviation (red dotted lines) and standard error of the mean (plotted as error bars). Precision (blue dotted lines), systematic (blue dash-dotted lines), and total (blue dashed lines) mean combined errors are shown, too. Top: v8 FR mode (left) and v8 OR mode (right) collocations; bottom: all FR plus OR v8 (left) and all FR plus OR v7 (right) collocations.

The MIPAS VMRs are 10% to 50% lower than ACE across the profile (5 km to 25 km) and all years between 2005 and 2012, but within the expected total error (see Figure 4-108). There are quite a few instances, particularly in the polar winters, where the C_2H_2 signal gives many negative values which means that some care needs to be taken with the data for scientific needs.

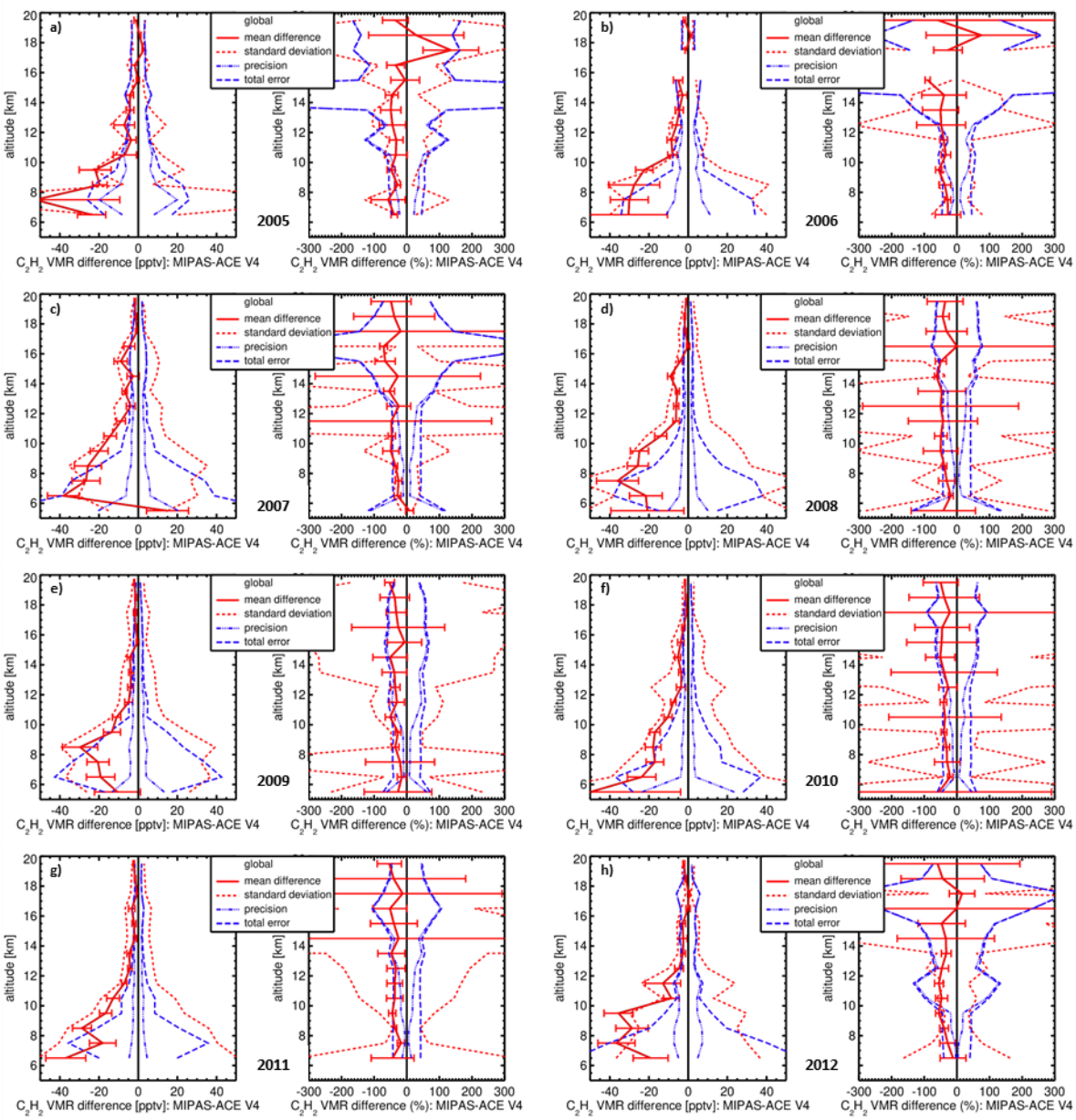

Figure 4-108. Mean absolute and relative C_2H_2 VMR difference of all match collocation (red numbers) between MIPAS and ACE version 4 data (red solid line) including standard deviation (red dotted lines) and standard error of the mean (plotted as error bars). Precision (blue dotted lines) and total (blue dashed lines) mean combined errors are shown, too. Global matchups. a) 2005, b) 2006, c) 2007, d) 2008, e) 2009, f) 2010 g) 2011, h) 2012.

4.19 Ethane (C_2H_6)

LEVEL 2 V8 ETHANE PRODUCTS										
Operational modes:	FR	RR	OR							
	NOM		NOM	UTLS1	MA	UA	AE	NLC	UTLS2	UTLS1_o
Nominal Vertical range [Km]	*6-42*	*9-30*	*7.5-31*	*10-34*	*---*	*---*	*8.5-29*	*---*	*12-29*	*8.5-31*
Useful range	*All altitudes up to 22 km (pressures greater than 60 hPa)*									
Microwindows:	*Link for downloading*									
Systematic errors:	*Link for downloading* *Link errors*									

Introduction

This molecule is a new molecule of MIPAS ESA L2V8 dataset.

Retrieval is performed with Optimal Estimation, with the a priori profile equal to the mean of the C_2H_6 climatological profiles. The diagonal element of the CM of the a priori are computed as the square of the sum of a constant (10^{-7} ppmv) plus the 90% of the a priori profile, while the non diagonal elements are computed assuming a correlation length of 5 km.

C_2H_6 is produced by biomass burning, natural gas losses and fossil fuel production. In Figure 4-109 we present the timeseries of V8 C_2H_6 in the latitude band 30N-60N.

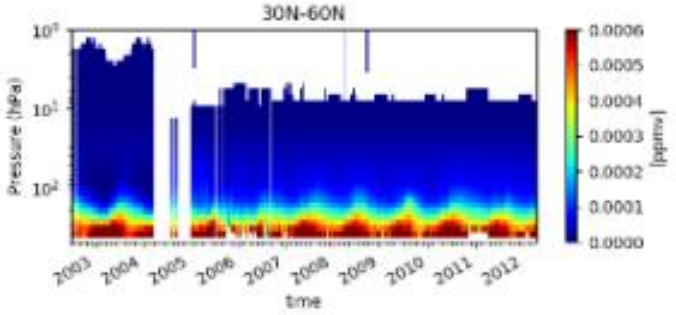

Figure 4-109 Timeseries of weekly mean of C_2H_6 on the full mission averaged on the latitude band 30N-60N

Quality quantifiers (AK and errors)

The vertical averaging kernels of the C_2H_6 retrieval are shown in Figure 4-110 for two representative profiles in Full Resolution nominal mode (left panel) and Optimised Resolution nominal mode (right panel). The selected scans are not affected by clouds. The vertical resolution profile of the considered scan is also reported in red in the same plot and the DOF distribution profile (see Sect. 3.5.2) in blue. A mean vertical resolution profile has been also computed considering all scans in the nominal mode of 2003 (for FR plots) and 2010 (for OR plots). It is about 5 km in a small interval around 10 km, it is 10-12 at 20 km, then it rapidly increases, and this it is true for both FR and OR measurements.

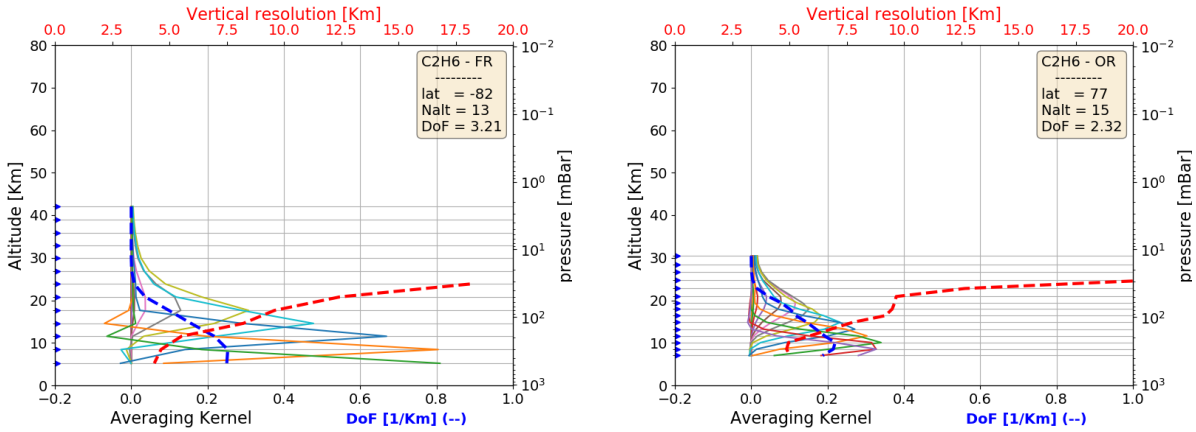

Figure 4-110 Example of C_2H_6 vertical averaging kernel (AK) computed for a representative Full Resolution (left panel) and Optimized Resolution (right panel) scan. Together with the AKs, the plots show the vertical resolution (red dashed line) and the Degree of Freedom for unity height (blue dashed line). The yellow box on the top right of each panel contains the latitude of the observation, the number of the measurement sweeps and the total Degree of Freedom (DoF)

Figure 4-111 shows the average C_2H_6 VMR profiles (left plots) and their associated average single scan random error profiles, in absolute (middle plots) and relative (right plots) scale. The average quantities are representative of 5 reference atmospheres, namely polar summer daytime, polar winter nightime, mid-latitudes (both daytime and nightime) and equatorial daytime atmospheres. The averages have been computed using information on retrieved profiles, noise error and pT error which are contained in the output files for each scan. For mid latitude atmospheres all scans in the nominal mode of 2003 (for FR plots) and 2010 (for OR plots) in the latitude band 30-60 (both hemispheres) have been taken into account (considering either daytime or nightime scans), for equatorial atmosphere the scans in the latitude band 30S-30N, for polar winter nighttime atmosphere all nightime scans in the nominal mode of June-July-August of 2003 (for FR) and of 2005-2011 years (for OR) in the band 60S-90S, for polar summer daytime atmosphere all daytime scans in the nominal mode of December-January-February of 2003 (for FR) and 2005-2011 (for OR) in the latitude band 60S-90S. Solid lines of middle and right plots represent the total random error, coming from the quadratic summation of the noise error (dotted curves, given by the mapping of the measurement error on the retrieved profile) and the pT error (given by the propagation of the random error of retrieved pressure and temperature profiles on VMR profile). The contribution to the random error coming from the pT error propagation is large for OR measurements. The single scan random error varies for the different atmospheres but it is never smaller than 25%.

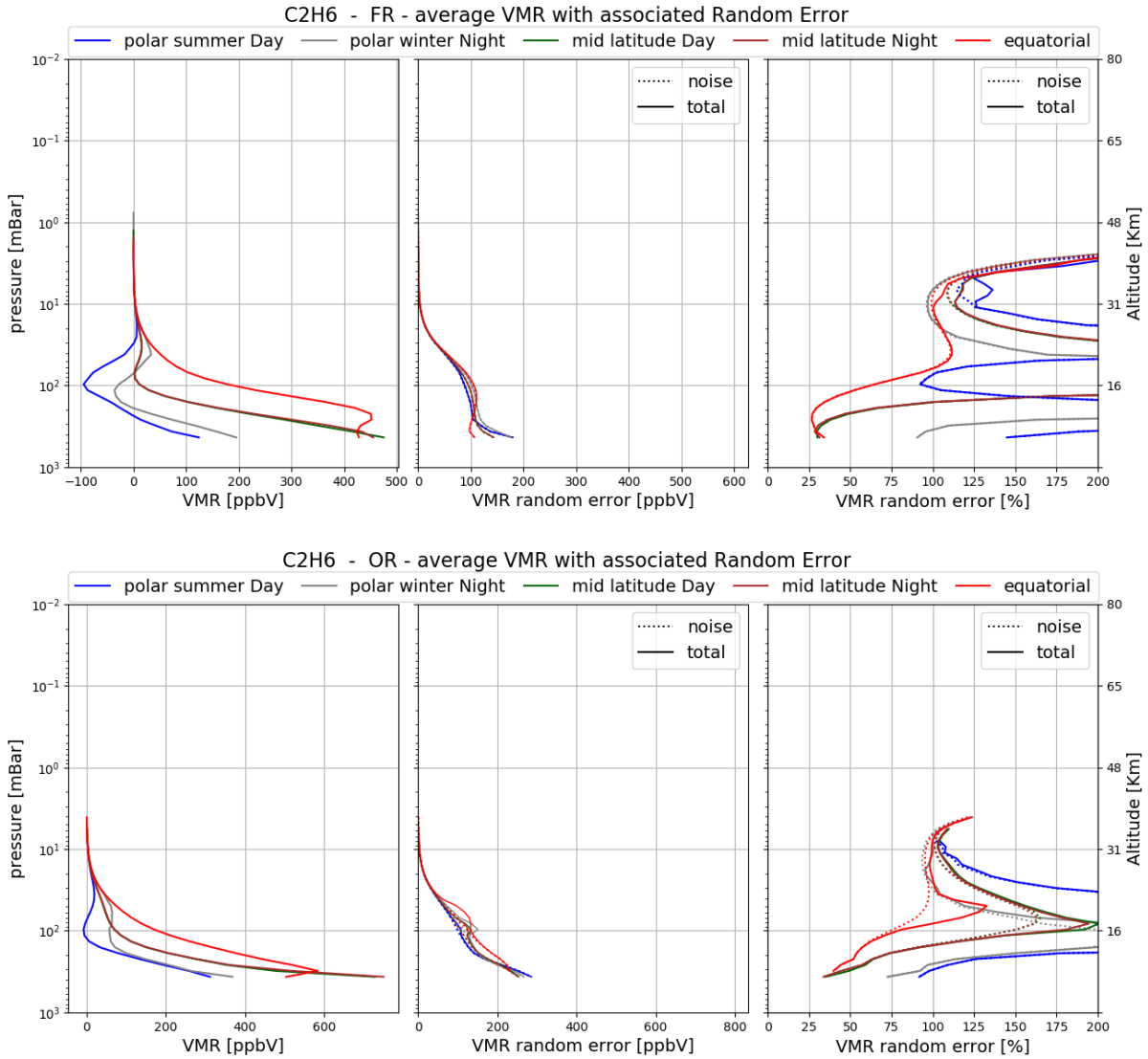

Figure 4-111 Average C_2H_6 VMR (left plots), absolute (mid plots) and relative (right plots) C_2H_6 random error for the 5 reference atmospheres described in the text. The noise error (dotted curves) is calculated by the retrieval; the total random error (solid curves) includes the contribution to the random error coming from propagation of the pT random error on VMR profiles. Top panel: Full Resolution nominal mode (average 2003); bottom panel: Optimized Resolution nominal mode (average on 2010).

Validation

Reference instrument	Source	Coverage validation analysis		
		Time	Horizontal	Vertical
MIPAS-B	KIT-IMK	8 flights + 2-day trajectories	3 sites, 68°N–5°S	200–50 hPa
ACE-FTS v4	U Waterloo	2005-2012	global	500-0.04 hPa

Comparisons with MIPAS-balloon in the OR period show very good consistency (within ±25%) in the altitude range 10-20 km, whereas MIPAS is up to 30% higher than ACE-FTS in the same range. In the FR period a significant negative bias of greater than 50% in some instances is observed by MIPAS with respect to the balloon-borne measurements. Details of results of validation are reported below.

C_2H_6 VMR differences between the two MIPAS instruments are within ±25% up to 19 km (see Figure 4-112). While a significant negative bias is obvious in the FR period (exceeding -50% limit above 13 km), no bias is seen in the MIPAS-E data below 20 km in the OR mode where differences are within a ±20% range. Lower stratospheric altitude regions in MIPAS-E retrievals sometimes show negative VMRs (in the Arctic). Consequently, C_2H_6 profiles should be carefully used in scientific studies.

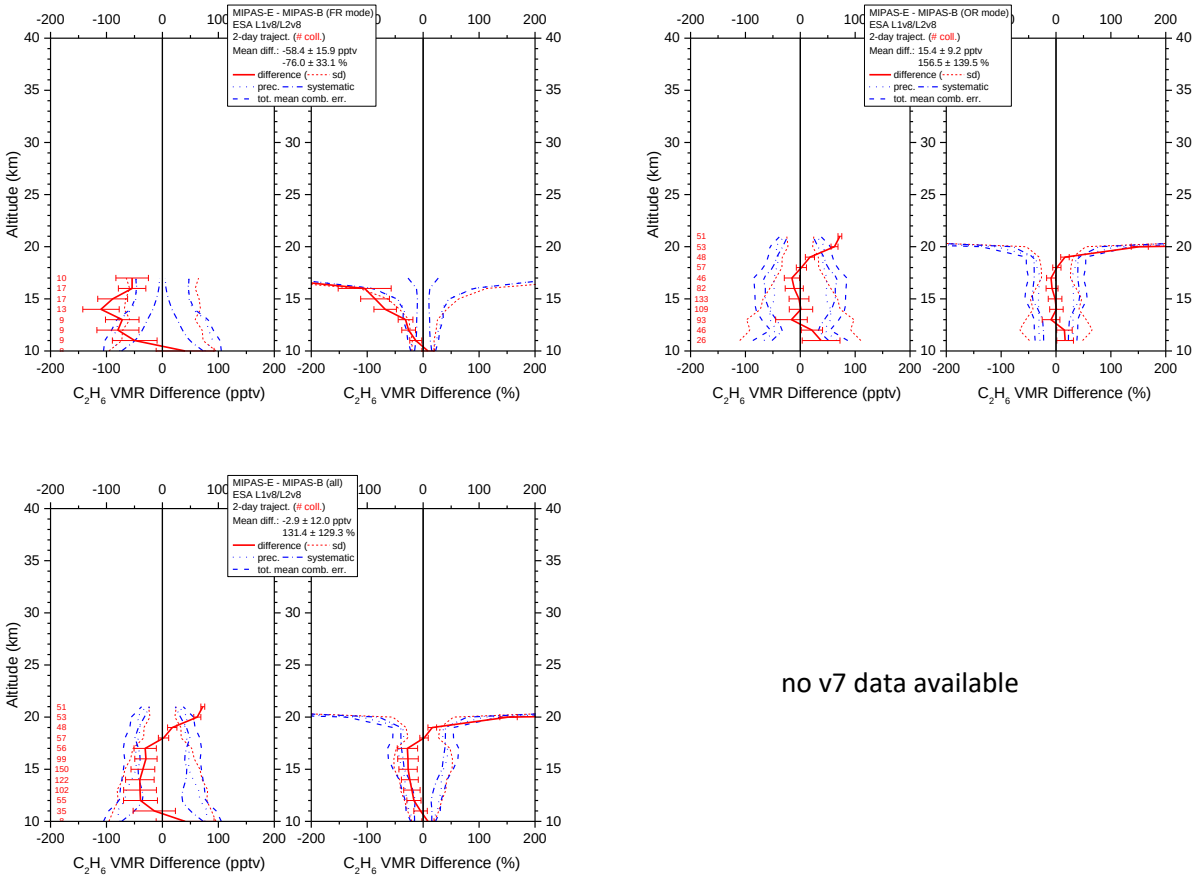

Figure 4-112 Mean absolute and relative C_2H_6 VMR difference of all trajectory match collocations (red numbers) between MIPAS-E and MIPAS-B (red solid line) including standard deviation (red dotted lines) and standard error of the mean (plotted as error bars). Precision (blue dotted lines), systematic (blue dash-dotted lines), and total (blue dashed lines) mean combined errors are shown, too. Top: v8 FR mode (left) and v8 OR mode (right) collocations; bottom: all FR plus OR v8 (left) and all FR plus OR v7 (right) collocations.

In the mid- to upper troposphere (6 km to 10 km) MIPAS ethane is between 30% and 50% higher than ACE, reducing to 20%-30% higher between 12 km and 14 km (see Figure 4-113). Above 15 km, there is a much larger spread in the differences, which may be related to issues with ACE data at higher altitude, first reported for version 3.5/3.6.

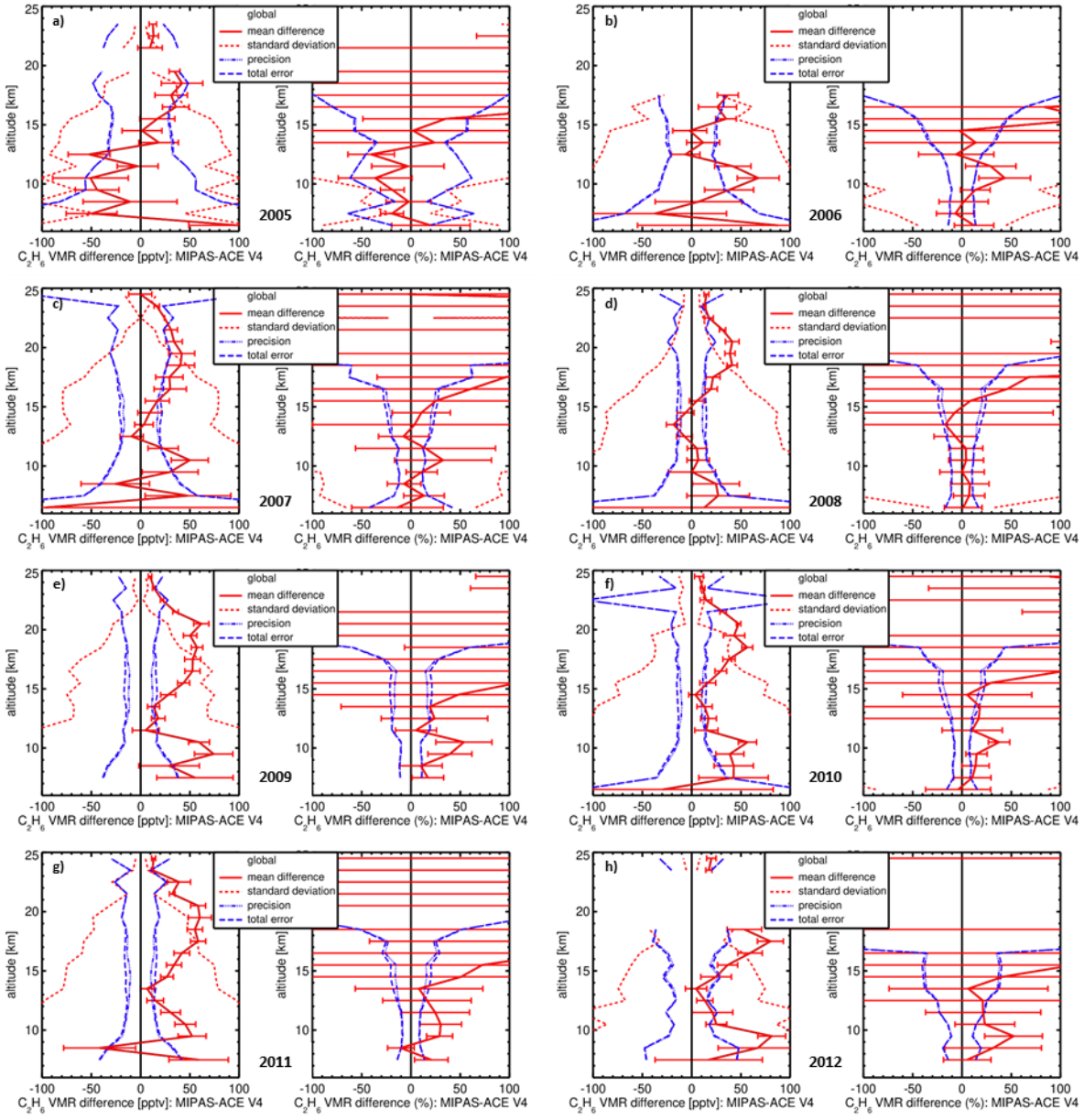

Figure 4-113. Mean absolute and relative C2H6 VMR difference of all match collocation (red numbers) between MIPAS and ACE version 4 data (red solid line) including standard deviation (red dotted lines) and standard error of the mean (plotted as error bars). Precision (blue dotted lines) and total (blue dashed lines) mean combined errors are shown, too. Global matchups. a) 2005, b) 2006, c) 2007, d) 2008, e) 2009, f) 2010 g) 2011, h) 2012.

4.20 Chloromethane (CH_3Cl)

LEVEL 2 V8 CHLOROMETHANE PRODUCTS										
Operational modes:	FR	RR	OR							
	NOM		NOM	UTLS1	MA	UA	AE	NLC	UTLS2	UTLS1_o
Nominal Vertical range [Km]	*12-42*	*6-39*	*10.5-40*	*8.5-43*	---	---	*7-38*	---	*12-37*	*8.5-39*
Useful range	*Up to 28 km (pressures larger than 20 hPa)*									
Microwindows:	*Link for downloading*									
Systematic errors:	*Link for downloading* *Link errors*									

Introduction

This molecule is a new molecule of MIPAS ESA L2V8 dataset.
CH_3Cl is the most abundant halocarbon in the atmosphere and originates from natural and anthropogenic sources. In Figure 4-114. we present the timeseries of CH_3Cl in the latitude band 30S-0.

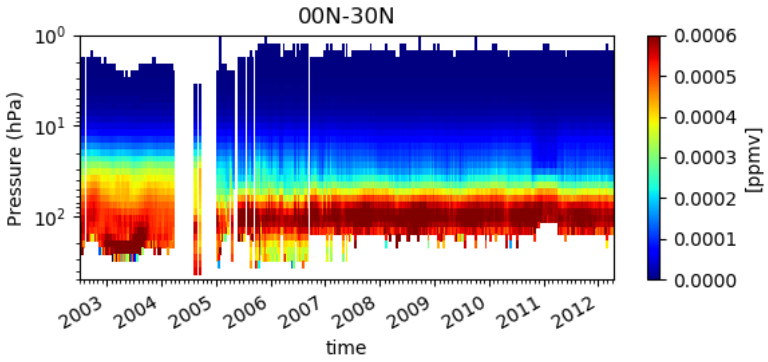

Figure 4-114 Timeseries of weekly mean of CH3Cl on the full mission averaged on the latitude band 30S-0.

Retrieval is performed with Optimal Estimation, with the a priori profile equal to the mean of the CH_3Cl climatological profiles. The diagonal element of the Covariance Matrix of the a priori are computed as the square of the sum of a constant (10^{-6} ppmv) plus the 95% of the a priori profile, while the non diagonal elements are computed assuming a correlation length of 4 km (for FR measurements) and of 6 km (for OR measurements).

Quality quantifiers (AK and errors)

The vertical averaging kernels of the CH_3Cl retrieval are shown in Figure 4-115 for two representative profiles in Full Resolution nominal mode (left panel) and Optimised Resolution nominal mode (right panel). The selected scans are not affected by clouds. The vertical resolution profile of the considered scan is also reported in red in the same plot and the DOF distribution profile (see Sect. 3.5.2) in blue. A mean vertical resolution profile has been also computed considering all scans in the nominal mode of 2003 (for FR plots) and 2010 (for OR plots). It is 5 km at 10 km, 7.5 at 20 km, 15-20 km at 30 km, for both FR and OR measurements.

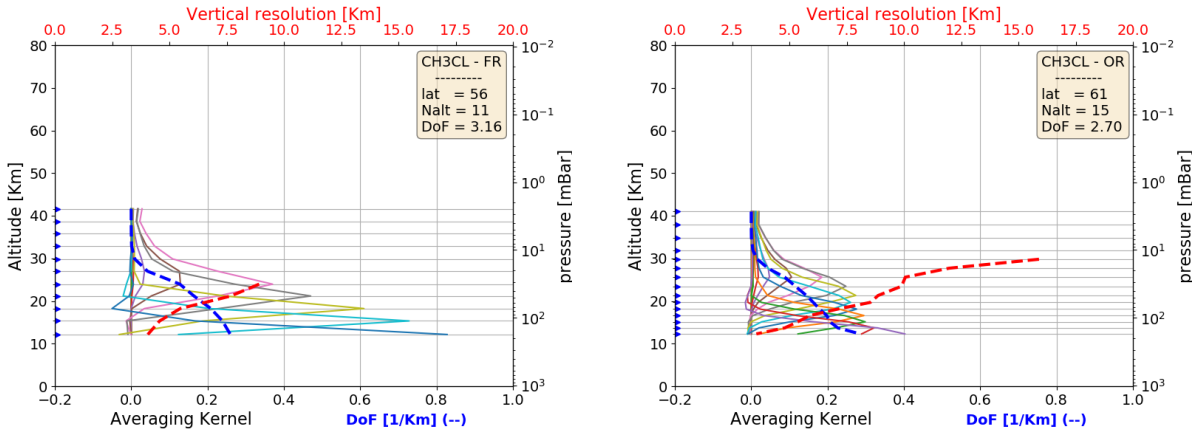

Figure 4-115 Example of CH_3Cl vertical averaging kernel (AK) computed for a representative Full Resolution (left panel) and Optimized Resolution (right panel) scan. Together with the AKs, the plots show the vertical resolution (red dashed line) and the Degree of Freedom for unity height (blue dashed line). The yellow box on the top right of each panel contains the latitude of the observation, the number of the measurement sweeps and the total Degree of Freedom (DoF)

Figure 4-116 shows the average CH3Cl VMR profiles (left plots) and their associated single scan average random error profiles, in absolute (middle plots) and relative (right plots) scale. The average quantities are representative of 5 reference atmospheres, namely polar summer daytime, polar winter nightime, mid-latitudes (both daytime and nightime) and equatorial daytime atmospheres. The averages have been computed using information on retrieved profiles, noise error and pT error which are contained in the output files for each scan. For mid latitude atmospheres all scans in the nominal mode of 2003 (for FR plots) and 2010 (for OR plots) in the latitude band 30-60 (both hemispheres) have been taken into account (considering either daytime or nightime scans), for equatorial atmosphere the scans in the latitude band 30S-30N, for polar winter nighttime atmosphere all nightime scans in the nominal mode of June-July-August of 2003 (for FR) and of 2005-2011 years (for OR) in the band 60S-90S, for polar summer daytime atmosphere all daytime scans in the nominal mode of December-January-February of 2003 (for FR) and 2005-2011 (for OR) in the latitude band 60S-90S. Solid lines of middle and right plots represent the total random error, coming from the quadratic summation of the noise error (dotted curves, given by the mapping of the measurement error on the retrieved profile) and the pT error (given by the propagation of the random error of retrieved pressure and temperature profiles on VMR profile). The contribution coming from the pT error propagation is generally smaller than the noise contribution. The relative random error varies for the different atmospheres and altitudes, but it is never smaller than 30%.

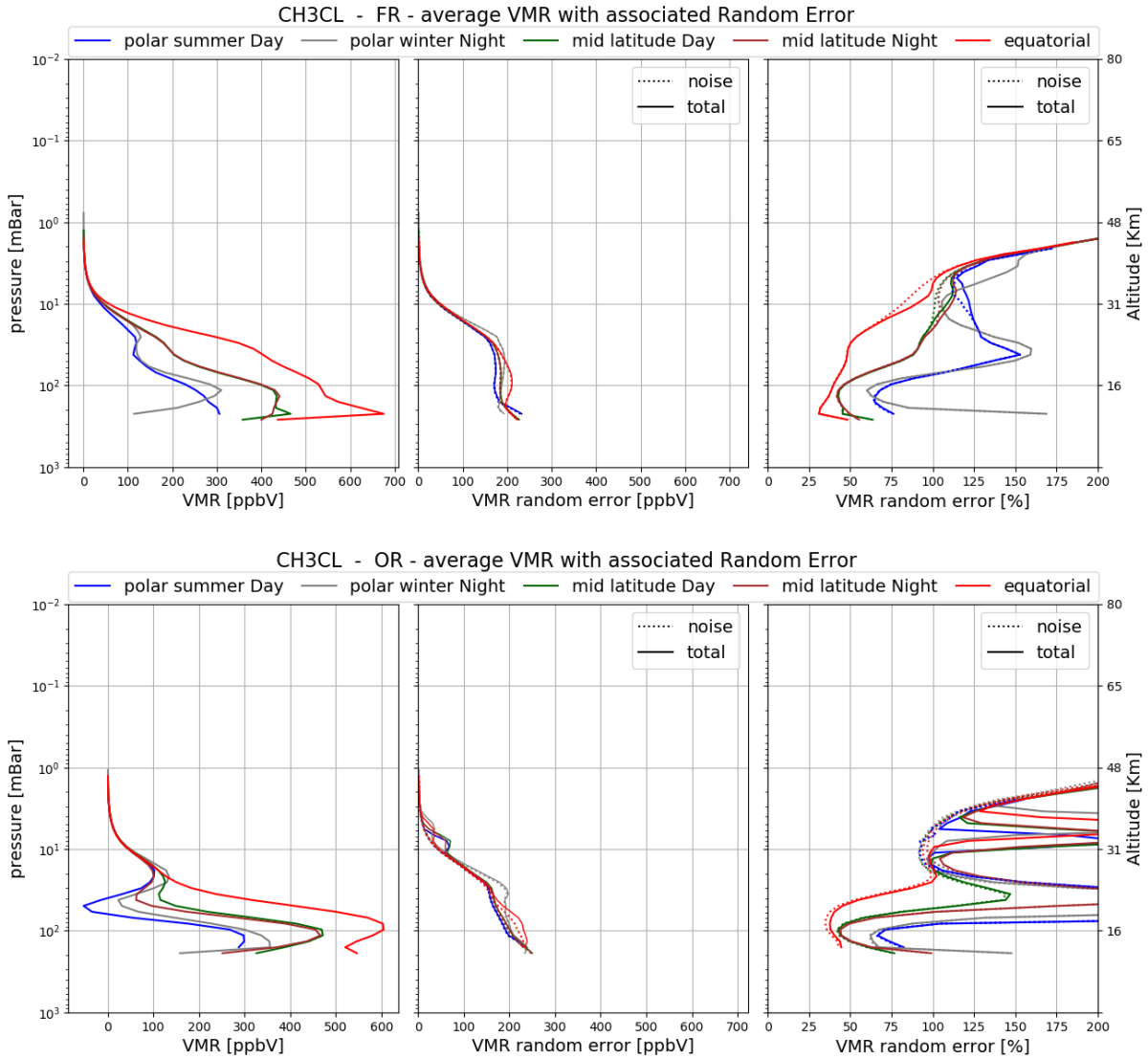

Figure 4-116 Average CH_3Cl VMR (left plots), absolute (mid plots) and relative (right plots) CH_3Cl random error for the 5 reference atmospheres described in the text. The noise error (dotted curves) is calculated by the retrieval; the total random error (solid curves) includes the contribution to the random error coming from propagation of the pT random error on VMR profiles. Top panel: Full Resolution nominal mode; bottom panel: Optimized Resolution nominal mode.

Validation

Reference instrument	Source	Coverage validation analysis		
		Time	Horizontal	Vertical
MIPAS-B	KIT-IMK	8 flights + 2-day trajectories	3 sites, 68°N–5°S	200–6 hPa
ACE-FTS v4	U Waterloo	2005-2012	global	500-0.04 hPa

Comparisons with the MIPAS-balloon in the OR period show very good consistency (within ±20%) in the upper troposphere and lower stratosphere, whereas MIPAS is up to 30% positively biased compared to ACE-FTS in the same range. In the FR period a significant positive bias is obvious above 16 km and significant negative bias below this altitude. Details of results of validation are reported below.

From the comparison of the two MIPAS instruments CH_3Cl VMR differences stay within ±20% between 13 and 22 km (full observation period) (see Figure 4-117). However, the comparison reveals a positive bias above 16 km and a negative bias below this altitude in the FR period. A negative bias within -35% between 19 and 26 km, increasing with altitude, and exceeding the combined systematic errors above 26 km is also visible in the OR period. Large deviations between both instruments occur at midlatitudes and in the Tropics (not shown).

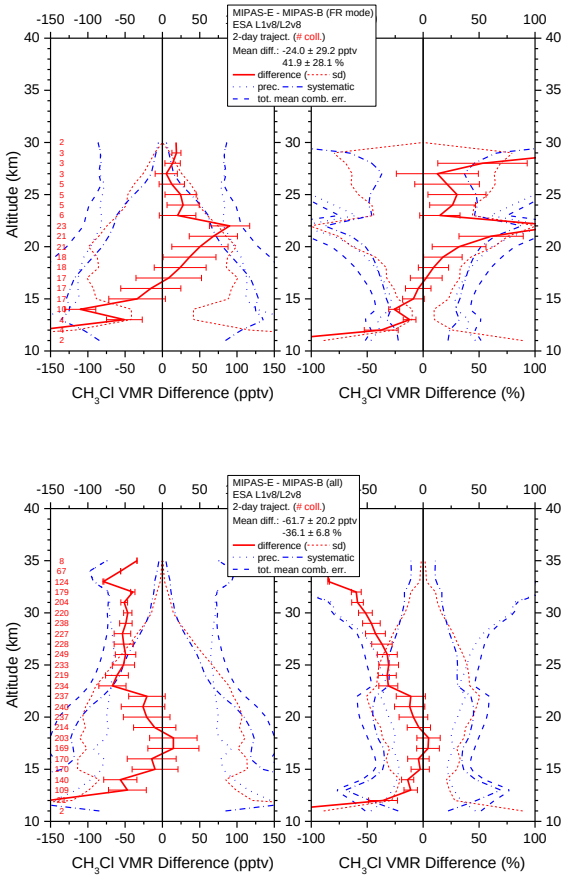

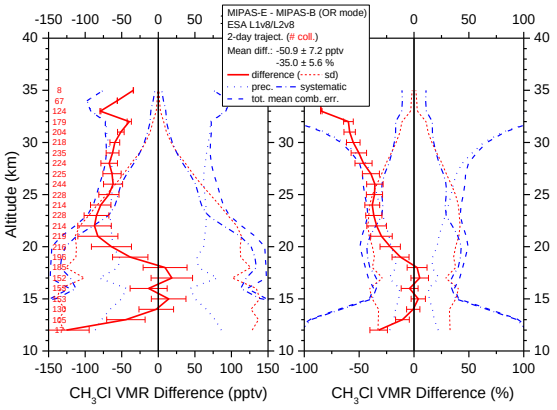

no v7 data available

Figure 4-117 Mean absolute and relative CH_3Cl VMR difference of all trajectory match collocations (red numbers) between MIPAS-E and MIPAS-B (red solid line) including standard deviation (red dotted lines) and standard error of the mean (plotted as error bars). Precision (blue dotted lines), systematic (blue dash-dotted lines), and total (blue dashed lines) mean combined errors are shown, too. Top: v8 FR mode (left) and v8 OR mode (right) collocations; bottom: all FR plus OR v8 (left) and all FR plus OR v7 (right) collocations.

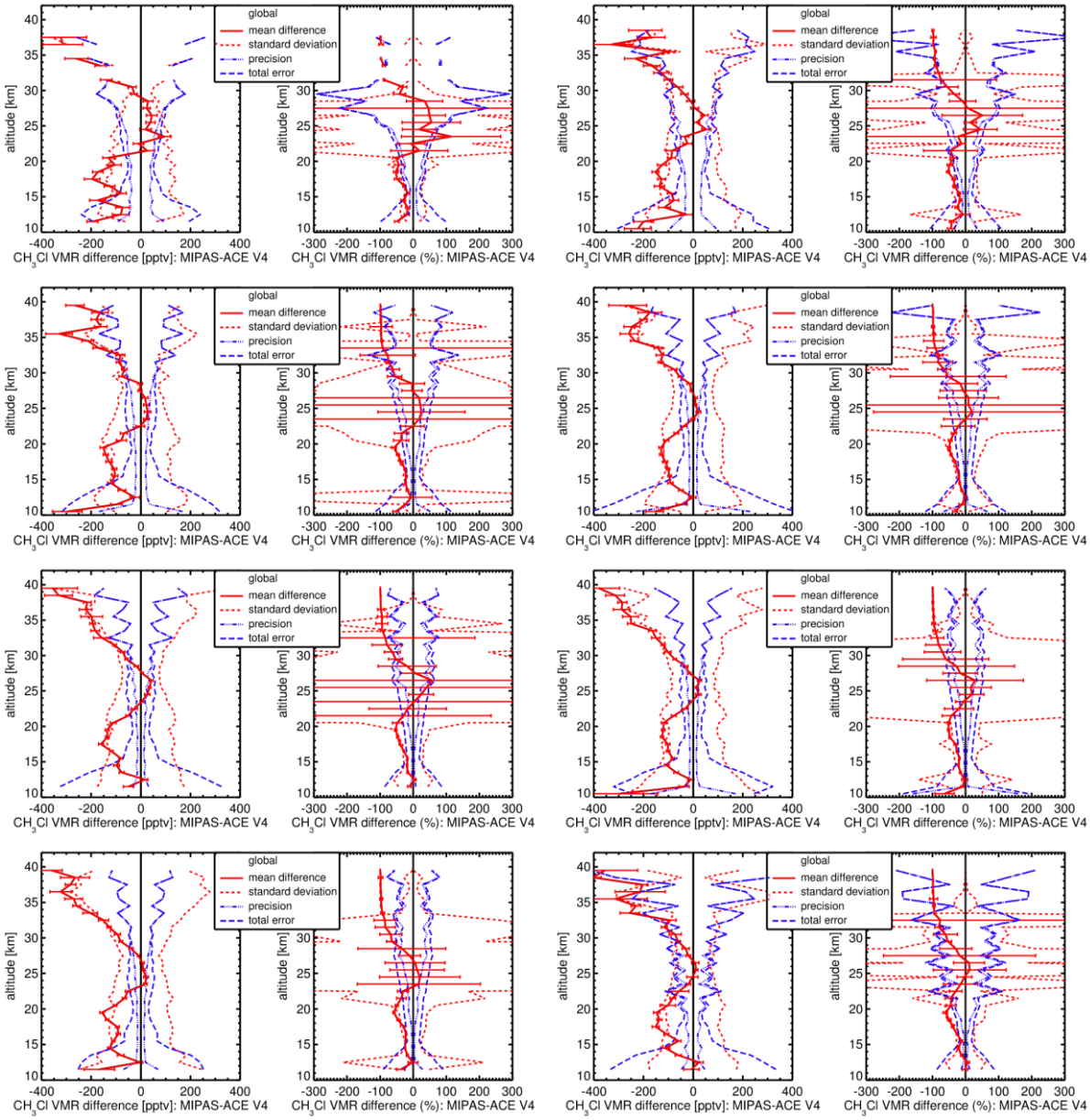

Figure 4-118. Mean absolute and relative CH_3Cl VMR difference of all match collocation (red numbers) between MIPAS and ACE version 4 data (red solid line) including standard deviation (red dotted lines) and standard error of the mean (plotted as error bars). Precision (blue dotted lines) and total (blue dashed lines) mean combined errors are shown, too. Global matchups. a) 2005, b) 2006, c) 2007, d) 2008, e) 2009, f) 2010 g) 2011, h) 2012.

MIPAS shows between 10-50% negative bias compared to ACE-FTS between 10 and 22 km, this increases to a maximum of 100% at altitudes greater than 26 km. The best agreement between the satellite datasets occurs between 22 and 26 km, with MIPAS showing a high bias in the profile of up to 30 %.

4.21 Phosgene ($COCl_2$)

LEVEL 2 V8 PHOSGENE PRODUCTS										
Operational modes:	FR	RR	OR							
	NOM		NOM	UTLS1	MA	UA	AE	NLC	UTLS2	UTLS1_o
Nominal Vertical range [Km]	*6--36*	*9-52*	*9-54*	*11.5-52*	*---*	*---*	*10-38*	*---*	*12-42*	*10-49*
Useful range	*All altitudes up to 28 km (pressures larger than 15 hPa)*									
Microwindows:	*Link for downloading*									
Systematic errors:	*Link for downloading* *Link errors*									

Introduction

$COCl_2$ is produced by chemical industries and, in the upper troposphere and in the stratosphere, from the decomposition of chlorocarbon compounds.

In Figure 4-119 we present the timeseries of V8 $COCl_2$ in the latitude band 60N-90N on the full mission. A negative trend is clearly visible in the timeseries (see Pettinari et al., in preparation).

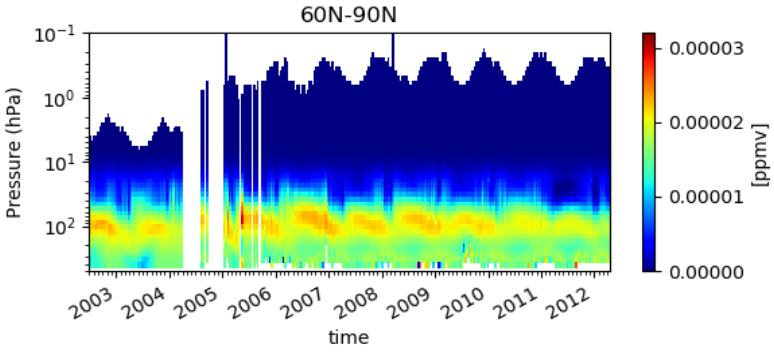

Figure 4-119 Timeseries of weekly mean of $COCl_2$ on the full mission averaged on the latitude band 60N-90N

Retrieval is performed with Optimal Estimation, with the a priori profile equal to the mean of the $COCl_2$ climatological profiles. The diagonal element of the Covariance Matrix of the a priori are computed as the square of the sum of a constant (10^{-7} ppmv) plus the 95% of the a priori profile, while the non diagonal elements are computed assuming a correlation length of 6 km.

The $COCl_2$ retrieval has been performed with new spectroscopic line list database described in Tchana et al., 2015, and this is responsible of an increase up to 2-3 pptb in the tropics in correspondence of the peak of the profile.

Quality quantifiers (AK and errors)

The vertical averaging kernels of the $COCl_2$ retrieval are shown in Figure 4-120 for two representative profiles in Full Resolution nominal mode (left panel) and Optimised Resolution nominal mode (right panel). The selected scans are not affected by clouds. The vertical resolution profile of the considered scan is also reported in red in the same plot and the DOF distribution profile (see Sect. 3.5.2) in blue. A mean vertical resolution profile has been also computed considering all scans in the nominal mode of 2003 (for FR plots) and 2010 (for OR plots). It is 3-5 km at 10 km, about 7.5 km at 20 km, 15-20 km at 30 km.

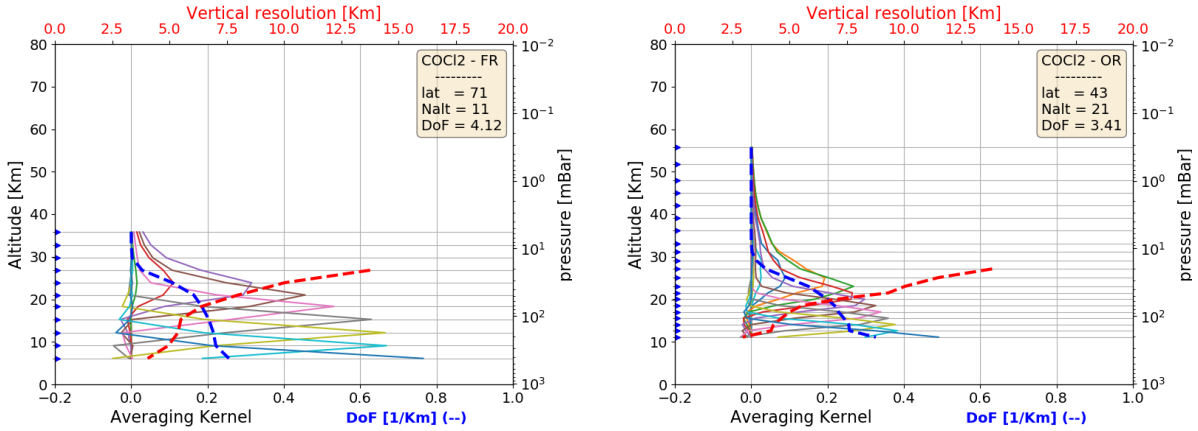

Figure 4-120 Example of $COCl_2$ vertical averaging kernel (AK) computed for a representative Full Resolution (left panel) and Optimized Resolution (right panel) scan. Together with the AKs, the plots show the vertical resolution (red dashed line) and the Degree of Freedom for unity height (blue dashed line). The yellow box on the top right of each panel contains the latitude of the observation, the number of the measurement sweeps and the total Degree of Freedom (DoF)

Figure 4-121 shows the average $COCl_2$ VMR profiles (left plots) and their associated single scan average random error profiles, in absolute (middle plots) and relative (right plots) scale. The average quantities are representative of 5 reference atmospheres, namely polar summer daytime, polar winter nightime, mid-latitudes (both daytime and nightime) and equatorial daytime atmospheres. The averages have been computed using information on retrieved profiles, noise error and pT error which are contained in the output files for each scan. For mid latitude atmospheres all scans in the nominal mode of 2003 (for FR plots) and 2010 (for OR plots) in the latitude band 30-60 (both hemispheres) have been taken into account (considering either daytime or nightime scans), for equatorial atmosphere the scans in the latitude band 30S-30N, for polar winter nighttime atmosphere all nightime scans in the nominal mode of June-July-August of 2003 (for FR) and of 2005-2011 years (for OR) in the band 60S-90S, for polar summer daytime atmosphere all daytime scans in the nominal mode of December-January-February of 2003 (for FR) and 2005-2011 (for OR) in the latitude band 60S-90S. Solid lines of middle and right plots represent the total random error, coming from the quadratic summation of the noise error (dotted curves, given by the mapping of the measurement error on the retrieved profile) and the pT error (given by the propagation of the random error of retrieved pressure and temperature profiles on VMR profile). The contribution coming from the pT error propagation is generally smaller than the noise contribution. The relative single scan random error varies for the different atmospheres but it is never smaller than 30%.

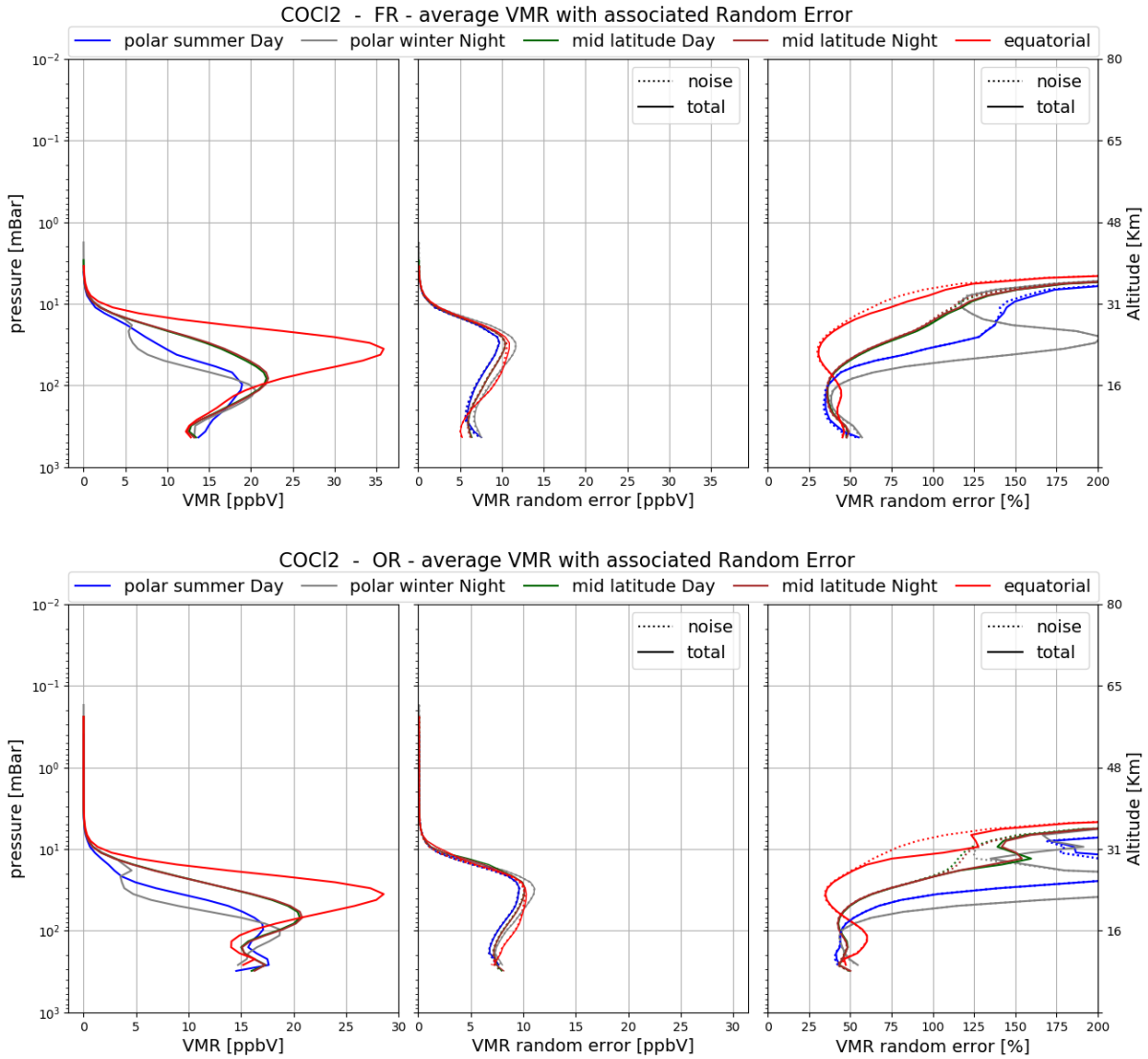

Figure 4-121 Average $COCl_2$ VMR (left plots), absolute (mid plots) and relative (right plots) $COCl_2$ random error for the 5 reference atmospheres described in the text. The noise error (dotted curves) is calculated by the retrieval; the total random error (solid curves) includes the contribution to the random error coming from propagation of the pT random error on VMR profiles. Top panel: Full Resolution nominal mode; bottom panel: Optimized Resolution nominal mode.

Validation

Reference instrument	Source	Coverage validation analysis		
		Time	Horizontal	Vertical
MIPAS-B	KIT-IMK	8 flights + 2-day trajectories	3 sites, 68°N–5°S	200–6 hPa
ACE-FTS v4	U Waterloo	2005-2012	global	500-0.04 hPa

It is difficult to draw conclusions from the comparison of MIPAS with ACE-FTS as there were significant changes between the v3.5 and v4 ACE products, which are still themselves to be validated. For the latest ACE-FTS version 4, MIPAS shows a significant positive bias of between 80% and 200% throughout the profile across all OR years. MIPAS comparison to balloon-borne measurements are more favourable and within ±20% up to 27 km altitude. An unexplained negative bias to the balloon-borne measurements above 27 km is observed. Further details of results of validation are reported below

Figure 4-122 shows that $COCl_2$ differences between both MIPAS instruments are within ±20% up to 27 km in both observation periods such that the general profile shapes (as measured by MIPAS-B) are reproduced by the satellite instrument. A negative bias is evident in the FR and OR period (except 22-27 km), unexplained (exceeding systematic error limits) at high altitudes. Deviations in the Tropics are quite large. Part of the differences found between MIPAS-ENVISAT and MIPAS-B can be ascribed to the different spectroscopic databases used for the analysis. Indeed, the analysis of MIPAS-B and ACE-FTS was performed with the $COCl_2$ spectroscopic database from Toon et al. (2001), while MIPAS-ENVISAT was performed with the new spectroscopic database described in (Valeri et al., 2016).

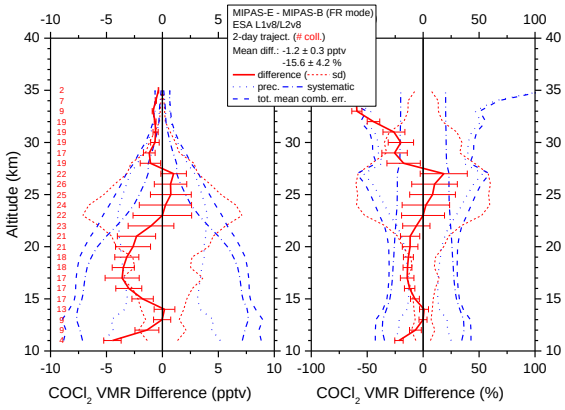

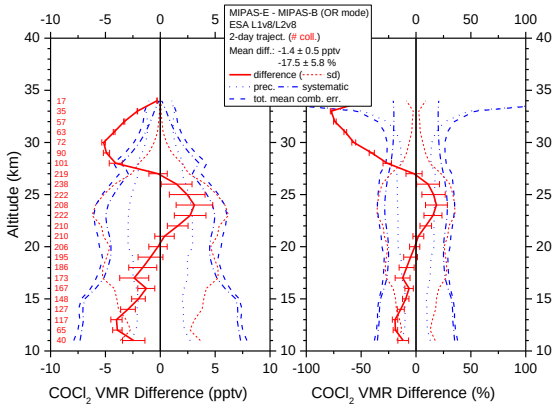

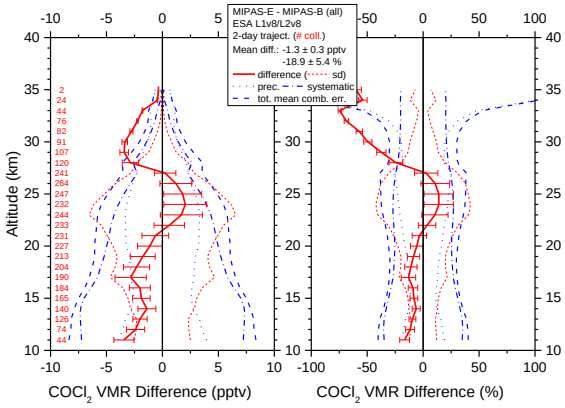

no v7 data available

Figure 4-122 Mean absolute and relative $COCl_2$ VMR difference of all trajectory match collocations (red numbers) between MIPAS-E and MIPAS-B (red solid line) including standard deviation (red dotted lines) and standard error of the mean (plotted as error bars). Precision (blue dotted lines), systematic (blue dash-dotted lines), and total (blue dashed lines) mean combined errors are shown, too. Top: v8 FR mode (left) and v8 OR mode (right) collocations; bottom: all FR plus OR v8 (left) and all FR plus OR v7 (right) collocations.

There is a very significant positive bias of MIPAS compared to ACE v4 throughout the retrieved profiles (8 km to 25 km) of between 80% and 200% (see Figure 4-123). The reason for this has to be ascribed to ACE-FTS v4, because significantly smaller differences were found with respect to ACE-FTS v3.5.

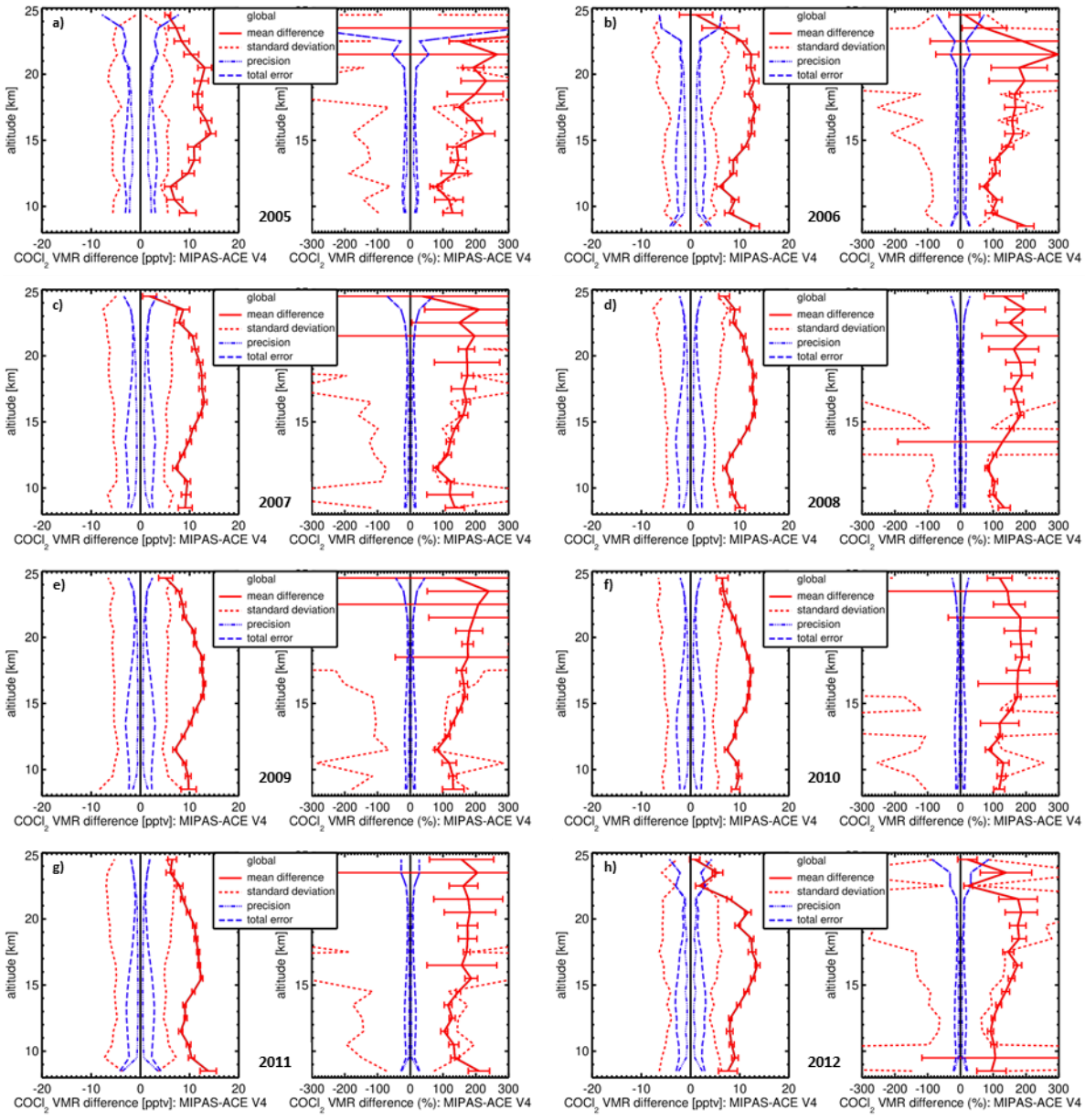

Figure 4-123. Mean absolute and relative $COCl_2$ VMR difference of all match collocation (red numbers) between MIPAS and ACE version 4 data (red solid line) including standard deviation (red dotted lines) and standard error of the mean (plotted as error bars). Precision (blue dotted lines) and total (blue dashed lines) mean combined errors are shown, too. Global matchups. a) 2005, b) 2006, c) 2007, d) 2008, e) 2009, f) 2010 g) 2011, h) 2012.

4.22 Carbonyl sulfide (OCS)

LEVEL 2 V8 CARBONYL SULFIDE PRODUCTS										
Operational modes:	FR	RR	OR							
	NOM		NOM	UTLS1	MA	UA	AE	NLC	UTLS2	UTLS1_o
Nominal Vertical range [Km]	*6--68*	*6-39*	*6-40*	*8.5-43*	---	---	*7-38*	---	*12-37*	*8.5-39*
Useful range	*All altitudes up to 26 km (pressures greater than 20 hPa)*									
Microwindows:	*Link for downloading*									
Systematic errors:	*Link for downloading* *Link errors*									

Introduction

This molecule is a new molecule of ESA L2V8 dataset.
OCS is the most prevalent sulphur-containing species which is transported into the stratosphere where it acts as prerequisite of the stratospheric aerosol layer. In Figure 4-124 we present the timeseries of V8 OCS in the latitude band 60N-90NS.

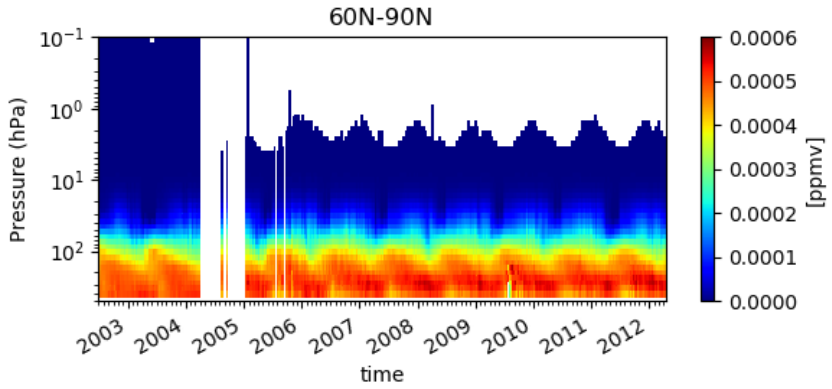

Figure 4-124 Timeseries of weekly mean of OCS on the full mission averaged on the latitude band 60N-90N

Retrieval is performed with Optimal Estimation, with the a priori profile equal to the mean of the OCS climatological profiles. The diagonal element of the CM of the a priori are computed as the square of the sum of a constant (10^{-7} ppmv) plus the 80% of the a priori profile, while the non diagonal elements are computed assuming a correlation length of 5 km.

Quality quantifiers (AK and errors)

The vertical averaging kernels of the OCS retrieval are shown in Figure 4-125 for two representative profiles in Full Resolution nominal mode (left panel) and Optimised Resolution nominal mode (right panel). The selected scans are not affected by clouds. The vertical resolution profile of the considered scan is also reported in red in the same plot and the DOF distribution profile (see Sect. 3.5.2) in blue. A mean vertical resolution profile has been also computed considering all scans in the nominal mode of 2003 (for FR plots) and 2010 (for OR plots). It is about 5 km in the altitude range 6-18 km, it rapidly increases above.

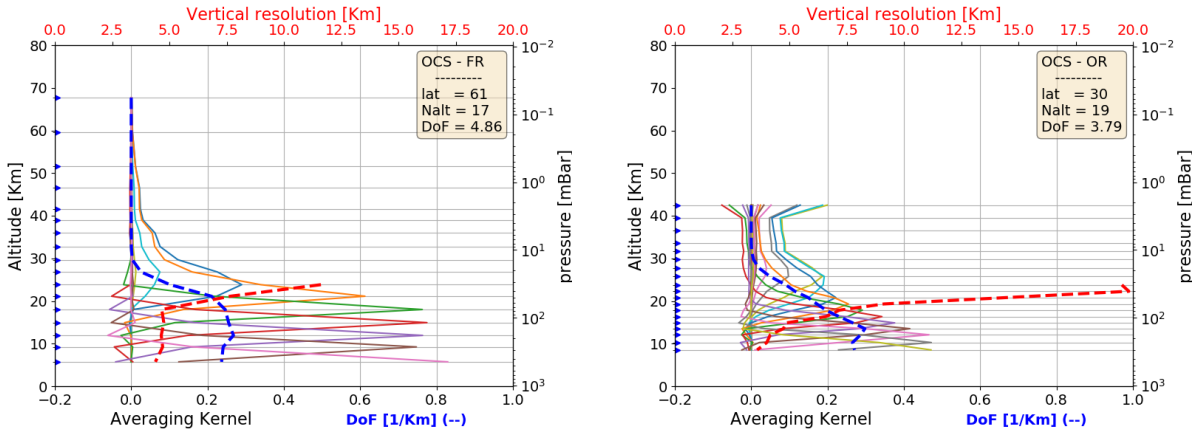

Figure 4-125 Example of OCS vertical averaging kernel (AK) computed for a representative Full Resolution (left panel) and Optimized Resolution (right panel) scan. Together with the AKs, the plots show the vertical resolution (red dashed line) and the Degree of Freedom for unity height (blue dashed line). The yellow box on the top right of each panel contains the latitude of the observation, the number of the measurement sweeps and the total Degree of Freedom (DoF).

Figure 4-126 shows the average OCS VMR profiles (left plots) and their associated average single scan random error profiles, in absolute (middle plots) and relative (right plots) scale. The average quantities are representative of 5 reference atmospheres, namely polar summer daytime, polar winter nightime, mid-latitudes (both daytime and nightime) and equatorial daytime atmospheres. The averages have been computed using information on retrieved profiles, noise error and pT error which are contained in the output files for each scan. For mid latitude atmospheres all scans in the nominal mode of 2003 (for FR plots) and 2010 (for OR plots) in the latitude band 30-60 (both hemispheres) have been taken into account (considering either daytime or nightime scans), for equatorial atmosphere the scans in the latitude band 30S-30N, for polar winter nighttime atmosphere all nightime scans in the nominal mode of June-July-August of 2003 (for FR) and of 2005-2011 years (for OR) in the band 60S-90S, for polar summer daytime atmosphere all daytime scans in the nominal mode of December-January-February of 2003 (for FR) and 2005-2011 (for OR) in the latitude band 60S-90S. Solid lines of middle and right plots represent the total random error, coming from the quadratic summation of the noise error (dotted curves, given by the mapping of the measurement error on the retrieved profile) and the pT error (given by the propagation of the random error of retrieved pressure and temperature profiles on VMR profile). The contribution coming from the pT error propagation is generally smaller than the noise contribution. The relative single scan random error is about 20% (25%) in the upper troposphere for FR (OR) measurements, then it rapidly increases.

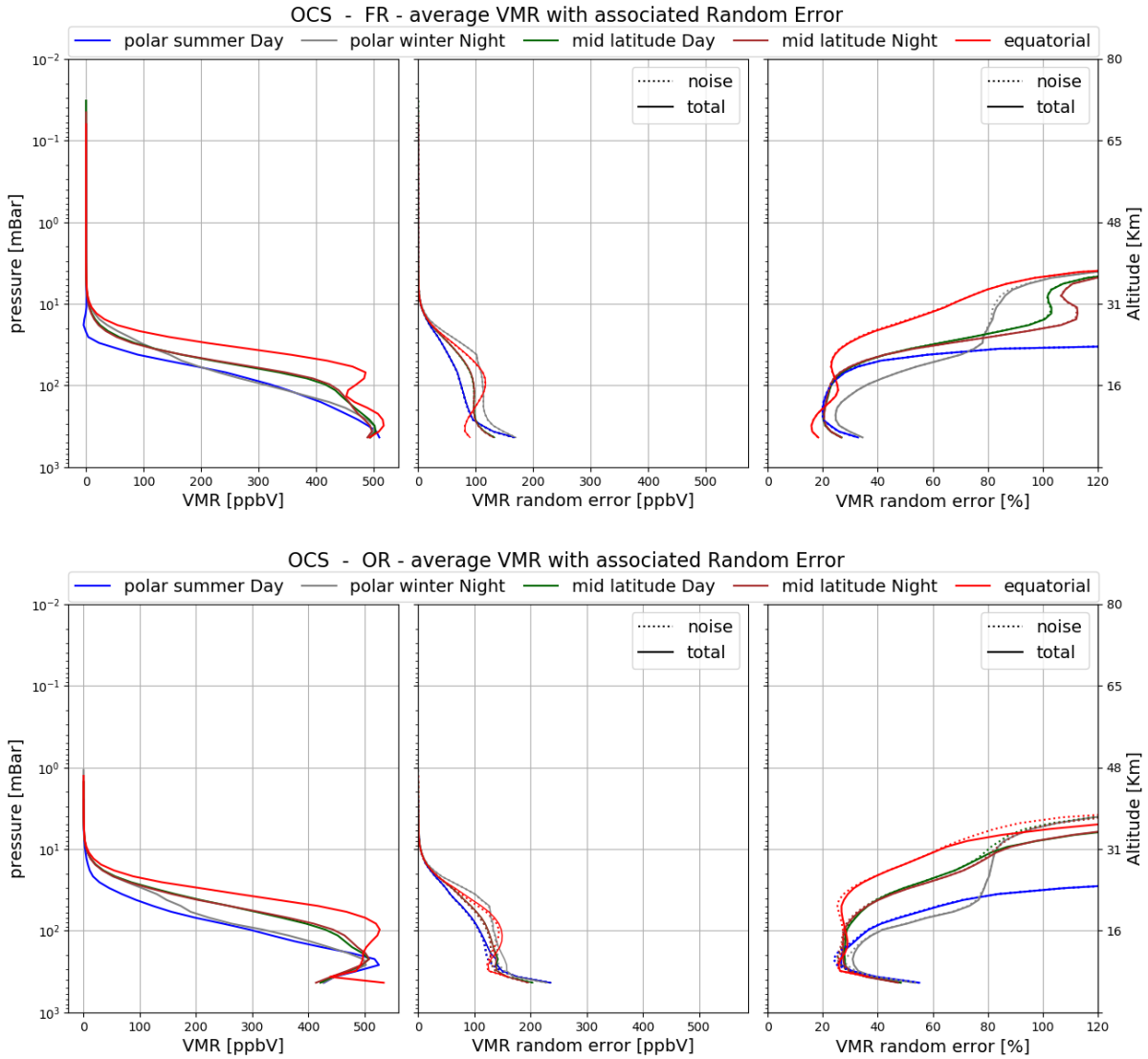

Figure 4-126 Average OCS VMR (left plots), absolute (mid plots) and relative (right plots) OCS random error for the 5 reference atmospheres described in the text. The noise error (dotted curves) is calculated by the retrieval; the total random error (solid curves) includes the contribution to the random error coming from propagation of the pT random error on VMR profiles. Top panel: Full Resolution nominal mode; bottom panel: Optimized Resolution nominal mode.

Validation

Reference instrument	Source	Coverage validation analysis		
		Time	Horizontal	Vertical
MIPAS-B	KIT-IMK	8 flights + 2-day trajectories	3 sites, 68°N–5°S	200–5 hPa

OCS VMR differences between both MIPAS instruments are within ±20% up to 24 km in the full measurement period (see Figure 4-127). A significant positive bias is visible below 22 km and a negative bias above this altitude in the OR period exceeding the ±50% limit and the combined systematic errors above 24 km. The agreement of the VMR profiles of both sensors is better in the FR period. Here, a significant (positive) bias is only visible between 14 and 18 km. In general, differences stay within ±20% for altitudes up to 26 km in the FR phase and ±25% up to 25 km in the OR period. Deviations in the Tropics are quite large.

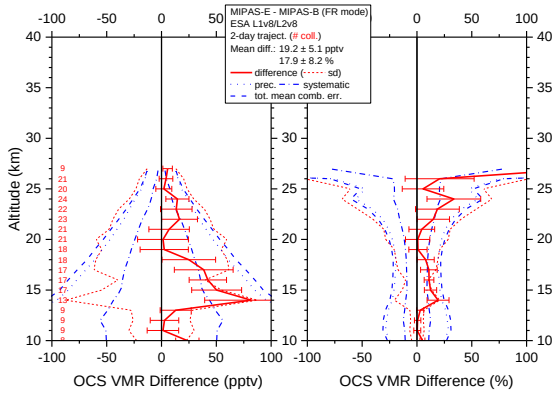

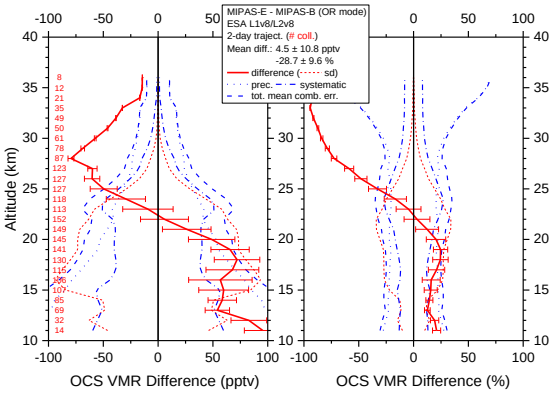

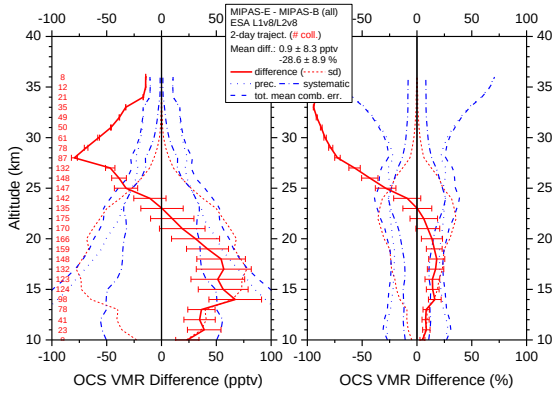

no v7 data available

Figure 4-127 Mean absolute and relative OCS VMR difference of all trajectory match collocations (red numbers) between MIPAS-E and MIPAS-B (red solid line) including standard deviation (red dotted lines) and standard error of the mean (plotted as error bars). Precision (blue dotted lines), systematic (blue dash-dotted lines), and total (blue dashed lines) mean combined errors are shown, too. Top: v8 FR mode (left) and v8 OR mode (right) collocations; bottom: all FR plus OR v8 (left) and all FR plus OR v7 (right) collocations.

4.23 Deuterium hydrogen oxide (HDO)

LEVEL 2 V8 DEUTERIUM HYDROGEN OXIDE PRODUCTS

Operational modes:	FR	RR	OR							
	NOM		NOM	UTLS1	MA	UA	AE	NLC	UTLS2	UTLS1_o
Nominal Vertical range [Km]	*6--68*	*6-52*	*6-58*	*8.5-52*	---	---	*7-38*	---	*12-42*	*8.5-49*
Useful range	*All altitudes up to 55 km (pressures greater than 0.4 hPa)*									
Microwindows:	*Link for downloading*									
Systematic errors:	*Link for downloading* *Link errors*									

Introduction

HDO is part of ESA L2 dataset for the first time.
More than 99.7% of water vapour exists in the form of $H_2{}^{16}O$. There are several minor isotopologues, such as $H_2{}^{18}O$ (0.20%), $H_2{}^{17}O$ (0.037 %), and $HD^{16}O$ (0.03 %). Although found in low abundance, the minor isotopologues can provide information on the process history of air parcels from their isotopic ratios relative to the main isotopologue, $H_2{}^{16}O$. In this regard, $HD^{16}O$ (hereafter referred to as HDO) is most interesting, as the isotopic ratio typically exhibits pronounced variations.

In Figure 4-128 we present the timeseries of V8 HDO in the latitude band 0-30N on the full mission, where we clearly see the typical tape recorder effect seen also in H_2O time series.

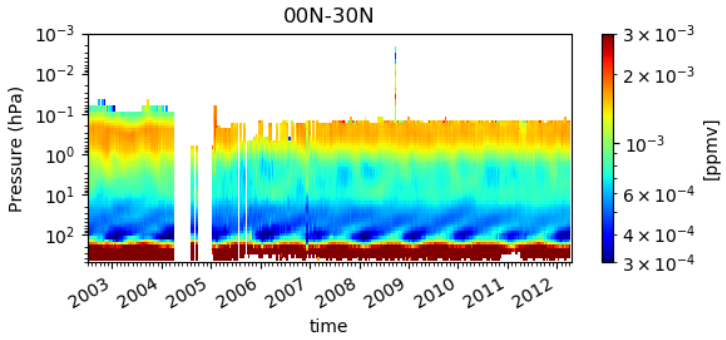

Figure 4-128 Timeseries of weekly mean of HDO on the full mission averaged on the latitude band 0-30N.

Retrieval is performed with Optimal Estimation, with the a priori profile equal to the retrieved H_2O profile, opportunely scaled according to the isotopic ratio. The diagonal element of the Covariance Matrix of the a priori are computed as the square of the sum of a constant (10^{-3} ppmv) plus the 100% of the a priori profile, while the non diagonal elements are computed assuming a correlation length of 10 km.

Quality quantifiers (AK and errors)

The vertical averaging kernels of the HDO retrieval are shown in Figure 4-129 for two representative profiles in Full Resolution nominal mode (left panel) and Optimised Resolution nominal mode (right panel). The selected scans are not affected by clouds. The vertical resolution profile of the considered scan is also reported in red in the same plot and the DOF distribution profile (see Sect. 3.5.2) in blue. A mean vertical resolution profile has been also computed considering all scans in the nominal mode of 2003 (for FR plots) and 2010 (for OR plots). It is, for FR measurements, about 5 km in the altitude range 6-30 km, it is 7.5 km at 40 km and 12.5 km at 50 km. For OR measurements it is better at very low altitudes (3-3.5 km in the range 6-10 km), then it is a bit worst then for FR measurements. The typical number of DOFs is 8 for both FR and OR measurements for clear sky profiles.

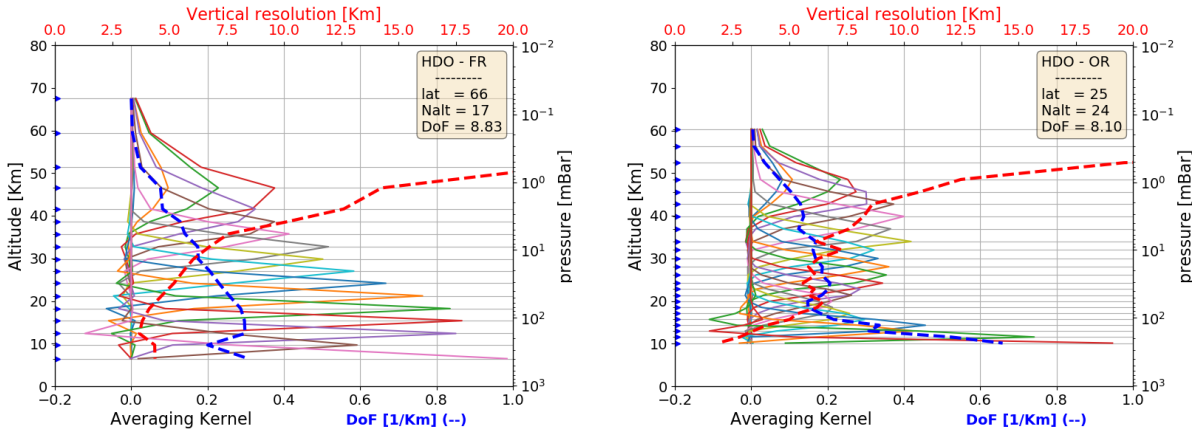

Figure 4-129 Example of HDO vertical averaging kernel (AK) computed for a representative Full Resolution (left panel) and Optimized Resolution (right panel) scan. Together with the AKs, the plots show the vertical resolution (red dashed line) and the Degree of Freedom for unity height (blue dashed line). The yellow box on the top right of each panel contains the latitude of the observation, the number of the measurement sweeps and the total Degree of Freedom (DoF)

Figure 4-130 shows the average HDO VMR profiles (left plots) and their associated average single scan random error profiles, in absolute (middle plots) and relative (right plots) scale. The average quantities are representative of 5 reference atmospheres, namely polar summer daytime, polar winter nightime, mid-latitudes (both daytime and nightime) and equatorial daytime atmospheres. The averages have been computed using information on retrieved profiles, noise error and pT error which are contained in the output files for each scan. For mid latitude atmospheres all scans in the nominal mode of 2003 (for FR plots) and 2010 (for OR plots) in the latitude band 30-60 (both hemispheres) have been taken into account (considering either daytime or nightime scans), for equatorial atmosphere the scans in the latitude band 30S-30N, for polar winter nighttime atmosphere all nightime scans in the nominal mode of June-July-August of 2003 (for FR) and of 2005-2011 years (for OR) in the band 60S-90S, for polar summer daytime atmosphere all daytime scans in the nominal mode of December-January-February of 2003 (for FR) and 2005-2011 (for OR) in the latitude band 60S-90S. Solid lines of middle and right plots represent the total random error, coming from the quadratic summation of the noise error (dotted curves, given by the mapping of the measurement error on the retrieved profile) and the pT error (given by the propagation of the random error of retrieved pressure and temperature profiles on VMR profile). The contribution coming from the pT error propagation is generally smaller than the noise contribution. The relative average single

scan random error varies with altitude for the different atmospheres, but it is never smaller than 10% for FR measurements and 25% for OR measurements.

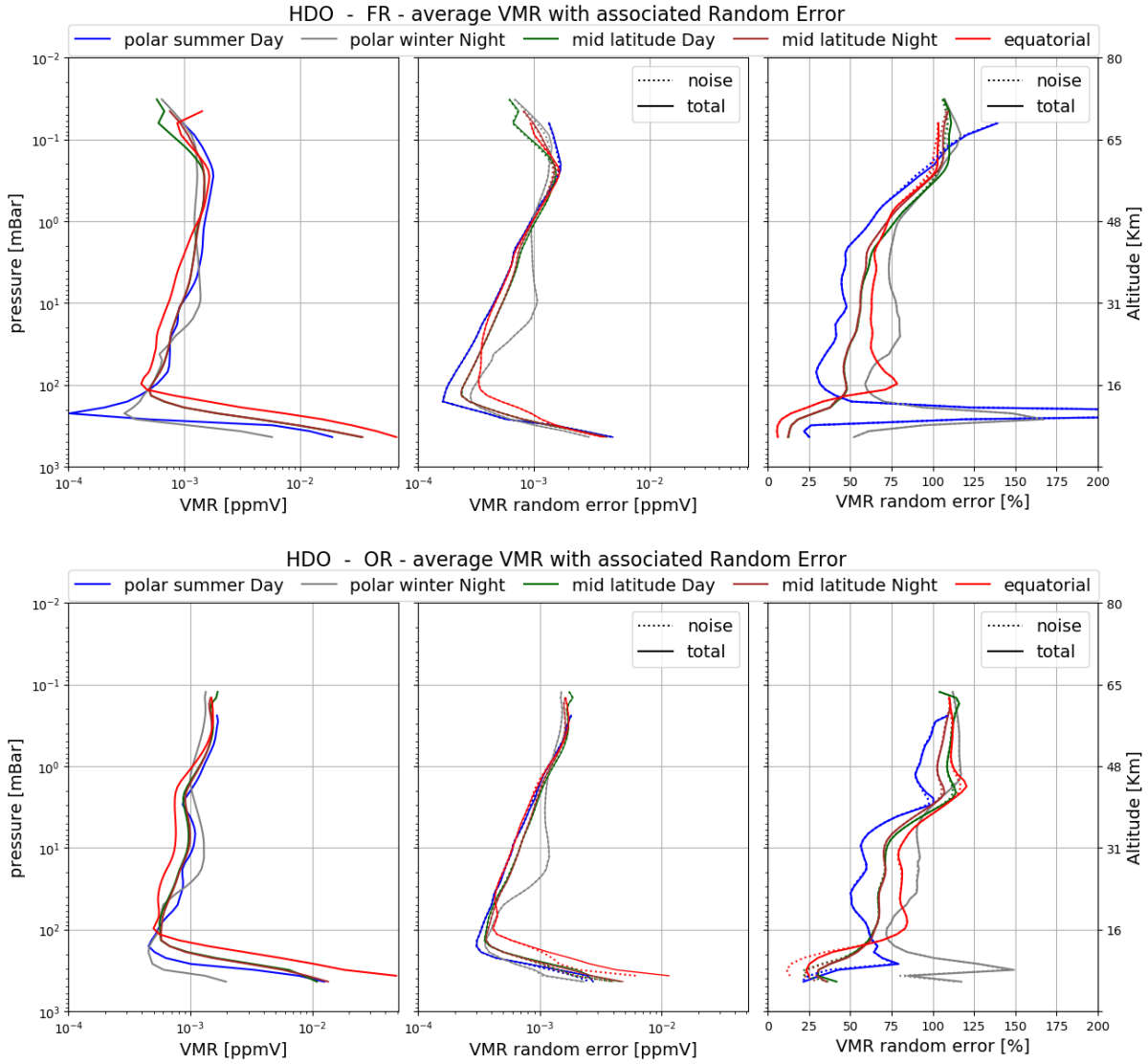

Figure 4-130 Average HDO VMR (left plots), absolute (mid plots) and relative (right plots) HDO random error for the 5 reference atmospheres described in the text. The noise error (dotted curves) is calculated by the retrieval; the total random error (solid curves) includes the contribution to the random error coming from propagation of the pT random error on VMR profiles. Top panel: Full Resolution nominal mode (average 2003); bottom panel: Optimized Resolution nominal mode (average on 2010).

Validation

Reference instrument	Source	Coverage validation analysis		
		Time	Horizontal	Vertical
ACE-FTS v4	U Waterloo	2005-2012	global	500-0.04 hPa

HDO VMRs show very good consistency, within ±20%, and generally better than 10% between 13 km and 35 km when compared to ACE. Below 13 km, MIPAS is between 10% and 50% lower than ACE (see Figure 4-131). Above 35 km, we see a similar low bias of MIPAS, being lower than ACE by between 20% and 50%.

Comparisons of MIPAS operational product to a research HDO from the Karlsruhe Institute of Technology (KIT), hereafter called HDO-KIT, yielded some very consistent and favourable results in the full-resolution data period (2002-2004) (see Figure 4-132). The best agreement overall was found to occur between the upper troposphere and the upper stratosphere (15 km to 50 km), within ±10%, which was also reproduced across all latitude regions in the regional analysis. Globally, operational MIPAS was lower than HDO-KIT by between 5% and 40% and this was representative of all regions. Below 9 km there was more inconsistency with the global average showing operational MIPAS data could be up to as much as 150% high , particularly in the arctic and northern hemisphere mid-lats.

During the optimised resolution period (2005-2012) there was also good consistency between the operational MIPAS HDO and HDO-KIT (see Figure 4-133). The highest consistency globally was between 15 km and 35 km, within ±15%. This was also represented across the five regional latitude bands, although the tropics showed less consistency of between ±30%. Below 15 km, MIPAS was between 10% and 100% lower than HDO-KIT. In the upper stratosphere (35 km to 50 km), MIPAS was lower by between 10%-30%. By the mesosphere (50 km to 65 km), MIPAS are higher by 10%-50%. Larger positive bias of MIPAS is found in the arctic mesosphere at up to 100%.

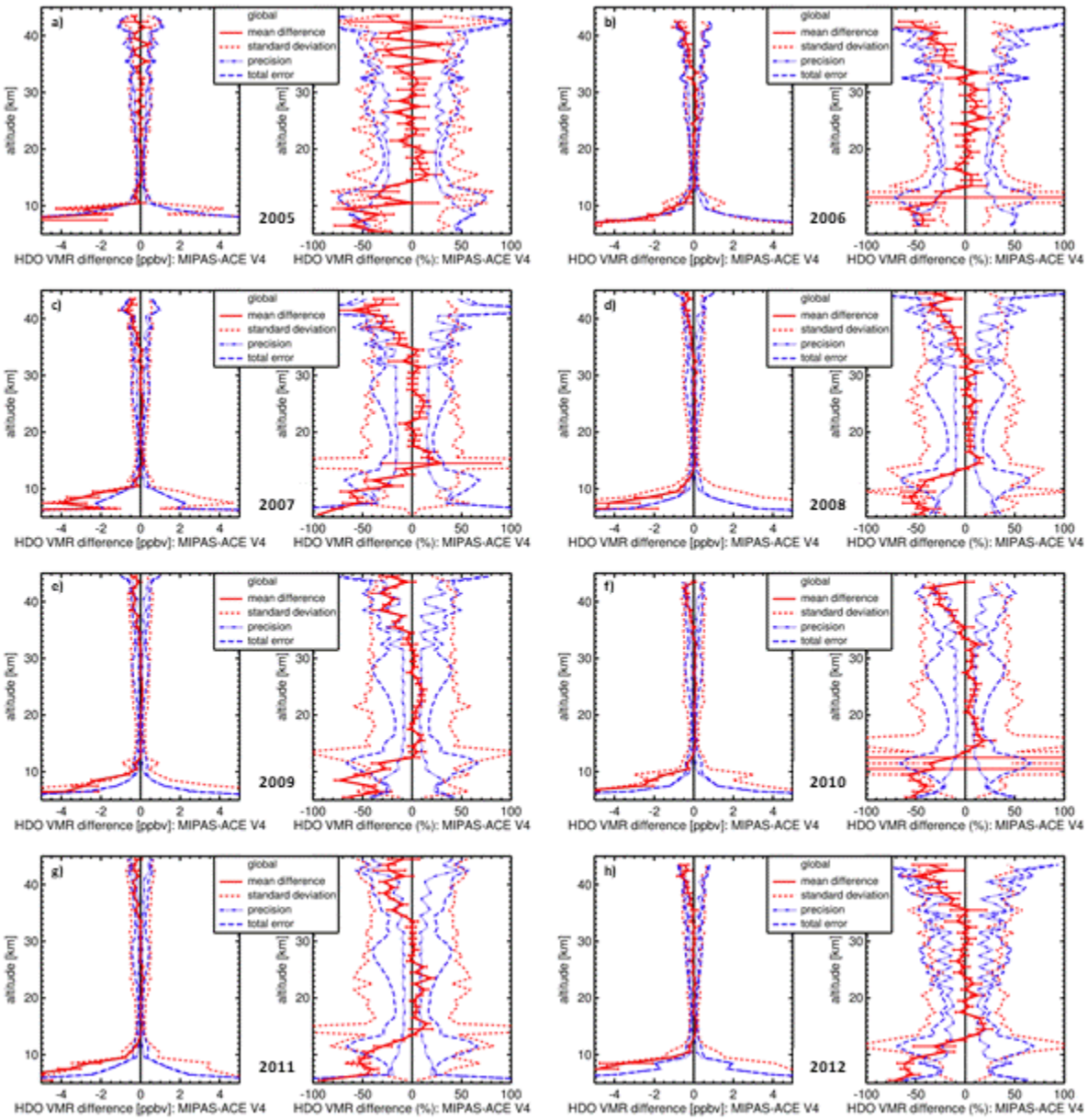

Figure 4-131. Mean absolute and relative HDO VMR difference of all match collocation (red numbers) between MIPAS and ACE version 4 data (red solid line) including standard deviation (red dotted lines) and standard error of the mean (plotted as error bars). Precision (blue dotted lines) and total (blue dashed lines) mean combined errors are shown, too. Global matchups. a) 2005, b) 2006, c) 2007, d) 2008, e) 2009, f) 2010 g) 2011, h) 2012.

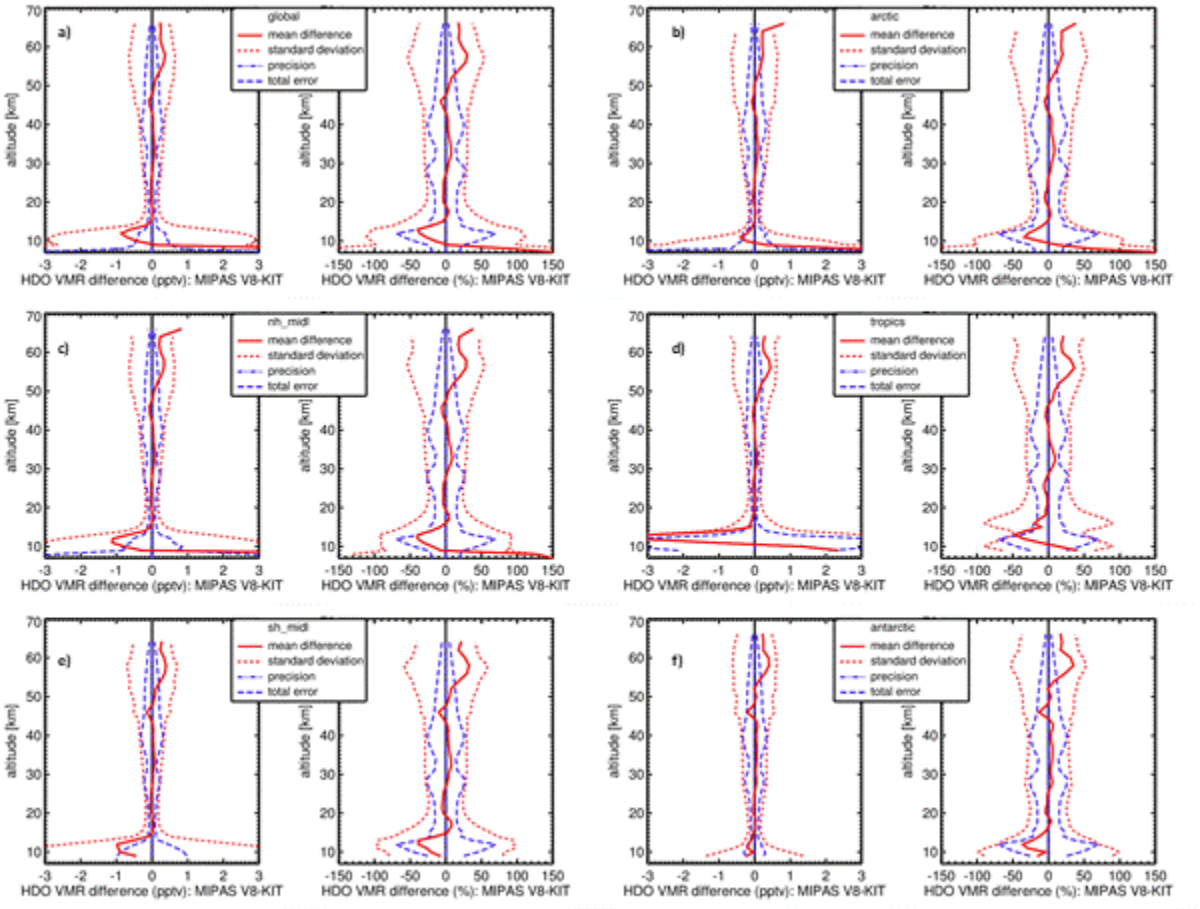

Figure 4-132. Mean absolute and relative HDO VMR difference of all match collocation (red numbers) between operational v8 MIPAS and KIT HDO data (red solid line) including standard deviation (red dotted lines) and standard error of the mean (plotted as error bars). Precision (blue dotted lines) and total (blue dashed lines) mean combined errors are shown, too for 2002-2004 during the MIPAS instrument full-resolution period. a) Global matchups, b) arctic [65N-90N], c) Northern Hemisphere mid-latitudes [20N-65N], d) tropics [20S-20N], e) Southern Hemisphere mid-latitudes [20S-65S], f) Antarctica [65S-90S].

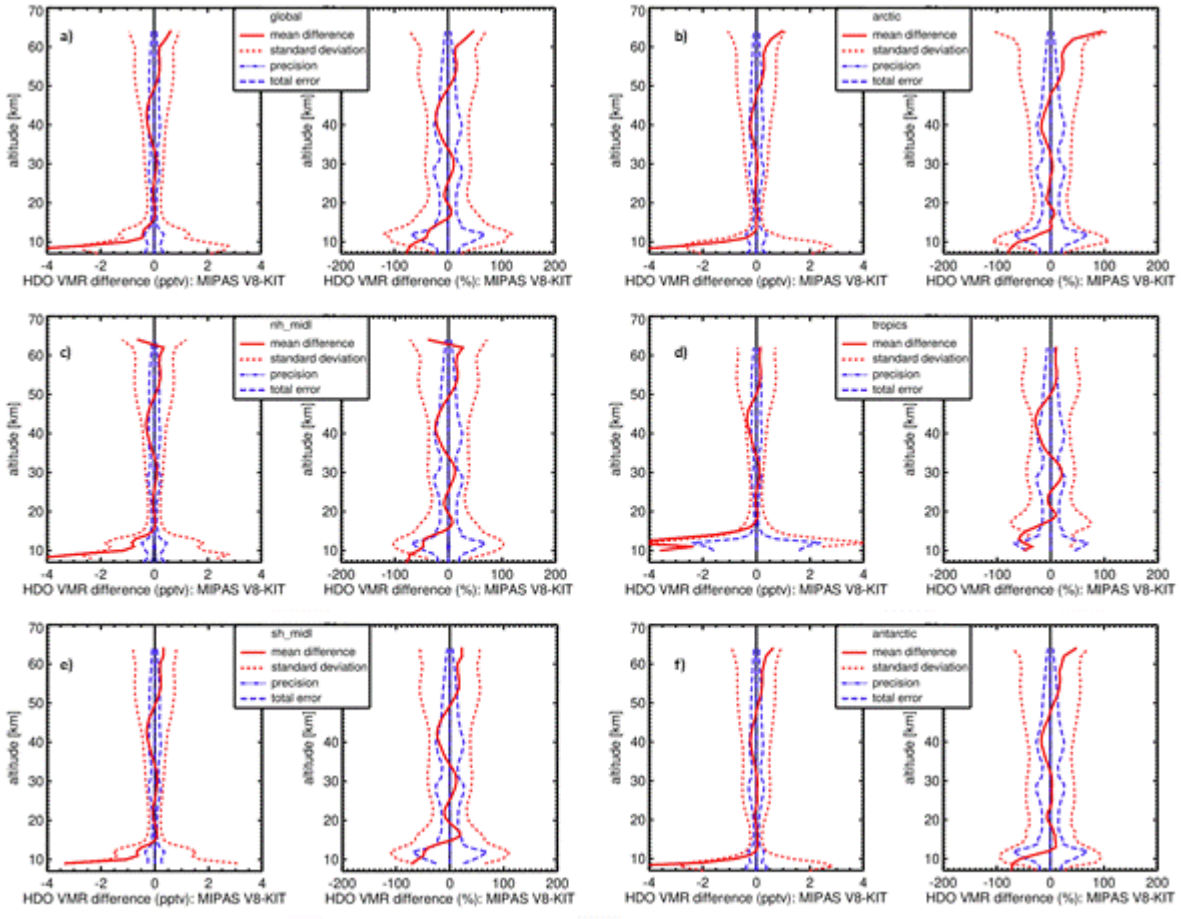

Figure 4-133. As Figure 4-132, but for 2005-2012.

5 Acronyms

ADC	Analogue to Digital Converter
ADF	Auxiliary Data File
ADS	Annotation Data Set
AK	Averaging Kernels
ATBD	Algorithm Theoretical Baseline Document
BEAT	Basic ENVISAT Atmospheric Toolbox
BIRA-IASB	Royal Belgian Institute for Space Aeronomy
CBB	Calibration Blackbody
CFI	Customer Furnished Items
CM	Covariance Matrix
CTI	Configuration Table Interface
DORIS	Doppler Orbitography and Radiopositioning Integrated by Satellite
DS	Deep Space
DSI	Data Service Initiative
ECMWF	European Centre for Medium-Range Weather Forecasts
ESA	European Space Agency
FPM	Fine Pointing Mode
FR	Full Resolution
FTIR	Fourier Transform InfraRed spectrometer
IAA	Instituto de Astrofísica de Andalucía
ID	Identifier
IDEAS	Instrument Data quality Evaluation and Analysis Service
IDU	Interferometer Drive Unit
IFOV	Instantaneous Field of View
ILS	Instrument Line Shape
IMK	Institute of Meteorology and Climate Research
IODD	Input / Output Data Definition
IPF	Instrument Processor Facility
IVS	Iterative variable strength
KIT	Karlsruhe Institute of Technology
L0	Level 0
L1b	Level 1b
L2	Level 2
LOS	Line Of Sight
LTE	Local Thermodynamic Equilibrium
MA	Middle Atmosphere
MDS	Measurements Data Set
MIPAS	Michelson Interferometer for Passive Atmospheric Sounding
MIPAS-B	MIPAS instrument (KIT) mounted on balloons
MPH	Main Product Header
MW	Microwindow
NESR	Noise Equivalent Spectral Radiance
NOM	Nominal
OM	Occupation Matrix
OR	Optimised Resolution

p	Atmospheric Pressure
PCD	Product Confidence Data
QWG	Quality Working Group
RR	Reduced Resolution
SODAP	Switch-On and Data Acquisition Phase
SPPA	Sensor Performance, Products and Algorithm
SYSM	Stellar Yaw Steering Mode
T	Atmospheric Kinetic Temperature
UA	Upper Atmosphere
UTLS	Upper Troposphere Lower Stratosphere
V6	Version 6 (MIPAS Level 2)
V7	Version 7 (MIPAS Level 2)
V8	Version 8 (MIPAS Level 2)
VMR	Volume Mixing Ratio
ZPD	Zero Path Difference

6 Reference Documents

Boone, C.D. , Bernath, P.F., Cok, D., Jones , S.C., Steffen, J., Version 4 retrievals for the atmospheric chemistry experiment Fourier transform spectrometer (ACE-FTS) and imagers, Journal of Quantitative Spectroscopy and Radiative Transfer, 2020

Calisesi, Y., Soebijanta, V. T., and van Oss, R.: Regridding of remote soundings: Formulation and application to ozone profile comparison, *J. Geophys. Res.*, 110, D23306, doi:10.1029/2005JD006122, 2005.

Carlotti, M.: Global-fit approach to the analysis of limb-scanning atmospheric measurements, Appl. Opt., 27, 3250–3254, 1988

Ceccherini, S., Carli, B., and Raspollini, P., "Equivalence of data fusion and simultaneous retrieval". In: Opt. Express 23.7 (Apr. 2015), pp. 8476–8488. doi: 1 0.1364/OE.23.008476. url: http://www.opticsexpress.org/abstract.cfm?URI=oe-23-7-8476.

S. Ceccherini, B. Carli and P. Raspollini, *Quality of MIPAS operational products*, Journal of Quantitative Spectroscopy and Radiative Transfer, Vol. **121**, 45-55 (2013), doi: 10.1016/j.jqsrt.2013.01.021

Ceccherini, S. and Ridolfi, M., "Technical Note: Variance-covariance matrix and averaging kernels for the Levenberg-Marquardt solution of the retrieval of atmospheric vertical profiles", Atmos. Chem. Phys. 10, 3131-3139 (2010).

Ceccherini, S.,"Analytical determination of the regularization parameter in the retrieval of atmospheric vertical profiles", Opt. Lett. 30, 2554–2556 (2005).

Dudhia, A., Jay, V. L., and Rodgers, C. D.: Microwindow selectionfor high-spectral-resolution sounders, Appl. Optics, 41, 3665–3673, 2002.

Errera, Q., Ceccherini, S., Christophe, Y., Chabrillat, S., Hegglin, M. I., Lambert, A., Ménard, R., Raspollini, P., Skachko, S., van Weele, M., and Walker, K. A.: Harmonisation and diagnostics of MIPAS

ESA CH_4 and N_2O profiles using data assimilation, Atmos. Meas. Tech., 9, 5895–5909, https://doi.org/10.5194/amt-9-5895-2016, 2016.

J.-M. Flaud, F. Kwabia Tchana, W.J. Laffertyb and C.A. Nixon , High resolution analysis of the m26 and 2m9–m9 bands of propane: modelling of Titan's infrared spectrum at 13.4 km
Molecular Physics, Vol. 108, No. 6, 20 March 2010, 699–704

Gordon a, I.E. *, L.S.Rothman a, C.Hill a,b, R.V.Kochanov a,c, Y.Tana, P.F.Bernath d, M.Birk e, V. Boudon f, A.Campargue g, K.V.Chance a, B.J.Drouin h, J.-M.Flaud i, R.R.Gamache j, J.T.Hodges k, D.Jacquemart l, V.I.Perevalovm, A.Perrin n, K.P.Shine o, M.-A.H.Smith p, J. Tennyson b, G.C.Toon h, H.Tran n, V.G.Tyuterev q, A.Barbe q, A.G.Császár r,rr, V.M.Devi s, T.Furtenbacher r, J.J.Harrison t,tt,ttt, J.-M.Hartmann n, A.Jolly i, T.J.Johnson u, T.Karman a,v, I. Kleiner i, A.A.Kyuberis a,w, J.Loos e, O.M.Lyulin m, S.T.Massie x, S.N.Mikhailenkom, N. Moazzen-Ahmadi y, H.S.P.Müller z, O.V.Naumenkom, A.V.Nikitinm, O.L.Polyansky b,w, M. Rey q, M.Rotger q, S.W.Sharpe u, K.Sung h, E.Starikovam, S.A.Tashkunm, J. VanderAuwera aa, G.Wagner e, J.Wilzewski a,e, P.Wcisło bb, S.Yuh, E.J.Zak b, The HITRAN2016 molecular spectroscopic database, Journal of Quantitative Spectroscopy & Radiative Transfer,3-69, 2017

Griessbach, S., Hoffmann, L., Spang, R., von Hobe, M., Müller, R., and Riese, M.: Infrared limb emission measurements of aerosol in the troposphere and stratosphere, Atmos. Meas. Tech., 9, 4399–4423, https://doi.org/10.5194/amt-9-4399-2016, 2016

Hanke, M.: A regularizing Levenberg-Marquardt scheme, with ap-plications to inverse groundwater filtration problems, InverseProblems, 13, 79–95, 1997.

Harrison, J. J., Boone, C. D., & Bernath, P. F. (2017). New and improved infrared absorption cross sections and ACE-FTS retrievals of carbon tetrachloride (CCl_4). *Journal of Quantitative Spectroscopy and Radiative Transfer, 186*, 139-149. doi:10.1016/j.jqsrt.2016.04.025

Harrison, J. J.: New and improved infrared absorption cross sections for chlorodifluoromethane (HCFC-22), Atmos. Meas. Tech., 9, 2593–2601, https://doi.org/10.5194/amt-9-2593-2016, 2016.

Harrison, J. J., New and improved infrared absorption cross sections for trichlorofluoromethane (CFC-11), Atmospheric Measurement Techniques, 5827--5836, 2018, https://www.atmos-meas-tech.net/11/5827/2018/, DOI = {10.5194/amt-11-5827-2018}

Höpfner, M., Blom, C. E., Echle, G., Glatthor, N., Hase, F., and Stiller, G. P.: Retrieval simulations for MIPAS–STR measurements, in: IRS 2000: Current Problems in Atmospheric Radiation, edited by: Smith, W. L. and Timofeyev, Y. M., A. Deepak Publishing, Hampton, VA, USA, 1121–1124, 2001.

Keppens, A., Compernolle, S., Verhoelst, T., Hubert, D., and Lambert, J.-C.: Harmonization and comparison of vertically resolved atmospheric state observations: methods, effects, and uncertainty budget, Atmos. Meas. Tech., 12, 4379–4391, https://doi.org/10.5194/amt-12-4379-2019, 2019

Kleinert, A., Birk, M., Perron, G., and Wagner, G.: Level 1b error budget for MIPAS on ENVISAT, Atmos. Meas. Tech., 11, 5657–5672, https://doi.org/10.5194/amt-11-5657-2018, 2018.

Levenberg, K.: A method for the solution of certain problems inleast squares, Q. Appl. Math., 2, 164–168, 1944.

Maki AG, Mellau GC, Klee S, Winnewisser M, Quapp W. High-temperature infrared measurements in the region of the bending fundamental of H12C14N, H12C15N, and H13C14N. J Mol Spectrosc 2000;202:67–82;

Maki AG, Quapp W, Klee S, Mellau GC, Albert S. Infrared transitions of H12C14N and H12C15N between 500 and 10000 cm"1. J Mol Spectrosc 1996;180:323–36

Marquardt, D. W.: An algorithm for the least-squares estimation ofnonlinear parameters, SIAM, J. Appl. Math., 11, 431–441, 1963

C.A. Nixon a,b,_, D.E. Jennings b, J.-M. Flaud c, B. B_ezard d, N.A. Teanby e, P.G.J. Irwin e, T.M. Ansty f, A. Coustenis d, S. Vinatier d, F.M. Flasar , Titan's prolific propane: The Cassini CIRS perspective, Planetary and Space Science 57 (2009) 1573–1585

Payan, S., Camy-Peyret, C., Oelhaf, H., Wetzel, G., Maucher, G., Keim, C., Pirre, M., Huret, N., Engel, A., Volk, M. C., Kuellmann, H., Kuttippurath, J., Cortesi, U., Bianchini, G., Mencaraglia, F., Raspollini, P., Redaelli, G., Vigouroux, C., De Mazière, M., Mikuteit, S., Blumenstock, T., Velazco, V., Notholt, J., Mahieu, E., Duchatelet, P., Smale, D., Wood, S., Jones, N., Piccolo, C., Payne, V., Bracher, A., Glatthor, N., Stiller, G., Grunow, K., Jeseck, P., Te, Y., and Butz, A., "Validation of version-4.61 methane and nitrous oxide observed by MIPAS", Atmos. Chem. Phys., 9, 413-442, doi:10.5194/acp-9-413-2009, 2009.

Perrin, A., Flaud, J.-M., Ridolfi, M., Vander Auwera, J., and Carlotti, M.: MIPAS database: new HNO_3 line parameters at 7.6 μm validated with MIPAS satellite measurements, Atmos. Meas. Tech., 9, 2067–2076, https://doi.org/10.5194/amt-9-2067-2016, 2016.

P. Raspollini, C. Belotti, A. Burgess, B. Carli, M. Carlotti, S. Ceccherini, B. M. Dinelli, A. Dudhia, J. M. Flaud, B. Funke, M. Hopfner, M. Lopez-Puertas, V. Payne, C. Piccolo, J. J. Remedios, M. Ridolfi, and R. Spang, "MIPAS level 2 operational analysis", Atmos. Chem. Phys. 6(12), 5605–5630 (2006).

P. Raspollini, B. Carli, M. Carlotti, S. Ceccherini, A. Dehn, B. M. Dinelli, A. Dudhia, J.-M. Flaud, M. López-Puertas, F. Niro, J. J. Remedios, M. Ridolfi, H. Sembhi, L. Sgheri, and T. von Clarmann, "Ten years of MIPAS measurements with ESA Level 2 processor V6 – Part 1: Retrieval algorithm and diagnostics of the products", Atmos. Meas. Tech.6, 2419-2439 (2013).

M. Ridolfi and L. Sgheri, "Iterative approach to self-adapting and altitude-dependent regularization for atmospheric profile retrievals", Opt. Express 19, 26696-26709 (2011).

M. Ridolfi, B. Carli, M. Carlotti, T. von Clarmann, B. M. Dinelli, A. Dudhia, J. M. Flaud, M. Höpfner, P. E. Morris, P. Raspollini, G. Stiller, and R. J. Wells, "Optimised forward model and retrieval scheme for MIPAS near-real-time data processing", Appl. Opt. 39(8), 1323–1340 (2000).

C. D. Rodgers, *Inverse Methods for Atmospheric Sounding: Theory and Practice*, Vol. 2 of Series on Atmospheric, Oceanic and Planetary Physics (World Scientific, 2000).

L.S. Rothman, I.E.Gordon, A.Barbe, D.ChrisBenner, P.F.Bernath, M.Birk, V.Boudon, L.R. Brown, A.Campargue, J.-P.Champion, K.Chance, L.H.Coudert, V.Dana, V.M.Devi, S. Fally, J.-M.Flaud, R.R.Gamache, A.Goldman, D.Jacquemart, I.Kleiner, N. Lacome, W.J.Lafferty, J.-Y.Mandin, S.T.Massie, S.N.Mikhailenko, C.E.Miller, N. Moazzen-Ahmadi, O.V.Naumenko, A.V.Nikitin, J.Orphal, V.I.Perevalov,

A.Perrin, A.Predoi-Cross, C.P.Rinsland, M.Rotger, M.Sˇimecˇkova´, M.A.H.Smith, K.Sung, S.A.Tashkun, J.Tennyson, R.A.Toth, A.C.Vandaele, J.VanderAuwera, The HITRAN 2008 molecular spectroscopic database, Journal of Quantitative Spectroscopy & Radiative Transfer, 533–572, (2009)

L.S. Rothman, I.E. Gordon, Y. Babikov, A. Barbe, D. Chris Benner,P.F. Bernath, M. Birk, L. Bizzocchi, V. Boudon, L.R. Brown, A. Campargue,K. Chance, E.A. Cohen, L.H. Coudert, V.M. Devi, B.J. Drouin, A. Fayt,J.-M. Flaud, R.R. Gamache, J.J. Harrison, J.-M. Hartmann, C. Hill,J.T. Hodges, D. Jacquemart, A. Jolly, J. Lamouroux, R.J. Le Roy,G.Li,D.A. Long, O.M. Lyulin, C.J. Mackie, S.T. Massie, S. Mikhailenko,H.S.P. Müller, O.V. Naumenko, A.V. Nikitin, J. Orphal, V. Perevalov,A. Perrin, E.R. Polovtseva, C. Richard, M.A.H. Smith, E. Starikova, K. Sung,S. Tashkun, J. Tennyson, G.C. Toon, Vl.G. Tyuterev, G. Wagner, The HITRAN2012 molecular spectroscopic database, 4-50, 2013, https://doi.org/10.1016/J.JQSRT.2013.07.002

Sembhi, H., Remedios, J., Trent, T., Moore, D. P., Spang, R.,Massie, S., and Vernier, J.-P.: MIPAS detection of cloud and aerosol particle occurrence in the UTLS with comparison to HIRDLS and CALIOP, Atmos. Meas. Tech., 5, 2537–2553,https://doi.org/10.5194/amt-5-2537-2012, 2012.

Sheese, P. E., Walker, K. A., Boone, C. D., Degenstein, D. A., Kolonjari, F., Plummer, D., Kinnison, D. E., Jöckel, P., and von Clarmann, T.: Model estimations of geophysical variability between satellite measurements of ozone profiles, Atmos. Meas. Tech. Discuss., https://doi.org/10.5194/amt-2020-207, in review, 2020.

Spang, R., Eidmann, G., Riese, M., Preusse, P., Offermann, D.,Pfister, L., and Wang, P. H.: CRISTA observations of cirrusclouds around the tropopause, J. Geophys. Res., 107, 8174,doi:10.1029/2001JD000698, 2002.
Spang, R., Remedios, J. J., and Barkley, M.: Colour indices forthe detection and differentiation of cloud types in infra-red limbemission spectra, Adv. Space Res., 33, 1041–1047, 2004.

Stiller, G. P., von Clarmann, T., Funke, B., Glatthor, N., Hase, F., Höpfner, M., and Linden, A.: Sensitivity of trace gas abundances retrievals from infrared limb emission spectra to simplifying approximations in radiative transfer modeling, J. Quant. Spectrosc. Ra., 72, 249–280, 2002.

Tchana FK, Lafferty WJ, Flaud J-M, Manceron L, Ndao M., High-resolution analysis of the ν1and ν5 bands of phosgene $^{35}Cl_2CO$ and $^{35}Cl^{37}ClCO$. Mol Phys, 2015; 113:3241–6, http://dx.doi.org/10.1080/00268976.2015.1015638

G. C. Toon, J.-F. Blavier, B. Sen, and B. J. Drouin , Atmospheric COCI measured by solar occultation spectrometry, GEOPHYSICAL RESEARCH LETTERS, 28, 2835-2838, 2001

Valeri, M., Carlotti, M., Flaud, J.-M., Raspollini, P., Ridolfi, M., and Dinelli, B. M.: Phosgene in the UTLS: seasonal and latitudinal variations from MIPAS observations, Atmos. Meas. Tech., 9, 4655–4663, https://doi.org/10.5194/amt-9-4655-2016, 2016.

Valeri, M., Barbara, F., Boone, C., Ceccherini, S., Gai, M., Maucher, G., Raspollini, P., Ridolfi, M., Sgheri, L., Wetzel, G., and Zoppetti, N.: CCl_4 distribution derived from MIPAS ESA v7 data: intercomparisons, trend, and lifetime estimation, Atmos. Chem. Phys., 17, 10143–10162, https://doi.org/10.5194/acp-17-10143-2017, 2017.

Vigouroux, C., De Mazière, M., Errera, Q., Chabrillat, S., Mahieu, E., Duchatelet, P., Wood, S., Smale, D., Mikuteit, S., Blumenstock, T., Hase, F., and Jones, N.: Comparisons between ground-based FTIR and MIPAS N_2O and HNO_3 profiles before and after assimilation in BASCOE, Atmos. Chem. Phys., 7, 377–396, https://doi.org/10.5194/acp-7-377-2007, 2007.

Wetzel, G., Bracher, A., Funke, B., Goutail, F., Hendrick, F., Lambert, J.-C., Mikuteit, S., Piccolo, C., Pirre, M., Bazureau, A., Belotti, C., Blumenstock, T., De Mazière, M., Fischer, H., Huret, N., Ionov, D., López-Puertas, M., Maucher, G., Oelhaf, H., Pommereau, J.-P., Ruhnke, R., Sinnhuber, M., Stiller, G., Van Roozendael, M., and Zhang, G.: Validation of MIPAS-ENVISAT NO_2 operational data, Atmos. Chem. Phys., 7, 3261–3284, https://doi.org/10.5194/acp-7-3261-2007, 2007.

Wetzel, G., Oelhaf, H., Berthet, G., Bracher, A., Cornacchia, C., Feist, D. G., Fischer, H., Fix, A., Iarlori, M., Kleinert, A., Lengel, A., Milz, M., Mona, L., Müller, S. C., Ovarlez, J., Pappalardo, G., Piccolo, C., Raspollini, P., Renard, J.-B., Rizi, V., Rohs, S., Schiller, C., Stiller, G., Weber, M., and Zhang, G.: Validation of MIPAS-ENVISAT H_2O operational data collected between July 2002 and March 2004, Atmos. Chem. Phys., 13, 5791–5811, https://doi.org/10.5194/acp-13-5791-2013, 2013a.

Wetzel, G., Oelhaf, H., Friedl-Vallon, F., Kleinert, A., Maucher, G., Nordmeyer, H., and Orphal, J.: Long-term intercomparison of MIPAS additional species $ClONO_2$, N_2O_5, CFC-11, and CFC-12 with MIPAS-B measurements, Annals of Geophysics, 56, Fast Track-1, doi:10.4401/ag-6329, 2013b.

TECHNICAL NOTES

[AD1] B. Carli, M. Carlotti, S. Ceccherini, M. Hoepfner, P. Raspollini, M. Ridolfi, L. Sgheri, MIPAS Level 2 Algorithm Theoretical Baseline Document (ATBD), IFAC_GA_2007_12_SC, issue 7.1, January 2020, https://earth.esa.int/eogateway/documents/20142/37627/atbd_issue_7.1.pdf/29fd8ac2-7784-2946-e76f-08009ca06b6b

[AD2] F. Barbara and P. Raspollini MIPAS Level 2 Processing Input/Output Data Definition (IODD), June 2020, https://earth.esa.int/eogateway/documents/20142/37627/IODD+mipasNetCDF4.pdf/21dd1b7f-e581-1205-9d62-e098a1773f57

[AD3] Hermann Oelhaf, MIPAS Mission Plan, issue 4.3, January 2008, https://earth.esa.int/documents/700255/707722/MIPAS_Mission_Plan_v4.3_final.pdf/34544a68-e45a-4476-9d7b-f93100ec5162

[AD4] Gerald Wetzel, Michael Höpfner, and Hermann Oelhaf, Report to MS6_2: L1v8/L2v8 FM comparison for GL1-GL3, Long-term validation of MIPAS ESA operational products using MIPAS-B measurements, January 2020 https://earth.esa.int/eogateway/documents/20142/37627/kit_ccn_2_esa_tn-fr_2020_01+GL1+GL3.pdf/3ecc56b5-cfce-8a1c-f8ff-4aa993ba1591

[AD5] David Moore and John Remedios, Long-term validation of MIPAS ESA operational products using ACE v3/v4 measurements, December 2019 https://earth.esa.int/eogateway/documents/20142/37627/UoL_validation_TN_dec_19-2_GS.pdf/f5f41c9a-6a1d-dfd7-8ec9-a12f28a693ec

[AD6] D. Hubert, A. Keppens, J. Granville and J.-C. Lambert, Ground-based validation of MIPAS ESA operational products (ORM 8.22) : T, altitude, O3, CH4, HNO3 and N2O, November 2020 https://earth.esa.int/eogateway/documents/20142/37627/TN-BIRA-IASB-MultiTASTE-Phase-F-MIPAS-ORM8-Iss1-RevB.pdf/da7b509c-21a6-b0a1-5ebb-baf37ce00b2e

[AD7] Product Quality Readme File for MIPAS Level 1b IPF 7.11 products, ENVI-GSOP-EOPGD-QD-15-0130, issue 1.1, 23 December 2015 https://earth.esa.int/documents/700255/707722/RMF_0130+MIP_NL__1P_issue1.1_final.pdf

[AD8] Product Quality Readme File for MIPAS Level 2 ML2PP V7 products, https://earth.esa.int/documents/700255/2635669/RMF_0141+MIP_NL__2P_issue1.pdf/59beb833-5ad4-4301-8422-f41001da36d4

[AD9] Anu Dudhia, Tech Note: Assessment of Molecular Cross-Section Data (v2), 18 Jan 2018 https://earth.esa.int/eogateway/documents/20142/37627/Assessment+of+Molecular+Cross-Section+Data_v2.pdf/b11ea16a-218b-335a-6eb4-1bc5f3ddcc06

[AD10] README FILE MIPAS L1V8 https://earth.esa.int/documents/700255/3711375/Read_Me_File_MIP_NL__1PY_ESA-EOPG-EBA-TN-1+issue1.1.pdf/e989ac1e-83b5-485d-8e25-b208891d84bf

MIPAS instrument
https://earth.esa.int/eogateway/instruments/mipas

- **Instrument performance**

https://earth.esa.int/eogateway/instruments/mipas/description

- **Instrument operations**

The list of events affecting the MIPAS mission can be found at:
https://earth.esa.int/eogateway/instruments/mipas/description

- **Processors documentation**

https://earth.esa.int/eogateway/instruments/mipas/products-information

- **Consolidated datasets**

https://earth.esa.int/eogateway/instruments/mipas/products-information

Annexes

7 A1. Platform pointing anomalies

- **Data quality degradation operational events**

The most significant deficiencies in the products are originated by the following causes:

- Decontaminations: along the mission, ice accumulated on the MIPAS optics with loss of signal at the detector. For this reason regular instrument decontaminations (cooler switch-off) were executed in order to remove the ice contamination. During these events, MIPAS was not in measurement mode. After decontamination periods the noise error was reduced.
- Temperatures stabilization: after planned or unplanned instrument switch-offs, the detector temperatures needed some time to reach operational thresholds and stabilise. During those time intervals the MIPAS measurements might be of a degraded quality.
- Platform pointing anomalies: the instrument pointing accuracy might be reduced during ENVISAT pointing anomalies, or when platform attitude modes different from the Stellar Yaw Steering Mode (SYSM) were operated (e.g. Yaw Steering Mode [YSM] or Fine Pointing Mode [FPM]). The list of affected mission intervals is provided in section 7.

Mission interval		Affected orbits	Anomaly
9 Dec 2003 10:00:00	12 Dec 2003 17:48:32	9280 - 9328	Platform attitude test
21 Jun 2004 07:56:33	22 Jun 2004 11:50:18	12070 - 12087	Platform attitude anomaly
13 Mar 2008 03:16:37	13 Mar 2008 19:28:44	31553 - 31559	Platform attitude anomaly
15 Feb 2009 03:38:34	16 Feb 2009 13:09:00	36402 - 36422	Platform attitude anomaly
5 Mar 2009 19:18:01	6 Mar 2009 15:10:02	36664 - 36681	Platform attitude anomaly
11 Jan 2010 11:34:56	11 Jan 2010 19:05:37	41130 - 41135	Platform attitude anomaly
26 May 2010 12:12:12	26 May 2010 16:26:04	43063 - 43066	Platform attitude anomaly
22 Oct 2010 04.20.01	02 Nov 2010 10.25.02	45191 - 45353	Orbit lowering manoeuvres